



**4<sup>th</sup> Iran National Zeolite Conference**  
**Golpayegan University of Technology, Golpayegan, Iran**  
**August 23-24, 2017**



# Book

of

**4<sup>th</sup> Iran National Zeolite Conference**

**Golpayegan University of Technology, 23-24 August 2017**



# 4<sup>th</sup> Iran National Zeolite Conference

## Golpayegan University of Technology, Golpayegan, Iran

### August 23-24, 2017



## Preface

Welcome all you to the 4<sup>th</sup> Iran National Zeolite Conference and I hope you have nice time in Golpayegan University of Technology.

After the first Iran international zeolite conference which was successfully held at Amir Kabir University in 2008, three others meetings were held on at Tehran University on 2010, Arak university on 2012 and Sciences and Technology university on 2015 (National conferences). Now, we are going to start 4<sup>th</sup> Iran National Zeolite Conference in the Golpayegan University of Technology. This conference brings together professionals from industry and academia center who are actively interested in science and technology of zeolite and zeotype materials.

The scientific program of the conference traditionally covers various fields of zeolites science and technology, with specific focus on the nanotechnology area detailed characterization and new area of their applications.

With the excellent involvement of colleagues working in area of zeolite science and technology, the INZC, organizing committee received more than 150 extend abstracts from Iran, in which the scientific committee has accepted 100 papers for presentation as orals and posters. The papers were subdivided into various sessions going from synthesize of materials to their properties and applications through their characterization. The evaluation was carefully reviewed by the members of the International and National Advisory Board.

The organizing committee has arranged 1 plenary lecture , 3 keynote lectures and 16 oral presentations in several separate sessions on Modification and characterization, Environmental applications, Catalysis, Adsorption and molecular sieve, Ion exchange, MOF (Metal organic Framework), Mesoporous materials, MMMs (Mix Matrix Membrane), Natural zeolites and also two poster presentation sessions. All accepted Extend abstract for 4<sup>th</sup> INZC published in a CD. In the point view of scientific committee of 4<sup>th</sup> INZC, the quality of the oral and poster papers which accepted for presentation is the same and due to limited time we choose a few oral presentations. Finally, the organizing committee has special thanks for some scientific companies including Behdash, Kimia Kavan Andishe, Pioneers clean environment, Golpayegan Pegah, Persian Jasmine Mineral Process, Fathe Alborz and Iran zeolite that supported us for this conferences.

**Dr. Mojgan Zendeheel**

**Scientific Chairman**

**4<sup>th</sup> Iran National Zeolite Conference**



**4<sup>th</sup> Iran National Zeolite Conference**  
**Golpayegan University of Technology, Golpayegan, Iran**  
**August 23-24, 2017**



**Conference Chairman Note**

It is our pleasure to welcome you to the 4th Iran National Zeolite conference, in the Golpayegan University in Golpayegan, Iran, from 23-24 August 2017. This conference is very important as it will provide an excellent opportunity for more than 160 well-established scientists both from the country and from abroad to present the latest scientific researches in the field of Zeolite.

I congratulate all organizer of 4th Iran National Zeolite conference and wish a greater success for this important event.

I wish you a successful participation in this conference and a very pleasant stay in Golpayegan.

**Prof. Dara Moazzami**

**Conference Chairman**

**4<sup>th</sup> Iran National Zeolite conference**



4<sup>th</sup> Iran National Zeolite Conference  
Golpayegan University of Technology, Golpayegan, Iran  
August 23-24, 2017



**Scientific Committee**

Chair  
Dr. Mojgan Zندهدل

Co Chair  
Amir Hossein Meysami

**International Advisory Board:**

- G. Bellussi (Italy)
- E. Chmielewska (Slovak Republic)
- G. Cruciani (Italy)
- F. Fajula (France)
- H. Kazemian (Canada)
- H. Oveisi (Japan)
- K. Pavelic (Croatia)
- G. Rodríguez Fuentes (Cuba)
- M. Signoretto (Italy)
- J. S. Yu (Korea)
- K. Surchi (Iraq)
- A. Dakovic (Serbia)

**National Advisory Board:**

- K. Akhbari (University of Tehran)
- A. Badiei (Tehran University, Iran)
- H. Faghihian (Islamic Azad Shahreza, Esfahan)



4<sup>th</sup> Iran National Zeolite Conference  
Golpayegan University of Technology, Golpayegan, Iran  
August 23-24, 2017



- F. Farzaneh (Alzahra university, Iran)
- T. Haji Ashrafi (Alzahra University)
- B. Ghanbari (Sharif University of Technology)
- M. Ghiasi (Isfahan University of Technology, Iran)
- S. A. Hosseini (Urmia University)
- M. Khatamian (Tabriz University)
- A. Mobinikhaledi (Arak University)
- M. Masteri-Farahani (Kharazmi University)
- B. Mazinani (Malayer University)
- N. Mir (Zabol University)
- B. Mirtamizdoust (University of Qom)
- H. Mohammadi-Manesh (Yazd University)
- A. Neshat (Institute for Advanced Studies in Basic Sciences)
- M. poor moghaddam (Ministry of Industry and Mining, Iran)
- M. M. Pour amini (Shahid Beheshti University, Iran)
- S. Rostamnia (University of Maragheh)
- M. Rezaee (AEOI)
- M. R. Pourjavid (AEOI)
- K. Saberyan (AEOI)
- M. Salavati Niasar (University of Kashan, Iran)
- S. M. Seyed Ahmadian (Shahid Madani University)
- Sh. Sohrabnezhad (Guilan University, Iran)
- M. soliman nejad (Arak University, Iran)
- A. Tadjarodi (Iran University of Science & Technology)



4<sup>th</sup> Iran National Zeolite Conference  
Golpayegan University of Technology, Golpayegan, Iran  
August 23-24, 2017



- A. S. Tarahhomi (Semnan University)
- A. A. Tarlani (Chemistry & Chemical Engineering Research Center of Iran)
- A. Tatar (Gorgan University of Agricultural Sciences and Natural Resources, Iran)
- M. Zanjanchi (Guilan University, Iran)
- R. Zendehtdel (Shahid Beheshti University, Iran)
- R. Amini Najafabadi (Golpayegan University of Technology)
- T. Dallali Esfahani (Golpayegan University of Technology)
- M. Rafiaie (Golpayegan University of Technology)
- M. Ardestani (Islamic Azad University, Science and Research Branch) B. Mazinani (Malayer University)
- Pr. MohammadReza Aboutalebi (Iran University of Science and Technology)
- S. Hossein Seiedein (Iran University of Science and Technology)
- H. Oveisi (Sabzevar University)
- M. Hajisafari (Islamic Azad University, Yazd Branch)
- R. Ghasemzadeh (Islamic Azad University, Karaj Branch)
- K. Saberyan (Atomic Energy Organization of Iran)
- A. Monshi (Isfahan University of Technology & Islamic Azad University – Ahvaz Branch)
- H. Paydar (Islamic Azad University – Tiran Branch)
- M. Razazi (Islamic Azad University, Majlesi Branch)
- H. Sharifi (University Of Shahrekord)
- R. Ebrahimi (Islamic Azad University – Najafabad Branch)
- Z. Obidov Rajabovich (Tajikistan Academy of Sciences)
- I. Ganiev Noroozovich (Tajikistan Academy of Sciences)
- M. Ahmadian (Isfahan University of Technology)
- R. Emadi (Isfahan University of Technology)



4<sup>th</sup> Iran National Zeolite Conference  
Golpayegan University of Technology, Golpayegan, Iran  
August 23-24, 2017



SM. Shariat (Payam Noor University of Golpayegan)

**Organizing Committee**

Prof. Dara Moazzami

Dr. Reza Amini Najafabadi

Dr. Mohsen Bahrami

Dr. Taghi Dallai Esfahani

Dr. Seyed Mehdi Rafiaei

Dr. Maryam Zare

Mr. Aliasghar Foroughifar

Mr. Eman Fakhari Golpayegani

Mr. Azizollah Bayati

Mr. Mohsen Jamali

Mrs. Fatemeh Ganji



4<sup>th</sup> Iran National Zeolite Conference  
Golpayegan University of Technology, Golpayegan, Iran  
August 23-24, 2017



# Plenary





# 4<sup>th</sup> Iran National Zeolite Conference

## Golpayegan University of Technology, Golpayegan, Iran

### August 23-24, 2017



## Zeolite materials for Solar thermal energy harvesting and Water remediation sustainable Technologies

Giuseppe Cruciani\*

*Department of Physics and Earth Sciences, University of Ferrara , Via G. Saragat 1, I-44122 Ferrara, Italy*

*\*Email: [giuseppe.cruciani@unife.it](mailto:giuseppe.cruciani@unife.it)*

Sustainable development is declared as “an overarching objective” of the European framework programme Horizon 2020. More in particular, the development of sustainable technologies and materials to exploit renewable energy sources, e.g. solar and geothermal energy, and to safeguard one of the most important primary resource of the Earth planet, namely water, is rated with high priority among the societal challenges.

Owing to several factors such as the rising world population and increasing life standards, the demand of energy could effectively grow by as much as 55% by 2030 and potentially double by 2050.<sup>1</sup> Although our reliance on fossil fuels is not expected to change significantly between now and 2050, reduction of primary energy consumption is strongly needed to reduce global warming, in line with the Kyoto Protocol (1998), which requires that industrialized nations reduce greenhouse gas emissions to below 1990 levels. Since a large fraction of energy production (e.g. up to 40% in Europe and to 80% in North America) is used for the heating and cooling of residential buildings, research on cheaper and environmentally clean energy sources and technologies is a key priority in many countries. In particular, the application of solar energy instead of electricity for air conditioning/refrigeration appears as a very promising technology owing to the close coincidence of high peak cooling demands with the maximum available solar thermal energy, especially in those countries with high solar irradiation.

Moreover, solar-powered refrigeration devices are suitable to meet requirements for the preservation of food, drugs and vaccines in remote areas.<sup>2</sup> Different physical phenomena can be exploited for the long-term ‘solar heat storage’ (SHS) including physisorption (based on weak Van der Waals forces and hydrogen bonding) or chemisorption (valency forces). Zeolites and related microporous minerals are among the best suited adsorbing materials owing to their tunable host-guest interaction strength, efficiency, and sustainability. The development of natural zeolite sorption refrigeration systems powered by solar energy emerged in the late 1970s, following the pioneering work of Tchernev<sup>3</sup> on mineral chabazite and its water adsorption properties. The exothermic enthalpy of hydration, thermodynamically stabilizing the otherwise metastable anhydrous zeolite structure, explains the endothermic nature of the dehydration phenomenon in these minerals.

Thermally activated sorption of zeolites can be used in Solar Coolers (SCs) as a possible alternative to electricity driven vapour compression refrigerator. Basically, in an adsorption cooling cycle the mechanical compressor of a conventional gas (refrigerant) compression system powered by electricity is replaced by a thermal compressor (zeolite) driven by low grade thermal energy like solar or geothermal energy to evaporate water. As a further advantage, the use of water vapour as the refrigerant fully complies with the Montreal protocol (1988) on substance that depletes the ozone layer. Alternatively, the zeolite water ad/desorption cycles can be used to increase efficiency of Adsorption Heat Pumps (AHPs) or in seasonal Solar Heat Storage (SHS) systems. The thermal stability of several zeolite topologies<sup>4</sup> makes the ad/desorption cycle fully reversible.

“Water”, the so-called “blue gold”, represents a primary resource for the planet Earth to be protected, for all the social, economic and geopolitical issues that arise. Water reserves represented by groundwater is seriously compromised in many industrial areas, especially in districts hosting petrochemical activities and oil. The development of the chemical and agrochemical industries has resulted in the release of chemical compounds into the environment. Aquatic ecosystems are especially vulnerable because they are used as recipients of potentially toxic liquids and solids from domestic, agricultural and industrial wastes. These chemicals, defined as emerging organic contaminants (EOCs), persist in the environment, can bioaccumulate throughout the food chain, and may be toxic to biotic communities. Approximately 500 Mt/y of hazardous wastes are produced by industry, which negatively affect global water resources.<sup>5</sup> For these reasons it is very important to develop technologies with low environmental impact



# 4<sup>th</sup> Iran National Zeolite Conference

## Golpayegan University of Technology, Golpayegan, Iran

### August 23-24, 2017



and high efficiency in order to overthrow the pollution of hydrocarbon cycle activities. Due to their particular chemical-physical and structural features, zeolite absorbers are crucial for the remediation of groundwater polluted by organic complexes, such as chlorinated compounds and hydrocarbons, deriving from petroleum activities and/or petrochemical industries. Zeolite materials are very reactive systems which can immobilize or decompose the contaminants into less dangerous products.

Recently, high-silica zeolites have been shown to be very effective in removing certain organics from water in Permeable Reactive Barriers (PRBs) technology<sup>6</sup>. To date, there are more than hundred PRB operating all over the world, most in the United States, and about twenty in Japan and Europe, respectively. In Italy, the research in this area has been primarily pushed by the national oil company Eni SpA and has led to publication of several patents<sup>7</sup> and scientific papers<sup>8-10</sup> describing the benefits arising from the use of hydrophobic synthetic zeolites. In particular, high-silica ZSM-5 is specific for hydrocarbons, since it can reduce of about 96% the hydrocarbons from C6 to C12 concentration.<sup>6</sup> Removal of pharmaceuticals and personal care products from natural water is another priority issue due to the harmful effects of these pollutants on the environment, even at very low concentration.<sup>11</sup> Among sewage-derived contaminants, the distribution and behavior of pharmaceutically active compounds (PhACs) have been extensively studied over the past decade for several reasons.

Firstly, many of these compounds are poorly degraded by conventional treatments in wastewater treatment plants. Secondly, although they are detected usually at very low concentrations in surface waters (parts per trillion), PhACs are biologically active substances that may cause long-term damage to most sensitive aquatic species. The occurrence of antibiotics in natural waters is one of the main reason of the spreading of microbial antibiotic resistance which, in its turn, makes the antibiotics less effective. For instance in Italy about fifteen hundred tons per year of pharmaceuticals are used and up to 90% of the administered dose, can be excreted unmetabolized in urine or stool and discharged into domestic wastewater. An example is sulfamethoxazole, belonging to the class of sulfa drugs which are the most widely administered antibiotics in animal husbandry, which occurs as one of the most abundant residual drug in surface waters in Italy and Europe.<sup>12</sup>

This lecture will focus on a few examples where zeolites, either natural or synthetic, can be successfully exploited for solution of the above problems. Particular emphasis will be given to the use of advanced powder X-ray diffraction (XRD) techniques to achieve a full understanding at the atomic level of the zeolite host-guest molecule intercalation undergone during the adsorption-desorption processes. Time-resolved Rietveld refinements of synchrotron radiation XRD powder data collected during 'in situ' heating provide a unique tool to monitor and catch transient and non-quenchable states, providing information on the dynamics of processes within the crystal structure. This kind of information is fundamental to clarify the collective phenomena occurring during adsorption of a given molecular species (e.g. water or hydrocarbons or pharmaceuticals) and optimize the adsorption/regeneration technology. For instance, the crystallographic knowledge of the ferroelastic behavior of diffusion-controlling phase transition in ZSM-5 and desorption kinetics by thermal treatment is fundamental for a cost-effective tuning of temperature during the adsorbent regeneration process.<sup>13</sup>

## References

- [1] Minea (2009) IEA Heat Pump Centre Newsletter, 27, 8.
- [2] Wang and Oliveira (2006) Prog. in Energy and Combustion Sci. 32, 424.
- [3] Tchernev (2001) MSA Rev. Miner. Geochem. 45, 589-617.
- [4] Cruciani (2006) J. Phys. Chem. Solids 67, 1973-1994.
- [5] UNESCO (2014).
- [6] Vignola et al. (2011) Chem. Eng. J. 178, 210.
- [7] Vignola et al. (2009) PCT Patent WO 2009/000429 A1.
- [8] Martucci et al. (2012) Microp Mesop Mater. 151, 358-367.
- [9] Martucci et al. (2015) Microp Mesop Mater. 215 175-182.
- [10] Rodeghero et al. (2016) Catalysis Today 277, 118-125.
- [11] Martucci et al. (2012) Microp Mesop Mater. 148, 174-183.
- [12] Riva et al. (2015) J. Pharm. Biomed. Anal. 15, 71-78.
- [13] Ardit et al. (2015) J. Phys. Chem. C 119, 7351-7359.



4<sup>th</sup> Iran National Zeolite Conference  
Golpayegan University of Technology, Golpayegan, Iran  
August 23-24, 2017



# Keynotes



4<sup>th</sup> Iran National Zeolite Conference  
Golpayegan University of Technology, Golpayegan, Iran  
August 23-24, 2017



Metal-Organic Frameworks as a New Class of Porous Materials in Catalytic  
Applications: Scope and Limitation

Mostafa M. Amini\*

Inorganic Division and Catalysis, Faculty of Chemistry, Shahid Beheshti University, Tehran 1983963113, Iran

\*Email: [m-pouramini@sbu.ac.ir](mailto:m-pouramini@sbu.ac.ir)

Metal-Organic Frameworks (MOFs) are a new class of crystalline porous materials with 3-D network structures, and they constructed from organic struts and metal-containing nodes as secondary building units (SBUs) [1-2]. MOFs with unique properties, including crystallinity, large and tuneable pore size and strong interaction between polytopic ligands and metal ions became an important class of porous materials. Since the discovery of the first MOF by Kinoshita and co-workers in 1954, a large number of MOFs with various metal ions and polytopic ligands have been reported. These classes of compounds have found their way through science by their fascinating framework topologies and design flexibility in which lead to broad applications in gas storage, gas separation, catalysis, sensors, and drug delivery systems. Metal-Organic Frameworks also can be classified as a subtitle of Porous Coordination Polymers (PCPs). MOFs with microporous structure can have a surface area as large as 5900 m<sup>2</sup>g<sup>-1</sup> and pore volume of 2 ml g<sup>-1</sup> with diverse topologies. More importantly, shape, size and chemical environment of pores of MOFs can be tailored by choosing suitable metal and SBUs in addition to functionalizing linkers by pre- or post-synthesis for a particular catalytic application. Figure 1 shows growth of catalytic applications of MOFs from 2005 up to 2014. Fast and steady growth of this class of compounds, as catalysts and support, shows their bright and promising futures for academic researchers and industrial applications. In this presentation, an overview of catalytic applications of MOFs will be discussed in addition to their scope and limitation in the catalytic process.

Finally, several ongoing works in catalytic applications of magnetic MIL-101-SO<sub>3</sub>H and MPCs@MIL-101 in organic transformation, including synthesis of 1,3,5-triarylbenzenes, 2,4,6-triaryl pyridines, oxidative amidation of aldehydes (Scheme 1) and also catalytic oxidation of dibenzothiophene by VO(OR)<sub>3-x</sub>(OH)<sub>x</sub>@MIL-101 to sulfone in a model fuel (Scheme 2) from our research group will be presented.

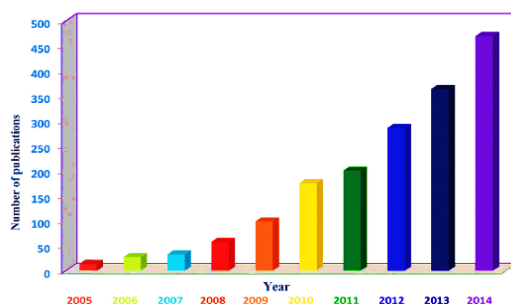
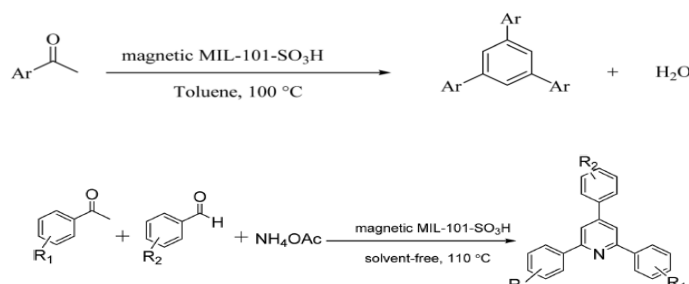


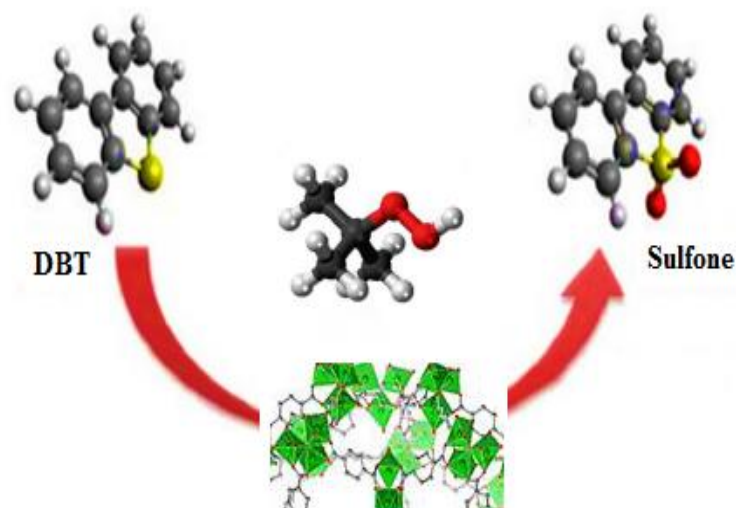
Fig.1. Growth of number of publication in catalytic applications of MOFs from 2005 to 2014.



Scheme 1. Synthesis of 1,3,5-triarylbenzenes and 2,4,6-triaryl pyridines using magnetic MIL-101-SO<sub>3</sub>H.



4<sup>th</sup> Iran National Zeolite Conference  
Golpayegan University of Technology, Golpayegan, Iran  
August 23-24, 2017



**Scheme 2.** Catalytic oxidation of dibenzothiophene by  $\text{VO}(\text{OR})_{3-x}(\text{OH})_x@ \text{MIL-101}$  to sulfone in a model fuel.

## References

1. R. J. Kuppler, D.J. Timmons, Q.-R. Fang, J.-R. Li, T.A. Makal, M.D. Young, D. Yuan, D. Zhao, W. Zhuang, H.-C. Zhou, *Coordination Chemistry Reviews*, 253 (2009) 304.
2. A. Corma, H. Garcia, F. X. Llabres i Xamen, *Chemistry Reviews* 110 (2010) 4606.
3. H. Furukawa, K.E. Cordova, M. O'Keeffe, O.M. Yaghi, *Science*, 341(2013) 974.
4. S. R. Batten, S.M. Neville, D.R. Turner, *Coordination Polymer, Design, Analysis and Application*, The Royal Society of Chemistry, Chapter 10, 2009, RSC Press, UK.
5. Y. Minyoung, R. Srirambalaji, K. Kim, *Chemistry Reviews* 112 (2012) 1196.
6. J. Liu, L. Chen, H. Cui, J. Zhang, L. Zhang, C-Y. Su, *Chemistry Society Reviews* 43 (2014) 6011.



# 4<sup>th</sup> Iran National Zeolite Conference

## Golpayegan University of Technology, Golpayegan, Iran

### August 23-24, 2017



## A review of strategic potentials of Iran's zeolites

Majid Poor Moghaddam\*

Researcher and mineral advisor of Ministry of Industry, Mine and Trade

\*\*Email: Dr.poormoghaddam@yahoo.com

### Introduction

In 2014, Iran ranked fifth in the world by the richest countries in the world to introduce the natural resources. English British Petroleum Company in its report Iran to the world's largest holder of gas reserves announced in 2016. They also have Halgart Institute in London in '94 by announcing the dawn of a big mining power called Iran, which has produced more than 40 mineral product. Iran also among the top 10 countries with 46 billion tons of proven reserves in the world, Asia and the Middle East is the third and quoted Majlis Research Center, Iran has produced 362 million tons of mineral products, mineral products manufacturer ninth with a total mine production totals the \$ 62 billion among the eight countries in the world in terms of total value of mineral production (2013, world mining Data). Iran, with 70 types of minerals, among the 15 countries in the world in terms of variety of minerals known as zeolites since Iran is known as 1/70 minerals, natural zeolites clinoptilolite Iran having a purity of 80% of the outstanding it is.

### 1. Zeolites' divisions and Types of Iran's Zeolites

Since zeolites are generally divided: volcanic and sedimentary zeolites

1-1) In the sedimentary zeolite of Si/Al ratio is greater than volcanic zeolite

2-1) Zeolite Iran's most natural zeolite-type sediments, while the majority of the world's volcanoes.

3-1) Most zeolites with a focus on Central Asia, Armenia and Georgia, as well as zones of Iranian zeolite, are deposited.

### 2. Geological age of Iran's zeolites:

Geological age of the majority of Iranian zeolite zones include Eocene, Pliocene, Oligocene

### 3. The condition for Zeolite formation:

1-3) Zeolites are often in layers of sediment, and buried after the formation of deposits, the reaction of aluminum silicate ( $\text{Al}_2\text{O}_3$ ) water ( $\text{H}_2\text{O}$ ) holes in joints and fractures are formed.

2-3) More zeolites in alkaline or saline lakes located in areas with hot and dry weather in parts of the acidity (PH) is about 5.9 the environment for the Zeolite, materials used in these lakes can conversion to zeolite include natural glass, tuffs, kaolinite and addition to zeolite, sodium and potassium feldspars and metal minerals containing boron are also formed.



# 4<sup>th</sup> Iran National Zeolite Conference

## Golpayegan University of Technology, Golpayegan, Iran

### August 23-24, 2017



3-3) All mineral zeolite groups of about 60 types have been identified so far, destruction or alteration of primary minerals and secondary minerals such as feldspar and feldspars, clay and finally arise from natural silicate gel.

#### 4. Impurities with zeolite reserves in Iran:

Iran often contains impurities with zeolite in plaster  $\text{CaSO}_4$ , lime  $\text{CaCO}_3$ , soil, clay (kaolin and bentonite Montemorlinite), Mordenite, sodium sulfate, salt, feldspar and quartz as well as silica or cristobalite is free.

1-4), usually in pursuit and exploration deposits of zeolite, a mineral impurities which is considered as a marker to identify zeolites are minerals Montemorlinite.

#### 5. Extraction of zeolite in Iran:

Most Iranian zeolite mines, and therefore suitable for open pit mining as an advantage mineral zeolite is easy. So consequently greatly reduced production costs, mining, given that Iran's natural zeolites, mainly affordable and accessible for different uses are considered.

#### 6. Zeolite production situation in Iran and the world:

Zeolite important manufacturers in China (75%), Cuba, Japan, America and Hungary are a total of over 3 million tons of zeolite, other countries, including South Africa, Italy, Canada, Bulgaria, Slovakia, the countries of Central Asia (Caucasus) are the next category of world production.

1-6) Some countries such as Argentina, Australia, Germany, Indonesia, Poland, Iran, France, Yugoslavia and Turkey have zeolite production, but a significant number are not accounted for.

#### 7. The status of a potential Iranian zeolite:

Iranian zeolite reserves to tens of millions of tons. These reserves, which in vast areas of the country are considered external sources. While allowing domestic industry, it also provides the possibility to export and exchange of technology.

1-7) There are zones of Iranian zeolite in Tehran Branch, Hesarbon and golden plains region south of Damavand, Taloqan, south Kahrizak, horseshoe-shaped neck Qom-Tehran road, mountain South Mountain logic routine, Varamin, Hormak area north of Zahedan, Ishlaq tea in Asia, South mountains Rustam Semnan and regional Aftar Semnan in the South east of semnan, South West Hshjyn in Ardabil, north Meshkinshar, South east and South West Bardsir Rafsanjan, Kerman Rhine, in the communication path Ardestān \_ Zafarghandi in Nain in the North east of Isfahan and ....

2-7) In general, Iran, in the field of zeolite has a very high capacity but the highest quality and most favorable zones of Iranian zeolites are zeolite deposits in Eastern Azarbaijan with Myaneh as the center, Semnan with Aftar as the center, and Tehran with Damavand as the center.

3-7) in Semnan province in terms of reserves and mining of zeolite has the highest rate in the country.



4<sup>th</sup> Iran National Zeolite Conference  
Golpayegan University of Technology, Golpayegan, Iran  
August 23-24, 2017



### 8. The quality of Iranian zeolite potential:

1-8) The Economic Zeolite and Valterparham, Clinoptilolite reserves in Iran with a mixture of more than 80% of its excellence in the world.

2-8) Iranian zeolite minerals of high quality and, therefore, for use in various industries mass produced by processing operations, but most of this production is consumed domestically.

3-8) zeolite in a form of silicates which are different physical and chemical properties and characteristics of a good zeolite clinoptilolite in Iran following:

$\text{SiO}_2 > \% 68$  ,  $\text{Ti}_2\text{O}_3 > \% 10$  ,  $\text{Fe}_2\text{O}_3 > \% 0.1$  ,  $\text{CaO} > \% 0.6$

$\text{K}_2\text{O} > \% 1.4$  ,  $\text{Na}_2\text{O} > \% 1.5$  ,  $0.5$  to  $1.1 \text{ gr} / \text{cm}^3 = \text{density}$

### 9. Compare the quality of natural and synthetic zeolites:

Natural zeolites due to the inconsistency in their properties, as well as the fact that their crystalline structure (natural zeolite) in size cavities are not suitable for many industrial users, so in terms of industrial, natural zeolites, fewer applications are, however, natural zeolites are cheaper and better access.

### 10. The natural zeolites and zeolite types that are found in nature:

1-10) among natural zeolites, only eight of them are found to be abundant in sediment and economic crisis. The eight types include Analcime, Chabazite, Clinoptilolite, Ariunite, Heulandite, Lamontite, Mordenite and Felipcite, the most abundant natural zeolite is clinoptilolite.

2-10) seven types of zeolites are found in Iran are as follows:

Clinoptilolite, Heulandite, Analcime, Chabazite, Natrolite, Stylbite, Lamontite







4<sup>th</sup> Iran National Zeolite Conference  
Golpayegan University of Technology, Golpayegan, Iran  
August 23-24, 2017



**11. Iran clinoptilolite zeolite (clinoptilolite):**

1-11) outcrops of clinoptilolite zeolites in Iran:

1-1-11) After the mineralization in the area is located in Semnan and 32 Kilometer North West, Eocene geologic age of the mineralization in cavities of basaltic rocks, Riolity and andesitic caused by the influence of hydrothermal fluids.

2-1-11) It is in Sabze hesarbon in the south west of Firoozkooh. Radial shapes and string beans are the pores, voids, cracks, fractures and veins have filled the stone. With secondary minerals include calcite and quartz.

3-1-11) The mineralization at the Myaneh Zone located in Ishlaq tea and north of the river is the urban challenges and zeolites this area, with tuff that fit the Eocene andesite, this tuff covered by Pliocene conglomerate, the zeolite with minerals quartz, crystobalite, feldspar and Monte Morilonite and the zeolite are associated with Eocene volcanic rocks are associated.

4-1-11) Peak located in South-East mineral district is the village of Aaron ear tuffs and zeolites with the peak Eocene sheet.

2-11) Clinoptilolite Iran often sodic-potassic and sodic potassic  $[\text{Na}_2 \text{K}_2 \text{Ca}]$  with values and bentonite are mordenite.

3-11) preparation of this mineral in Iran is very cheap and useful.

3-11) Clinoptilolite chemical formula  $(\text{Na K Ca})_x (3 [\text{Al}_3 (\text{Al, Si})_2 \text{Si}_{13}\text{O}_{36}]) \cdot 12\text{H}_2\text{O}$

1-4-11) is a collection of minerals and a fracture is rough, crystal shape, wide and short.

2-4-11) colors including white and red

3-4-11) Crystal System: Monoclinic and the classification of hydrothermal silicate and its origin is located.

5-11) The mineral applications in industry:

1. toothpaste containing fluoride is used as a polish.
2. shows more stability against degradation and destruction of their radioactivity.
3. Purification of petroleum products have a key role.
4. Productive livestock fattening male squared.



# 4<sup>th</sup> Iran National Zeolite Conference

## Golpayegan University of Technology, Golpayegan, Iran

August 23-24, 2017



### 12. Zeolites Analcime in Iran:

1-12) The mineral abundant in the North and North West of Ardabil province is located Meshkinshar.

2-12) analcime chemical formula  $\text{Na} [\text{AlSi}_2\text{O}_6] \cdot \text{H}_2\text{O}$

1-2-12) Crystal System: cubic and the family are silicates.

3-12) Analcime as secondary minerals in cavities Bazaltic igneous rocks and sedimentary rocks can be seen, there Analcime in magmatic rocks of avsn in North Meshkinshar been established.

4-12) The mineral applications in industry:

1. When the water molecules crystallize out of the building, creating an empty hole in the zeolite molecular structure, causing it to be unstable, it causes these minerals tend to bond with other molecules have, therefore, this feature of the application it has increased in the industry.

2. Application as chemical filters.

3. audio and video system or leather industry .

4. The chemical industry as an absorbent.



### 13. Zeolite natrolite in Iran (Natrolite):

1-13) outcrops of natrolite zeolites in Iran:



4<sup>th</sup> Iran National Zeolite Conference  
Golpayegan University of Technology, Golpayegan, Iran  
August 23-24, 2017



The mineralization in the area Haramak, north of Zahedan in Iran's South East as well as in the area along the route Tehran-Qom highway Hassan Abad in the south Kahrizak and also Brdsyrkrman in the region is exposed.

2-13) natrolite chemical formula  $\text{Na}_2\text{Al}_2\text{Si}_3\text{O}_{10}$

1-2-13) Crystal System: orthorhombic with barely 5-5 .5 and a specific gravity of 2.25g / cm<sup>3</sup>

3-13) The mineral applications in industry:

1. as a catalyst effective, natural, recyclable heterogeneous and in synthesis of urea and Nitrile are used (Nasrollahzadeh, Bu-Ali Sina's PhD thesis, 91)
2. in many areas of pollution control and environmental cleaning applications.



**14. Zeolites Heulandite Iran (Heulandite):**

1-14) After this mineralization in the area is abundant in Semnan and 32 km North West Eocene-Oligocene age

2-14) Heulandite chemical formula  $\text{CaAl}_2\text{Si}_6\text{O}_{16} \cdot 5\text{H}_2\text{O}$

1-2-14) Crystal System: Monoclinic coffin-shaped crystal shape, hardness of 3-4 and a specific gravity of 2.2 g/cm<sup>3</sup>, the Heulandite type has 4+ and strontium. Heulandite and stilbite are generally similar.

3-14) Heulandite in fact is the name of a series of Tektosilicate groups and from a variety of Heulandites, the first of its kind in terms of more frequent and basically Heulandite is rich in potassium and Silicon.

4-14) Heulandite with other zeolites and Stilbite in caves amigdolity basaltic igneous rocks, gneiss and hydrothermal veins to be found.



**15. Zeolites stilbite in Iran (Stilbite):**



4<sup>th</sup> Iran National Zeolite Conference  
Golpayegan University of Technology, Golpayegan, Iran  
August 23-24, 2017



1-15) outcrops of stilbite zeolites in Iran:

20 km northwest of mineral Hashjin, the southwestern province of Ardebil and stilbite main mineral zeolite alteration zones and quartz is present as minor minerals.

2-15) stilbite chemical formula  $(\text{Na}_2\text{Ca})(\text{Al}_2\text{Si}_7)\text{O}_{18}\cdot 7\text{H}_2\text{O}$

1-2-15) Crystal System: Monoclinic and with barely 3.5- 4 and a specific gravity of 2. 1 - 2. 2g / cm<sup>3</sup> and its origin is volcanic hydrothermal.

3-15) The mineral applications in industry:

1. The removal of iron and manganese perfect tool for artesian wells
2. The removal of chromium from industrial sewage waters
3. The absorption of heavy metals



**16. Zeolites Chabazite Iran (Chabazite):**

1-16) mineralization in the southern part of Rafsanjan East and South West Bardsir hip Eocene outcrops. The mineral usually empty environments and Badamkhay basaltic rocks are volcanic and metamorphic rocks are a little form, this mineral also be formed around hot springs.

2-16) chabazite chemical formula  $(\text{Na}_2\text{Ca})(\text{Al}_2\text{Si}_4)\text{O}_{12}\cdot 6\text{H}_2\text{O}$

1-2-16) Crystal System: Rhombohedral and silicates with a hardness rating of 4-5 and a hydrothermal origin, post-volcanic.

3-16) The mineral applications in industry:

1. Absorb mercury and silver, separating the alcohol compound.
2. Auxiliary radioactive contamination efficient.
3. purification of petroleum products have a key role.
4. Some gases such as nitrogen absorbent used in Iran as a dietary supplement for livestock.
5. The reserve of solar energy.



4<sup>th</sup> Iran National Zeolite Conference  
Golpayegan University of Technology, Golpayegan, Iran  
August 23-24, 2017



**17. Zeolites Lamontite in Iran (Lamontite):**

1-17) The deposit of zeolite in the communication path Ardestān Zafarghandi 6 kilometers East North Esfahan is Nain, along with clays and carbonate minerals clay (albite, lime) and due to thermal alteration of zeolitic tuff rock formation (see Saeed Abedi, an organization of 90)

2-17) chemical formula  $\text{Ca}(\text{Al}_2\text{Si}_4)\text{O}_{12}\cdot 4\text{H}_2\text{O}$  crystallization system orthorhombic

3-17) this mineralization is very similar to Bavnite minerals and paragenesis are fluorite and albite and pegmatite formation of hydrothermal origin.

4-17) The mineral applications in industry: alcohol, paraffin attract the best use of it.

**18. Problems and Challenges of Iranian zeolite deposits and deposits:**

1-18) lack of efficient technical knowledge and lack of serious investment in connection with the processing of natural and industrial production and a variety quintal that must be taken to transfer and processing technology has done.

2-18) study this material and create value-added processing production lines and the modernization of grain processing (such as aggregation only takes place in our country) and serious movement for export zeolite materials to be processed.

3-18) Given that the livestock and poultry specialists are familiar with the mineral zeolite, which unfortunately sometimes used only as feed for livestock and poultry.

4-18) exploits intellectual property laws in our country that could do in there, be resolved.

5-18) environmental problems are especially severe in grading micron and nano level there is lining this, unfortunately, is not much that can cause lung problems, the process of environmental pollution should be considered.

6-18) Setting up specialized workshops for familiarizing audience interested in this fascinating material.



# 4<sup>th</sup> Iran National Zeolite Conference

## Golpayegan University of Technology, Golpayegan, Iran

### August 23-24, 2017



## Novel Functional Nanoporous Catalytic Materials for Synthesis of Fine Chemicals

Ajayan Vinu\*

*Future Industries Institute, University of South Australia, Mawson Lakes 5095, South Australia, Australia*

\*Email: [Ajayan.vinu@unisa.edu.au](mailto:Ajayan.vinu@unisa.edu.au); [vinu.ajayan@gmail.com](mailto:vinu.ajayan@gmail.com)

Nanoporous carbon materials have attracted much attention in the recent years due to their enormous applications in the fields of adsorption, catalysis, and fuel cells [1-5]. However, the incorporation of hetero atoms such as boron and nitrogen in the carbon materials can significantly change their electronic and semi-conducting properties. Recently our group has discovered a new family of nanoporous materials such as nanoporous carbon nitride with different structures, morphology, and pore diameters. In the first part of the talk, I will discuss about the preparation techniques, basics and the mechanism behind the synthesis of various nanoporous nitride materials with different pore structure and textural parameters [6-9]. One of the important features of the materials is that they have inbuilt basic sites in the form of NH<sub>2</sub> or NH groups and can be used as a metal free basic catalyst. I will also demonstrate the basic catalytic performance of these materials in the transesterification of beta-ketoesters with different alcohols, aldol and Knoevenagel reactions and their ability to capture acidic CO<sub>2</sub> molecules. In the second part of the talk, I will be focusing mainly on the fabrication and the catalytic application of amorphous and crystalline metallosilicate catalysts with 3D structure. Especially, the conversion of non-catalytic pure silica materials such as SBA-1, SBA-15, and KIT-5 into highly active catalytic materials by incorporating metal species in the framework in a highly acidic medium will be demonstrated. I introduced two novel concepts for the metal incorporation in the silica framework. These concepts involve: 1. Controlling the water to hydrochloric acid molar ratio in the synthesis gel for the fabrication of metal substituted SBA-15 and KIT-5, which can reduce the pH of the synthesis medium and can enhance the interaction between the metal species and the silica species in the acidic medium; and 2. Changing the local concentration of the H<sup>+</sup> ions in the synthesis mixture to promote local contact between the Si and metal species (for SBA-1) as the synthesis procedure is highly sensitive. The catalytic applications of the materials including alkylation, acylation, multicomponent coupling and condensation reaction will be presented. At the end of my talk, the fabrication of highly crystalline and acidic nanoporous metallosilicate materials and heteropolyacids with different morphology will be presented. These porous superacidic materials with HPA and highly crystalline metallosilicate framework have well-ordered porous structure and exhibit high acidity and excellent textural parameters. These factors are highly critical for their applications especially in catalysis. The catalytic applications of these materials in alkylation and acylation of aromatics, polymerization, and oxidation of aromatics will also be demonstrated [10-11].

### References

1. Vinu et al. Chem. Soc. Rev., 2017, 46, 72.
2. Vinu et al. Angew Chem. Inter. Ed. 2017, In press.
3. Vinu et al. Angew. Chemie Inter. Ed. 2009, 48, 7358.
4. Vinu et al. Angew. Chemie. Int. Ed. 2008, 47, 7254.
5. Vinu et al. Adv. Funct. Mater. 2008, 18, 640.
6. Vinu et al. Adv. Mater. 2005, 17, 1648.
7. A. Vinu, Adv. Func. Mater. 2008, 18, 816.
8. Vinu et al. Chem. Mater. 2007, 19, 4367.
9. Vinu et al. Angew. Chemie Intl. Ed. 2009, 48, 7884.
10. Vinu et al. Angew. Chem. Intl. Ed. 2010, 49, 5961-5965.
11. Vinu et al. Angew. Chem. Intl. Ed. 2012, 51, 2859.



4<sup>th</sup> Iran National Zeolite Conference  
Golpayegan University of Technology, Golpayegan, Iran  
August 23-24, 2017



# Invited Speakers



4<sup>th</sup> Iran National Zeolite Conference  
Golpayegan University of Technology, Golpayegan, Iran  
August 23-24, 2017



**Post-synthetic ion-exchange process in nanoporous metal-organic frameworks; an effective way for modulating their structures and properties**

Kamran Akhbari\*

*School of Chemistry, College of Science, University of Tehran, P.O. Box 14155-6455, Tehran, Islamic Republic of Iran.*

*\*Email: akhbari.k@khayam.ut.ac.ir*

In recent years, MOFs have amused fundamental attention because of their unique properties and their applications in gas sorption, catalysis, separation, drug delivery and synthesis of nano materials. Up to now, two bunches of exchange that occurred in metal nodes and secondary building units (SBUs) of MOFs have been studied. In the first group, M. Lalonde and co-workers, have reported metal exchange involving metal nodes in MOFs have been reported.<sup>1</sup> Their discussion focused on the system where metal cations were exchanged directly in the node. C. K. Brozek and co-workers, in the other group, has checked the cation exchange at MOF's SBUs.<sup>2</sup> They also ambient their discussion to substitution that just occurs at SBUs and not in the pores. In addition, both of them studied the cation exchange, while the ion exchange that occurs at MOFs doesn't confine to cation exchange. Ion-exchange is one of the interesting properties of anionic or cationic MOFs which do not have neutral frameworks. We want to outline the available observations of all types of ion exchange at MOFs pores. When the factors that make ions in the pores exchangeable are explaining, particular materials could be selected for ion-exchange including cation exchange & anion exchange, and their exact compounds could be designed. In this section, we classified two branches of ion-exchange on their examples and reported cases and their applications.

### **Anion-exchange**

For MOFs that have cationic coordination frameworks, the anions are generally included for charge balance and/or serving as templates in the available empty spaces. As a result, anion-exchange properties for such MOFs materials have been extensively foraged.

### **Cation-exchange**

Sometimes the exchange of metal ions or organic cations within anionic MOFs can modulate the chemical properties of a MOF and this could be achieved simply by merging the sample into a solution containing certain metal salt or organic cations to generate a turned anionic MOF. Ion exchange has already yielded some amazing results and new materials that have not been accessible otherwise, but the limit of its usage for architecting new MOFs in a systematic & predictive manner depends on understanding its mechanism. We contemplated to provide a blueprint towards this goal.





4<sup>th</sup> Iran National Zeolite Conference  
Golpayegan University of Technology, Golpayegan, Iran  
August 23-24, 2017



### Applications of ion-exchange process in metal-organic frameworks

The ion exchange that has been introduced by us has some efficient applications. Some of these applications and their effects that happened after exchange have been studied by different research groups and we tried to focus on them during this work. Working on more applications specially gas adsorption of exchanged-materials of MOFs, can be an ideal worth aspiring.

They can be summarized as:

- 1) Separation Process
- 2) Catalytic Properties
- 3) Adsorption properties
- 4) Luminescent Properties
- 5) Other application

These cases can be appeal many communities with different fields. For examples, in the water treatment industry, the ability of MOFs to separate different ions can be used. Modulating gas adsorption property of MOFs after exchange can also be used in various fields, such as the replacement of CNG with ANG, using in fuel cells and cleaning the exhaust gas of factories. It seems that, post-synthetic ion exchange and especially cation exchange process can be a suitable method for modulating the properties of metal organic frameworks.

### References

- 1) M. Lalonde, W. Bury, O. Karagiari, Z. Brown, J. Hupp, O. K. Farha, *J. Mater. Chem. A.*, 2013, 1, 5453.
- 2) C. K. Brozek, M. Dinca, *Chem. Soc. Rev.*, 2014, 43, 5457.



# 4<sup>th</sup> Iran National Zeolite Conference Golpayegan University of Technology, Golpayegan, Iran August 23-24, 2017



## Engineering of hybrid nanoreactors; a promising porous materials for green organic transformations

Sadegh Rostammia \*

Organic and Nano Group (ONG), Department of Chemistry, Faculty of Science, University of Maragheh, P.O.B 55181-83111, Maragheh, Iran

\*Email: [rostammia@gmail.com](mailto:rostammia@gmail.com); [rosammia@maragheh.ac.ir](mailto:rosammia@maragheh.ac.ir)

### Introduction

Engineering of mesoporous silica has emerged as a nanoreactor in various fields, especially in material chemistry, industrials and medicine [1-2]. As our ongoing research interest in the development of catalytic applications of mesoporous silica materials [2], we recently discussed and reviewed organocatalysts which are supported inside the mesopores [3]. Herein, we aimed to review recent advances in the catalytic applications of sulfonic acid-based mesostructures and metal-organic frameworks as nanoreactor (Figure 1) in a comprehensive paper.

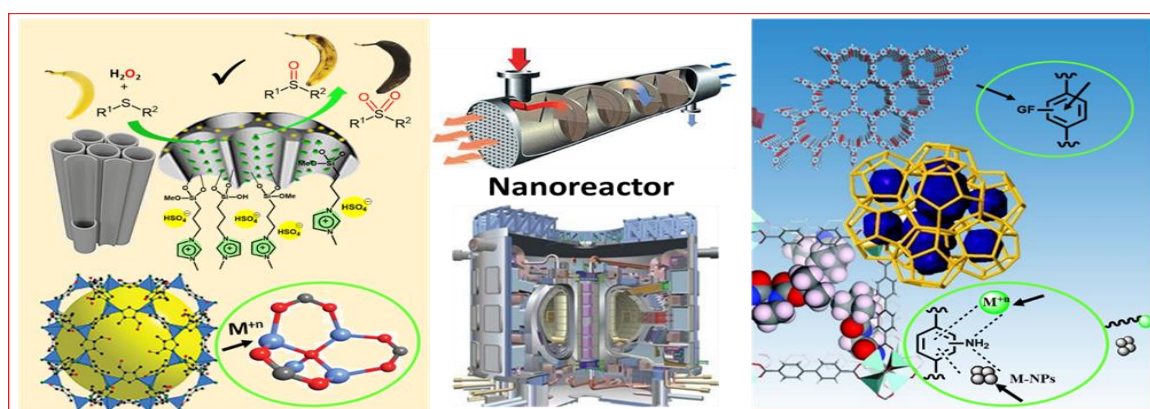
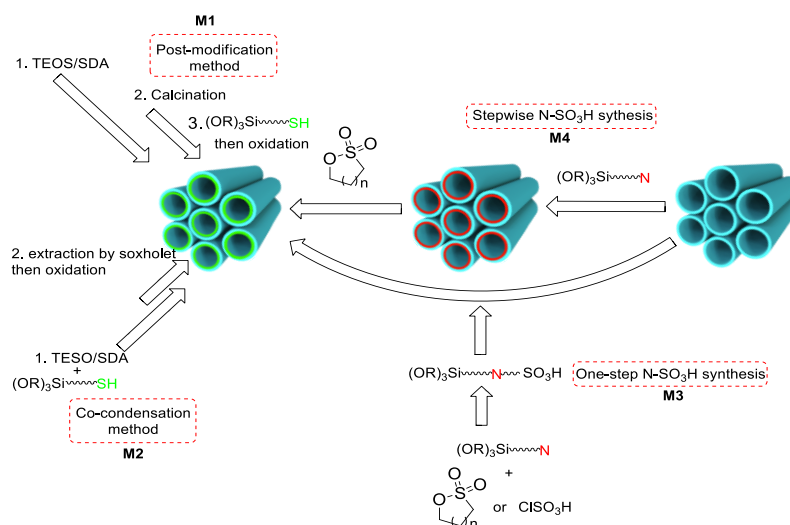


Fig 1. Reactor and Nanoreactor.

Primary reports on sulfonic acid-based precursors go back to 1998 [4], in which the earliest versions of SAPs in mesoporous silicas were prepared by two general routes: 1) post-functionalization of mesoporous silica with 3-mercaptopropyltrimethoxysilane (MPTS) (**M1**) and 2) co-condensation of MPTS and silica source, specifically tetraethyl/methylorthosilicate (TEOS and TMOS, respectively) (**M2**). Here, the final key step to produce SAPs was to oxidate the thiol groups to sulphonic acid using  $H_2O_2$ . Generally, four methods have been developed for preparation of SAPs and functionalization of mesoporous silica materials which are depicted in scheme 1. So far, many developments had been performed by various research groups [5]. For instance, enhancing the capacity of MPTS loading by coating method [6], co-condensation method by using TMOS rather than TEOS [4], replacing calcination with extraction [7]. Most of the sulfonic acid based silica mesopores (SASM) were primarily employed in biomass production [4-7].



# 4<sup>th</sup> Iran National Zeolite Conference Golpayegan University of Technology, Golpayegan, Iran August 23-24, 2017



Scheme 1.

Propylsulfonic acid-based precursor ( $S_{pr}AP$ ) is the earlier type of SAPs which can be obtained by functionalization of MPTS and further oxidation of it.  $S_{pr}AP$  is a most common and available precursor which is extensively used in various catalytic applications. It was first incorporated into MCM-type mesostructures by some pioneering groups in 1998 [4-6]. Rhijn and coworkers [8] used MCM type mesostructure as a catalyst for the synthesis of 2,2-bis(5-methylfuryl)propane which was obtained from condensation of acetone and 2-methylfuran. They also applied it in the esterification of D-sorbitol with lauric acid [9]. Then, Jacobs *et al.* [10] disclosed the synthesis of monolaurin through direct esterification of glycerol with lauric acid over reusable MCM-41 and HMS-Pr-SO<sub>3</sub>H which were far more active than H-USY zeolite and even than commercial sulfonic-acid resins. Mahdavinia and Sepehrian reported the three-component synthesis of 3,4-dihydropyrimidinones (DHP) using MCM-41-Pr-SO<sub>3</sub>H as a mild heterogeneous catalyst through Biginelli reaction (Scheme 2) [11].

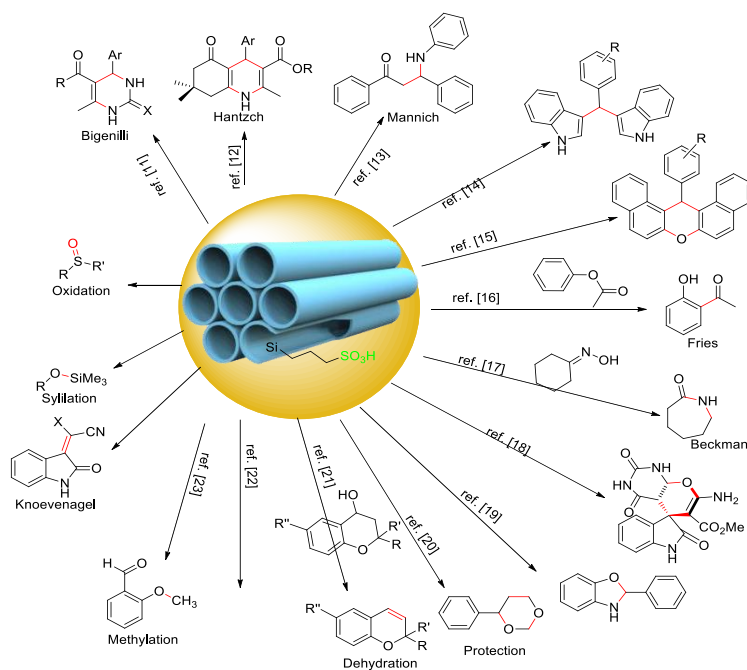
So far, a wide range of catalytic applications are developed by mesoporous silica-propyl-SO<sub>3</sub>H (Meso-Pr-SO<sub>3</sub>H) with no further modifications or improvements. Because explaining all of them by details is overwhelming, we schematically illustrated some of them in Scheme 2. Synthesis of polyhydroquinoline derivatives,  $\beta$ -amino carbonyls synthesis (Mannich reaction), Xanthenes and bis(indolyl)methanes syntheses, and Fries rearrangement, Beckmann rearrangement, multicomponent synthesis of spiro[indole-tetrahydropyrano(2,3-d)pyrimidine] derivatives, synthesis of benzoxazole derivatives, synthesis of 4-phenyl-1,3-dioxane, synthesis of chromenes from chromanols, esterification of salicylic acid with dimethyl carbonate, oxidation of sulphides to sulfoxide, trimethylsilylation of alcohols, etc. [12] are of these examples (Scheme 2).



# 4<sup>th</sup> Iran National Zeolite Conference

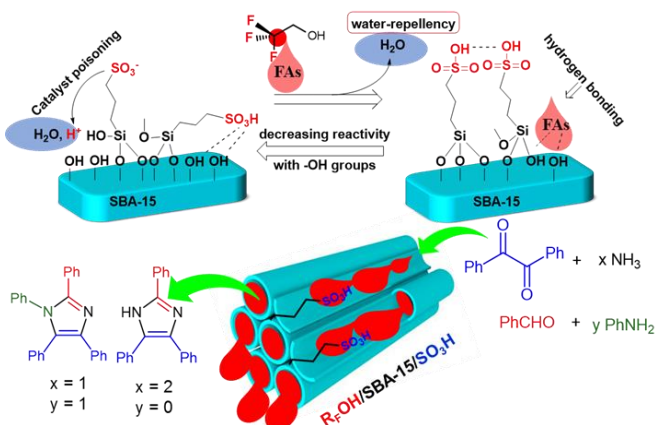
## Golpayegan University of Technology, Golpayegan, Iran

### August 23-24, 2017



Scheme 2.

Recently, we have turned our attention to studying the effect of fluorinated alcohols (FA) on the surface activity of mesoporous silica [13]. Thus, we investigated the the effect of FAs on the catalytic activity of mesoporous silica SBA-15. We found that in the presence of a FA, surface of SBA-15 acts as a catalyst and therefore it can be incorporated in the reactions as a catalyst. Moreover, FAs can increase the mass transfer inside the mesochannels. Then we studied the effect of FAs on the catalytic activity of SBA-15-Pr-SO<sub>3</sub>H. This investigation disclosed the unique effect of FAs on the SBA-15-Pr-SO<sub>3</sub>H. -SO<sub>3</sub>H groups can be interact with silanols of surface and therefore, the catalyst activity may be decreased. We believe that, perfluoroualkyl chains of FAs with a strong hydrogen bonding can interact with silanols and keep them away from availibility of -SO<sub>3</sub>H groups. On the other hand, it can raise the acidity of -SO<sub>3</sub>H with hydrogen bonding which together can raise the catalyst activity of SBA-15-Pr-SO<sub>3</sub>H. also, the hydrophobic nature of perfluoroalkyl chains can have a water repellency effect (Scheme 3). This effect may increase the mass transfer and decrease the catalyst poisoning by water.



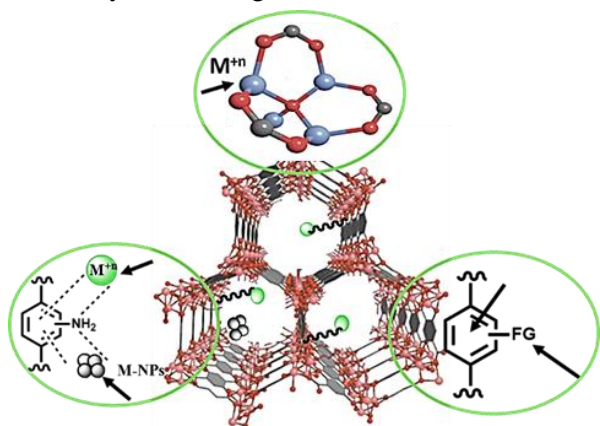


4<sup>th</sup> Iran National Zeolite Conference  
Golpayegan University of Technology, Golpayegan, Iran  
August 23-24, 2017



Scheme 3.

Solid porous coordination polymers (metal-organic frameworks -MOFs) Metal organic frameworks (MOFs) are crystalline solids, in which the structure is formed by inorganic clusters or metal ions (generally transition metal) held in place by multifunctional organic ligands. Application of the porous coordination polymers of MOFs is much interest in exploiting the advantages that MOFs offer as catalysts, including a large surface area, high metal content, flexibility in the design of the active sites in the framework [14-15].



Scheme 4.

Likewise IRMOF-3, NH<sub>2</sub>-MIL-53 is an amine-reached MOF which can be used as a catalyst. NH<sub>2</sub>-MIL-53(Al) material can be prepared by 2-aminoterephthalic acid (H<sub>2</sub>ATA) and aluminium chloride hexahydrate in DMF by a solvothermal method. The porous NH<sub>2</sub>-MIL-53 have crystalline structure with diamond-shaped and one-dimensional (1D) pores (Fig. 1). We used it as a porous lewis acid in the formylation of aromatic amines, and fortunately, it had good results [16].

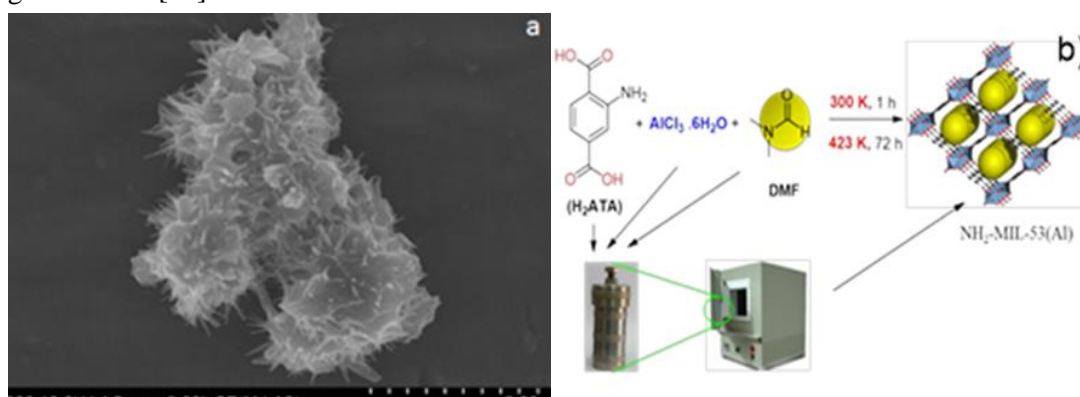


Fig. 2. a) Preparation process of NH<sub>2</sub>-MIL-53(Al), b) SEM image of NH<sub>2</sub>-MIL-53(Al) crystal.

## Conclusion

In summary, there are various types of SAPs and metal-organic frameworks which can be used for mesoporous silica and MOFs nanomaterials. These porous materials have many catalytic applications by denoting acidic nature to solid mesoporous. Depending on the reaction conditions, and by knowing the properties of SAPs and MOFs, we can manufacture an efficient solid acid catalyst.



# 4<sup>th</sup> Iran National Zeolite Conference

## Golpayegan University of Technology, Golpayegan, Iran

### August 23-24, 2017



#### References

1. O.M. Yaghi, G. Li, H. Li, *Nature*, **1995**, 378, 703-706.
2. W.V. Rhijn, D.D. Vos, W. Bossaert, J. Bullen, B. Wouters, P. Grobet, P. Jacobs, Sulfonic acid bearing mesoporous materials as catalysts in furan and polyol derivatization, in: F.B.C.D.S.G. L. Bonneviot, S. Kaliaguine (Eds.) *Studies in Surface Science and Catalysis*, Elsevier, **1998**, pp. 183-190.
3. S. Rostamnia, E. Doustkhah, *RSC Adv.*, **2014**, *4*, 28238-28248.
4. M.H. Lim, C.F. Blanford, A. Stein, *Chem. Mater.*, **1998**, 10, 467-470.
5. W. M. Van Rhijn, D. E. De Vos, B. F. Sels, W. D. Bossaert, *Chem. Commun.* **1998**, 317-318.
6. W.V. Rhijn, D.D. Vos, W. Bossaert, J. Bullen, B. Wouters, P. Grobet, P. Jacobs, Sulfonic acid bearing mesoporous materials as catalysts in furan and polyol derivatization, in: F.B.C.D.S.G. L. Bonneviot, S. Kaliaguine (Eds.) *Studies in Surface Science and Catalysis*, Elsevier, **1998**, pp. 183-190.
7. M. Boveri, J. Aguilar-Pliego, J. Pérez-Pariente, E. Sastre, *Catalysis Today*, **2005**, 107-108, 868-873.
8. W. M. Van Rhijn, D. E. De Vos, B. F. Sels, W. D. Bossaert, *Chem. Commun.*, **1998**, 317-318.
9. J.n. Pérez-Pariente, I. Díaz, F. Mohino, E. Sastre, *Applied Catalysis A: General*, **2003**, 254, 173-188.
10. W.D. Bossaert, D. De Vos, W. Van Rhijn, J. Bullen, P.J. Grobet, P.A. Jacobs, *J. Catalysis*, **1999**, 182, 156-164.
11. G.H. Mahdavinia, H. Sephrian, *Chin. Chem. Lett.*, **2008**, 19, 1435-1439.
12. S.Rostamnia, E.I Doustkhah, *Nanochem. Res.*, **2016**, 1, 19-32.
13. S. Rostamnia, A. Zabardasti, *J. Fluorine Chem.*, **2012**, 144, 69-72.
14. S. Rostamnia, Z. Karimi, *Inorgan. Chim. Acta.*, **2015**, 428, 133-137.
15. S. Rostamnia, H. Xin, *Appl. Organometal. Chem.* **2014**, 28, 359-363.
16. S. Rostamnia, A. Morsali, *RSC Advances*, **2014**, 4, 10514-10518.

## Photo-activated degradation of tartrazine by H<sub>2</sub>O<sub>2</sub> as catalyzed by both bare and Fe-doped methyl-imogolite nanotubes and the related collapsed phases

Elnaz Bahadori,<sup>a</sup> Vincenzo Vaiano,<sup>b</sup> Serena Esposito,<sup>c</sup> Marco Armandi,<sup>a</sup> Diana Sannino,<sup>b,\*</sup> Barbara Bonelli<sup>\* a,d</sup>

<sup>a</sup> Department of Applied Science and Technology, Politecnico di Torino, Corso Duca degli Abruzzi 24, 10129 Turin (Italy).

<sup>b</sup> Department of Industrial Engineering, University of Salerno, via Giovanni Paolo II, 84084 Fisciano, SA, Italy.

<sup>c</sup> Department of Civil and Mechanical Engineering, Università degli Studi di Cassino e del Lazio Meridionale, Via G. Di Biasio 43, 03043 Cassino, FR, Italy.

<sup>d</sup> INSTM Unit of Torino Politecnico, Corso Duca degli Abruzzi 24, 10129 Turin (Italy).

\*Email: [dsannino@unisa.it](mailto:dsannino@unisa.it), [barbara.bonelli@polito.it](mailto:barbara.bonelli@polito.it)

#### Abstract

Synthetic azo dyes, widely used by textile, cosmetic, photographic, pharmaceutical and food industries, represent an environmental concern and must be removed from both wastewater and groundwater [1] due to their potential toxicity to humans and environment, along with the visibility problems connected to their presence in water. One of the most widely used food coloring agents, *i.e.* Tartrazine E102 (TRZ), is recalcitrant to biodegradation under aerobic conditions, and appears to be responsible of the most allergic and/or intolerance reactions in comparison to the other



4<sup>th</sup> Iran National Zeolite Conference  
Golpayegan University of Technology, Golpayegan, Iran  
August 23-24, 2017



azo dyes [2]. Among nanomaterials with potential application as heterogeneous catalysts, there is a growing interest for imogolite-related materials, as testified by the recent studies on their synthesis [3], structure [4], electronic states

[5], stability [5], and application as catalyst and/or catalytic support [6]. Proper imogolite is a hydrous aluminum silicate with chemical formula  $(\text{OH})_3\text{Al}_2\text{O}_3\text{SiOH}$  [7], occurring as single walled nanotubes (NTs) with  $\text{Al}(\text{OH})\text{Al}$  and  $\text{Al}-\text{O}-\text{Al}$  groups at the outer surface, and silanols ( $\text{SiOH}$ ) at the inner one. Subject of this study is instead the catalytic behavior of the hybrid organic/inorganic analogue of imogolite, i.e. methyl-imogolite (MeIMO), along with that of novel Fe-doped MeIMO obtained by ionic exchange and of the phases stemming by the thermal collapse of NTs.

MeIMO NTs (chemical formula  $(\text{OH})_3\text{Al}_2\text{O}_3\text{SiCH}_3$ ) have an inner (hydrophobic) surface lined by  $\text{SiCH}_3$  groups (Figure 1) [8], and an outer surface resembling that of imogolite. In the dry powder, NTs form bundles with hexagonal packing, giving rise to three kinds of pores and related surfaces (Figure 1). In MeIMO, intra-tube pores (A) have  $\cong 2.0$  nm diameter; inter-tube pores (B) among three aligned NTs in a bundle have ca. 0.45 nm diameter and larger C mesopores are disordered slit-pores occurring among bundles.

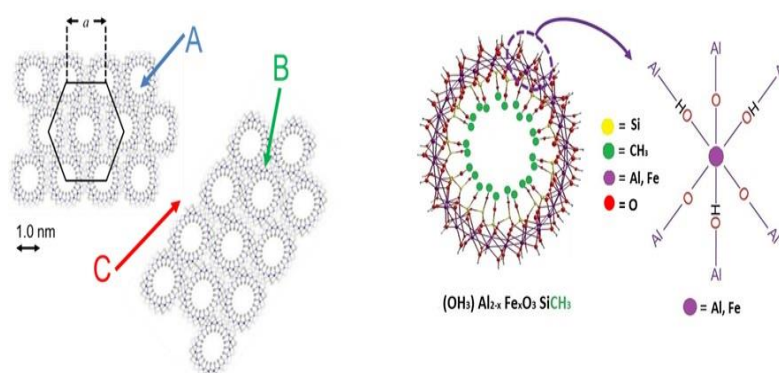


**Figure 1:** (left) Representation of two bundles of hexagonally packed MeIMO NTs; (right) frontal view of a single-walled MeIMO NT exposing Si-CH<sub>3</sub> groups at the inner surface and Al(OH)Al and Al-O-Al groups at the outer surface

So far, no specific study has been devoted to Fe-doped MeIMO NTs, nor to their application as heterogeneous catalysts in the degradation of TRZ. Shafia *et al.* obtained Fe-doped imogolite NTs by both direct synthesis and post-synthesis ionic exchange [9]. Doping Fe in imogolite NT structure decreases the band gap ( $E_g$ ) of imogolite, an insulator with  $E_g = 4.9$  eV, to 2.4-2.8 eV in Fe-doped NTs that ultimately show semiconducting properties [10].

In this work, Fe-doping was obtained by ionic exchange of preformed MeIMO NTs. Two Fe contents were considered: 0.7 and 1.4 wt. % Fe, as different authors agree that Fe may isomorphically substitute for Al up to 1 wt. %, whereas at Fe loadings as high as 1.4 wt. % Fe oxo-hydroxide clusters formation occurs along with IS, NTs formation being instead hindered at higher loadings [10].

A further aspect considered in the present paper was the catalytic activity of the structure stemming from NTs thermal degradation: previous work showed that after thermal treatment at 773 K MeIMO NTs collapse into a buckled structure, which retains high surface area and porosity remaining suitable for catalytic purposes [11]. The photocatalytic activity of such collapsed phases was also addressed in this paper. After MeIMO NTs thermal collapse, the Al coordination changes from octahedral to both tetrahedral and pentacoordinated Al [11], which could lead to the formation of more reactive Al-OOH groups, whereas the new environment surrounding Fe in the collapse phase is expected to affect its photo-Fenton performance, when the material is exposed to H<sub>2</sub>O<sub>2</sub> and UV light.



# 4<sup>th</sup> Iran National Zeolite Conference

## Golpayegan University of Technology, Golpayegan, Iran

### August 23-24, 2017



#### References

1. Lata, H., Garg, V.K., and Gupta, R.K., (2008), Adsorptive removal of basic dye by chemically activated Parthenium biomass: equilibrium and kinetic modeling. *Desalination*. 219: pages 250-261.
2. Wawrzekiewicz, M. and Hubiki, Z., (2009), Kinetic studies of dyes sorption from aqueous solutions onto the strongly basic anion-exchanger Lewatit MonoPlus M-600. *Chemical Engineering Journal*. 150.
3. Koenderink, G.H., Kluijtmans, S.G.J.M., and Philipse, A.P., (1999), On the Synthesis of Colloidal Imogolite Fibers. *Journal of Colloid and Interface Science*. 216: pages 429-431.
4. MacKenzie, K.J.D., Bowden, M.E., Brown, I.W.M., and Meinhold, R.H., (1989), Structure and Thermal Transformations of Imogolite Studied by <sup>29</sup>Si and <sup>27</sup>Al High-Resolution Solid-State Nuclear Magnetic Resonance. *Clays and Clay Minerals*. 37: pages 317-324.
5. Guimarães, L., Enyashin, A.N., Frenzel, J., Heine, T., Duarte, H.A., and Seifert, G., (2007), Imogolite Nanotubes: Stability, Electronic, and Mechanical Properties. *ACS Nano*. 1: pages 362-368.
6. Ookawa, M., (2012), Synthesis and Characterization of Fe-Imogolite as an Oxidation Catalyst. *Clay Minerals in Nature - Their Characterization, Modification and Application*. InTech.
7. Yoshinaga, N. and Aomine, S., (1962), Imogolite in some ando soils. *Soil Science and Plant Nutrition*. 8: pages 22-29.
8. Bottero, I., Bonelli, B., Ashbrook, S.E., Wright, P.A., Zhou, W., Tagliabue, M., Armandi, M., and Garrone, E., (2011), Synthesis and characterization of hybrid organic/inorganic nanotubes of the imogolite type and their behaviour towards methane adsorption. *Phys Chem Chem Phys*. 13: pages 744-50.
9. Shafia, E., Esposito, S., Armandi, M., Bahadori, E., Garrone, E., and Bonelli, B., (2015), Reactivity of bare and Fe-doped aluminosilicate nanotubes (imogolite) with H<sub>2</sub>O<sub>2</sub> and the azo-dye Acid Orange 7. *Catalysis Today*.
10. Shafia, E., Esposito, S., Armandi, M., Manzoli, M., Garrone, E., and Bonelli, B., (2016), Isomorphic substitution of aluminium by iron into single-walled aluminosilicate nanotubes: A physico-chemical insight into the structural and adsorption properties of Fe-doped imogolite. *Microporous and Mesoporous Materials*. 224: pages 229-238.
11. Zanzottera, C., Vicente, A., Armandi, M., Fernandez, C., Garrone, E., and Bonelli, B., (2012), Thermal Collapse of Single-Walled Aluminosilicate Nanotubes: Transformation Mechanisms and Morphology of the Resulting Lamellar Phases. *The Journal of Physical Chemistry C*. 116: pages 23577-23584.

## Zeolite as an efficient molecular sieve for improvement of catalyst performance in photocatalytic processes

Masoumeh Khatamian\*

<sup>a</sup>Department of Inorganic Chemistry, Faculty of Chemistry, University of Tabriz, Tabriz, Iran.

\*Email: : Khatamian@tabrizu.ac.ir

Zeolites represent an interesting and extreme test case for replication strategies; because the dimensions of their cages and channels are quite similar to those of the organic polymers. Zeolites are hydrated aluminosilicate minerals made from interlinked tetrahedra of alumina (AlO<sub>4</sub>) and silica (SiO<sub>4</sub>). In simpler words, they're solids with a relatively open, three-dimensional crystal structure built from the elements aluminum, oxygen, and silicon, with alkali or alkaline-Earth metals (such as sodium, potassium, and magnesium) plus water molecules trapped in the gaps between them.





# 4<sup>th</sup> Iran National Zeolite Conference

## Golpayegan University of Technology, Golpayegan, Iran

### August 23-24, 2017



Zeolites are widely used as ion-exchange beds in domestic and commercial water purification, softening, and other applications. In chemistry, zeolites are used to separate molecules (only molecules of certain sizes and shapes can pass through), and as traps for molecules so they can be analyzed.

In our recent researches, it can be distinguished that one of the conventional methods for enhancing the activity of a nano semiconductor as a photocatalyst is to use an efficient support material such as metalosilicates (isomorphous substitution of metal ion as Fe, Cr, B, Mn and ... for aluminum in zeolite framework), which can increase its effective surface area; metalosilicate as a support, can offer a very high surface area and also provides an effective and homogenous dispersion of semiconductor particles on the external surface or within the pores of its structure. Moreover, the metalosilicate structure with electron-accepting and donating properties can play an important role in the control of charge transfer processes. Furthermore the strong electrostatic field present in the metalosilicate framework can effectively separate the electrons and holes produced during photo-excitation of nano semiconductor and so resulted in lower recombination of them and higher photodegradation efficiency. According to the results, it can be observed that in the case of supporting nano semiconductors on metalosilicates the efficiency of the photocatalysts increase significantly for semiconductor nano particles as well as the band gap width of the semiconductor change. Thus using metalosilicates leads to an improvement the photocatalytic activity of the prepared semiconductor nanoparticles.

#### References

1. Khatamian, M., Fazayeli, M., & Divband, B. (2014). Preparation, characterization and photocatalytic properties of polythiophene-sensitized zinc oxide hybrid nanocomposites. *Materials Science in Semiconductor Processing*, 26, 540-547.
2. Khatamian, M., Hashemian, S., Yavari, A., & Saket, M. (2012). Preparation of metal ion (Fe 3+ and Ni 2+) doped TiO 2 nanoparticles supported on ZSM-5 zeolite and investigation of its photocatalytic activity. *Materials Science and Engineering: B*, 177(18), 1623-1627.
3. Khatamian, M., Hashemian, S., & Sabaee, S. (2010). Preparation and photo-catalytic activity of nano-TiO 2-ZSM-5 composite. *Materials Science in Semiconductor Processing*, 13(3), 156-161.
4. Khatamian, M., Divband, B., & Jodaei, A. (2012). Degradation of 4-nitrophenol (4-NP) using ZnO nanoparticles supported on zeolites and modeling of experimental results by artificial neural networks. *Materials Chemistry and Physics*, 134(1), 31-37
5. Khatamian, M., Alaji, Z., & Khandar, A. A. (2011). Synthesis and characterization of polycrystalline ZnO/HZSM-5 nanocomposites. *Journal of the Iranian Chemical Society*, 8, S44-S54.
6. Khatamian, M., & Alaji, Z. (2012). Efficient adsorption-photodegradation of 4-nitrophenol in aqueous solution by using ZnO/HZSM-5 nanocomposites. *Desalination*, 286, 248-253.

## Applications of Zeolites in Nano Medicine

Baharak Divband \*

*Research Center for Pharmaceutical Nanotechnology, Tabriz University of Medical Sciences, Tabriz, Iran.*

*\*Email: divband@tabrizu.ac.ir*

#### Abstract

A particular structural feature of zeolites relative to other aluminosilicate materials, and other crystalline materials in general, is the existence of channels and/or cavities linked by channels. One of the characteristics that distinguishes



# 4<sup>th</sup> Iran National Zeolite Conference

## Golpayegan University of Technology, Golpayegan, Iran

### August 23-24, 2017



zeolites from other porous materials is their variety of pore sizes and shapes. The size and shape of channels/cavities in zeolites therefore define the structural parameters of a given type of zeolite. The basic structure of zeolites is biologically neutral. Zeolites can have water as part of their structure; after the water has been driven off by heating, the basic framework structure is left intact. Subsequently, other solutions can be put through the structure, and thus the zeolite acts as a delivery system for the new fluid. This process has been exploited and applied in medicine [1]. They are biocompatible and are used as safe oral magnetic resonance imaging (MRI) contrast agents [2].

Examples demonstrate that different zeolites can be exchanged with cations, functionalized or loaded with drug molecules for specific biomedical applications. Different parameters were varied such as aluminum content in the zeolite, effect of distribution of functional groups and the method of surface modification. Controlled release in zeolites has been achieved through modifying the external surface of the zeolites with functional groups. The release is controlled by a number of factors such as the pore size, the nature of the grafted functional groups, and the nature of intermolecular interactions. By changing the physicochemical properties of the host materials we can change the nature of interactions of the guest (drug) molecules and as a result of which we have better control over the loading and release properties of drug molecules in these materials [3]. Drug delivery systems are basically classified based on their release mechanism and the method of their preparation. The different types of drug delivery systems include; (a) physical systems such as porous monoliths and biodegradable systems, (b) chemical systems which involve the immobilization of the drug molecules, and (c) biological systems which include gene therapy [4, 5].

Exploring the possibility of using zeolites in tissue engineering scaffolds is a potential approach in regenerative medicine because of their biocompatibility and other properties mentioned before. Tissue engineering scaffolds are porous structures fabricated from synthetic and naturally derived biodegradable polymers which serve as transitory artificial extracellular matrix that promotes cell attachment and 3 dimensional (3D) tissue formation. Zeolites in 3D porous scaffolds allow high cell seeding density for dermal tissue growth and diffusion of nutrients and waste products from the cells [6]. Wound infections are caused due to invasion of injured tissues by microorganisms that trigger body's immune system, induce inflammation, tissue damage and impede the healing process [7].

There are several examples of biomedical applications of zeolites reported in the literature including imaging, wound treatment, and drug delivery.

## References

- [1] M. Khatamian, B. Divband, F. Farahmand-zahed, *Materials Science and Engineering C*, 2016, 66, 251–258.
- [2] Z. Atashi, B. Divband, A. Keshtkar, M. Khatamian, F. Farahmand-Zahed, A. Kiani Nazarloo, N. Gharehaghaji. *Journal of magnetic and magnetism materials*, 2017.
- [3] G. Mittal, M. N. V. R. Kumar, *Journal of Pharmaceutical Sciences* 2009, 98, 3730.
- [4] J. L. Vivero-Escoto, I. I. Slowing, B. G. Trewyn, V. S.-Y. Lin, *Small*. 2010, 6(18), 1952–1967.
- [5] R. Amorim, N. Vilaça, O. Martinho, R. M. Reis, M. Sardo, J. Rocha, A. M. Fonseca, F. Baltazar and I. C. Neves, *J. Phys. Chem. C*, 2012, 116, 25642–25650.
- [6] N. Ninan, Y. Grohens, A. Elain, N. Kalarikkal, S. Thomas, *European Polymer Journal*, 2013, 49, 2433–2445.
- [7] N. Ninan, M. Muthiah, N. A. Bt. Yahaya, et al. *Colloids and Surfaces B: Biointerfaces*, 2014, 115, 244–252.



4<sup>th</sup> Iran National Zeolite Conference  
Golpayegan University of Technology, Golpayegan, Iran  
August 23-24, 2017



**Zeolite 4A; General Properties and Applications in Detergent Industry – BEHDASH Experience**

Vahid Ameri Dehabadi <sup>a\*</sup>, Hodjat Hakkakpour <sup>b</sup>, Davoud Abedi Amoli <sup>c</sup>

<sup>a</sup> Deputy Director of Research & Development, Behdash Chemical Co., Vard Avarid Blvd, 19th km Karaj Makhsous Rd, Tehran, Iran, Postal Code: 13981-63171

<sup>b</sup> Plant Manager of Inorganic Products, Behdash Chemical Co., Mahd – e – Taje Group.

<sup>c</sup> CEO, Behdash Chemical Co., Mahd – e – Taje Group.

\*Email: [yahid.ameri@mahdetaje.com](mailto:yahid.ameri@mahdetaje.com)

### Abstract

Detergent powders are consisting of several chemicals, including surfactants, special functional materials and builders, as well. For almost all types of detergents applications builders are of major importance, in which in terms of production volume sodium-A-Type zeolites is one of the most important builders in household and laundry washing products.

Providing a fast and efficient softening of water of the wash liolitequor under a wide range of performance conditions (usually in combination with acrylic-maleic copolymers) is the main function of A-type zeolites, which is carried out by rapidly exchanging sodium ions of heavy water. Ze 4A is the alternative of STTP (sodium tripolyphosphate), which its usage in detergent industry has been already banned due to its potential environmental and human health hazards. Behdash Chemical Co. was the first company in Iran, which installed and launched the complete line of zeolite 4A plant with capacity of 40,000 ton/year.



4<sup>th</sup> Iran National Zeolite Conference  
Golpayegan University of Technology, Golpayegan, Iran  
August 23-24, 2017



# Lectures



4<sup>th</sup> Iran National Zeolite Conference  
Golpayegan University of Technology, Golpayegan, Iran  
August 23-24, 2017



**Preparation and characterization of 4-aminopyridine-functionalized zeolite-HY and application as a basic nanocatalyst in the synthesis of polyhydroquinolines**

Mahdia Hmidinasab,<sup>a</sup> Mojgan Zendehtdel,<sup>a</sup> Mohammad Ali Bodaghifard<sup>a,b,\*</sup>

<sup>a</sup> Department of Chemistry, Faculty of Science, Arak University, Arak, 38156-88349, Iran

<sup>b</sup> Institute of Nanosciences & Nanotechnology, Arak University, Arak, Iran

\*Email: m-bodaghifard@araku.ac.ir

## 1. Introduction

Combining inorganic and organic material is of interest for various applications, including catalysis, separation, and adsorption agents [1-4]. For catalysis, many kinds of organic acid and alkali were functionalized on various support materials such as amine compound-MCM-41, amine compound-SBA-15, carboxylic acid MCM-41, carboxylic acid-SBA-15,[5] and sulphonic acid-SBA-15 [6]. Zeolitic material, a crystalline aluminosilicate mineral, was more interesting than silica for functionalized support due to its large surface area, high chemical and thermal stability, and pore diameter that is selective to small organic molecules. Moreover, zeolite Y had a great density of silanol groups (Si-OH), potentially allowing a high density of functional groups to be attached.

1,4-dihydropyridyl compounds have various pharmaceutical and biological activities [7]. Thus development of a simple and efficient method for preparation of PHQ derivatives is an active research area, and there is a scope for further improvement involving milder and less hazardous reaction conditions.

In this study, the preparation and characterisation of a basic catalyst with functionalized pyridine moiety on zeolite HY was introduced. The zeolite HY was functionalized with 4-aminopyridine compound and its catalytic activity was investigated in the synthesis of polyhydroquinoline derivatives.

## 2. Experimental

### *Preparation of the 4-Aminopyridine-Functionalized Zeolite Y:*

In preparation, the zeolite HY (1 g) was suspended in 30 mL of anhydrous toluene at a temperature of 110 °C for 30 min. Then, the required amount of the respective 3-chloropropyltrimethoxy silane was added to the mixture and stirred for the desired reaction time (12 h) under reflux conditions. The mixture was then cooled and the solid portion was separated by filtration. 1 gr pre-treated zeolite HY was suspended in 30 mL of anhydrous toluene and reacted with 1 gr 4-aminopyridine in the presence of 1 mL triethylamine under nitrogen atmosphere and reflux condition for 12 h. The mixture was then cooled and the solid portion was separated by filtration. The aminopyridine-functionalized zeolite was dried at 100 °C in an oven for 12 h.

### *Characterization of the Functionalized Zeolite Y:*

Fourier transform infrared (FT-IR) spectroscopy, field emission scanning electron microscopy (FE-SEM), energy dispersive X-ray spectroscopy (EDS), X-ray diffraction (XRD), thermo-gravimetric analysis (TGA) were used to identify and characterize the prepared catalyst. The concentration of amino groups in the fresh catalyst and each cycle of spent catalyst was quantified by back-titration.

### *General Procedure for the Synthesis of polyhydroquinolines*

A mixture of aldehyde (1.0 mmol), dimedone or 1,3-cyclohexanedione (1.0 mmol), ethyl acetoacetate (1.0 mmol), ammonium acetate (2.0 mmol), and aminopyridine-functionalized zeolite (0.05 gr) was heated at 80 °C for an



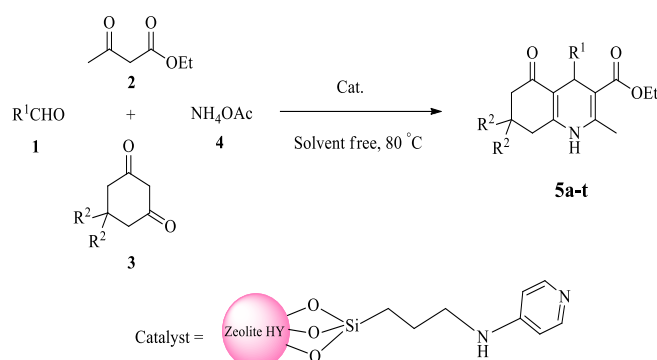
4<sup>th</sup> Iran National Zeolite Conference  
Golpayegan University of Technology, Golpayegan, Iran  
August 23-24, 2017



appropriate time (TLC). The resulting solid product was treated with hot ethanol and then filtered. The filtrate was concentrated to afford the crude product. The pure product was obtained by recrystallization from absolute ethanol.

### 3. Results and discussion

After optimization of the reaction condition, the generality of the present protocol investigated which found that is equally effective for aromatic, unsaturated, and heterocyclic aldehydes and more than 20 derivatives have been synthesized (Scheme 1). Moreover, the experimental procedure is very simple, and there was no undesirable side product.



**Scheme 1.** 4-Aminopyridine-functionalized zeolite HY efficiently catalyzed the synthesis of polyhydroquinolines.

### 4. Conclusions

In conclusion, we have demonstrated that the four-component Hantzsch reaction can effectively synthesize PHQ derivatives with the promotion of a functionalized zeolite as a novel basic organic-inorganic hybrid nanocatalyst, which provides a simple and efficient method. Mild reaction conditions, high yields, generality, and simplicity of the procedure, stability and reusability of the catalyst, and avoidance of using harmful organic solvents are features of this new protocol.

### Acknowledgments

We acknowledge the financial support from Research council of Arak University.

### References

- [1] S. Hamoudi, A. El-Nemr, M. Bouguerra, K. Belkacemi, *Can. J. Chem. Eng.*, **2012**, *90*, 34.
- [2] V. V. Guerrero, D. F. Shantz, *Ind. Eng. Chem. Res.*, **2009**, *48*, 10375.
- [3] W. Xie, L. Zhao, *Fuel*, **2013**, *103*, 1106.
- [4] K. F. Yee, J. C. S. Wu, K. T. Lee, *Biomass Bioenerg.*, **2011**, *35*, 1739.
- [5] S. Sumiya, Y. Kubota, Y. Oumi, M. Sadakane, T. Sano, *Appl. Catal. A. Gen.*, **2010**, *372*, 82.
- [6] G. M. Ziarani, N. Lashgari, A. Badiei, *J. Mol. Catal. A. Chem.*, **2015**, *397*, 166.
- [6] H. Nakayama, Y. Kanaoka, *Heterocycles*, **1996**, *42*, 901.



# 4<sup>th</sup> Iran National Zeolite Conference Golpayegan University of Technology, Golpayegan, Iran August 23-24, 2017



## Mesoporous SiO<sub>2</sub> immobilized HClO<sub>4</sub> for synthesis of DHPMs and DHPs Heterocycles

Sadegh Rostamnia \*

Organic and Nano Group (ONG), Department of Chemistry, Faculty of Science, University of Maragheh, P.O.B 55181-83111, Maragheh, Iran

\*Email: srostamnia@gmail.com; rosamnia@maragheh.ac.ir

### 1. Introduction

Recently, ordered mesoporous silica of SBA-15 has emerged as a catalyst in various organic transformations, especially when low amount of catalyst loading of the catalyst are used [1-3]. Based on our interest in multicomponent reactions [4-6], in this respect, we are used a neat heterogeneous and reusable catalytically ordered mesoporous silica supported perchloric acid (SBA-15/HClO<sub>4</sub>) mediate for ring-opening reaction of diketene6 in presence of alcohols and aldehydes for preparation of the DHPMs and DHPs heterocycles via urea and ammonium acetate as nucleophile, respectively (Figure 1). The neat approach, simplicity and variability in derivatives of the present four-component procedure makes it an interesting alternative to three-component usual approaches.

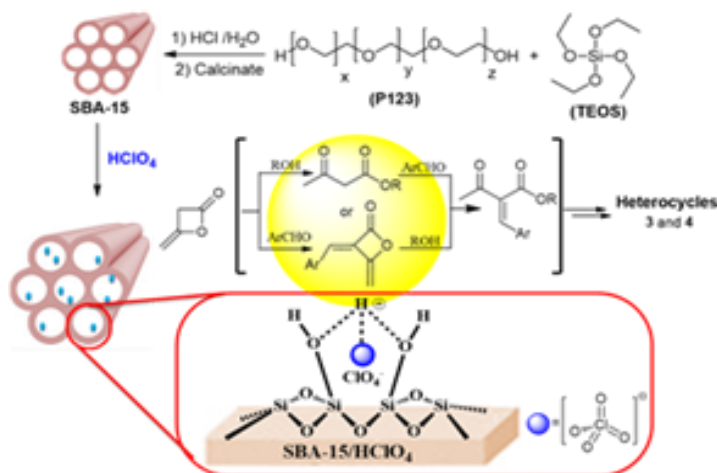


Fig 1. SBA-15/HClO<sub>4</sub> catalyzed synthesis of DHPMs and DHPs.

### 2. Experimental

#### Chemicals and apparatus

All reagents were obtained from Merck (Germany) and Fluka (Switzerland) and were used without further purification. Melting points were measured on an Electrothermal 9100 apparatus. Progress of reactions was monitored by Thin Layer Chromatography (TLC). <sup>1</sup>H and <sup>13</sup>C NMR spectra were measured (CDCl<sub>3</sub>) with a Bruker DRX-300 AVANCE spectrometer at 300 and 75 MHz, respectively.

#### Mesoporous silica supported HClO<sub>4</sub>



4<sup>th</sup> Iran National Zeolite Conference  
Golpayegan University of Technology, Golpayegan, Iran  
August 23-24, 2017



For synthesis of SBA-15, in a typical synthesis batch, triblock copolymer surfactant as a template (P123, 4.0 g) was dissolved in 30 mL of H<sub>2</sub>O and 120 g of 2 M HCl solution. Then, TEOS (9 g) was added to reaction mixture which was stirred for 8 h at 40 °C. The resulting mixture was transferred into a Teflon-lined stainless steel autoclave and kept at 100 °C for 20 h. After cooling down to room temperature, the product was filtered, washed with water and dried overnight at 70 °C in air. After that, the as-synthesized sample was calcinated at 550-600 °C for 6 h to remove the template. Then, the calcinated SBA-15 (1 g) was functionalized by perchloric acid (HClO<sub>4</sub>) in toluene (2 mmol) under reflux conditions for 24 h. Finally to achieve the SBA-15/HClO<sub>4</sub> the extra HClO<sub>4</sub> was then washed and the solid was dried at 55-60 °C.

*General procedure for the synthesis of DHPMs and DHPs*

equivalent amount of neat adduct diketene, alcohol in excess amount of equivalent, and aldehyde in SBA-15/HClO<sub>4</sub> (10 mol%) for 10 min at reflux condition, NH<sub>4</sub>OAc or urea was added, and then heated in neat state with stirring in refluxing condition, for an appropriate time (table 1 and 2). The reaction was cooled to room temperature and the solid was washed with cooled water, petroleum ether/ether. All the products were previously reported by three-component method [2 and 3] and were characterized by comparing physical data with those.

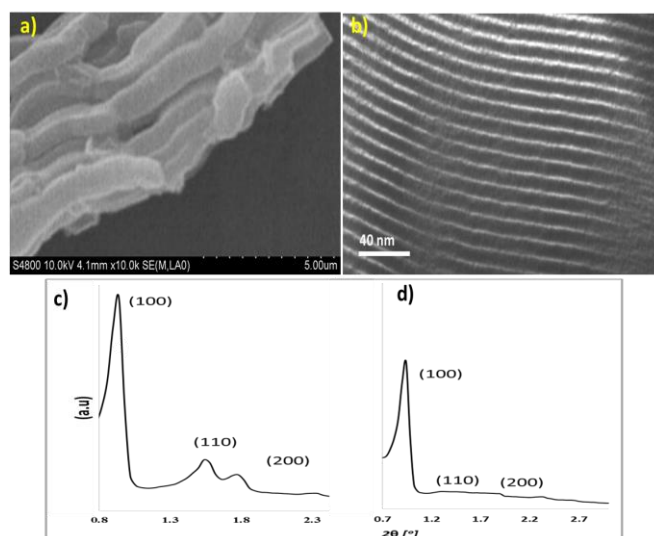


**Fig. 1.** SEM (a) and TEM (b) images SBA-15/HClO<sub>4</sub>. XRD patterns of SBA-15/HClO<sub>4</sub>: (c) newly prepared; (d) used 10 times.

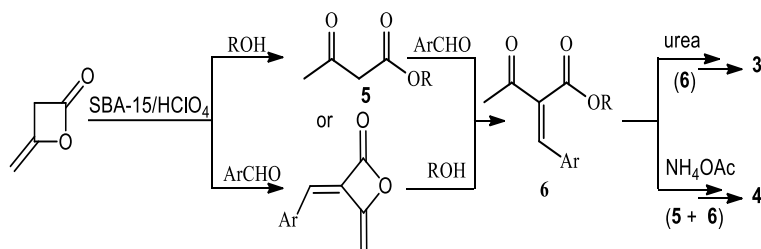
### 3. Results and discussion

The use of SBA-15/HClO<sub>4</sub> (Figure 1) has received considerable attention as a heterogeneous and recyclable catalyst to afford the corresponding products in excellent yields. Our study is based on the use of diketene as an in situ source of various  $\beta$ -ketoesters in the four-component synthesis of dihydropyrimidinones and dihydropyridines (Scheme 1). Solid acid catalyst can be easily prepared from the readily available ingredients, perchloric acid and silica source TEOS.





4<sup>th</sup> Iran National Zeolite Conference  
Golpayegan University of Technology, Golpayegan, Iran  
August 23-24, 2017

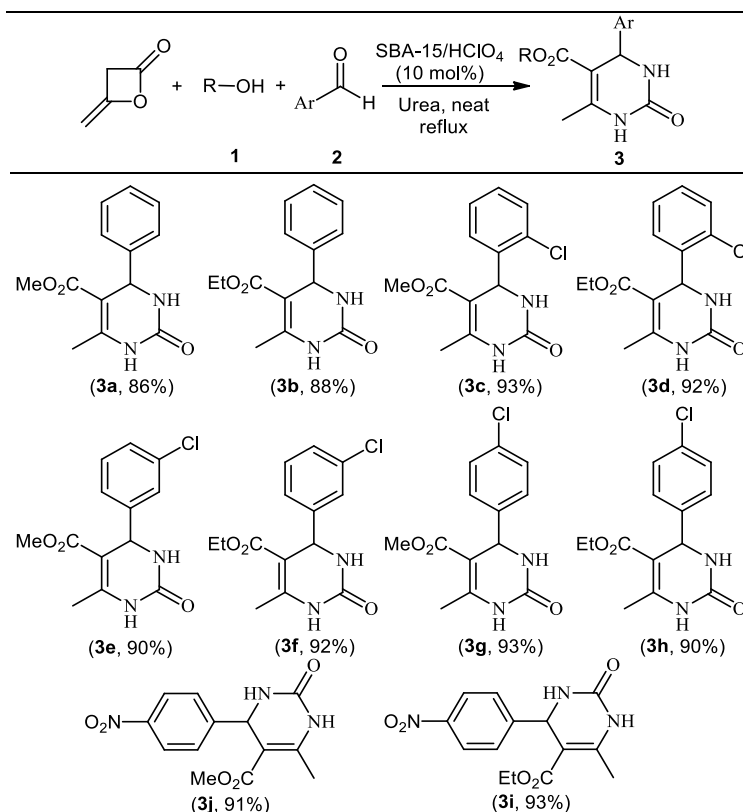


Scheme 1. Four-component synthesis of DHPMs and DHPs by SBA-15/HClO<sub>4</sub> catalyst.

The reaction of diketene, arylaldehydes 1, and alcohols 2, with urea in the presence of a catalytically amount of SBA-15/HClO<sub>4</sub> undergoes a Biginelli-type cyclocondensation reaction at reflux to produce 3,4-dihydropyrimidin-2(1H)-one derivatives 3 in 86-93% yields (Table 1).

1,4-dihydropyridine products 4 afforded in good yields with ammonium acetate. The results are summarized in Table 2. A possible explanation on the mechanism of these reactions is proposed in Scheme 2. On the basis of the established chemistry of diketene, it is reasonable to assume that the 3,4-dihydropyrimidinones and 1,4-dihydropyridines apparently result from the initial addition of the alcohol or aldehyde to diketene to generation  $\beta$ -dicarbonyl 5 and unsaturated adduct 6 under acidic and refluxing conditions, followed by Biginelli-type and Hantzsch-type conditions. These in situ generated intermediates under the reaction conditions give the corresponding 3,4-dihydropyrimidinones and 1,4-dihydropyridines derivatives (Tables 1 and 2).

Table 1: SBA-15/HClO<sub>4</sub> catalyzed Biginelli-type condensation.





# 4<sup>th</sup> Iran National Zeolite Conference

## Golpayegan University of Technology, Golpayegan, Iran

### August 23-24, 2017



### Conclusions

In summary, un-covalently functionalization of perchloric acid onto the ordered mesoporous silica (SBA-15/HClO<sub>4</sub>) as a inexpensive heterogeneous, green and reusable catalyst for ring-opening diketene-based heterocycles skeleton synthesis is successfully achieved. A variety of annulated DHPMs and DHPs are accessible using this method, that this solid acidic catalytic procedure based on neat conditions, is highly preparative in nature of unreusable homogenous methods, avoids the use of expensive catalyst and solvents or other additives. This rapid, green and reusable four-component method should be an interesting alternative to the application of other three-component synthetic method. In other hand, one-pot entry into the synthesis of DHPM and DHP heterocycles of potential synthetic and pharmaceutical interest.

The recycling possibility and ability of the SBA-15/HClO<sub>4</sub> catalyst, the preparation of the 3h and 4g as model reactions was studied. During this study, in the end of reaction completion (Table 1 and 2), the catalyst was easily separated from the product by centrifuged. As indicate in Figure 2, which clearly demonstrates the practical recyclability of this catalys.

**Table 2:** SBA-15/HClO<sub>4</sub> catalyzed Hantzsch-type condensation.

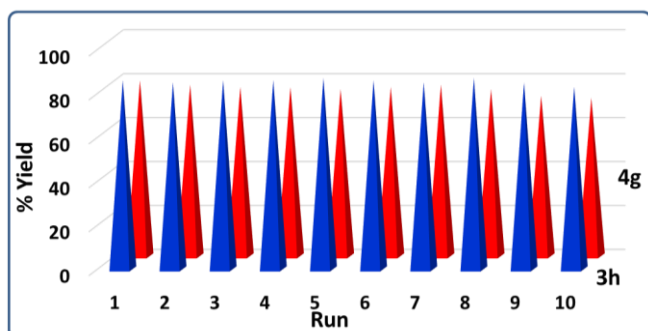
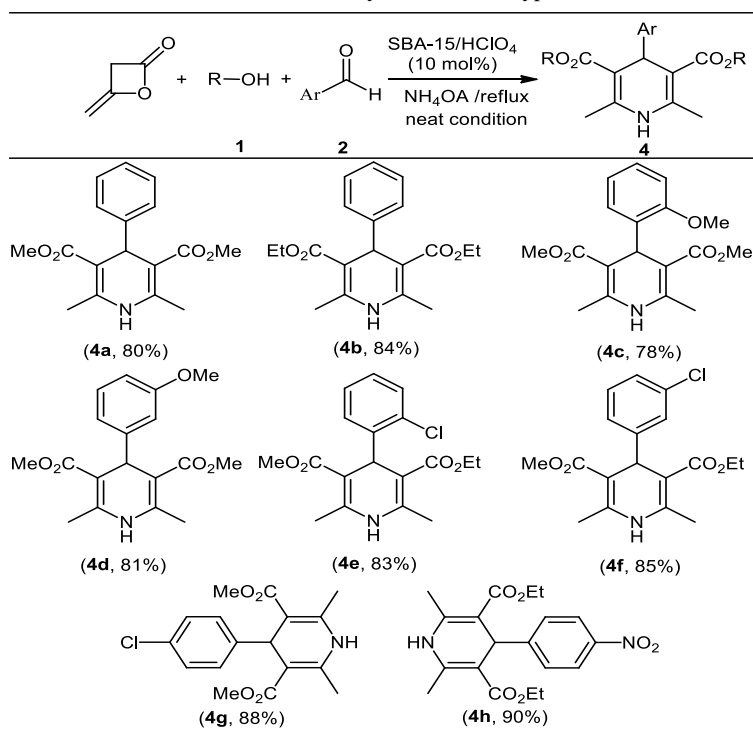


**Fig 2.** Recyclability study of SBA-15/HClO<sub>4</sub> in synthesis of 3h and 4g.



4<sup>th</sup> Iran National Zeolite Conference  
Golpayegan University of Technology, Golpayegan, Iran  
August 23-24, 2017



## References

1. Q. Yang, M. Kapoor, N. Shirokura, M. Ohashi, S. Inagaki, J. N. Kondo, K. Domen, *J. Mater. Chem.*, 15, **2005**, 666-673.
2. Q. Yang, M. Kapoor, S. Inagaki, N. Shirokura, J. N. Kondo, K. Domen, *J. Mol. Catal. A: Chemical*, 230, **2005**, 85-89.
3. B. Karimi, M. Vafaezadeh, *Chem. Commun.*, **2012**, 3327-3329.
4. Rostamnia, S.; Lamei, K. *Synthesis* **2011**, 3080.
5. S. Rostamnia, H. Xin, X. Liu, K. Lamei, *J. Mol. Catal. A: Chem.* **2013**, 374-375, 85.
6. Rostamnia, H. Xin, *Appl. Organomet. Chem.* **2013**, 27, 348

## Preparation, characterization and application of SO<sub>3</sub>H@zeolite-Y as a high efficient nano-catalyst for rapid and facile synthesis of perimidine derivatives

Mehdi Kalhor<sup>a\*</sup>, Raheleh Gaeini<sup>a</sup>, Bahar Molaei<sup>a,b</sup>

<sup>a</sup> Department of Chemistry, Payame Noor University, 19395-4697, Tehran, Iran

<sup>b</sup> Young Researchers and Elite Club, Shahr-e-Qods Branch, Islamic Azad University, Tehran, Iran

\* E-mail: mekalhor@pnu.ac.ir

### 1. Introduction

The zeolite can act as a catalyst, Lewis and Brønsted acid, as well as an oxidizing agent. One of the significant properties allowing zeolites to act as catalysts is their ability to exchange cations without decomposing the crystalline structure [1]. Also, the use of solid heterogeneous catalysts in organic synthesis and industrial chemical manufacture, is interesting, remarkable and increasing [2]. They have many advantages such as thermal stability, persistence in all organic solvents, low cost handling, nontoxic and environmentally safe. In recent decades, there has been special attention in the application of solid acids as a catalyst for a variety of organic reactions [3].

Perimidines [4] are tricyclic heterocycles containing a dihydropyrimidine ring *ortho* and peri-fused to the naphthalene structure. These heterocyclic systems, which have been shown to be interesting candidates for biological studies, are widely applied in industry, agriculture, and medicine [5]. Because of their importance, several methods have been reported for synthesis of these compounds, including reaction of 1,8-diaminonaphthalene with the carbonyl groups. However, despite their potential utility, these methods suffer from one or more disadvantages. Thus, there is still much demand for alternative synthetic routes to perimidine derivatives. For these reasons, and as a part of our research interest in the development of new methods for the synthesis of heterocyclic compounds [6,7], we report a clean and facile synthetic procedure for preparation of 2-substituted 2,3-dihydro-1H-perimidines, using SO<sub>3</sub>H@zeolite-Y as an efficient nano-catalyst.

### 2. Experimental

#### Preparation of nano SO<sub>3</sub>H@zeolite-Y



4<sup>th</sup> Iran National Zeolite Conference  
Golpayegan University of Technology, Golpayegan, Iran  
August 23-24, 2017



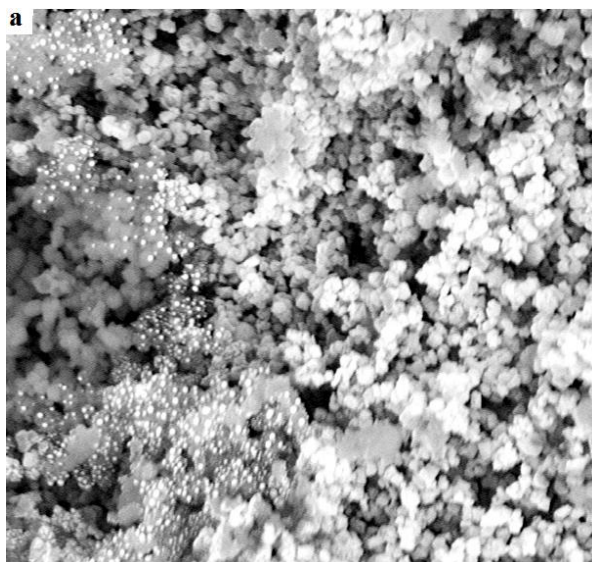
0.192g of chlorosulphonic acid was added dropwise during 30 min under nitrogen atmosphere to 2.0 g NaY zeolite in a 150-mL flask. After adding all of the chlorosulphonic acid, the reaction mixture was stirred for another 30 min under nitrogen atmosphere. Then the solution was filtered and washed with water to remove the unreacted chlorosulphonic acid. Finally, the white solid powder of SO<sub>3</sub>H/zeolite-Y was obtained.

**The procedure for preparation of 2-aryl perimidines:**

To a solution of 1,8-diaminonaphthalene (0.05g) in ethanol (2 mL), the appropriate aromatic aldehyde and nano SO<sub>3</sub>H@zeoliteY (0.0025 g) were added. Reaction mixture was stirred at room temperature for desired time. After completion of the reaction, the catalyst was isolated by filtration. The precipitated product was isolated by filtration, washed with water–ethanol (80:20), and air dried.

**3. Results and discussion**

First, nano-SO<sub>3</sub>H/zeolite-Y (NSZ) was prepared in our laboratory by use of a previously reported procedure. The scanning electron microscopy (SEM) image of the SO<sub>3</sub>H-Y zeolite nano-particles is shown in (Fig. 1, a). The particles size was mainly about 65-85 nm. In the Energy Dispersive X-ray (EDX), Peak appeared in the region of 2.3 eV confirmed the presence of sulfur atom deposited on zeolite, respectively (Fig. 1, b). In the next step, to obtain the optimal method conditions, the effect of solvent, the amount of efficient catalyst on the yield of the reaction were examined.





4<sup>th</sup> Iran National Zeolite Conference  
Golpayegan University of Technology, Golpayegan, Iran  
August 23-24, 2017

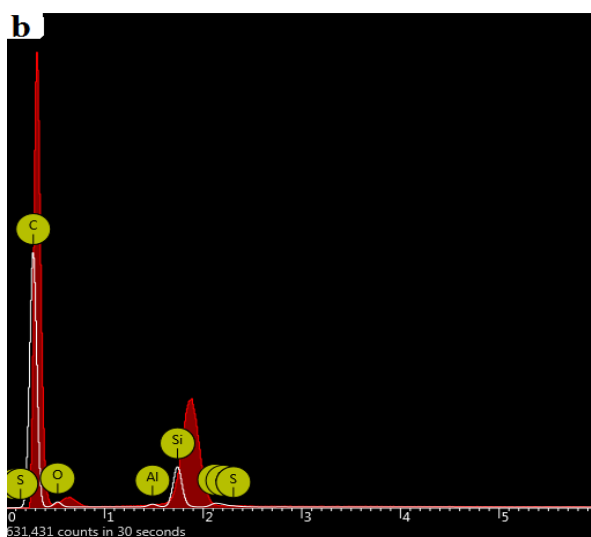
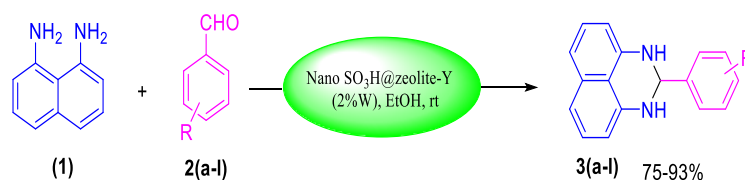


Figure 1. SEM image (a) and EDX spectrum (b) of SO<sub>3</sub>H/Zeolite-Y nanoparticles

2W% of NSZ as the best catalyst, made the highest yield (93%) and EtOH in a model reaction of 4-nitrobenzaldehyde and 1,8-diaminonaphthalene. By generality of this method, the Some 2-aryl perimidines **3a-l** were prepared *via* one-pot reaction by employing 1,8-diaminonaphthalene and various aryl aldehydes under the same conditions (Scheme 1).



Scheme 1. Synthetic method for compounds **3a-l**

For investigation of the reusable of the catalyst, was carried out chosen model reaction, under the same optimized conditions. Then the first reaction filtrated catalyst, recovered by refluxing in ethanol for 4h, drying at oven to 100 °C and reused in subsequent reactions with a small decreasing in activity even after the fourth run.

#### 4. Conclusions

In summary, we successfully used nano-SO<sub>3</sub>H/zeolite- Y as environmental friendly catalyst for easy synthesis 2-aryl perimidines **3a-l** derived from a one-pot condensation reaction of 1,8-diaminonaphthalene and various aryl aldehydes. The attractive features of this procedure are its good conversions, easy workup, inexpensive and recyclable catalyst and short reaction times, making it a useful practical method for the simple synthesis of the target compounds.

#### Acknowledgment

The gratitude of authors goes to the research commute of Chemistry Department of Payame Noor University who provided financial and technical supports for this project.



4<sup>th</sup> Iran National Zeolite Conference  
Golpayegan University of Technology, Golpayegan, Iran  
August 23-24, 2017



## References

- [1] J. Ward, *J. Coll. Int. Sci.* **1968**, 28, 269.
- [2] R.A. Sheldon, R.S. Downing, *Appl. Catal. A*, **1999**, 189, 163.
- [3] V. Sakthivel, S. Thirumeni, P. Kasi, *J. Nanomater.* **2008**, 49, 1818.
- [4] A. F. Pozharskii, V.V. Dalnikovskaya, *Russ. Chem. Rev.* 1981, 50, 816.
- [5] J. M. Herbert, P. D. Woodgate, W. A. Denny, *J. Med. Chem.* **1987**, 30, 2081.
- [6] M. Kalhor, N. Khodaparast, *Res. Chem. Intermed.* **2015**, 41, 3235.
- [7] M. Kalhor, N. Khodaparast, M. Zendehtdel, *Lett. Org. Chem.* **2013**, 10, 573.

## Effect of substituted-hydroxyl groups on porphyrin ring in the photodegradation of 4-Nitrophenol

M. Moosavifar<sup>a\*</sup>, S. Bagheri<sup>a</sup>

<sup>a</sup>Department of Chemistry, Faculty of Science, University of Maragheh, P.O. Box 55181-83111, Maragheh, Iran

\* E-mail: m.moosavifar90@gmail.com

### 1. Introduction

Photodegradation of pollutants is gaining extensive attention from the point of view eco-friendly. TiO<sub>2</sub> is believed to be one of the most active photocatalysts. However, critical drawbacks of TiO<sub>2</sub> are the large band gap and low surface area. Immobilization of TiO<sub>2</sub> on support is a good manner to overcome to these disadvantages. On the other hand, Photosensitized catalysis is the initiation of degradation or transformation reactions of molecules using a combination of light and photoactive materials as catalysts [1,2].

Photodegradation of 4-Nitro phenol was performed in the presence of H<sub>2</sub>O<sub>2</sub> as oxidant reagent. However, H<sub>2</sub>O<sub>2</sub> is an oxidative material and may be have some drawback [3,4].

Motivation above work, Here we wish to report synthesise of the heterogenized functional metalloporphyrin with various number of OH group and investigation of their catalytic activity in the photodegradation of 4-Nitrophenol.

### 2. Experimental Part or Theoretical Details

All materials were of the commercial reagent grade were purchased from Sigma-Aldrich, Merck and Fluka. Photocatalyst was prepared using a related procedure. In a typical procedure, pyrrole, benzaldehyde and para-hydroxy benzaldehyde with various ratio in propionic acid was mixed to obtain functional porphyrin ligand. Then ligand was metalated and finally metallocomplex was synthesized into nanocage of zeolite by zeolite synthesis method. TiO<sub>2</sub> was entered into zeolite cage using impregnation method. The photocatalytic activity of obtained photocatalysts were investigated in the photodegradation of 4-NP.



4<sup>th</sup> Iran National Zeolite Conference  
Golpayegan University of Technology, Golpayegan, Iran  
August 23-24, 2017



### 3. Results and discussion

CeTPP(OH)<sub>n</sub>/NaY/TiO<sub>2</sub> (n=1-4) nanocomposites were prepared into nanocage of Y zeolite. Based on formation of catalyst into zeolite cage, the color of zeolite was changed which proved encapsulation of catalyst inside zeolite cage. The XRD pattern of the photocatalyst indicated that the catalyst has crystallinity almost identical to that of the parent NaY zeolite. This proved metallocomplexes dispersion as fine particles [5]. However, the presence of peaks in the region of TiO<sub>2</sub> improved the insertion of TiO<sub>2</sub> in zeolite cages.

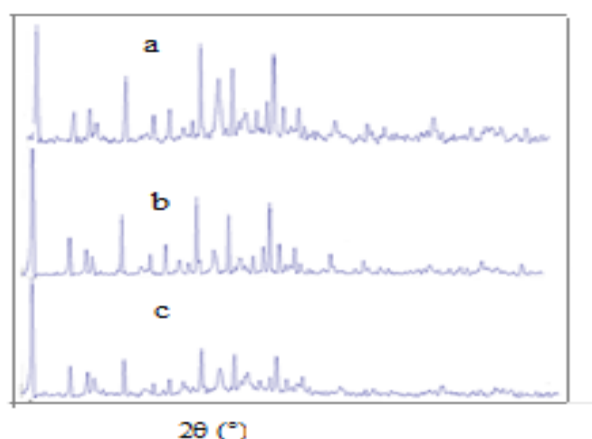


Fig. 1. XRD pattern of a) Ce Di HPP/NaY/ TiO<sub>2</sub> b) Ce Te HPP/HY/TiO<sub>2</sub> c) zeolite Y

The FT-IR of catalysts confirmed the presence of metalloporphyrin and TiO<sub>2</sub> into nanocage of zeolite.

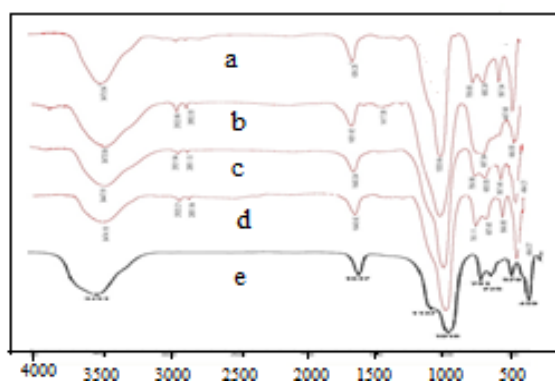


Fig. 2. FTIR spectra a) Ce Mo HPP/ NaY/TiO<sub>2</sub> b) Ce Di HPP/ NaY/ TiO<sub>2</sub> c) Ce Tr HPP/HY/ TiO<sub>2</sub> d) Ce Te HPP / HY/TiO<sub>2</sub> e) zeolite

FESEM of catalyst indicated the cubo-octahedral units that proved upon the formation of complexes into zeolite cage, the morphology is preserved. In addition the presence of species in nanometer size proved the insertion of TiO<sub>2</sub> into pores of zeolite.



4<sup>th</sup> Iran National Zeolite Conference  
Golpayegan University of Technology, Golpayegan, Iran  
August 23-24, 2017

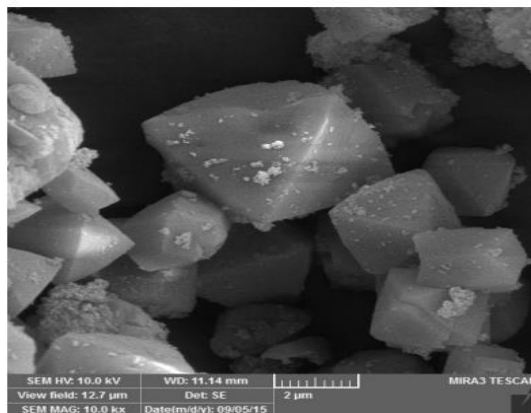


Fig. 3. micrograph of CeTPP(OH)<sub>2</sub>/TiO<sub>2</sub>/NaY

The photocatalytic activity of catalysts were investigated in the photodegradation of 4-NP. The results showed based on increasing OH group, the photocatalytic activity of systems increases. It seems hydroxyl group in the para-position can be produces OH radical which in turn acts as well as H<sub>2</sub>O<sub>2</sub> and therefore, oxidation of organic pollutant is accelerated.

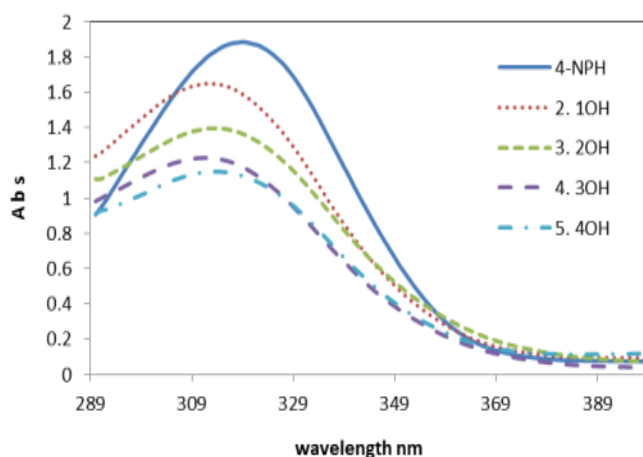


Fig.4. Effect of amount of hydroxyl group on the photodegradation of 4-NP

#### 4. Conclusions

In this study, the preparation of CeTPP(OH)<sub>n</sub>/TiO<sub>2</sub>/NaY catalysts were performed using zeolite synthesis and impregnation methods respectively. XRD studies showed that based on incorporation of the metal complex into zeolite nanocage, crystallinity of the zeolite matrix is unchanged. In addition, the presence of peaks in the 2θ=28 indication of TiO<sub>2</sub> in anatase form which proved insertion of TiO<sub>2</sub> in nanopores of zeolite. The catalyst displays an efficient photoactivity for the degradation of 4-NP in absence of H<sub>2</sub>O<sub>2</sub>. It can be concluded these catalytic systems are efficient photocatalysts which degraded 4-NP in the absence of H<sub>2</sub>O<sub>2</sub>.

#### References

- 1) W. SUN, J. Li, X. Lü, F.Zhang, F. Res Chem Intermed. **2013** 39 , 1447-1457.





4<sup>th</sup> Iran National Zeolite Conference  
Golpayegan University of Technology, Golpayegan, Iran  
August 23-24, 2017



- 2) M. Zanjanchi, A. Ebrahimian, M. Arvand, J. hazard.mater. **2010**. 175, 992-1000.
- 3) L. Sanchez, J. Peral, X. Domenech, Appl. Catal. B **1998**, 19, 59-65.
- 4) Y. Kim, M. Yoon, J. Mol. Catal. A: Chemical **2001**, 168, 257-263.
- 5) M. Moghadam, S. Tangestaninejad, V. Mirkhani, I. Mohammadpoor-Baltork, M. Moosavifar, **2009**. J. Mol. Catal. A: Chemical 302, 68-75.

## Molecular Dynamics Simulations of CS<sub>2</sub> Diffusion in the nanoporous of the Cu-BTC

Afsaneh Sadat Modarreci,<sup>a</sup> Hossein Mohammadi-Manesh,<sup>a</sup> \*

<sup>a</sup>Department of Chemistry, Yazd University, Yazd, 89195-741, Iran

\*Email: mohammadimanesh@yazd.ac.ir

### 1. Introduction

The class of coordination polymers known as metal-organic frameworks (MOFs) has three-dimensional porous structures that are considered as a promising alternative to zeolites and other nanoporous materials for catalysis, adsorption, and separation applications. MOFs based on metal-oxide building blocks linked together with organic molecules have very stable structures with high porosity.<sup>1-3</sup> In the present work a copper-based MOF was selected, the so-called CuBTC (BTC = benzene-1,3,5-tricarboxylate), also named HKUST-1 and initially developed by Chui et al.<sup>4</sup> In this paper, we calculated dynamical properties such as Mean square displacement, self-diffusion coefficient and activation energy. Molecular dynamics simulations are performed to study the guest behavior at loading 20 and different temperatures (100, 200, 300, 400, and 500).

### 2. Theoretical Details

In this work we have used DLPOLY 2.18 to perform all molecular dynamics simulations. Cu-BTC MOF framework is kept fixed and CS<sub>2</sub> molecule are allowed to move during the simulation. A simulation time step of 1 fs was used in the simulation. Simulations were performed at constant pressure of 1 atmosphere and cutoff of 13 Å. Self-diffusion coefficient isotherm were obtained using NVE ensemble. The volume V, the number N and The energy E are kept fixed but before for equilibration of the system at the desired Temperature, an NVT simulation is used. For equilibration of the system at the desired temperature, an NVT simulation with  $15 \times 10^4$  steps is used and for computing the structural and dynamical properties, the ensemble is switched to NVE with  $5.7 \times 10^5$  steps which the first  $7 \times 10^4$  steps used for equilibration.

### 3. Results and discussion

MSD was calculated by Einstein equation (1).



# 4<sup>th</sup> Iran National Zeolite Conference

## Golpayegan University of Technology, Golpayegan, Iran

### August 23-24, 2017



$$\langle r(t)^2 \rangle = \langle |r_i \vec{r}(t) - r_i \vec{r}(0)|^2 \rangle \quad (1)$$

In equation (1)  $r_i \vec{r}(t)$  is the position of particle  $i$  at time  $t$ . Symbol  $\langle \rangle$  denotes averaging over all the atoms are moving. The total MSD of CS<sub>2</sub> in the Cu-BTC at the range of 100-500 K are calculated and shown in Fig. 1. This shows MSD value increases with increasing temperature. As the temperature increases the kinetic energy of the molecules increases and molecules at a greater distance within the specified time. Also, The calculated MSD for the center of mass of the CS<sub>2</sub> molecules in the X, Y and Z-directions are calculated shown in Fig. 2. This figure shows that the motion of CS<sub>2</sub> is homogeneous in the Cu-BTC and there is isotropic translational diffusion for CS<sub>2</sub> in the Cu-BTC.

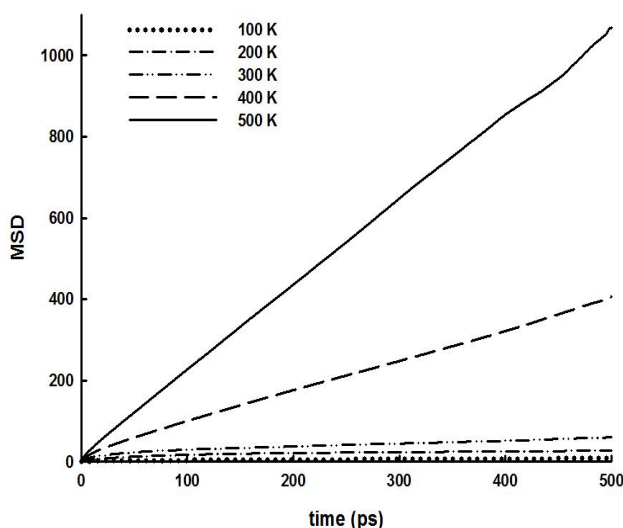


Figure 1. The total MSDs of CS<sub>2</sub> in Cu-BTC for range of 100–500 K.

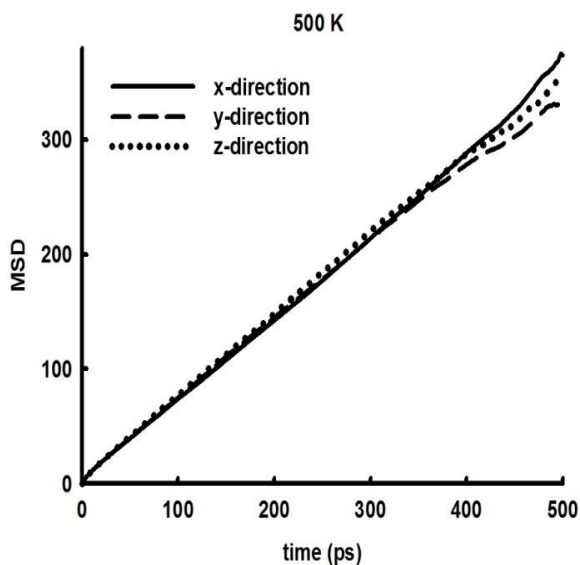


Figure 2. The x-, y-, and z-components of MSD for CS<sub>2</sub> in Cu-BTC at 500 K.

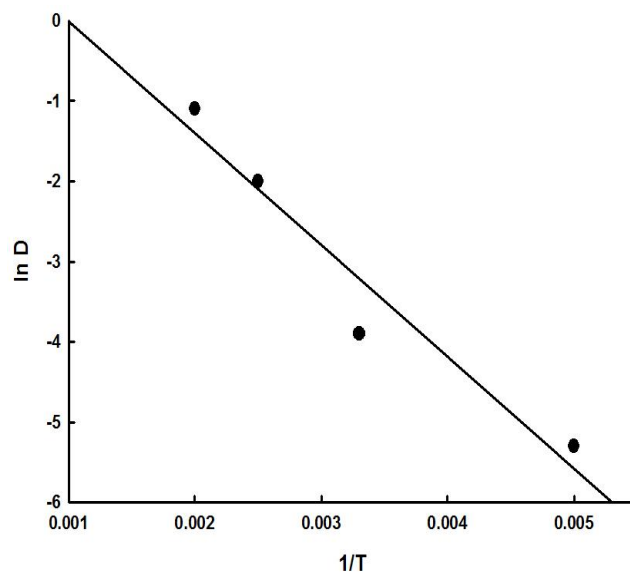


Figure 3. The temperature dependence of the self-diffusion coefficient CS<sub>2</sub>.



# 4<sup>th</sup> Iran National Zeolite Conference

## Golpayegan University of Technology, Golpayegan, Iran

### August 23-24, 2017



Self-diffusion coefficient ( $D_s$ ) was calculated from the linear region of the plot of MSD with respect to time at large  $t$ .

**Table 1.** The x, y, z components and total of activation energy (KJ/mole)

Loading	$E_{Total}$	$E_x$	$E_y$	$E_z$
20	4.96	4.68	4.64	4.66

The diffusion coefficients as a function of temperatures is plotted and shown in Fig 3. It is observed that self-diffusion coefficient increase as the temperature is increased.

Activation energy of diffusion for carbon monoxide in the Cu-BTC was calculated by Arrhenius equation (2):

$$\ln D = \ln D_0 - E_{act}/RT \quad (2)$$

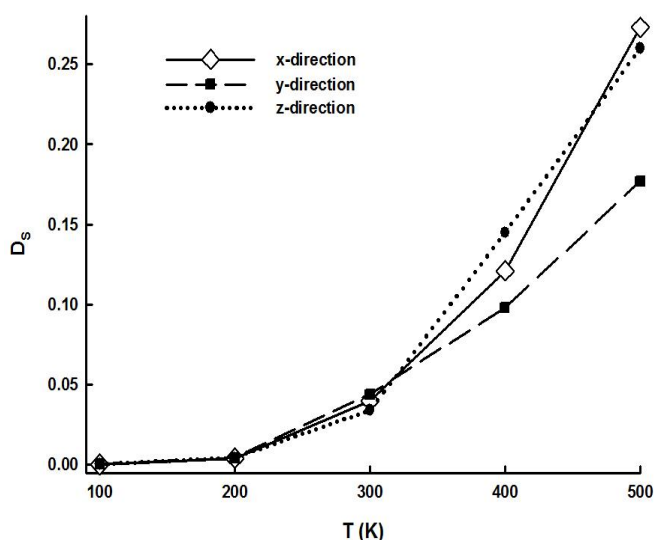


**Figure 4.** Arrhenius plots showing activation energy

Where  $D$ ,  $E_{act}$ ,  $R$ ,  $T$  are self-diffusion coefficient, activation energy, gas constant and temperatures simulation respectively. For calculated activation energy  $\ln D$  plot as function of  $1/T$  is plotted (Fig 4). The slope of the graph is equal to  $E_{act}/RT$ . The result of calculated activation energies are shown in table 1.

#### 4. Conclusions

The diffusion properties of  $CS_2$  in Cu-BTC were studied using molecular dynamic simulation. The calculated self-diffusion coefficient with increasing temperature is increased, due to  $CS_2$  obtain extra energy and jump small octahedral cage to large cage. In large cage  $CS_2$  have extra moving, increase molecular mass is reduced. To verify that sorption kinetics and diffusion of  $CS_2$  in Cu-BTC we calculated activation energy. Where activation energy of diffusion for  $CS_2$  was found to be around  $4.73 \text{ KJ.mole}^{-1}$ .



# 4<sup>th</sup> Iran National Zeolite Conference

## Golpayegan University of Technology, Golpayegan, Iran

### August 23-24, 2017



#### Acknowledgments

All financial, software and hardware resources needed for this work were supported by Yazd University. We would like to thank Yazd University for providing software and hardware resources.

#### References

- 1) Eddaoudi, M.; Li, H. L.; Yaghi, O. M. *J. Am. Chem. Soc.* **2000**, *122*, 1391-1397.
- 2) Eddaoudi, M.; Moler, D. B.; Li, H. L.; Chen, B. L.; Reineke, T. M.; O'Keeffe, M.; Yaghi, O. M. *Acc. Chem. Res.* **2001**, *34*, 319-330.
- 3) Yaghi, O. M.; O'Keeffe, M.; Ockwig, N. W.; Chae, H. K.; Eddaoudi, M.; Kim, J. *Nature* **2003**, *423*, 705-714.
- 4) Chui, S. S.-Y., Lo, S. M.-F., Charmant, J. P., Orpen, A. G., & Williams, I. D. **1999**. 283, 1148-1150.

## Zeolite modification to generate mesoporosity for adsorption of pollutants

S. Esmaili, M.A. Zanjanchi\*

*Department of Chemistry, Faculty of Science, University of Guilan, P.O. Box 1914, Rasht, Iran*

\*Email: zanjanchi@guilan.ac.ir

### 1. Introduction

Zeolites always have been considered as useful materials in different chemical processes especially as adsorptive, catalyst support or ion-exchanger. Many chemical procedures require adsorption of molecules from gas or solution onto/into zeolite as a preliminary step. Ordered microporous structure of zeolites is one of their unique properties that can define and determine their potential adsorptive and consequently catalytic performance [1]. Mordenite and zeolite Y are considered as microporous structures. Larger pores or so-called mesopores can modify the favorable functions of these substances as catalyst or adsorbent. In this work we report the effects of sonication and combination of sonication and other mesopore-inducing approaches on characteristics of mordenite and zeolite Y. In current study these parameters were investigated.

### 2. Experimental

The mordenite was prepared based on previous report and was designated as MOR [2]. Then it was converted to NaMOR, NH<sub>4</sub>MOR and HMOR. All these samples were subjected to acid-treatment, alkaline treatment and sonication or a combination of these treatments.

Preparation of zeolite Y was based on our previously published report [3]. Then it was converted to NH<sub>4</sub>Y, HY and NaY forms. These samples were subjected to treatment with various amounts of ammonium hexafluorosilicate (AHFS) during a solid-state reaction. Adsorption of methylene blue (MB) was chosen as the criteria to assess the success of treatments in formation of mesopores. All prepared substrates were characterized with XRD, SEM, BET, BJH and FT-IR.



# 4<sup>th</sup> Iran National Zeolite Conference

## Golpayegan University of Technology, Golpayegan, Iran

### August 23-24, 2017



### 3. Results and discussion

In case of mordenite, it was found that employing combination of acid treatment ( $\text{HNO}_3$ ) and ultrasound irradiation (*via* ultrasound probe) provides adequate means to get highly adsorptive mordenite. Exploitation of this porous structure eliminates rhodamine B as a moderately large dye molecule from aqueous solution within short time. These results can be considered very promising in manipulating the porous structure of already existed/prepared zeolites in order to use them in environmental applications especially removal of large-size pollutants. In case of zeolite Y, treatment with AHFS showed an improved adsorptive ability. Fig. 1 shows  $\text{N}_2$  dsorption- desorption isotherm for zeolite Y.

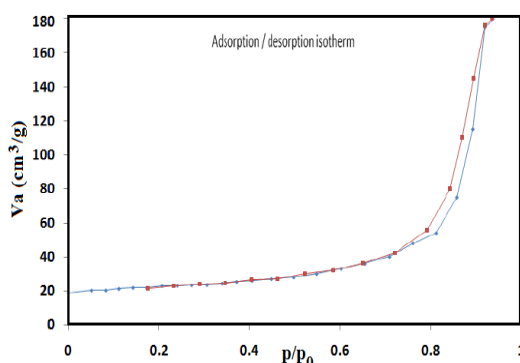


Figure 1.  $\text{N}_2$  dsorption - desorption isotherm for AHFS-modified zeolite Y

### 4. Conclusions

The certain modification methods showed higher capability for the modified zeolite in terms of adsorption of MB presented in aqueous solutions.

### References

- [1] P. Misaelides, Microporous Mesoporous Mater. **2011**, 144, 15-18.
- [2] A. A. Shaikh, P. N. Joshi, N. E. Jacob, V. P. Shiralkar, Zeolites, **1993**, 13, 511-517.
- [3] M. A. Zanjanchi, K. Tabatabaiean, M. Moosavifar, J. Inclu. Phenom. **2001**, 40, 193-198.

## Synthesis process and evaluation of zeolite-based micromotors

Fatemeh Abedini<sup>a\*</sup>, H.R. Madaah Hosseini<sup>a</sup>

<sup>a</sup>Material science and engineering department, Sharif university of technology, Tehran 14584, P. O. Box 11365-9466, Iran

\*Email: f.abedini@gmail.com

### 1. Introduction

Micro/nano motor is a general term to describe a class of manmade tiny devices with the ability to exhibit mechanical motion often in a liquid or liquid/gas interface <sup>[1]</sup>. Autonomous propulsion in such objects arises from chemical



# 4<sup>th</sup> Iran National Zeolite Conference

## Golpayegan University of Technology, Golpayegan, Iran

### August 23-24, 2017



reaction of a catalyst coated asymmetrically on particles' surface and the fuel molecule dissolved in motion media <sup>[2]</sup>. These motors has the potential to be used in various applications ranging from biomedical <sup>[3]</sup> to environmental remediation <sup>[4]</sup>.

We describe here the synthesis process of a novel zeolite-based micromotor with the potential of chemical and biological detoxification of water.

Among zeolite family, zeolite 4A is well known for its ability to remove heavy metals from water <sup>[5]</sup>, non-toxic nature, availability and low cost <sup>[6]</sup>. It is also reported that silver exchanged zeolite has antibacterial capability in spite of its low toxicity <sup>[7]</sup>. Combining these properties with micromotor advantages, i.e. move and destroy contamination, can be beneficial for water remediation purposes.

One of the known fuels of micromotors is aqueous hydrogen peroxide ( $H_2O_2$ ) which has antiseptic feature <sup>[4]</sup>. Hydrogen peroxide can decompose to water and oxygen in the presence of proper catalysts such as Pt or Ag <sup>[1]</sup>.

Micromotors with the purpose of water remediation both chemically and biologically can be fabricated by using masking technique to coat Ag asymmetrically on cubic silver-zeolite particles <sup>[9]</sup>.

## 2. Experimental Part or Theoretical Details

The fabrication of catalytic silver-zeolite micromotors includes two steps:

### *Synthesis of silver-zeolite particles:*

Zeolite 4A purchased from "Iran zeolite" with average particle size of 4  $\mu m$  used as base particles. Silver-zeolite particles were prepared using conventional ion exchange method with some modifications. The particles added to solution of 0.1M silver nitrate (Merck) and stirred for 16 hours at room temperature in darkness. Then filtered and washed with deionized water. In order to assure complete silver exchange, the process repeated twice. The particle obtained dried at 100°C in vacuum oven over night.

### *Synthesis of silver-zeolite micromotor:*

As prepared silver-zeolite particles were used to fabricate Janus micromotors. A dilute suspension of particles were prepared and sprayed over cleaned glass slides and dried at room temperature. The deposition of Ag coating was carried out by means of dc magnetron sputtering with Ar pressure of  $3 \cdot 10^{-2}$  Torr and at room temperature.

The surface of particle in touch with glass slide was fully masked. In order to obtain an asymmetrical coating, the sample were also set up parallel to the Ag target.

## 3. Results and discussion

Figure 1 represents scanning electron microscope (SEM) images and energy-disperse x-ray spectroscopy (EDS) of different elements in (A) sodium-zeolite and (B) silver-zeolite particles. Comparison of Na and Ag EDS patterns of zeolite 4A and silver-zeolite shows that Ag has replaced Na in zeolite structure, which confirms the successful silver ion exchange process. The XRD result of both sodium-zeolite and silver-zeolite had same pattern with slight differences. This shows that silver ion exchange didn't change the crystal structure of zeolites significantly (Figure 2).



4<sup>th</sup> Iran National Zeolite Conference  
Golpayegan University of Technology, Golpayegan, Iran  
August 23-24, 2017

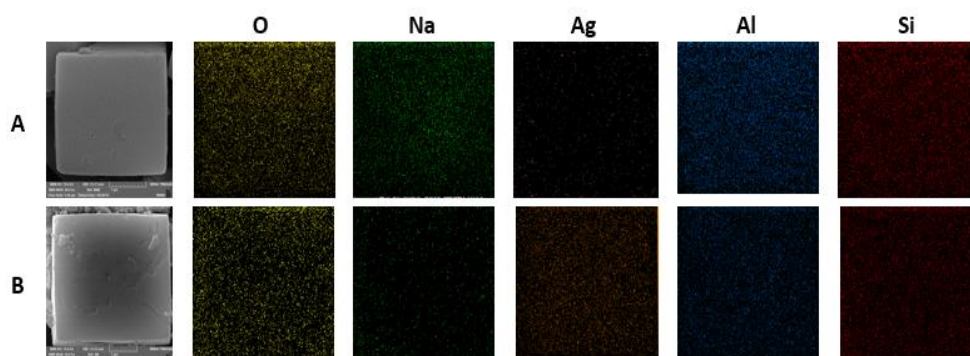


Figure 1. SEM image and EDS pattern showing different elements distribution in (A) zeolite 4A (B) silver-zeolite.

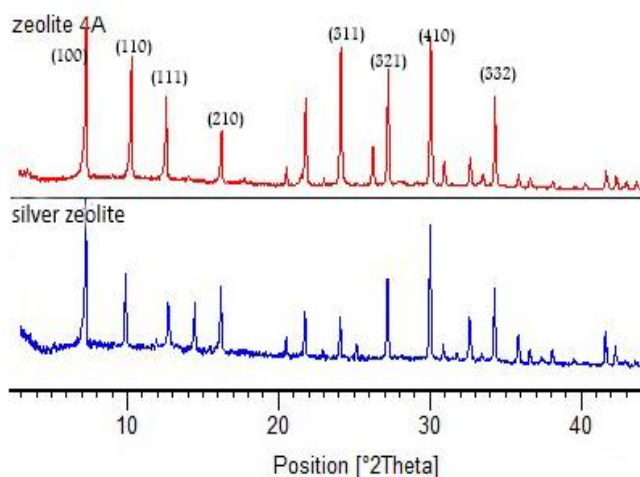


Figure 2. XRD pattern of zeolite 4A and silver-zeolite.

A schematic of Zeolite-based janus particles illustrated in figure 3. As indicated before a part of zeolite particle masked before coating and therefore only exposed side of zeolite were coated with Ag. This asymmetric coating is vital for directional oxygen bubble production and mechanical movement of motor particles.

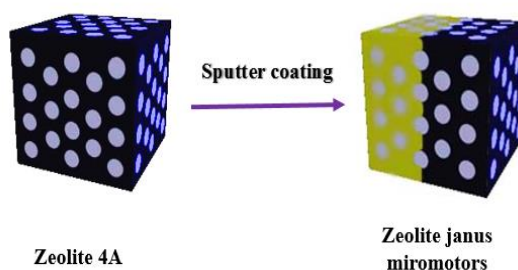


Figure 3. Schematic representation of zeolite janus miromotors.

Grazing XRD from surface of glass slides after sputtering approved the formation of Ag coating on zeolite particles (Figure 4). This coating has the ability to catalyze hydrogen peroxide to produce bubbles and supply the thrust needed for motion of micromotors. It can also help to enhance antibacterial effect of particles.



4<sup>th</sup> Iran National Zeolite Conference  
Golpayegan University of Technology, Golpayegan, Iran  
August 23-24, 2017

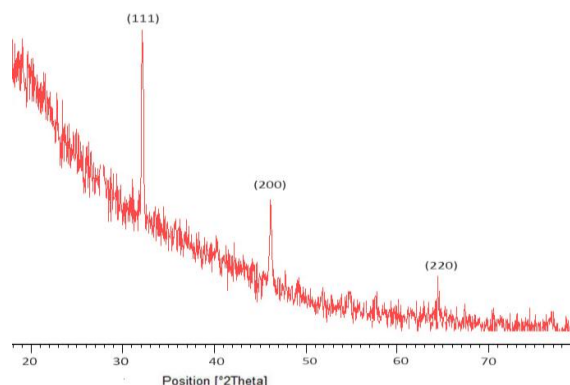


Figure 3. XRD pattern of Ag coating after sputtering.

#### 4. Conclusions

Silver-zeolite janus micromotors synthesized successfully by immobilization (masking) procedure with the help of sputtering technique. Particles synthesized in this report has the potential to purify water both chemically and biologically with low cost. The movement path and velocity of these micromotors and their ability to purify water could be evaluated in future works.

#### References

- [1] S. J. Ebbens and J. R. Howse, *Langmuir* **2011**, *27*, 12293-12296.
- [2] A. I. Campbell and S. J. Ebbens, *Langmuir* **2013**, *29*, 14066-14073.
- [3] L. K. Abdelmohsen, F. Peng, Y. Tu and D. A. Wilson, *Journal of Materials Chemistry B* **2014**, *2*, 2395-2408.
- [4] W. Gao and J. Wang, *Acs Nano* **2014**, *8*, 3170-3180.
- [5] S. Mehdizadeh, S. Sadjadi, S. J. Ahmadi and M. Outokesh, *Journal of Environmental Health Science and Engineering* **2014**, *12*, 7-7.
- [6] M. M. Khin, A. S. Nair, V. J. Babu, R. Murugan and S. Ramakrishna, *Energy & Environmental Science* **2012**, *5*, 8075-8109.
- [7] Y. Zhang, S. Zhong, M. Zhang and Y. Lin, *Journal of materials science* **2009**, *44*, 457-462.
- [8] S. Ebbens, M. H. Tu, J. R. Howse and R. Golestanian, *Phys Rev E Stat Nonlin Soft Matter Phys* **2012**, *85*, 020401.
- [9] a) J. Hu, S. Zhou, Y. Sun, X. Fang and L. Wu, *Chem Soc Rev* **2012**, *41*, 4356-4378; b) V. V. Singh, B. Jurado - Sánchez, S. Sattayasamitsathit, J. Orozco, J. Li, M. Galarnyk, Y. Fedorak and J. Wang, *Advanced Functional Materials* **2015**, *25*, 2147-2155.

## Zeolite Supported Palladium Nanoparticles Catalyzed Nitroarenes Reduction

Seyed Mahdi Rafiaei<sup>a</sup>, Mohammadreza Shokouhimehr<sup>b\*</sup>

<sup>a</sup> Department of Materials Science and Engineering, Golpayegan University of Technology, Isfahan, Iran.

<sup>b</sup> Department of Material Science and Engineering, Iran University of Science and Technology, Tehran, Iran,

\*Email: shokouhimehr@gmail.com

#### 1. Introduction

The catalytic reduction of nitroaromatics to anilines is an important transformation in both laboratory and chemical





4<sup>th</sup> Iran National Zeolite Conference  
Golpayegan University of Technology, Golpayegan, Iran  
August 23-24, 2017



industries [1-3]. Recyclable catalysts are very important for the reduction of nitroarene compounds and a number of transition metals (*e.g.*, Pd, and Pt.) are reported to be efficient for this process [4-7]. Heterogeneous catalysts have attracted attention in catalytic reactions because of their high activities and the benefit of recycling [8-10]. In addition, the catalysts without any support generally aggregate after a single use in catalytic reactions which causes rapid activity decay [11-14]. The aggregation of catalysts reduces the active surface area resulting in less effective chemical reactions [15-17]. To resolve these drawbacks, catalysts are immobilized on inexpensive solid supports such as carbon, mesoporous silica, and zeolites. Among the various catalyst supports, zeolite materials have been extensively employed in heterogeneous catalysis due to their desirable properties including, chemical inertness and good mechanical stability [18-20].

## 2. Experimental Part

The general procedures for the aforementioned catalytic reaction using the Pd catalysts are as follows. The reduction of nitroarenes were catalyzed using Pd catalysts (1 mol%) dispersed in ethanol in a round-bottom flask (25 ml). Then, nitrobenzene (0.5 mmol), hydrazine (2 equiv.), and a small stirring bar were added to the flask. The flask containing reaction mixture was placed in an oil bath (90 °C) and stirred under air atmosphere. After completion of reaction, the mixture was cooled to room temperature and zeolite supported Pd catalysts were separated using a filter. The separated catalysts were washed several times with EtOH. The products were analyzed by a GC-MS.

## 3. Results and discussion

The TEM image of the zeolite (Fig. 1a) shows well-ordered structures. The TEM images of the Pd catalysts loaded on zeolite reveal that the Pd NPs are uniform with average size of ~5 nm and well disperse without any obvious aggregation (Fig. 2b).

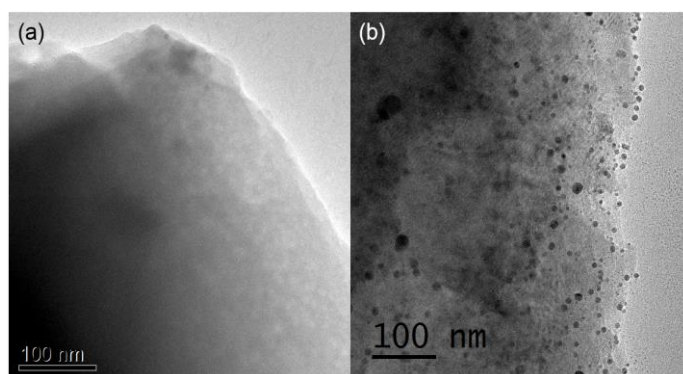


Fig. (1). TEM image of zeolite (a). TEM image of Pd catalysts on zeolite (b).

Fig. (2) exhibits representative existence of Pd species on the designed zeolite catalyst ascertained by XPS analysis.



4<sup>th</sup> Iran National Zeolite Conference  
Golpayegan University of Technology, Golpayegan, Iran  
August 23-24, 2017

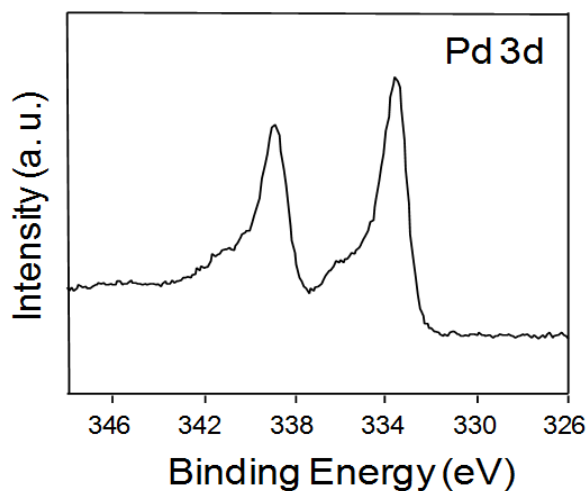


Fig. (2). XPS analyses of Pd 3d for the zeolite Pd catalysts.

We investigated the catalytic efficiency of the Pd catalysts supported on zeolite in the reduction of structurally diverse nitro compounds. Table 1 shows the catalysts exhibited excellent activity in nitro group reduction. Reusability of the catalyst is very important for the industrial applications. We examined the recycling and reusability of the zeolite supported Pd catalysts for the reduction of nitrobenzene. The catalysts were successfully separated by a simple filtration and reused for five consecutive cycles of the reduction of nitrobenzene with no significant loss of activity (Fig. 3).

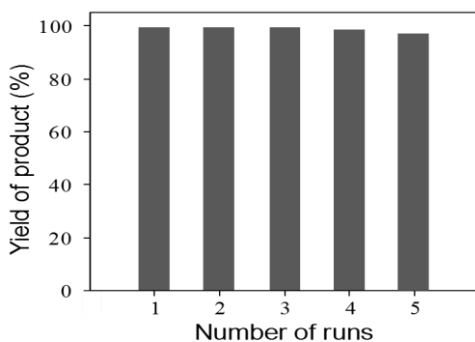
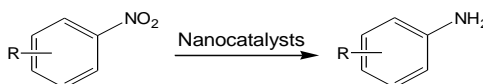


Fig. (3). Recycling of the zeolite supported Pd catalysts in the reduction of nitrobenzene.

Table 1. Reduction of substituted nitrobenzenes with hydrazine.<sup>a</sup>

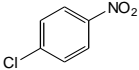
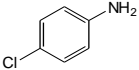
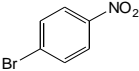
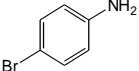
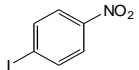
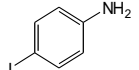
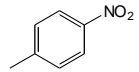
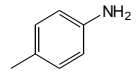
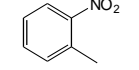
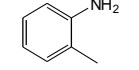
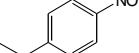
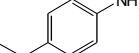


Entry	Substrate	Product	Yield (%) <sup>b</sup>
1			97



4<sup>th</sup> Iran National Zeolite Conference  
Golpayegan University of Technology, Golpayegan, Iran  
August 23-24, 2017



2			95
3			93
4			91
5			91
6			89
7			88

<sup>a</sup> Reaction conditions: substituted nitrobenzene (1 mmol), hydrazine (2 equiv.), Pd (1 mol %), EtOH (10 ml), 90 °C, 5 h.

<sup>b</sup> The yields were determined by GC-MS with respect to an internal standard.

#### 4. Conclusions

In conclusion, we have demonstrated a new sustainable palladium nanoparticles supported on zeolite prepared by a simple and economical synthetic process. The efficiency of this catalysts was verified in reduction of nitroaromatics providing excellent product yields. The catalyst could be reused for five consecutive cycles in reduction of nitrobenzene without significant loss of activity.

#### References

- [1] S. Cenini and F. Ragaini, *Catalytic Reductive Carbonylation of Organic Nitro Compounds*, Springer (1997).
- [2] A. M. Tafesh and J. Weiguny, *Chem. Rev.* 96, 2035 (1996).
- [3] D. C. Sherrington, A. P. Kybett, *Supported Catalysts and Their Applications*, RSC (2001).
- [4] M. Benaglia, *Recoverable and Recyclable Catalysts*, Wiley (2009).
- [5] D. Sahu, C. Sarmah, and P. Das, *Tetrahedron Lett.* 55, 3422 (2014).
- [6] N. Koizumi, X. Jiang, J. Kugai, and C. Song, *Catal. Today* 194, 16 (2012).
- [7] P. Luo, K. Xu, R. Zhang, Huang, J. Wang, W. Xing, and J. Huang, *Catal. Sci. Technol.* 2, 301 (2012).
- [8] R. A. Sheldon and H. van Bekkum, *Fine Chemicals through Heterogeneous Catalysis*, Wiley-VCH (2008).
- [9] U. Heiz and U. Landman, *Nanocatalysis*, Springer (2006).
- [10] V. Polshettiwar and T. Asefa, *Nanocatalysis*, Wiley (2013).
- [11] J. Zhi, D. Song, Z. Li, X. Lei, and A. Hu, *Chem. Commun.* 47, 10707 (2011).
- [12] J. M. Thomas, W. J. Thomas, *Principles and Practice of Heterogeneous Catalysis*, Wiley-VCH (1997).
- [13] J. R. H. Ross, *Heterogeneous Catalysis*, Elsevier (2011).
- [14] J. Lu and P. H. Toy, *Chem. Rev.* 109, 815 (2009).
- [15] C. Perego and R. Millini, *Chem. Soc. Rev.* 42, 3956 (2013).
- [16] F. Zaera, *Chem. Soc. Rev.* 42, 2746 (2013).
- [17] L. Yin and J. Liebscher, *Chem. Rev.* 107, 133 (2007).
- [18] G. A. Somorjai and B. Chaudert, *Nanomaterials in Catalysis*, Wiley-VCH (2013).
- [19] G. Centi, R.A. van Santen, *Catalysis for Renewables*, Wiley-VCH (2007).



4<sup>th</sup> Iran National Zeolite Conference  
Golpayegan University of Technology, Golpayegan, Iran  
August 23-24, 2017



[20] J. T. Richardson, Principles of Catalyst Development, Plenum Press, New York (1989).

## Selective and efficient BTX yield from methanol over low-Si/Al-ratio ZSM-5 impregnated with Mo

Bahram Ghanbari<sup>a,\*</sup> Fatemeh Kazemi Zangeneh<sup>a</sup>

<sup>a</sup> Department of Chemistry, Sharif University of Technology, Tehran, PO Box 11155-3516, Iran

\*Email: ghanbari@sharif.edu

### 1. Introduction

Nowadays, aromatic compounds such as benzene (B), toluene (T) and xylene (X), which are known as BTX, are significant chemical intermediates in fine chemical industries, which their commercial demands sharply grow up.<sup>1,2</sup> Reforming of petroleum fractions aromatic hydrocarbons are the central source of aromatics while working on new non-petroleum substitute is industrially crucial.<sup>3-5</sup> During the recent decades, the research on solid acid catalysts for the conversion of methanol to aromatics (MTA) process has fascinated both scientists and industrial organization, because since methanol is produced from various resources as syngas, natural gas, coal, biomass and any other carbon-based gasifiable feedstock.<sup>6,7</sup> Some reports unveiled that the yield of aromatics hydrocarbons production could be improved where the conversion of methanol was executed over the upgraded ZSM-5 zeolite with some metal species.<sup>8</sup>

In this work, the catalytic conversion of methanol to aromatic hydrocarbons has been studied over Mo impregnated-low-silica ZSM-5 (Si/Al=11) catalyst with various metal loadings (0, 1, 2 and 4 wt. %).

### 2. Experimental

The ZSM-5 zeolite was prepared via hydrothermal method according to the general technique reported by Karimi et al.<sup>9</sup>, with few modifications. The gel molar composition was  $1\text{Al}_2\text{O}_3:22\text{SiO}_2:2.7\text{TPAOH}:5\text{Na}_2\text{O}:2500\text{H}_2\text{O}$ . The Mo-promoted catalysts were prepared by impregnation of ZSM-5 zeolite with an aqueous solution of ammonium molybdate tetrahydrate ( $(\text{NH}_4)_6\text{Mo}_7\text{O}_{24}$ ) to achieve 1, 2 and 4 wt. % Mo loading. The impregnated samples dried at 110°C

overnight and then calcined at 550 °C for 6 h. The resultant catalysts were denoted as Mo-1-ZSM-5, Mo-2-ZSM-5 and Mo-4-ZSM-5, respectively.

A fixed-bed tubular reactor was applied to determine the performance of the catalyst samples in MTA process at 375 °C under ambient pressure. A graduated burette using a micro tube pump (prep pump, Chem Tech Co. Ltd.) at a



# 4<sup>th</sup> Iran National Zeolite Conference

## Golpayegan University of Technology, Golpayegan, Iran

### August 23-24, 2017



flow rate of 0.1 mL/min Liquid methanol was applied for pumping of liquid methanol for WHSV of 2 h<sup>-1</sup>. Also a GC-Varian 3800 instrument was applied to analyze off-line the liquid products.

### 3. Results and discussion

Figure 1 shows the XRD diffraction patterns of catalysts. Five diffraction patterns found in the XRD patterns ( $2\theta = 8.1^\circ, 8.9^\circ, 23.1^\circ, 23.3^\circ$  and  $23.8^\circ$ ) were assigned to the orthorhombic structure of ZSM-5. As shown in Figure 1, modification of zeolite structure by loading it by Mo, make no change in the peaks of XRD graphs.

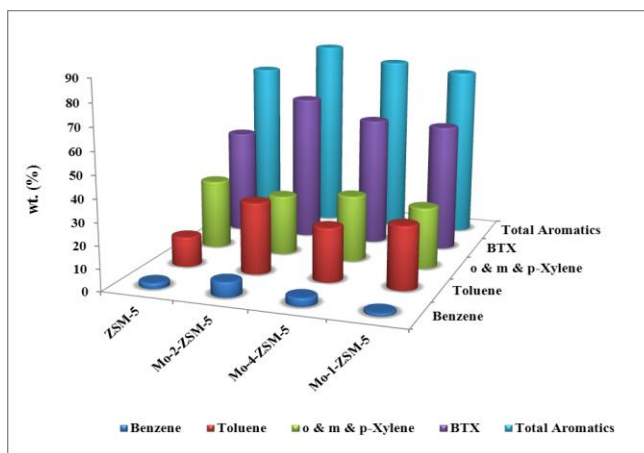
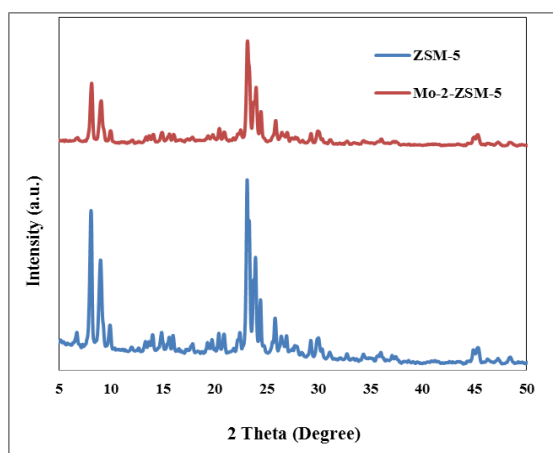


**Figure 1.** The XRD patterns of the ZSM-5 and Mo-2-ZSM-5.

**Figure 2.** BTX selectivity over ZSM-5 and Mo-1-ZSM-5, Mo-2-ZSM-5 and Mo-4-ZSM-5 zeolites (Reaction condition: T = 375 °C, WHSV = 2 h<sup>-1</sup>).

In order to discuss more about catalytic performance of the prepared catalysts, the liquid hydrocarbons of the product in MTA process was analyzed by GC and GC-MS methods. As inferred from Figure 2, the aromatics selectivity over Mo-2-ZSM-5 was largely higher than that from the parent ZSM-5. Also, Figure 2 represents higher percentage of BTX in the product applying Mo-2-ZSM-5 catalyst than the parent ZSM-5.

Also, product distributions for MTA process over ZSM-5 and Mo-2-ZSM-5 is shown in Table 1.

**Table 1.** Product distributions for MTA process catalyzed by ZSM-5 and Mo-2-ZSM-5 at T<sub>R</sub>= 375 °C.

Sample	ZSM-5 (0% Mo)	Mo-2-ZSM-5 (2% Mo)
<b>Component (wt. %)</b>		
i-C <sub>5</sub>	2.3	0.9
C <sub>6</sub> Saturated	0.7	0.2
Benzene	2.5	6.7
C <sub>7</sub> Saturated	1.3	0.1
Toluene	13.5	32.1
Ethyl Benzene	2.0	1.6
o & m & p-Xylene	31.1	26.9
M-E-Benzene	3.2	1.8
3M-Benzene	7.0	8.0
Ar-C <sub>10</sub>	14.0	8.9



4<sup>th</sup> Iran National Zeolite Conference  
Golpayegan University of Technology, Golpayegan, Iran  
August 23-24, 2017



C <sub>10</sub> <sup>+</sup>	12.5	8.8
Others	9.9	4.0
Sum	100	100

Table 2 represents that Mo-2-ZSM-5 catalyst was capable to produce 86.0 wt. % aromatics with BTX selectivity 65.7%.

**Table 2.** BTX and total aromatics distribution for MTA process catalyzed by ZSM-5 and Mo-2-ZSM-5 at T<sub>R</sub>= 375 °C.

Sample Component (wt. %)	ZSM-5 (0% Mo)	Mo-2- ZSM-5 (2% Mo)
BTX	47.1	65.7
Total Aromatics	73.3	86.0

#### 4. Conclusions

Mo impregnated-low-silica ZSM-5 catalysts with various metal loadings (0, 1, 2 and 4 wt. %) prepared and its catalytic performance in the aromatization of methanol was studied. The results indicated that the BTX yield increased following the trend of ZSM-5 < Mo-1-ZSM-5 < Mo-4-ZSM-5 < Mo-2-ZSM-5 zeolites. 2wt. % Mo-ZSM-5 zeolite catalyst (optimized sample) improved the production of aromatics and BTX about 12.7% and 18.6% in weight percent, respectively rather than the parent ZSM-5 zeolite.

#### Acknowledgments

The research was supported by Research Office of Sharif University of Technology.

#### References

- 1) H. Hu, Q. Zhang, J. Cen, X. Li, *Catal. Commun.* **2014**, 57, 129-133.
- 2) Y. Gao, G. Wu, F. Ma, C. Liu, F. Jiang, Y. Wang, A. Wang, *Microporous Mesoporous Mater.* **2016**, 226, 251-259.
- 3) M.A. Fahim, T.A. Alsahhaf, A. Elkilani, *Fundamentals of Petroleum Refining*, The Netherlands, **2010**, pp. 95-111.
- 4) C. Yang, M. Qiu, S. Hu, X. Chen, G. Zeng, Z. Liu, Y. Sun, *Microporous Mesoporous Mater.* **2016**, 231, 110-116.
- 5) A. Zheng, Z. Zhao, S. Chang, Z. Huang, H. Wu, X. Wang, F. He, H. Li, *J. Mol. Catal. A: Chem* **2014**, 383, 23-30.
- 6) T. Wang, X. Tang, X. Huang, W. Qian, Y. Cui, X. Hui, W. Yang, F. Wei, *Catal. Today* **2014**, 233, 8-13.
- 7) S. Ilias, A. Bhan, *ACS Catal.* **2013**, 3, 18-31.
- 8) X. Niu, J. Gao, Q. Miao, M. Dong, G. Wang, W. Fan, Z. Qin, J. Wang, *Microporous Mesoporous Mater.* **2014**, 197, 252-261.
- 9) R. Karimi, B. Bayati, N. Charchi Aghdam, M. Ejtemaee, A.A. Babaluo, *Powder Technol.* **2012**, 229, 229-236.



# 4<sup>th</sup> Iran National Zeolite Conference

## Golpayegan University of Technology, Golpayegan, Iran

### August 23-24, 2017



## Application of Zeolite Coverage on Gachsaran Formation in Gotvand olya Dam to reduce the dissolution of salt

Behnaz Shahrokh<sup>a\*</sup>, Mohammad taghi Mansouri kia<sup>b</sup>

<sup>a</sup> Research Manager of Banian Pey Geotechnical consulting engineering , Ahvaz, Iran

<sup>b</sup> Director on Dams executive office , Khuzestan water and power authority (KWPA).

\*Email: r10719853@yahoo.com

### 1. Introduction

Gotvand dam reservoir with over 90 km length is surrounded by Gachsaran, Mishan, Aghajari and Bakhtiari formations. The noticeable point in the dam reservoir is the presence of Gachsaran Formation that is composed of considerable volume of salt located 4 km upstream of dam. Salinity of dam water due to dissolution of salt in reservoir water can cause serious environmental problems. In addition to direct dissolution of salt in contact with reservoir water, slope instability can also influence on this process. Probable sliding in salty layers of slopes will insert a significant volume of salt in contact with reservoir water in a short time [1].

Due to tectonic pressure, salt is compressed and turned into a vertical mass with high thickness. Due to physical properties and fluidity, Gypsum and salt formation creates certain structural form called salt tectonic at the time of rogeny. At the time of orogeny, the pressure and heat is high in depth of the earth and the evaporated water leads to severe hydration of salt. In this condition, stones and rocks are not as stable as in earth surface, instead they are plastic paste and evaporated rocks and other plastic rocks like clay and marl will be the same in salt orogeny process [1].

### 2. Theoretical Details

Initial investigation conducted by the design consultant upper dam Scroll indicated the presence of a mass in the salt reservoir dam Gotvand Olya Gachsaran is the most important and most orogeny salt mountain near the dam axis is located. Concerning the consequent problems, whether environmental like salinity of dam

lack and river or technical and engineering problems related to the main and subordinate structures of Gotvand Olya dam, which might happen especially for power plant, Finally, the treatment method including covering the outer level of salt mass by the use of clay and Riprap construction material was approved [2]. The obtained results indicate that sliding in reservoir area are mostly shallow and are caused by dissolution of salty layer.

Concerning the collapse of clay wall at the first stage of impounding, and the results obtained from testing the water on the upstream and downstream of the salt mountain and it becomes obvious that the quality of water in downstream has reduced meaningfully.

In addition to direct dissolution of salt in contact with reservoir water, slope instability can also influence on this process.

After the construction operation and before beginning the inundation, constructors proceed to build a clay blanket on the salt formations. But, signs of cracking were observed on clay blanket just three days after the edges of these blankets went under water. Dissolving rate of formation salt accelerates with a larger value of flow quantity as demonstrated the experiment, revealing that solution movement accelerated the convection effect and diffusion effect of formation salt. Therefore, in practice, properly controlling the freshwater injection rate will have a more effect of



4<sup>th</sup> Iran National Zeolite Conference  
Golpayegan University of Technology, Golpayegan, Iran  
August 23-24, 2017



mineral dissolution for salt formation. The clay blanket density is less than 3kg/lit, thus it moved easily with reservoir level changes. Laboratory results showed that clay blankets is not enough to prevent the penetration of water into Gachsaran Formation (Fig. 1)

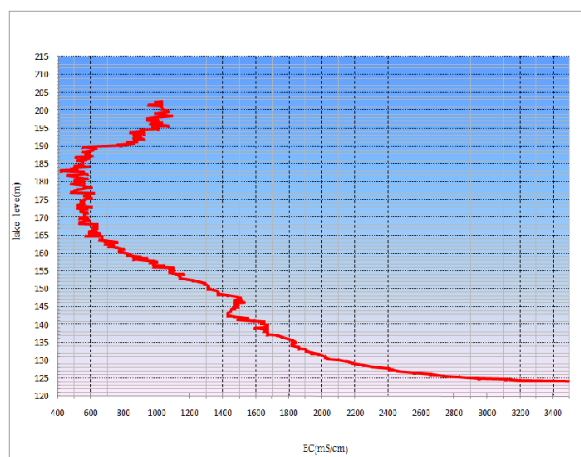


Fig 1. Changes of electrical conductivity based on the reservoir levels (annual average)

The main aim of this study is to determine the ability of the natural zeolites (clinoptiolite and perlite[4, 5]) to get the best results for reduce of the dissolution of salt. Using of zeolites coverage on the clay blanket can be decrease salt solution if the density of blanket is more than 6kg/litter. Additionally, this density will be absorbed ions on zeolites and will be stabilized surface. The ion shield prevents more ions out.

The chemical behavior of natural zeolites in different aqueous environments in Dam reservoir will be find. Geochemical and technological studies, monitoring of pH and EC and theirs changes are very important for zeolite usage at real environments. Zeolites can interact with hydrogen or hydroxyl ions present in solutions consequently, certain physicochemical phenomena such as hydrolysis of solids, degradation, dissolution and even phase transformations can be occurred. All these phenomena again depend on the structural characteristics and the chemical composition of the used zeolite.

### 3. Results and discussion

When water permeates through coverage zeolite , ions are adsorbed on the zeolite coverage and form a layer with high ions concentration near the zeolite coverage surface(between clay blanket and coverage zeolite). Due to the high ions concentration in the layer, ion tend to diffuse back to the bulk as long as they are not fixed in gel/cake layer. The concentration profile settles at the equilibrium between convective ion transport to coverage surface and diffusive ions back transport to the bulk solution. This is so called concentration polarization phenomenon that fundamentally increases the coverage performance. Concentration polarization refers to the concentration gradient of salts on the high pressure side of the zeolite coverage surface created by the less than immediate redilution of salts behind as water permeates through the coverage itself. The salt concentration in this boundary layer exceeds the concentration of the bulk water. This phenomenon impacts the performance of the zeolite coverage by increasing the osmotic pressure at the coverage's surface leading to the following:

- 1)Reduced flux
- 2) Increased salt leakage

Increasing the velocity (turbulence) of the brine stream helps to reduce the concentration polarization.

In Fig 2. The relationship between the diffusion coefficient and the concentration at the deep- Sea is shown.





4<sup>th</sup> Iran National Zeolite Conference  
 Golpayegan University of Technology, Golpayegan, Iran  
 August 23-24, 2017

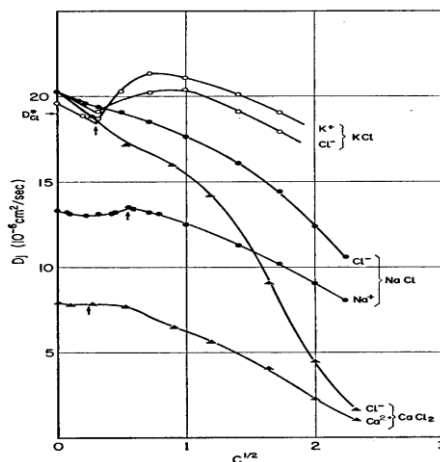


Fig 2. The tracer-diffusion coefficient of ions in different single or salt solution, as a function  $c^{1/2}$ [3]

Due to changes of electrical conductivity based on the reservoir levels (Fig. 1) and the diffusion coefficient of ions (Fig. 2) three layers is predictable. (1) Dissolution layer, (2) ion transfer layer (3) saturated layer (Fig. 3).

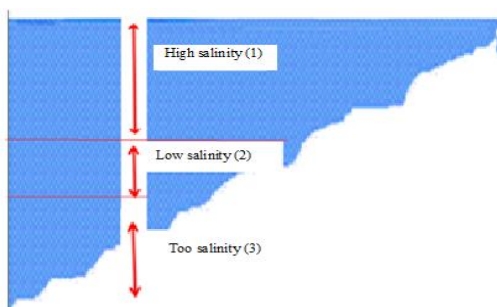


Fig 3. Reservoir water properties based on electrical conductivity (1) high salinity, (2) low salinity and (3) too salinity

The results showed that the use of the clay blanket is not enough. According to the diffusion coefficient (Fig. 2) of sodium ions and chloride, one of the best methods of using an ion shield to stabilize ion on salt formation. Using ion shields such as membranes is very difficult and expensive.

For the first time this idea is presented by this paper" a curtain of natural zeolites/clay ( with 25 cm layers) can be save a huge dam reservoir from salt solution at acceptable limits. After preparation procedures including transport of zeolit to site and scattering, the final thickness of zeolit layer will be 15 cm.

Due to the increased too salinity layer in dam reservoir, gate chamber, drain valves and other Hydraulic equipment will be damaged. Thus it is necessary that salinity layer is drained near the Gachsaran formation( this formation have salt) and so far from Dam body. According to diffusion coefficient of salt (NaCl), the EC of reservoir water gradually will decrease at near Dam body.

#### 4. Conclusions

For the first time, introducing the treatment method based on construction of a zeolite coverage, the same as ion shell, for rehabilitation of huge reservoir of an arched dam. Salt dome will be controlled by this proposal. Natural resources zeolites are abundant and low cost, high adsorption characteristic and it is used by simple method. The zeolite and clay



4<sup>th</sup> Iran National Zeolite Conference  
Golpayegan University of Technology, Golpayegan, Iran  
August 23-24, 2017



blanket (curtain) is a good membrane for sealing and it will reduce diffusion of ions. Then rate of salinity in reservoir will be decrease.

### References

- 1) A Sepasad Engineering Company. (2011). *Report: Introduction and Explanation of the Actions Taken for Treatment of Gachsaran Formation Plan.*
- 2) Iran Water and Power Resources Development Company,(2008) "*General specification of Gotvand Olya project and power plant*", *Iran Tehran.*
- 3) Y. H. Li, *Geochemical et Cosmochimica Acta*, 1974, 38, 703.
- 4) F. Shokrian, K. Solaimani, G. H. Nematzadeh and P. Biparva, *International Journal of Farming and Allied Sciences* 2015, 4 (1), 50-54.
- 5) W. J. Cho, Y. Seo, S. J. Jung, W. G. Lee, B. C. Kim, G. Mathieson, and K. H. Yu, *Bull. Korean Chem. Soc.* 2013, 34( 6) 1693.



4<sup>th</sup> Iran National Zeolite Conference  
Golpayegan University of Technology, Golpayegan, Iran  
August 23-24, 2017



# Posters



# 4<sup>th</sup> Iran National Zeolite Conference

## Golpayegan University of Technology, Golpayegan, Iran

### August 23-24, 2017



## Application of the zeolite on reducing TDS of waste water in great industrial town of shiraz

S. H. Ghetmiri <sup>a\*</sup>, M. Karimi <sup>a</sup>, S. Deilami <sup>a</sup>

<sup>a</sup> Department of Geology, shiraz Branch , Islamic Azad university, shiraz, Iran

\*Email: Hosseinghetmiri@yahoo.com

### 1. Introduction

Industrial sewages depend on the type of industry and processed materials have different combinations. These sewages could be simply biologically analyzed or potentially poisonous, in regard of strong organic element (Ghazban .2002). it means that the amount of impurities of water on that might be 10 to thousands milligram per liter. Nonpurified industrial sewage add pollutants to the receptor waters.receptor waters could include pools, lakes, rivers,coastal waters and seas . Finally leads to environmental pollutions. if the industrial sewages will be refined in an appropriate method , they could be used as the safe and valuable sources in the mentioned cases (Habibollahi 2014).

### 2. Experimental part

In this study the efficiency of zeolite on the TDS factor as catalysis in the exit backwater refinery of shiraz grand industrial town was investigated. Great industrial town of shiraz is located in 15 km of shiraz – Fasa road. and with 1300 hectares area. Activities begin from 1992. This town include food , chemical, cellulose, metallic, weaving ,electronic, minerals industries and services. Zeolite is a network hydrous silicate with strong cation exchange.They forming in alkali lakes, alkali soils, from volcanic tuffs alteration and deep sea sediments. Nearly 40 types zeolite has known in nature. So these minerals are produced synthetically(Evans 1993). Zeolite used in refinery sewage. In iran has found in Rodehen, Qom,Taleghan etc (ghorbani 2002). For doing study there works had performed. Design and make laboratory pilots, set up and calibration, reactor starting, Primary tests and watch process, pilot loading in different sets, change of independent variables, use of softwares for results evaluate. Figures 1 and 2 shown laboratory pilot and used zeolite.



Figure1. Graded zeolite 1 to 3 mm size



Figure2. Active reactor with ground zeolite

In this study by use of Semnan mine zeolite grading 1 to 3 mm as absorbent to be measured qualitative parameters such as TDS, TSS, Ec, pH and COD on the daily to rate 20 liters refined waste water with 24 hours staying duration 3 months.

### 3.Results and discussion

Results obtained from this study in 3 months (february, march and april) has present in table 1.



# 4<sup>th</sup> Iran National Zeolite Conference

## Golpayegan University of Technology, Golpayegan, Iran

### August 23-24, 2017



Table 1 . Decrease of TDS duration 3 months

Time (month)	Entry Average TDS (mg/lit)	Exit Average TDS (mg/lit)	TDS decrease (%)
February	1111	998	10
March	1392	868	37
April	2150	612	71

#### 4. Conclusions

With attention to results obtained, zeolite as catalysis has decreased TDS factor in backwater of refinery sewage of industrial town in shiraz . The results of examinations present that the best operation of zeolite caused 71 percent decreasing in TDS. This method was performed successfully on the exit backwater.

#### Acknowledgments

We acknowledge the management of great industrial town of shiraz.

#### References

- 1)Ghazban F. Environmental Geology. Tehran university press . 2002
- 2)Habibollahi S, Hajjalizadeh A. The study on TDS decrease of industrial sewages by natural zeolite.5th water sewage and garbage conference. 2014
- 3)Evans.A. Introduction ore Deposits 1993.
- 4)Ghorbani M. EconomicGeology.Arian zamin press 2002

## Designing a multi component reaction for facile synthesis of some novel 2-aryl thiazolidin-4-ones bearing benzimidazole moiety by Nano-NiY Zeolite as an Efficient Nano Catalyst

Mehdi kalhor <sup>a\*</sup>, Soodabeh Banibairami <sup>a</sup>, Seyed Ahmad Mirshokraie <sup>a</sup>

<sup>a</sup> Department of Chemistry, Payame Noor University, 19395-4697, Tehran, Iran

\*Email: [mekalhor@gmail.com](mailto:mekalhor@gmail.com), [mekalhor@pnu.ac.ir](mailto:mekalhor@pnu.ac.ir)

#### 1. Introduction

Development the multicomponent chemical reaction (MCRs) in modern organic chemistry is due to the ability of this method in synthesis of wired natural-product-like molecules. Multicomponent reaction as a powerful tools can couples more than two starting reagent to a single pure product which contains the essential parts of starters. [1-2]



4<sup>th</sup> Iran National Zeolite Conference  
Golpayegan University of Technology, Golpayegan, Iran  
August 23-24, 2017



1,3-thiazolidin-4-ones by having sulfur and nitrogen in a five membered ring, are belong to thiazolidones that can be found as a core structure in various synthetic pharmaceutical and agricultural compounds and displaying a broad spectrum of biological activities. They have been employed in the preparation different important drugs such as famotidine, mebendazole and astemizole.[3-4] Nowadays their antifungal, antimicrobial, anticancer, antidiabetic, antiviral and anti HIV activities are reported [5].

On the other hand, biologically and physiologically activity of natural and synthetic molecules that have benzimidazole core have been proved [6]. By considering biological activities of both thiazolidinone and benzimidazole moieties and furthermore, as a part of our ongoing studies on the catalytic synthesis of compounds by benzimidazole nucleus as an important class of fungicides plant, [7] we showed that 2-aminobenzimidazole as an aromatic amine, aromatic aldehydes, and 2-mercaptoacetic acid, under a mild multicomponent reaction that catalyzed by Nano-NiY Zeolite can yield to 2-((1H-benzo[d]imidazol-2-ylamino)(aryl) 1,3-thiazolidin-4-ones **4a-l**.

## 2. Experimental Part

To a mixture of aromatic aldehyde (1 mmol, **2a-l**), 2-aminobenzimidazole (1 mmol, **1**) and thioglicolic acid (1.2 mmol, **3**) in 5ml ethanol, Nano-NiY Zeolite (10W%) as catalyst was added. The reaction mixture stirred magnetically at room temperature for appropriate time as shown in Table 2 (The progress of reaction being monitored by TLC and using n-hexane/ethyl acetate (2:1 v/v) as an eluent). After completion of the reaction, the catalyst was separated by simple filtration and 5 ml water was added and the precipitate product was filtrated and washed with cold ethanol-water. The residue was recrystallized from ethanol-water and air dried.

## 3. Results and discussion

Some novel 2-((1H-benzo[d]imidazol-2-ylamino)(aryl) 1,3-thiazolidin-4-ones were prepared *via* one-pot multicomponent reaction by employing various aromatic aldehydes under the same conditions (Figure 1). The results are presented in Table 1.

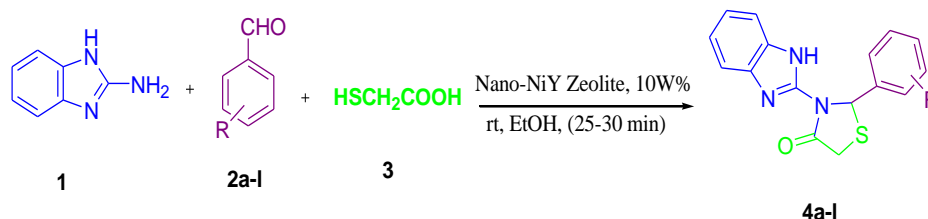


Figure 1. Synthetic method for compounds **4a-l**

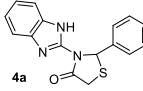
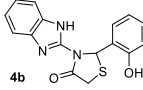
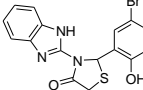
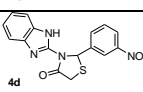
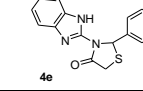
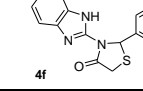
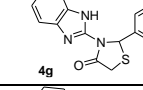
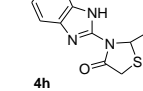
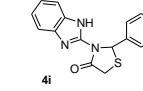
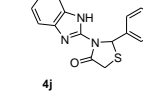
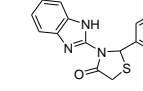
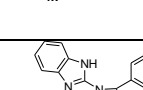
All products are new and their structures were assigned using the spectroscopic data. In the <sup>1</sup>H-NMR spectra, two diastereotopic hydrogen that clearly appears as a doublet and doublet with  $J = 16.23-16.53$  Hz around 3.88 - 4.24 ppm are attributed to the methylene group of the thiazolidinone ring and the singlet signal at 12.40 ppm is refer to the resonance of NH proton of benzimidazole ring. ( Figure 2 ) The other signals were observed at the expected region which is consistent with their structures. In the mass spectra, molecular ion peak (25-100%) can be seen for all of compounds.



4<sup>th</sup> Iran National Zeolite Conference  
Golpayegan University of Technology, Golpayegan, Iran  
August 23-24, 2017



**Table 1.** Synthesis of 2-((1H-benzo[d]imidazol-2-ylamino)(Aryl) 1,3-thiazolidin-4-ones, 4a-l in the presence of 10 W% Nano-NiY Zeolite in ethanol at room temperature.

Entry	R	Product	Time (min)	Yield (%) <sup>a</sup>
1	H	 4a	30	85
2	2-OH	 4b	25	90
3	2-OH-5-Br	 4c	30	93
4	3-NO <sub>2</sub>	 4d	25	93
5	4-NO <sub>2</sub>	 4e	25	95
6	4-Cl	 4f	25	92
7	4-Br	 4g	25	94
8	2-OMe	 4h	30	81
9	4-OMe	 4i	30	84
10	3,4-diOMe	 4j	30	86
11	3-Cl	 4k	30	93
12	4-Me	 4l	30	80



4<sup>th</sup> Iran National Zeolite Conference  
Golpayegan University of Technology, Golpayegan, Iran  
August 23-24, 2017

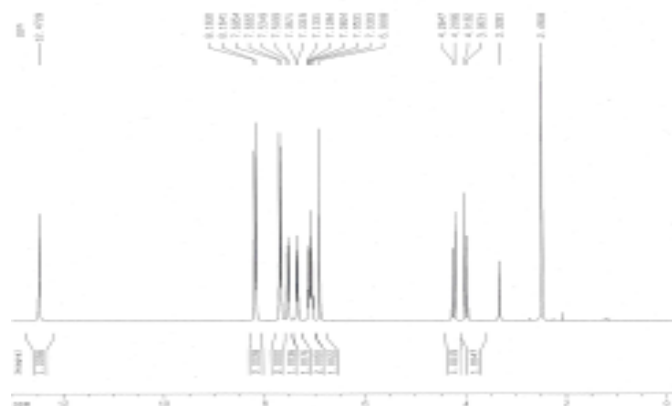


Figure2. <sup>1</sup>H-NMR of (4e)

#### 4. Conclusions

Some novel derivatives of 2-((1*H*-benzo[*d*]imidazol-2-ylamino)(aryl)1,3-thiazolidine-4-one based on 2-aminobenzimidazole core were synthesized in the little amount of ethanol as a solvent via one-pot reaction of 2-aminobenzimidazole, aromatic aldehydes and thioglicolic acid in the presence of catalytic amount of Nano-NiY Zeolite at room temperature. Considering short reaction time, high yield, eliminate the temperature and using of nontoxic solvent and reusable catalyst, we can claim that our chemical design consistent with the goal of green chemistry.

#### References

1. Weber, L. Multicomponent reactions and evolutionary chemistry. *Drug Discov. Today*, **2002**, 7, 143–147.
2. Menendez, J. C. Multicomponent reactions, *Synthesis*, **2006**, 2624–2624.
3. Pola, s. Significance of Thiazole-based Heterocycles for Bioactive Systems, **2016**.
4. Cruz, A., Padilla-Martínez, I. I., García-Báez, E. V., Guerrero-Muñoz, G., Synthesis and Structure of Sulfur Derivatives from 2-Aminobenzimidazole, *Molecules*, **2014**, 19, 13878-13893.
5. Jain, A.K., Vaidya, A., Ravichandran, V., Kashaw, S. K., Agraval, R.K., Recent developments and biological activities of thiazolidinone derivatives: A review, *Bioorg. Med. Chem.*, **2012**, 20, 11, 3378-3395.
6. Panda, S. S., Ritu Malikk, A. B., Jainb, S. C., Synthetic Approaches to 2-Arylbenzimidazoles: A Review, *Current Organic Chemistry*, **2012**, 16, 1905-1919.





4<sup>th</sup> Iran National Zeolite Conference  
Golpayegan University of Technology, Golpayegan, Iran  
August 23-24, 2017



Synthesis and characterization of Zeolite : TiO<sub>2</sub> nanocomposite

B. Barghi<sup>a</sup>, M. Zendehtdel<sup>a\*</sup>

<sup>a</sup> Department of Chemistry, Faculty of Science, Arak University, Arak38156-8- 8349; Iran

\*Email: m-zendehtdel@araku.ac.ir

### 1. Introduction

In today's word, many efforts have been made on synthesis, characterization and application of TiO<sub>2</sub> nanocomposite. Since there are a lot of opportunity to making improvement and modification in the existing method, so synthesis and characterization of new compound will be breakthrough to future designing. In this study we considered a zeolite as a substrate for TiO<sub>2</sub>. then we characterized the feature of synthesized composite by FT-IR, XRD, SEM, DRS.

### 2. Experimental Part or Theoretical Details

The starting materials used in this study included Silica gel, sodium hydroxide, aluminum hydroxide, titanium dioxide and deionized water. All chemical materials supplied by Merck and aqueous solutions were made dissolving them in deionized water. XRD and FT-IR, were used to characterization of obtained product. At first different percent of TiO<sub>2</sub> was mixed with zeolite gel and then nanocomposite of Zeolite:TiO<sub>2</sub> synthesized with hydrothermal method at 100°C for 26 h. The powder was filtered and characterized with FT-IR, XRD, TGA, DRS and SEM.

### 3. Results and discussion

X-ray diffraction pattern of Zeolite:TiO<sub>2</sub> is shown in Fig.1, Some diffraction peaks such as 2θ= 6.20°, 10.10°, 18.65°, 23.50°, 29.45° and 31.25° can be indexed as the Zeolite and 2θ= 25.30°, 37.80°, 40.10° can be indexed as the Titanium Dioxide.

Figure 2 demonstrates the infrared spectra of TiO<sub>2</sub>/zeolite. A shoulder between 3600 and 3450 cm<sup>-1</sup> is assigned to the asymmetrical stretching of H–O–H or O–H bonds, and the bending vibration of the water molecules appears in 1750–1550 cm<sup>-1</sup>. and in these peaks of 1050–950 and 550–400 cm<sup>-1</sup> are Si–O and Al–O bonds respectively. In addition, the Ti–O bond appears in the peaks of 650–500 cm<sup>-1</sup>. So, it can be concluded that the nano-TiO<sub>2</sub> particles have no effect on the structure of the zeolite.

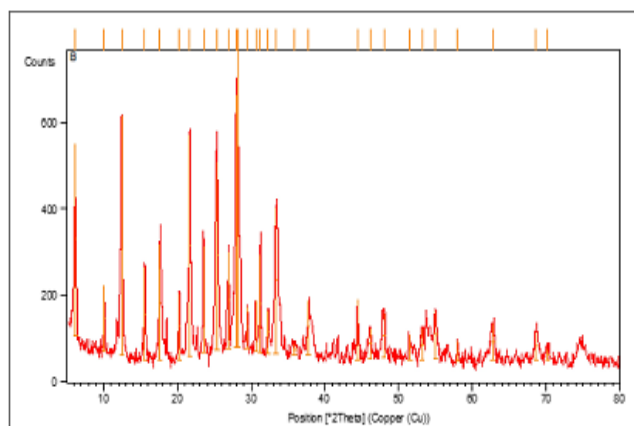


Figure 1 XRD pattern of Zeolite:TiO<sub>2</sub> nanocomposite,



# 4<sup>th</sup> Iran National Zeolite Conference

## Golpayegan University of Technology, Golpayegan, Iran

### August 23-24, 2017

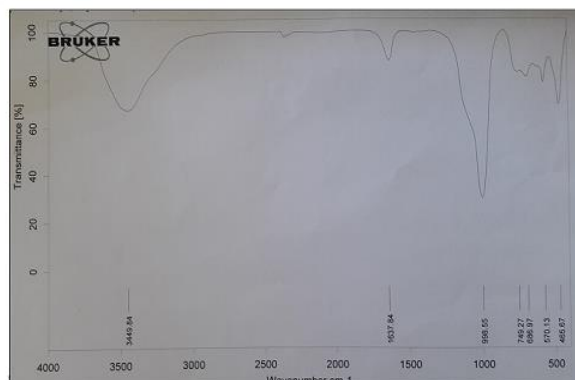


Figure 2 FT-IR spectra of Zeolite:TiO<sub>2</sub> nanocomposite

The SEM picture for nanocomposite shows that there are two phase in the composite. As shown in Fig. 3, it is easy to find that the nano-TiO<sub>2</sub> particles were just supported on the surface of the zeolite, and the size of TiO<sub>2</sub> particles is a few nanometers.

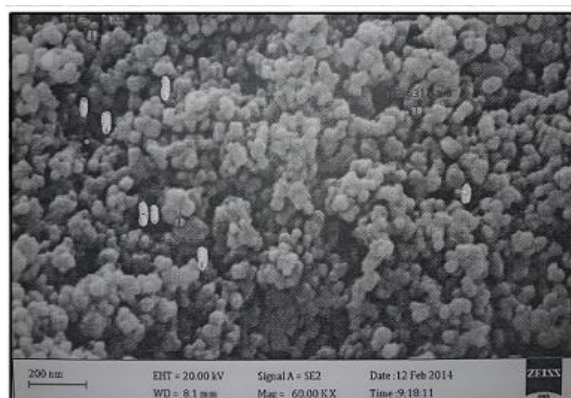


Figure 3 SEM micrograph of Zeolite:TiO<sub>2</sub> nanocomposite

### Acknowledgments

Thanks are due to the Iranian Nanotechnology Initiative and the Research Council of Arak University of Technology and Center of Excellence in the Chemistry Department of Arak University of Technology for supporting of this work.

### References

- 1) Review Article Zeolite Y: Synthesis, Modification, and Properties—A Case Revisited.
- 2) ASTM D3906 Standard Test Method for Determination of Relative X-ray Diffraction Intensities of Faujasite-Type Zeolite-Containing Materials.
- 3) T.A.AL-Dhahir Diyala Journal For Pure Sciences Vol: 9 No: 2, May 2013
- 4) Kheamrutai Thamaphat<sup>1\*</sup>, Pichet Limsuwan<sup>1</sup> and Boonlaer Ngotawornchai<sup>2</sup> Kasetsart J. (Nat. Sci.) 42 : 357 - 361 (2008)
- 5) <https://web.chemdoodle.com/demos/iza-zeolite-explorer/>



# 4<sup>th</sup> Iran National Zeolite Conference

## Golpayegan University of Technology, Golpayegan, Iran

### August 23-24, 2017



## Adsorption and desorption of water in nanoporous sodium metal–organic framework

Zarin Moghadam<sup>a</sup>, Zhaleh Moradi<sup>a</sup>, Kamran Akhbari<sup>\*a</sup>

<sup>a</sup> Department of Chemistry, Faculty of Science, University of Tehran, Tehran 14155-6455, Iran

\*Email: akhbari.k@khayam.ut.ac.ir

### 1. Introduction

Coordination compounds with infinite structures have been intensively studied, in particular, compounds with backbones constructed from metal ions as connectors and ligands as linkers, the so-called “coordination polymers. [1-2] Metal–organic frameworks (MOFs) are materials that are constructed from metal-based nodes and organic linkers [3-4]. The combination of these two building units leads to the formation of crystalline, porous structures, which, in many instances have unique chemical functionality. [5-6] Continuing our previous works on synthesizing of  $[\text{Na}(\text{HB-4-hps})(\text{H}_2\text{O})]_n$  ( $1 \cdot \text{H}_2\text{O}$ ) as metal organic framework, in this work we focused on modulation of the compound structure by reversible removal of guest molecules. Thus, in this work, we wish to report an example of the one which is a reversible exchange of solvent molecules in a sodium metal-organic framework complex without important change in its structure.

### 2. Experimental

All reagents and solvents for the synthesis and analysis were commercially available and were used as received. To prepare the nanostructure of compound ( $1 \cdot \text{H}_2\text{O}$ ) by sonochemical process we used ultrasonic bath. so nano particle of  $[\text{Na}(\text{HB-4-hps})(\text{H}_2\text{O})]_n$  was obtained. the Nano powder of compound ( $1 \cdot \text{H}_2\text{O}$ ) was heated at 180 °C in a furnace and stayed for 3h in atmosphere of air so  $[\text{Na}(\text{HB-4-hps})]_n$  (1) was obtained. In order to study adsorption of water and the reversibility in these Na metal organic -framework, the nano particle of 1 was immersed in water for three days.

### 3. Results and discussion

A comparison between the XRD patterns simulated from single crystal X-ray data (Fig. 1a) and that of the prepared powder (Fig. 1b), approved the formation of  $[\text{Na}(\text{HB-4-hps})(\text{H}_2\text{O})]_n$  ( $1 \cdot \text{H}_2\text{O}$ ). Fig 1c shows the XRD pattern of ( $1 \cdot \text{H}_2\text{O}$ ) after thermal treatment at 180°C. It shows that the structure of 1 approximately is similar to  $1 \cdot \text{H}_2\text{O}$  but with no crystalline water molecules. In order to check the reversibility of this process, we immersed 1 in water for three days. XRD pattern of it is exactly similar to the simulated pattern form from single crystal X-ray data (Fig.1a) the experimental pattern of the as-synthesized phase approved the reversibility of this desorption and adsorption process of water in  $1 \cdot \text{H}_2\text{O}$ .



4<sup>th</sup> Iran National Zeolite Conference  
Golpayegan University of Technology, Golpayegan, Iran  
August 23-24, 2017

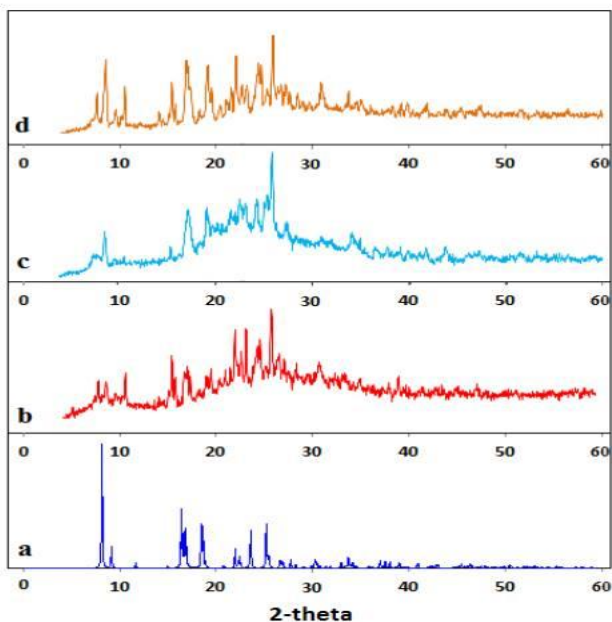


Fig. 1 XRD patterns; a) simulated pattern based on single crystal data of compound  $[\text{Na}(\text{HB}-4\text{hps})(\text{H}_2\text{O})]_n \cdot 1.5\text{H}_2\text{O}$ , b) compound  $1.5\text{H}_2\text{O}$  nanoparticles synthesized by sonochemical process, c) nanoparticles of  $[\text{Na}(\text{HB}-4\text{hps})]_n \cdot 1$  metal-organic framework after thermal treatment of  $1.5\text{H}_2\text{O}$  at  $180^\circ\text{C}$ , d) compound  $1.5\text{H}_2\text{O}$  obtained after immersing 1 in water.

Figure 2 a-c shows the SEM images of compound  $1.5\text{H}_2\text{O}$  during water desorption-adsorption process. It shows that

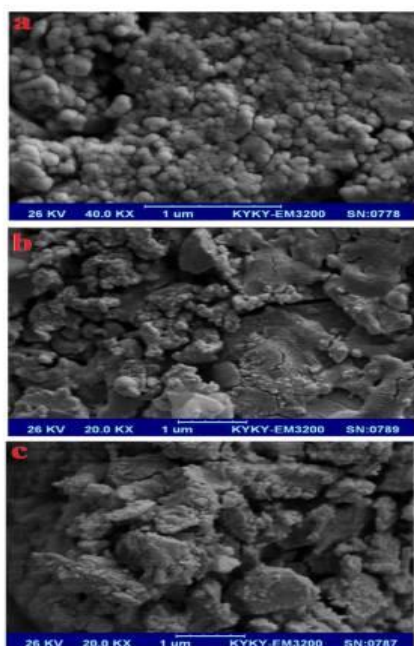


Fig.2 SEM images of a) compound  $1.5\text{H}_2\text{O}$  nanoparticles synthesized by sonochemical process, b) nanoparticles of  $[\text{Na}(\text{HB}-4\text{hps})]_n \cdot 1$  metal-organic framework after thermal treatment of  $1.5\text{H}_2\text{O}$  at  $180^\circ\text{C}$  and c) compound  $1.5\text{H}_2\text{O}$  obtained after immersing 1 in water.

during this solid-state process, the morphology of it changes and agglomeration was occurred.



4<sup>th</sup> Iran National Zeolite Conference  
Golpayegan University of Technology, Golpayegan, Iran  
August 23-24, 2017



#### 4. Conclusions

In summary, nanoparticles of  $[\text{Na}(\text{HB}-4\text{-hps})(\text{H}_2\text{O})]_n$  ( $1.\text{H}_2\text{O}$ ) metal-organic framework morphology was synthesized by sonochemical process. Guest water molecules can be removed from the nanopores of  $1.\text{H}_2\text{O}$  by thermal treatment at  $180\text{ }^\circ\text{C}$  in a furnace and static atmosphere of air for 3 h. This process is reversible. nanoparticles of  $[\text{Na}(\text{HB}-4\text{-hps})]_n$  (1) can easily absorb water again by immersing in water.

#### Acknowledgments

The authors would like to acknowledge the financial support of University of Tehran for this research under Grant number 01/1/389845

#### References

- [1] X.W. Lou, L.A. Archer, Z. Yang, *Adv. Mater.* 20, 3987 (2008)
- [2] Y. Zhao, L. Jiang, *Adv. Mater.* 21, 3621 (2009)
- [3] S. Kitagawa, R. Kitaura, S-I. Noro, *Angew. Chem. Int. Ed.* 43 (2004) 2334-2375.
- [4] M. O'Keeffe, M. A. Peskov, S. J. Ramsden and O. M. Yaghi, *Acc. Chem. Res.*, 2008, 41, 1782–1789.
- [5] G. Ferey, *Chem. Soc. Rev.*, 2008, 37, 191–214.
- [6] S. Horike, S. Shimomura and S. Kitagawa, *Nat. Chem.*, 2009, 1, 695–704.

## Host (nanocavity of dealuminated zeolite-Y)-guest (substituted heteropoly acid) as an efficient photocatalyst in the removal of methyl orange

M. Moosavifar<sup>a\*</sup>, F. Mavadat, B. Pezeshki

<sup>a</sup>Department of Chemistry, Faculty of Science, University of Maragheh, P.O. Box 55181-83111, Maragheh, Iran

\*Email: m.moosavifar90@gmail.com)

#### 1. Introduction

Heteropoly acids are known to be active, exhibit the unique property of structural stability and redox activity which facilitate photocatalytic activity because of suitable HOMO-LUMO gap [1,2]. These systems act as “electron reservoirs” because of their high capacity of accepting electrons without a major change in their structure. This, in turn causes heteropoly acids were tested as photocatalysts in the degradation of aqueous pesticides [3]. Meanwhile, the substituted heteropoly acid introduced to improvement the physico-chemical properties and catalytic activity [4]. However, the main drawback of homogeneous heteropoly acid is low surface area and its high solubility in polar solvent which recovery and separation become difficult. Here, we wish to report the zeolite-supported Ti-substituted POM to increase the photocatalytic activity. The photocatalytic activity of these systems was investigated in the photodecoloration of methyl orange.



# 4<sup>th</sup> Iran National Zeolite Conference

## Golpayegan University of Technology, Golpayegan, Iran

### August 23-24, 2017



## 2. Experimental Part

All materials were of the commercial reagent grade and were used without any purification. In a typical procedure, NaY zeolite was dealuminated by chemical operation with EDTA treatment. In a typical procedure, Ti-substituted 12-molybdophosphoric acid was prepared in the nanocage of the dealuminated Y zeolite by ship-in-a-bottle method with different stoichiometric ratios of Mo and Ti. The prepared photocatalysts were used in the photodecoloration of methyl orange.

## 3. Results and discussion

NaY was dealuminated by post-synthesis method with EDTA treatment which causes increasing in hydrophobicity of surface, therefore the absorption of organic dye on zeolite surface enhances which followed by increasing in the photocatalytic activity. The FT-IR spectra confirm the existence of MPA intonanocage of dealuminated Y zeolite (Fig. 1).

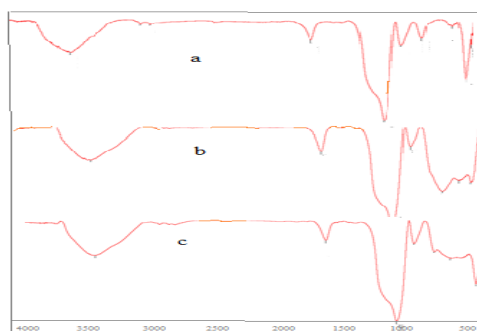


Fig. 1. FTIR spectra a)  $H_3PMo_{12}O_{40}/Y/TiO_2$  b)  $H_5PMo_{11}TiO_{40}/Y$  c)  $H_5PMo_{10}Ti_2O_{40}/Y$

FESEM of the  $Ti_n$ HPA/HY indicated the cubo-octahedral units that proved zeolite structure was preserved after the insertion of  $Ti_n$ HPA in the nanocage of zeolite (Fig. 2).

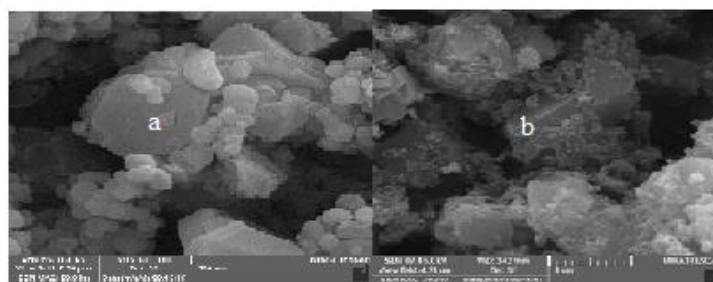


Fig. 2. FESEM micrograph of a)  $H_5PMo_{11}TiO_{40}/Y$  b)  $H_5PMo_{10}Ti_2O_{40}/Y$

Analysis of tri point EDS proved the presence of Ti-HPA on zeolite surface and zeolite nanocage (Fig. 3).

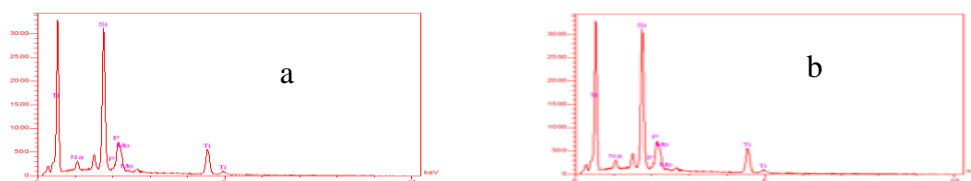


Fig. 3. EDS analysis of a)  $H_5PMo_{11}TiO_{40}/Y$  b)  $H_5PMo_{10}Ti_2O_{40}/Y$



4<sup>th</sup> Iran National Zeolite Conference  
Golpayegan University of Technology, Golpayegan, Iran  
August 23-24, 2017



The photocatalytic activity of these systems investigated in the photodecoloration of methyl orange. The results showed base on the increasing in Ti content, the photocatalytic activity of systems enhanced and decoloration performed efficiently (Fig. 4).

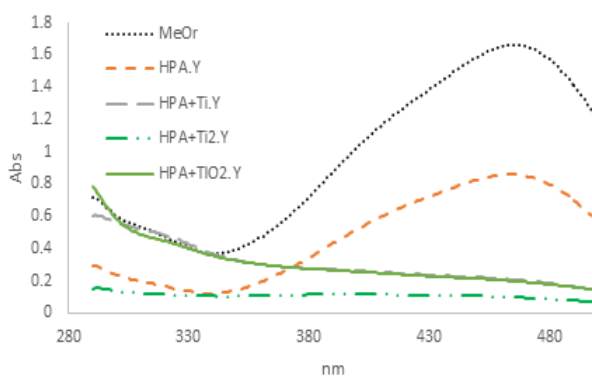


Fig.4. Effect of Ti amount on the photodecoloration of Methyl orange

In this case, Ti incorporated in HPA structure, in the other hand, Mo was substituted by Ti atoms ( $H_5PMo_{10}Ti_2O_{40}/Y$ ), therefore, not only acts as well as HPA/TiO<sub>2</sub>/Y and decolorated methyl orange in the presence of UV but also the leaching of Ti is ignorable in comparison with HPA/TiO<sub>2</sub>/Y and photocatalytic activity is preserved. photodecoloration process proved this claim (Fig. 4).

#### 4. Conclusions

In this work,  $H_{3+2x}PMo_{12-x}Ti_xO_{40}/Y$  were synthesized using ship-in-a-bottle method. These heterogeneous catalysts were characterized by XRD, FT-IR, FESEM, ICP AND EDS technique. The photocatalytic activity of these systems was investigated in the photodecoloration of methyl orange. With increasing in Ti content, the photocatalytic activity enhanced.

#### References

- 1) C. Tiejun, L. Yuchao, P. Zhenshan, L. Yunfei, W. Zongyuan, D. Qian J. Environ. Sci. **2009**, 21, 997 .
- 2) S. Anandan, M. Yoon, Sol. Energy Mater. Sol. Cells **2007**, 91, 143.
- 3) Y. Guo, Y. Wang, C. Hu, Y. Wang, E. Wang, Y. Zhou, S. Feng, Chem. Mater. **2000**, 12, 3501.
- [4] O.A. Kholdeeva, Topics in Catalysis **2006**, 40, 229.
- [5] V. Dufaud , F. Lefebvre, Materials 2010,3, 682.



4<sup>th</sup> Iran National Zeolite Conference  
Golpayegan University of Technology, Golpayegan, Iran  
August 23-24, 2017



**Design and synthesis of nanocrystalline MnFe<sub>2</sub>O<sub>4</sub>-modified natural clinoptilolite and their catalytic application in chalcone and pyridine derivative synthesis**

Noshin Mir\*, Reza Arian, Amin Kharadeh

Department of Chemistry, University of Zabol, P.O. Box 98615-538, Zabol, Islamic Republic of Iran

\*Email: n.mir@uoz.ac.ir

### 1. Introduction

The development of environment friendly technologies has promoted much research in heterogeneous catalysis and in particular the heterogenization of known active homogeneous catalysts. Natural porous products have been recently considered as one of the promising materials for catalytic applications in terms of being eco-friendly, cost-effective, highly porous, and very effective. One of the natural porous materials suitable for this purpose is natural clinoptilolite which is abundantly found in Semnan region, Iran. One of the disadvantages of this material is its low catalytic activity. This problem could be raised with incorporation of some Lewis acids in the porous structure of the substrate. MnFe<sub>2</sub>O<sub>4</sub>, a magnetic nanomaterial is known as an efficient Lewis acid for the synthesis of organic compounds [1]. Due to its magnetic properties, the final MnFe<sub>2</sub>O<sub>4</sub>/clinoptilolite could be easily separated from the solution by the aid of an external magnet. In the present study, nanocrystalline MnFe<sub>2</sub>O<sub>4</sub>-modified natural clinoptilolite possessing redox properties have been designed and synthesized. Then, these nanocatalysts have been applied in the synthesis of chalcone and pyridine derivatives and their effect on the reaction rates, products' yields and products' purity has been studied. Chalcone derivatives are one of the building blocks presented in the structure of flavonoids which have exhibited numerous pharmacological activities as anticancer, antiinflammatory, antireproduction and antioxidant agents.

### 2. Experimental

In order to prepare the homoionic Na<sup>+</sup>-exchanged form of the clinoptilolite, the required amount was stirred in 2 mol L<sup>-1</sup> of NaCl solution for 50 about 24 h at 25 °C, and then the Na<sup>+</sup>-nanozeolite clinoptilolite was filtrated and washed with distilled water (50 mL) two times. The Na<sup>+</sup>-nanozeolite was dried in an oven at 100 °C. The Na<sup>+</sup>-nanozeolite clinoptilolite (5 g) was taken into a 250 mL round bottom flask and 100 mL 4 M sulfuric acid was added to it [2]. Then the required amount of the prepared zeolite was added to water. Fe<sub>2</sub>(SO<sub>4</sub>)<sub>3</sub>.H<sub>2</sub>O (3 mmol) and MnCl<sub>2</sub> (3 mmol) were used in a stoichiometric ratio of 2 : 1. A homogeneous aqueous solution of 1g CTAB was prepared by stirring for 10 min. Then the CTAB solution was added to the zeolite solution. After that, MnCl<sub>2</sub> was added to the solution under N<sub>2</sub> atmosphere on vigorous stirring and the reaction temperature was kept between 90–100 °C 1 h. After that aqueous ammonium hydroxide was added into the reaction mixture to maintain the pH of 13–14, and the resulting solution was magnetically stirred for another 2 h. On completion of the reaction, the solution was transferred to a Teflon-line autoclave and was heated at 250 °C for 4h. After cooling the autoclave, the obtained black precipitate was washed with deionized water and then dried at 100 °C for 12 h. Three different catalysis as well as pure MnFe<sub>2</sub>O<sub>4</sub> were prepared with different concentrations of the nanoparticles including 10, 20, and 30 weight percent of MnFe<sub>2</sub>O<sub>4</sub> nanocrystals in clinoptilolite which are denoted as 3, 2, and 1, respectively.

### 3. Results and discussion

The SEM pattern for the Zeolite-MnFe<sub>2</sub>O<sub>4</sub> nanocrystals is shown in Fig. 1. It is observed that agglomerated nanoparticles with the size of less than 100 nm are formed in the zeolite substrate.





4<sup>th</sup> Iran National Zeolite Conference  
Golpayegan University of Technology, Golpayegan, Iran  
August 23-24, 2017

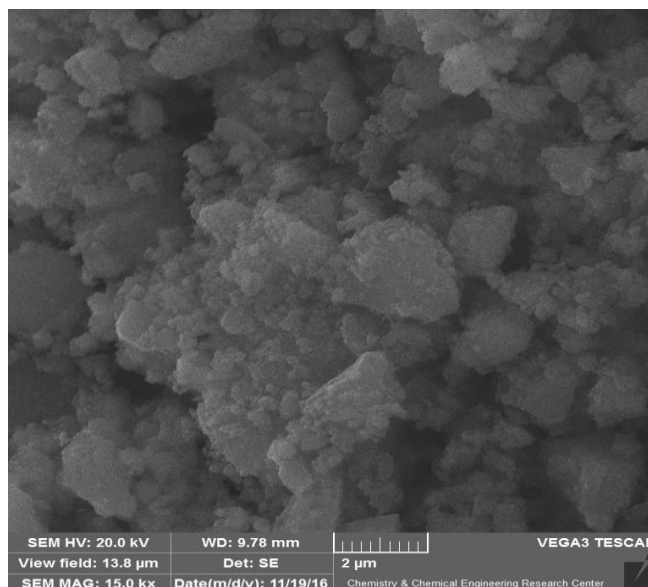


Figure 1. SEM image of MnFe<sub>2</sub>O<sub>4</sub>-modified natural clinoptilolite (sample 1).

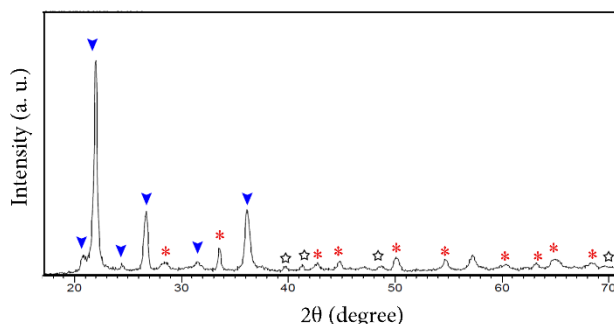


Figure 2. XRD pattern of the prepared MnFe<sub>2</sub>O<sub>4</sub>-modified natural clinoptilolite (sample 1).

Blue arrow: clinoptilolite red stars: MnFe<sub>2</sub>O<sub>4</sub>, empty stars: Fe<sub>2</sub>O<sub>3</sub>

The XRD patterns of sample 3 is shown in Figure 2.. The characteristic lines of clinoptilolite crystallites are assigned which have good agreement with JCPDS No. 39-1383. The XRD pattern reflections of MnFe<sub>2</sub>O<sub>4</sub> phase are labelled with red stars which agree with JCPDS No. 01-074-2403. Some weak peaks representative of slight amount of Fe<sub>2</sub>O<sub>3</sub> impurities are also observed which are labelled with black empty stars.

The interactions between benzaldehyde and acetophenone are represented schematically in Figure 3. The results of the catalytic reaction including the reaction time and yield are presented in Table 1. It is observed that sample 1 with the highest weight percent of MnFe<sub>2</sub>O<sub>4</sub> gives the best results.



4<sup>th</sup> Iran National Zeolite Conference  
Golpayegan University of Technology, Golpayegan, Iran  
August 23-24, 2017

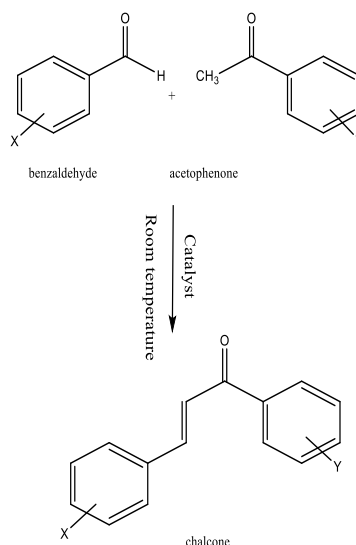


Figure 3. Synthesis of chalcone derivatives by Zeolite/MnFe<sub>2</sub>O<sub>4</sub>

Table 1. Comparison of the nanocatalysts

Catalyst	Benzaldehyde	Acetophenone	Yield %	Time (min)
1	4-chloro	acetophenone	96	15
2	4-chloro	acetophenone	92	25
3	4-chloro	acetophenone	90	25
MnFe <sub>2</sub> O <sub>4</sub>	4-chloro	acetophenone	90	50

#### 4. Conclusions

Manganese ferrite (MnFe<sub>2</sub>O<sub>4</sub>) and three Zeolite-MnFe<sub>2</sub>O<sub>4</sub> nanocrystals were synthesized by a hydrothermal method. The results indicate that the use of novel MnFe<sub>2</sub>O<sub>4</sub>-modified natural clinoptilolite nanocatalysts led to improving the reaction factors such as yields and the reaction times. Moreover, ambient reaction temperatures, simple product purification, not using harmful and toxic organic solvents and good catalyst reusability are the other significant advantages of using these novel nanocatalysts for the synthesis of chalcone derivatives.

#### References

- [1] G. Brahmachari, S. Laskar, P. Barik, Magnetically separable MnFe<sub>2</sub>O<sub>4</sub> nano-material: an efficient and reusable heterogeneous catalyst for the synthesis of 2-substituted benzimidazoles and the extended synthesis of quinoxalines at room temperature under aerobic conditions, RSC Advances, 3 (2013) 14245-14253.
- [2] S.M. Baghbanian, Synthesis, characterization, and application of Cu<sub>2</sub>O and NiO nanoparticles supported on natural nanozeolite clinoptilolite as a heterogeneous catalyst for the synthesis of pyrano[3,2-b]pyrans and pyrano[3,2-c]pyridones, RSC Advances, 4 (2014) 59397-59404.



4<sup>th</sup> Iran National Zeolite Conference  
Golpayegan University of Technology, Golpayegan, Iran  
August 23-24, 2017



**Synthesis of a new nanoporous metal-organic framework and Sodium Sulfate nanostructure from it**

Sahar Usefi<sup>a</sup>, Zhaleh Moradi<sup>a</sup>, Kamran Akhbari\*<sup>a</sup>

<sup>a</sup> School of Chemistry, College of Science, University of Tehran, Tehran, 14155-6455, Islamic Republic of Iran

\*Email: akhbari.k@khayam.ut.ac.ir

### 1. Introduction

Metal-organic frameworks (MOFs) represent a new class of hybrid organic-inorganic supramolecular materials comprised of ordered networks formed from organic electron donor linkers and metal cations [1, 2]. Now constituting thousands of distinct examples, MOFs are an intriguing class of hybrid materials that exist as infinite crystalline lattices with inorganic vertices and molecular-scale organic connectors [3, 4]. Solid-state coordination chemistry is a versatile greener alternative to conventional synthesis, offering quantitative yields, enhanced stoichiometric and topological selectivity, access to a wider range of precursors, as well as to molecules and materials not readily accessible in solution or solvothermally [5]. In this work we investigate the reaction between bis (4-hydroxyphenyl) sulfone ligand (H<sub>2</sub>B-4-hps) and NaOH, provides a crystalline material with formula [Na(HB-4-hps) (H<sub>2</sub>O)]<sub>n</sub> (1).

### 2. Experimental

All chemicals and reagents were used as received without purification. [Na(HB-4-hps)(H<sub>2</sub>O)]<sub>n</sub> was prepared by reacting between NaOH(1mmol), H<sub>2</sub>B-4-hps(1mmol) and distilled water (25cc). All reactions were carried out under ambient conditions. To prepare the [Na(HB-4-hps)(H<sub>2</sub>O)] (1) by sono-chemical process, an ultrasonic bath is used with the power 28 kHz. The initial concentrations ratios of the reactants (NaOH : H<sub>2</sub>B-4-hps) for the sample are 0.8 : 0.16 M. A solution of NaOH (10 ml) was added dropwise to the solution of H<sub>2</sub>B-4-hps (10ml) under sonication. The solid were separated and dried. For preparation of Na<sub>2</sub>SO<sub>4</sub> nanoparticles thermal decomposition of compound 1 nanostructure was done at 600 °C in static atmosphere of air for 3hours.

### 3. Results and discussion

Structural determination by single crystal X-ray diffraction was done for 1. The initial building block of the molecular structure of this compound is shown in Fig1-a. The HB-4-hps ligand has not been completely deprotonated and binds to four sodium ions. Sodium atoms bind to five oxygen atoms of HB-4-hps ligand and one oxygen atoms of H<sub>2</sub>O, and are six coordinated. The structure of this nanoporous metal-organic framework that have pores channels with diameter of 0.7×0.7 nm is shown in Fig 1.b. The pores of this compound was empty in the crystal structure, and no guest water molecules that was used as solvents, was observed. To investigate the thermal stability of the single crystal 1, TG-DTA in the temperature range of 20-560 °C in nitrogen atmosphere was carried out. TG-DTA data show that the endothermic elimination of water molecules in single crystals 1 starts at 117 °C and the process of weight loss continues up to 160 °C with 4.9% of weight loss. The remaining compounds that may be considered as anhydrous compounds of [Na(HB-4-hps)] is stable till 327 °C and the endothermic peak that appear at 360 °C showed the decomposition of this compound. A comparison between the XRD simulated pattern of single crystal X-ray crystal data of 1(Fig.2a) and its nano structures prepared by sono chemical process (Fig.2b) confirmed the formation of compound 1. Fig 3a shows the original morphologies of it. Compound 1 nanostructure were used as new precursor for synthesis of Na<sub>2</sub>SO<sub>4</sub> nanostructures. Fig.2c, shows the XRD pattern obtained from this reaction and Fig.3b shows the SEM image of Na<sub>2</sub>SO<sub>4</sub> nanoparticles obtained from this process.



4<sup>th</sup> Iran National Zeolite Conference  
Golpayegan University of Technology, Golpayegan, Iran  
August 23-24, 2017

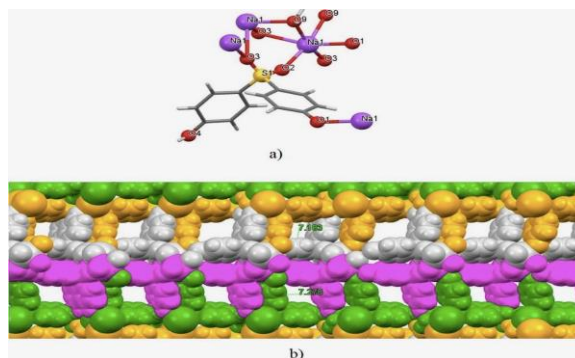


**Figure 1.** a) The initial building block of compound  $[\text{Na}(\text{HB-4hps})(\text{H}_2\text{O})]_n$ . b) The structure of this nanoporous metal-organic framework that have pores channels with diameter of  $0.7 \times 0.7$  nm.

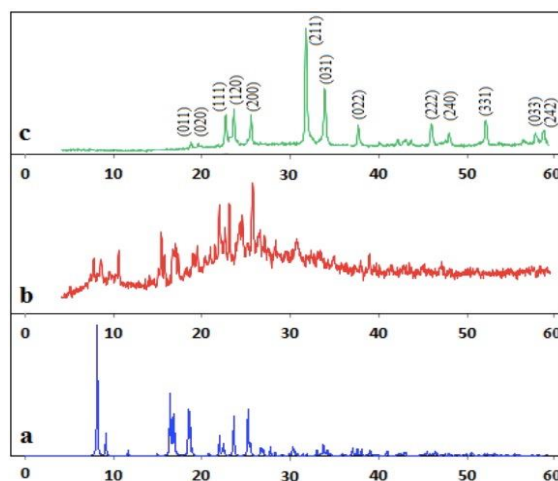


**Figure 2.** a) XRD patterns; a) simulated pattern based on single crystal data of  $[\text{Na}(\text{HB-4hps})(\text{H}_2\text{O})]_n$ . b) 1 nanostructures prepared by sonochemical process. c)  $\text{Na}_2\text{SO}_4$  nanoparticles synthesized by thermal decomposition of 1 at  $600^\circ\text{C}$ .

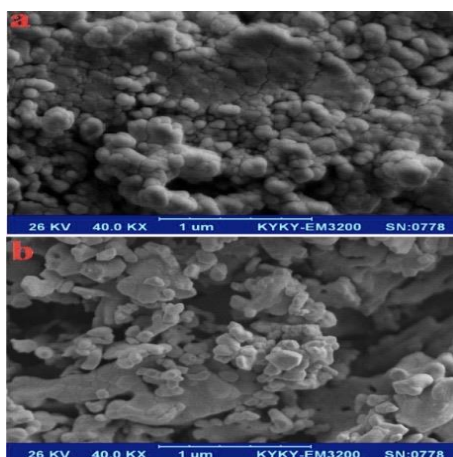


**Figure 3.** SEM images of a) 1 nanostructures prepared by sonochemical process. b)  $\text{Na}_2\text{SO}_4$  nanoparticles synthesized by thermal decomposition of 1 at  $600^\circ\text{C}$

#### 4. Conclusions

In summary,  $[\text{Na}(\text{HB-4hps})(\text{H}_2\text{O})]_n$  (1) was synthesized from the reaction between  $\text{H}_2\text{B-4hps}$  and  $\text{NaOH}$ . The



# 4<sup>th</sup> Iran National Zeolite Conference

## Golpayegan University of Technology, Golpayegan, Iran

### August 23-24, 2017



structure of this nanoporous metal-organic framework that have pores channels with diameter of  $0.7 \times 0.7$  nm was synthesized and its structure was determined by Single crystal X-ray crystallography. The pores of this compound was empty in the crystal structure, and no guest water molecules that was used as solvents was observed in them. Nano structure of 1 was synthesized by sonochemical process and used for preparation of  $\text{Na}_2\text{SO}_4$  nanoparticles.

#### Acknowledgments

The authors would like to acknowledge the financial support of University of Tehran for this research under Grant number 01/1/389845

#### References

- 1) Scott. T. Meek, Jeffery. A. Greathouse, Mark. A. Allendorf, Adv. Mater. 2011, 23, 249–267.
- 2) J. Mater. Chem., 2006,16, 626-636
- 3) J. Am. Chem. Soc., 2008, 130 (42), 13850–13851
- 4) Y. Li, H. Bux, A. Feldhoff, G. Li, W. Yang, J. Caro, Mater, 2010, 22, 3322-3326.
- 5) C. Mottillo, T.Friscic, Molecules 2017, 22, 144.

## The use of Clinoptilolite Zeolite to prevent of lethal concentration by ammonia in, Beluga Sturgeon (*Huso huso*) in vitro

Omid Ehsaniyan<sup>a</sup>, Mohammad Farhangi\*<sup>a</sup>,

<sup>a</sup> Departments of Natural Resources and Agriculture, Gonbad Kavous, Gonbad Kavous University, Iran.

\*Email: s.farhangi@yahoo.com

### 1. Introduction

Ammonia is the original nitrogenous pond products of fishes that emanated from decomposition of unused diets and fish excrements in water environments (Frances *et al.*, 2000). Ammonia appears to have a direct effect on the growth of aquatic animals (Colt, 2006) and cause decreased growth, disease resistance (Lemarie *et al.*, 2004) or even killed the culturing fishes (Wang *et al.*, 2000). Zeolites are one of the most effective materials that able to absorb the ammonia compounds. One of the best zeolites in ammonia removal is Clinoptilolite (Bergero *et al.*, 1994). This research tried to determine lethal concentration (LC96) of ammonia compounds on beluga sturgeon and survey the effects of Clinoptilolite zeolite to removal of ammonia compounds from water environment.

### 2. Materials and methods

The trial performed in Shahid Marjani Sturgeon Culturing Center, Iran. Temperature in all stages maintained to 26°C and pH were equivalent 8.2. Used ammonia was ammonium chloride (made by Merck Company; Germany). Total ammonia concentrations were measuring with hack colorimeter DR/890 (made by USA). All testing procedures were conducted to static water method. This experiment consists of two stages preliminary and main test:

In first, the experiment was conducted to determine the lethal concentration of total ammonia at 96 h in juvenile Beluga sturgeons and also from different amounts 0, 15, 30, 50, 75 mg/lit of ammonia salt were used with five



# 4<sup>th</sup> Iran National Zeolite Conference

## Golpayegan University of Technology, Golpayegan, Iran

### August 23-24, 2017



treatments in triplicate, also In each basin 6 fishes with average weight  $46 \pm 5$  g and total length  $22 \pm 4$  cm were placed. After determine the lethal concentration of ammonia (LC96) in Beluga juveniles, the main test to measure the efficiency of zeolite was assessed in removal of ammonia lethal concentration. The used zeolite was Clinoptilolite type with 90 % purity. In this stage, 180 fishes in 12 basins (with 35 liters capacity) were used and in each basin 15 fishes with the same weight and total length in first stage were placed. Initially the amount of substantial ammonia in the water was measured and then each basin equivalent to 50 mg/lit ammonia salt was added according to preliminary test. Granulated zeolite at 3 treatments in 5, 10, 15 g/lit with three replications for each treatment and a control treatment was used. Until the end testing, once every 12 hours the amount of ammonia in the water basin was measured. Air-stone has been used in treatment as an aerator. Samples were taken from gill, kidney and liver of fish and histopathological sections were prepared. The results were compared by ANOVAs (Analysis of Variance).

### 3. Results and discussion

Based on the results in preliminary stage, highest mortality rate in doses of 50 and 75 mg/lit were observed. Ionized ammonia lethal concentrations were equivalent to 50 mg/lit in sturgeon fishes at 96 hours (Fig. 1). In first treatment as control treatment no mortality was observed. First behavioral symptoms such as gasping, swallowing water, the curvature of muscles, hit the basin sides, lack of balance and severe reaction to external factors were observed in fishes and over time, sat on the floor of the basins while resting back and eventually died. With increasing zeolite in each treatment, the survival rate of fish also increased significantly ( $p < 0.05$ ). Figure 2 indicate ionized ammonium decreased after 96 h in treatments. Application of 15g/l granulated zeolite could be prevented the mortality after 96 hours (fig. 3). The studied of histological samples show that, The common lesions of fish gill exposed to ammonia lethal concentration were hyperplasia, edema, hyperemia, hemorrhage, expansion of secondary lamella, epithelial cells necrosis of gill and inflammation. In control group and zeolite without ammonia group less hyperplasia in tip of gill filaments and edema observed too. The major lesions in kidney were such as expansion of Bowman's capsule, hemorrhage, hyperemia, degenerated tubules of kidney, epithelial cells necrosis of kidney and a lot of monocellular. In fishes kidney of control absorb any lesions. The lesions in liver were hyperemia, hemorrhage, inflammatory cells infiltration and hepatocytes necrosis. In control group and zeolite without ammonia group absorb any lesions. The fish exposed to lethal concentration of  $N-NH_4^+$  adding Clinoptilolite zeolite the lesions were observed just less toxicity of ammonia (fig. 4, 5)

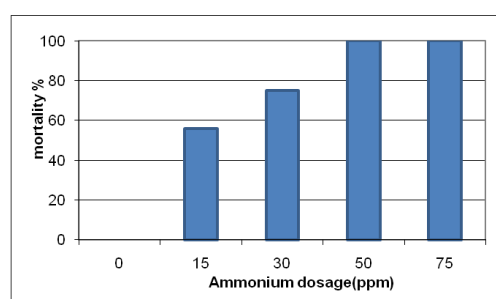


Fig. 1- Fish mortality in different dosage of ammonia

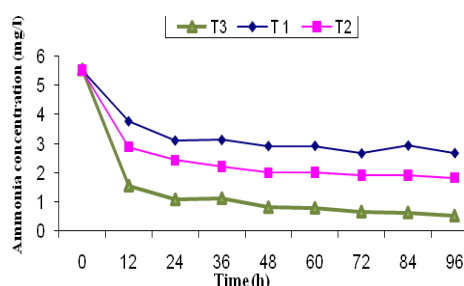


Fig. 2- Decreasing the ammonia (NH<sub>3</sub>) concentration during



# 4<sup>th</sup> Iran National Zeolite Conference

## Golpayegan University of Technology, Golpayegan, Iran

### August 23-24, 2017

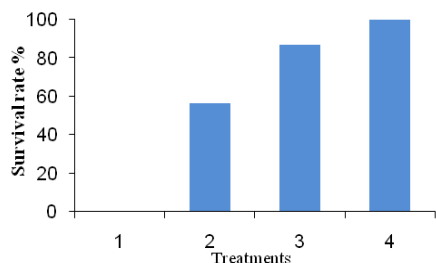


Fig. 3- Survival rate of the fishes in main test

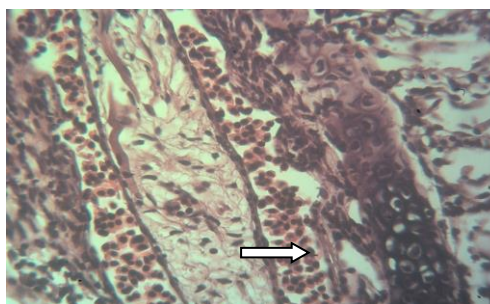


Fig 4- Gill histological section that exposure to lethal ammonia toxicity. Arrows show hyperemia (\* 400).

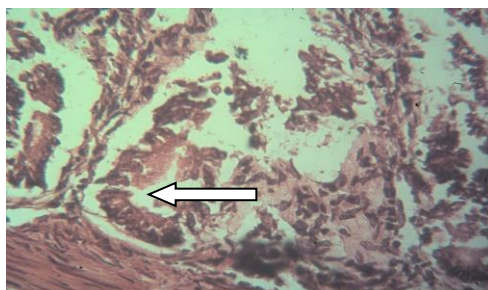


Fig 5- kidney histological sections that exposure to lethal ammonia toxicity. Arrows show degenerated tubules of kidney (\* 400).

#### 4. Conclusions

The survival rate in beluga fishes by adding the amount of zeolites were increased (fig. 3). Applying of zeolites was directly relative to removal of ammonia compounds in this study. So, the most efficient of removal rate of ammonia by zeolite was achieved when granulated zeolite was applied at 15g/l concentration. However during the trial fishes showed many severe reactions like disquiet and spasm. after the specific time zeolites reach to saturation point. Therefore, we should use a particular amount of zeolites due to prevent ammonia compounds. However, the use of zeolite seems promising in intensive aquaculture systems.

#### References

- 1) Bergero D, Boccignone M, Palmegiano GB. 1994. Ammonia removal capacity of European natural zeolite tuffs: Application to aquaculture waste water. *Aquaculture and fisheries* 25:81-86.
- 2) Lemarie´ G, Dosdat A, Coves D, Dutto G, Gasset E, Ruyet JPG. 2004. Effect of chronic ammonia exposure on growth of European seabass (*Dicentrarchus labrax*) juveniles. *Aquaculture* 229: 479-491.
- 3) Colt J. 2006. Water quality requirements for reuse systems. *Aquacultural engineering* 34: 143-156.
- 4) Frances J, Nowak BF, Allan GL. 2000. Effects of ammonia on juvenile (*Bidyanus bidyanus*). *Aquaculture* 183: 95–103.



4<sup>th</sup> Iran National Zeolite Conference  
Golpayegan University of Technology, Golpayegan, Iran  
August 23-24, 2017



**Epoxidation of Alkenes Catalyzed by the Nanocluster Polyoxomolybdate  
Supported on SBA-15**

Mojtaba Bagherzadeh\* , Hadigheh sadat Hosseini

*Department of Chemistry, Faculty of Science, Tehran University, P.O. Box 11155-3615, Iran*

\*Email: [bagherzadeh@sharif.edu](mailto:bagherzadeh@sharif.edu)

### 1. Introduction

Polyoxometalates (POMs) are a particular class of transition-metal oxoanion nanosized clusters which exhibit a great structural diversity of shapes, sizes and nuclearities<sup>1</sup>. POMs have attracted great interest as homogenous catalysts for the oxidation of alkenes, aromatics and alcohols. The immobilization of soluble POMs onto surfaces is preferred since they can easily be separated from a reaction mixture and recovered<sup>2</sup>. Recently, mesoporous SBA-15 have deserved general attention as support of heterogeneous catalysts due to its high surface area, uniform and large pores, tunable pore size and high thermal stability<sup>3</sup>.

### 2. Experimental

The mesoporous material, SBA-15, was prepared according to the literature. Polyoxomolybdate was prepared and supported on the SBA-15. The prepared material was characterized by means of FT-IR, inductively coupled plasma optical emission spectrometry (ICP-OES), powder X-ray diffraction (XRD), N<sub>2</sub> absorption-desorption, field emission scanning electron micrograph (FE-SEM) and transmission electron microscopy (TEM). The catalytic activity of the prepared catalyst was evaluated in the epoxidation of alkenes.

### 3. Results and discussion

ICP-OES, BET surface area and TEM analyses confirmed the immobilization of polyoxomolybdate. XRD analysis and FT-IR spectroscopy reveal that the structure of support remains intact after immobilization of polyoxomolybdate. The catalytic investigations showed that supported polyoxomolybdate is efficiently active and recyclable catalyst in liquid phase alkene epoxidation in dichloroethane at 80 °C.

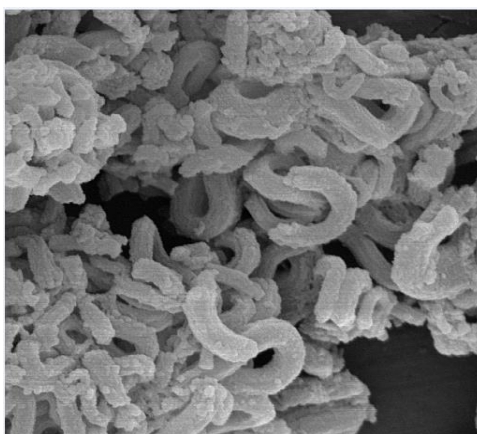


**Figure 1.** FE-SEM of POM@ SBA-15 with the scale bar of 500nm.





4<sup>th</sup> Iran National Zeolite Conference  
Golpayegan University of Technology, Golpayegan, Iran  
August 23-24, 2017

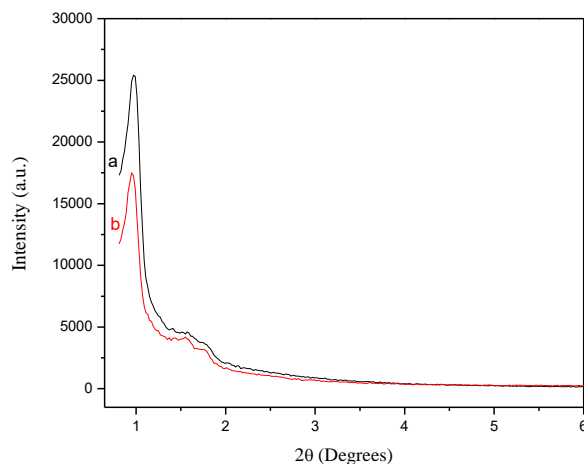


Figure 2. XRD patterns of the SBA-15 (a) and POM@SBA-15 (b)

Table 1. Textural properties (pore volume  $V_p$ , BET surface area  $a_{s,BET}$  and average pore size  $r_{p,peak}$ ) of POM and POM@SBA-15

Sample	$a_{s,BET}(m^2/g)$	$V_p(cm^3/g)$	$r_{p,peak}(BJH)(nm)$
SBA-15	381.85	0.8719	4.61
POM@SBA-15	315.98	0.7115	4.61

#### 4. Conclusions

In this study, supported polyoxomolybdate has been prepared and characterized by several techniques. The results confirm the immobilization of POM on SBA-15. The prepared material can be efficiently used as active and recyclable catalyst for the epoxidation of alkenes.

#### Acknowledgments

Financial support of this study was provided by the Research Council of Sharif University of Technology.

#### References

- 1) M. Mirzaei, H. Eshtiagh-Hosseini, M. Alipour, A. Frontera, *Coord.Chem.Rev* **2014**,275, 1-18.
- 2) Y. Zhou, G. Chen, Z. Long, J. Wang, *RSC Adv* **2014**, 4, 42092-42113.
- 3) M. Bagherzadeh, M. Zare, V. Amani, A. Ellern, L. Keith Woo, *Polyhedron* **2013**, 53, 223–229



# 4<sup>th</sup> Iran National Zeolite Conference

## Golpayegan University of Technology, Golpayegan, Iran

### August 23-24, 2017



## Construction of titanium-based porous photocatalyst using a new precursor

Tahereh Jabbari Manjili<sup>a</sup>, M.A. zanjanchi<sup>\*b</sup>

<sup>a</sup>University of guilan, Rasht, P.O.Box 1914, Iran

<sup>b</sup>University of guilan, Rasht, P.O.Box 1914, Iran

\*Email:Zanjanchi@guilan.ac.ir

### 1. Introduction

A photocatalyst is generally defined as a material that induce chemical reactions in presence of light [1]. The efficiency of the photocatalyst is a function of the balance between charge separation, ease of interfacial electron transfer and energy-wasting charge recombination [2]. Organic pollutants especially dyes are the side-products from different manufacturing industries like as insecticides, paint and dye textiles and pharmaceuticals. They are released into the the aquatic ecosystem and must be removed for environmental protection. TiO<sub>2</sub> is an attractive material for numerous photocatalytic applications. The method of synthesis of TiO<sub>2</sub> generally influences the photocatalytic activity of the catalyst. In this study we use adequate precursor for preparation of active TiO<sub>2</sub> photocatalyst [3].

### 2. Experimental

Synthesis of TiO<sub>2</sub> nanoparticles was carried out by thermal hydrolysis process. Both soloublized TiOSO<sub>4</sub> in sulfuric acid and solid TiOSO<sub>4</sub> were used for the synthesis as titanium precursors. Selected surfactant (including cetyltrimethylammonium bromide CTAB) were used in certain synthesis. The obtained white precipitate were finally calcined at 450, 550 and 650 °C for 4 h. TiO<sub>2</sub>-incorporated into zeolite 4A were also prepared. The prepared photocatalysts were charact-erized with XRD, SEM, EDX, FTIR and BET methods. They were tested for degradation of methylene blue as a pollutant probe molecule using a photocatalytic testing apparatus.

### 3. Results and discussion

In this study, we used adequate precursor for preparation of active TiO<sub>2</sub> photocatalyst. TiOSO<sub>4</sub> is a precursor that has not been studied comprehensively for the preparation of active TiO<sub>2</sub>. The preparation of TiO<sub>2</sub> from TiOSO<sub>4</sub> were done using several procetures. The variavles such as synthesis temperature, synthesis time and pH, calcination temperatures and addition of surfactant to the synthesis gel were studied. It was found that calcinations at 450 °C of the samples synthesized in presence or absence of CTAB provide higher activity in photocatalytic tests. TiO<sub>2</sub>-incorporated into 4A zeolite shows moderate activity either using titanium isopropoxide or titanium chloride. The work is in progress to find out how the activity of TiO<sub>2</sub>-4A samples could be improved. The patterns shown in Fig.1 indicated that the as-prepared and calcined TiO<sub>2</sub> samples were in the form of anatase crystalline structure.

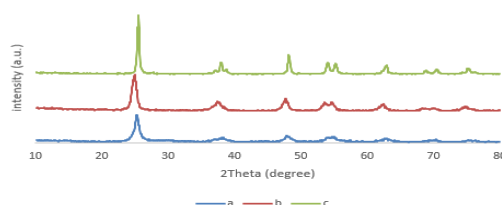


**Figure 1.** XRD patterns of porous TiO<sub>2</sub> samples prepared from TiOSO<sub>4</sub> and calcined at (a) 450 (b) 550 and (c) 650 °C for 4h.



# 4<sup>th</sup> Iran National Zeolite Conference

## Golpayegan University of Technology, Golpayegan, Iran

### August 23-24, 2017



#### 4. Conclusions

In summary, the porous TiO<sub>2</sub> were prepared via a simple and efficient low-temperature method using TiOSO<sub>4</sub> as titanium sources. The work also includes preparation of TiO<sub>2</sub>-incorporated 4A zeolite. The prepared materials were active in photocatalytic tests for degradation of methylene blue. Our results found great potential of the obtained TiO<sub>2</sub> for use as highly efficient photocatalyst.

#### Acknowledgments

We gratefully acknowledge the Research Department of University of Guilan for supporting this work.

#### References

- 1) AL. Linsebigler, L. Guanquan, T. John, Chemical reviews 95(1995) 735-758.
- 2) R. Nagarjuna, S. Challagulla, N. Alla, R. Ganesan, S. Roy, Materials and Design 86 (2015) 621–626.
- 3) R. Nagarjuna, S. Roy, R. Ganesan, Microporous and Mesoporous Materials 211 (2015) 1-8

## Removal of bacteria from aqueous solution by novel Hydroxyapatite/Zeolite nanocomposite

Parisa Maleki<sup>b</sup>, Bahareh Shoshtari Yeganeh<sup>a</sup>, Mojgan Zendehtdel<sup>a\*</sup>

<sup>a</sup> Department of Chemistry, Faculty of Science, Arak University, Arak 38156-8- 8349, Iran

<sup>b</sup> Department of Biology, Faculty of Science, Arak University, Arak 38156-8- 8349, Iran

\*Email: Mojganzendehtdel@yahoo.com

#### 1. Introduction

Hydroxyapatite (HAp), Ca<sub>10</sub>(PO<sub>4</sub>)<sub>6</sub>(OH)<sub>2</sub>, is a class of materials from different origins (mineral, synthetic, and derived from animal and fish bones) [1]. HAp special in nano form has high biocompatibility and bioactivity properties [2]. Zeolites are naturally aluminosilicates which can be also obtained by synthesis and characterized by high internal and external surface areas. Several types of moieties like water and alkaline/alkaline earth metals can be hosted or adsorbed in both natural and synthetic zeolites porous and channels. Herein, we report the synthesis and characterization of hydroxyapatite/Zeolite nanocomposite and in vitro antibacterial activity of these nanocomposites was evaluated against Bacillus subtilis (as Gram-positive bacteria) and Pseudomonas aeruginosa (as Gram-negative bacteria) via utilizing the agar disc diffusion method under anaerobic conditions and compared with standard drugs.

#### 2. Experimental

Various aliquots (0.175, 0.350, and 0.700 g) of the prepared hydroxyapatite were initially added to a zeolite gel (NaP). The mixtures were then placed in an autoclave after ageing at 100°C for 26 h. The three composites with different



4<sup>th</sup> Iran National Zeolite Conference  
Golpayegan University of Technology, Golpayegan, Iran  
August 23-24, 2017



ratio HAP were synthesized and then filtered and washed with deionized water repeatedly in order to reach pH of 7. For comparison a nanocomposite of Clinoptilolite /HAP was prepared [3]. HAP/Zeolite nanocomposite was then characterized by Fourier transform infrared (FTIR), (XRD), (SEM), (EDAX), (BET) and (TG/DTA).

### 3. Results and discussion

Results suggested that the nanocomposite crystals of HAP were dispersed onto the zeolite external surface and/or encapsulated within the zeolite channels and pores.

#### Antibacterial activity study

The in vitro antibacterial activity of the investigated compounds was tested against pathogenic Gram-negative bacteria's such as *P. aeruginosa* (ATCC 27853) and Gram-positive bacteria's such as *B. subtilis* (ATCC 6633) using the paper disc diffusion method according to the procedure described by Hwang and Ma [4]. This method is a way to measuring efficiency of an antibacterial agent against the mentioned bacterial growth. Muller Hinton broth was used for preparing culture media for the bioassay of the organisms. A lawn culture from 0.5 Mac Farland suspension of each strain was prepared on Muller Hinton agar. The agar medium was sterilized in autoclave and cooled to room temperature, then introduce into sterilized petri dishes. The bacteria are swabbed uniformly across a culture plate, while the petri dishes are cooled over 24 h. Discs of samples were placed on the surface of the medium and finally, all petri dishes containing bacteria and antibacterial reagents were incubated and maintained at 37 °C for 24 h. The diameters of the inhibition zones formed around each disc were determined and presented in mm.

#### Biological studies

The in vitro antibacterial activities of HAp nanopowder and HAP/zeolite (0.5:1, 1:1, and 2:1) were studied with two standard antibacterial drugs, vancomycin, and nalidixic acid. The microorganisms used in this study include *B. subtilis* (as Gram-positive bacteria) and *P. aeruginosa* (as Gram-negative bacteria). Comparing the biological activity of the HAp nanopowder and HAP/zeolite (0.5:1, 1:1, and 2:1) with standard drugs, indicate incorporated nano HAP to composite show more inhibition on bacterial growth.

Table 1. antibacterial activity data of HAp and HAp/zeolite

Compounds	Inhibition zone (mm)	
	<i>B. subtilis</i> (Gram(+))	<i>S. aeruginosa</i> (Gram(-))
HAp	14	10
HAp/ zeolite (0.5:1)	18	12
HAp/ zeolite (1:1)	21	13
HAp/ zeolite (2:1)	22	15
HAp/ Clin (0.5:1)	15	16
HAp/ Clin (1:1)	19	12
Vancomycine	23	-
Nalidixic acid	22	-

It seems the aggregation effect is very significant in antibacterial activity of nano hydroxyapatite that decrease with incorporated of zeolite. It is apparent that toxicity toward Gram-positive bacteria is more than Gram negative strains and because peptidoglycan are negatively charged and HAP nanoparticles are positively charged [4]. The reason is the



# 4<sup>th</sup> Iran National Zeolite Conference

## Golpayegan University of Technology, Golpayegan, Iran

### August 23-24, 2017



difference in the structure of the cell wall. The walls of Gram-negative cells are more complex than those of Gram-positive cells and lipopolysaccharides form an outer lipid membrane and contribute to the complex antigenic specificity of Gram-negative cells. Also, we know that some bacteria such as *P. aeruginosa* are a group of resistant microorganism to many standard drugs, and they were found to have no activity against it. Then, it is interesting that *P. aeruginosa* was inhibited by these nanocomposites [5]. (Table 1)

#### 4. Conclusions

Results suggested that the nanocomposite crystals of HAp were dispersed onto the zeolite external surface and/or encapsulated within the zeolite channels and pores.

we found that the antibacterial activity of these nanocomposites was very good against bacteria such as *Bacillus subtilis* (as Gram-positive bacteria) and *Pseudomonas aeruginosa* (as Gram-negative bacteria).

#### Acknowledgments

Thanks are due to the Research Council of Arak University of Technology and Center of Excellence in the Chemistry Department of Arak University of Technology for supporting of this work.

#### References

- [1] A. Corami, S. Mignardi, V. Ferrini, J.Hazard.Mater. 146, 164 (2007)
- [2] H. S. Ragab , F. A. Ibrahim , F. Abdallah , Attieh A. Al-Ghamdi , Farid El-Tantawy , F. Yakuphanoglu, Journal of Pharmacy and Biological Sciences. 9, 77 (2014)
- [3] Mojgan Zendehtdel , Bahareh Shoshtari-Yeganeh, Giuseppe Cruciani, J IRAN CHEM SOC  
DOI 10.1007/s13738-016-0908-9
- [4] J.J. Hwang, T.W. Ma, Mater. Chem. Phys. 136, 613 (2012)
- [5] R.Juan-Luis,F.Alian,Pseudomonas, 2nd edn. (Springer, Virulence and Gene Regulation, 2007)

## A novel PrNH<sub>2</sub>/Fe<sub>3</sub>O<sub>4</sub>/SiO<sub>2</sub> magnetic nanoparticle (MNPs) for water purification from heavy metals

Sadegh Rostammia<sup>a\*</sup>, Mahin Abdollahi<sup>b</sup>, Moslem Sadeghi<sup>b</sup>, Ahmad Sohrabi Noor<sup>b</sup>

<sup>a</sup> Organic and Nano Group (ONG), Department of Chemistry, Faculty of Science, University of Maragheh, P.O.B 55181-83111, Maragheh, Iran

<sup>b</sup> Maragheh Chemistry Association, University of Maragheh, P.O. Box 55181-83111, Maragheh, Iran

\*Email: [srostammia@gmail.com](mailto:srostammia@gmail.com)

#### 1. Introduction

Due to the task-specific properties of amino groups, core-shell nanostructures of PrNH<sub>2</sub>/Fe<sub>3</sub>O<sub>4</sub>@SiO<sub>2</sub> have been extensively investigated as advanced adsorbents; however, most studies on surface modification of Fe<sub>3</sub>O<sub>4</sub>@SiO<sub>2</sub>



# 4<sup>th</sup> Iran National Zeolite Conference

## Golpayegan University of Technology, Golpayegan, Iran

### August 23-24, 2017



substances were of environmentally inefficient grafting methods [1-3]. Herein, we demonstrated that monodispersed and spherical magnetic nanoparticle of  $\text{Fe}_3\text{O}_4$  to  $\text{Fe}_3\text{O}_4@ \text{SiO}_2$  nanomaterials and then preparation of the  $\text{PrNH}_2/\text{Fe}_3\text{O}_4@ \text{SiO}_2$  can be facily prepared by co-condensation of TEOS with APTMS employing a green sol-gel process.

On the other hand, with the increasingly discharged heavy metal containing wastewater into the environment, removal of heavy metal ions from wastewater has been an extensive research topic. These pollutants are not biodegradable and tend to accumulate in living organisms and many heavy metal ions are known to be toxic or carcinogenic [3-5].

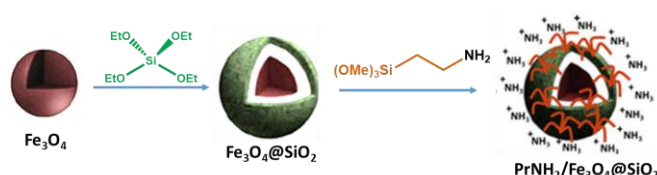
## 2. Experimental

Magnetic  $\text{Fe}_3\text{O}_4$  MNPs were prepared by a solvothermal method as previously reported [3]. Briefly,  $\text{FeCl}_3 \cdot 6\text{H}_2\text{O}$  (1.62 g),  $\text{NaOAc}$  (14.0 g) and  $\text{Na}_3\text{Cit}$  (15 g) were dissolved in EG (60 mL), after vigorous stirring for 1h, the obtained yellow solution was transferred to controlled Teflonline stainless-steel autoclave, then sealed and heated at 190 °C. After reaction for 12 h, the autoclave was cooled to room temperature. The obtained  $\text{Fe}_3\text{O}_4$  MNPs were washed several times with water and ethanol. Finally, the products were collected with a magnet and then re-dispersed in 80 mL water for further use.

The  $\text{Fe}_3\text{O}_4$  MNPs were then modified sequentially with TEOS and APTMS to introduce amine groups. Typically, 20 mL magneto-fluid was diluted with 100 mL ethanol, and the mixture was homogenized by ultrasonic for 10 min prior to the addition of 1 mL  $\text{NH}_3$ . After being stirred vigorously for 30 min at 30 °C, 2 mL TEOS was dropped into the solution. The reaction was performed for 45 min and then 1 mL APTMS was introduced and lasted reaction for another 4 h; during the mentioned stages, the amount of APTMS was systematically investigated to correlate the dependence of physicochemical properties of  $\text{PrNH}_2/\text{Fe}_3\text{O}_4@ \text{SiO}_2$  on the key preparation parameters.

## 3. Results and discussion

The  $\text{Fe}_3\text{O}_4$  MNPs were directly used for one-pot amino-functionalization without any other treatment by an optimized sol-gel process under the following conditions; that is, a mixture of 20 mL magneto-fluid, 100 mL EtOH and 1 mL of  $\text{NH}_3$ , was homogenized by ultrasonic, then 2 mL of TEOS as the hydrolysis precursor was added into the mixture. After the mixture was hydrolyzed, 1 mL APTMS was added to functionalize the MNPs with  $-\text{NH}_2$  groups (Scheme 1).



**Scheme 1.** Illustration of the synthesis of  $\text{PrNH}_2/\text{Fe}_3\text{O}_4@ \text{SiO}_2$  on the formation of core/shell structures.

Figure 1 shows TEM image of  $\text{PrNH}_2/\text{Fe}_3\text{O}_4@ \text{SiO}_2$  MNPs obtained by a solvothermal procedure, particles with diameter of about 110 nm are clearly present.



4<sup>th</sup> Iran National Zeolite Conference  
Golpayegan University of Technology, Golpayegan, Iran  
August 23-24, 2017

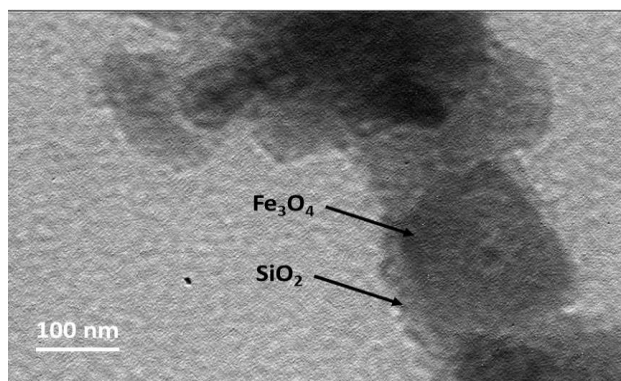


Figure 1. TEM images of PrNH<sub>2</sub>/Fe<sub>3</sub>O<sub>4</sub>@SiO<sub>2</sub>.

Figure 2 shows the dependence of PrNH<sub>2</sub>/Fe<sub>3</sub>O<sub>4</sub>@SiO<sub>2</sub> towards Pb (II) from aqueous solutions. It is clear that with increasing amount of MNPs based on amino functionality, the adsorption will have increased. However, MNPs exhibit remarkable Pb (II) withdrawal capacities. The adsorption results suggest that aqueous Pb(II) adsorption percentage clearly increases with the amino group content in the adsorbents, revealing amino groups worked as efficient chelating sites for Pb(II) adsorption under performed conditions.

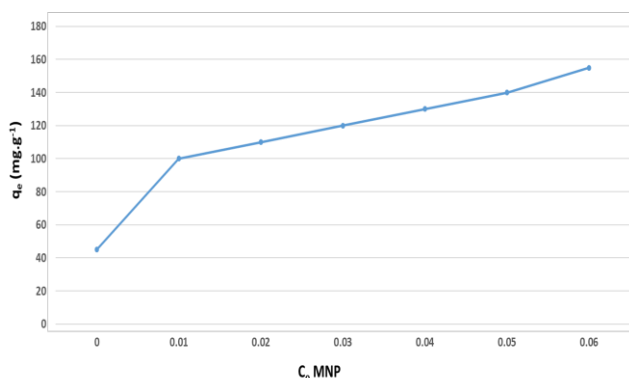


Figure 2. Effect of the PrNH<sub>2</sub>/Fe<sub>3</sub>O<sub>4</sub>@SiO<sub>2</sub> usage on the adsorption of towards Pb (II) from aqueous solution.

#### 4. Conclusions

Magnetic nanoparticles of PrNH<sub>2</sub>/Fe<sub>3</sub>O<sub>4</sub>@SiO<sub>2</sub> with core-shell structure and relatively good loading of NH<sup>2</sup>-functionality were prepared via a proposed sol-gel process. As-synthesized PrNH<sub>2</sub>/Fe<sub>3</sub>O<sub>4</sub>@SiO<sub>2</sub> were employed in adsorption of Pb (II) ions from water.

#### Acknowledgments

We acknowledge the financial support from “Vice Chancellor of Socio-Cultural” of University of Maragheh.

#### References

- 1) N.K. Srivastava, C.B. Majumder, *J. Hazard. Mater.* **2008**, 151, 1–8.
- 2) H. Gurer-Orhan, H.U. Sabir, H. Ozgunes, *Toxicology* **2004**, 195, 147-154.
- 3) D. Clifford, S. Subramonian, T. Sorg, *J. Environ. Sci. Technol.* **1986**, 20, 1072-1080.
- 4) E. Dana, A. Sayari, *Desalination* **2012**, 285, 62-67.
- 5) A. Saeed, M. Iqbal, M.W. Waheed, *J. Hazard. Mater.* **2005**, 117, 65-73.



4<sup>th</sup> Iran National Zeolite Conference  
Golpayegan University of Technology, Golpayegan, Iran  
August 23-24, 2017



Highly selective olefin epoxidation with the hydrogen peroxide in the presence of hematite nanoparticles ( $\alpha$ -Fe<sub>2</sub>O<sub>3</sub>-NP)

Fatemeh Parchegani<sup>\*a</sup>, Hassan Hosseini Monfared<sup>a</sup>

<sup>a</sup> Department of chemistry, Faculty of Science, Zanzan University, P.O. Box 45195-395, Zanzan, I.R. Iran

\*Email: [f-Parchegani94@phd.araku.ac.ir](mailto:f-Parchegani94@phd.araku.ac.ir)

### 1. Introduction

Metal oxide nanoparticles have been applied for detection and separation of proteins<sup>i</sup>, to immunoassay<sup>ii</sup>, drug<sup>iii</sup> and gene delivery<sup>iv,v</sup>. Moreover, the use of nanoparticles attracted a lot of attention in the field of catalysis due to their high surface area. Therefore given the far lower cost, less toxicity and greater abundance of iron over the more precious metals, it is clear that iron derived catalysts would provide a range of benefits if they could be made practical, stable, active and selective. The catalytic properties of the NPs can be modified by particles size. The most obvious size-dependence relationship results from the change in the percentage of surface atoms which are responsible for the catalytic properties when changing the diameter. In this work we report a facile solvothermal approach to the synthesise of hematite nanoparticles ( $\alpha$ -Fe<sub>2</sub>O<sub>3</sub>-NP) and their applications in the catalytic oxidation of olefins.

### 2. Experimental

The oxidation of olefin with hydrogen peroxide was performed in a 25-mL round-bottom flask placed in a thermostatic oil bath. In a typical experiment the flask was charged with the suspension of  $\alpha$ -Fe<sub>2</sub>O<sub>3</sub>-NP (1.0 mg) in 3 mL acetonitrile, n-octane as internal standard and olefin (2 mmol). The oxidation reaction was started with addition of 6 mmol aqueous 30% hydrogen peroxide and the mixture was stirred vigorously with magnetic stirrer bar at 80°C for 6 h. At appropriate intervals, aliquots were removed and analyzed by gas chromatograph.

### 3. Results and discussion

The synthesized sample was characterized by different techniques. The XRD pattern of ( $\alpha$ -Fe<sub>2</sub>O<sub>3</sub>-NP) synthesized show the sharp and intense peaks indicate the good crystallinity of the sample. The diffraction peaks can be well corresponded to the standard hematite nanoparticles (Fig 1).

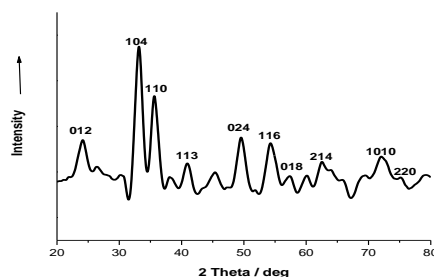


Fig. 1. X-ray diffraction pattern of  $\alpha$ -Fe<sub>2</sub>O<sub>3</sub>-NP





4<sup>th</sup> Iran National Zeolite Conference  
Golpayegan University of Technology, Golpayegan, Iran  
August 23-24, 2017



The size, shape and size distribution of the nanoparticles of hematite nanoparticles were examined by SEM. SEM images show (Fig 2) that all of the hematite particles obtained have nearly spherical shape and uniform size. The synthesized  $\alpha$ -Fe<sub>2</sub>O<sub>3</sub>-NP show the highest particle size ( $188 \pm 105$ ).



Fig 2. SEM image of  $\alpha$ -Fe<sub>2</sub>O<sub>3</sub>-NP

H<sub>2</sub>O<sub>2</sub> was used as oxidant for catalytic studies because it is readily available, inexpensive and the only by-product is water. The catalytic works results showed that cyclohexene and cyclooctene could be oxidized easily to corresponding epoxides with 100% selectivity at very good conversion. The optimum conditions were obtained by studying solvent and oxidant molar ratios effect.

#### 4. Conclusions

Easily prepared  $\alpha$ -Fe<sub>2</sub>O<sub>3</sub>-NP has been shown to be an active, stable, and highly selective catalyst for oxidations of cyclic olefins applying with 3 equiv aqueous 30% H<sub>2</sub>O<sub>2</sub>. Activation of H<sub>2</sub>O<sub>2</sub> by this complex raises the prospect of using this type of simple catalyst for selective organic syntheses. Because of its simple recyclability, the catalyst is well-suited for continuous processes.

#### Acknowledgment

The authors are grateful to the University of Zanjan for financial support of this study.

#### References

1. Y. Deng, D. Qi, C. Deng, X. Zhang, D. Zhao, J. Am. Chem. Soc. 130 (2008) 28
2. A. Agrawal, T. Sathe, S.M. Nie, J. Agric. Food Chem. 55 (2007) 3778.
3. M.K. Yu, Y.Y. Jeong, J. Park, S. Park, J.W. Kim, J.J. Min, K. Kim, S. Jon, Angew.Chem. Int. Ed. 47 (2008) 5362.
4. X.L. Wang, L.Z. Zhou, Y.J. Ma, X. Li, H.C. Gu, Nano Res. 2 (2009) 365.
5. B.R. Hao, R. Xing, Z. Xu, Y. Hou, S. Gao, S. Sun, Adv. Mater. 22 (2010) 2729.



# 4<sup>th</sup> Iran National Zeolite Conference

## Golpayegan University of Technology, Golpayegan, Iran

### August 23-24, 2017



## Alkyl amino pyridine-functionalized NaY zeolite (synthesis and characterize)

Hakimeh Behyar<sup>a</sup>, Zahra Kalateh<sup>a</sup>, Mohammad Ali Bodaghi Fard<sup>a</sup>, Mojgan Zendehtdel<sup>\*a</sup>

<sup>a</sup> Department of Chemistry, Faculty of Science, Arak University, Arak 38156-8- 8349; Iran

\*Email: [m-zendehtdel@araku.ac.ir](mailto:m-zendehtdel@araku.ac.ir)

### 1. Introduction

Homogeneous organic catalyst such as Alkyl amino pyridines have been used as active catalysts for many different organic reactions. The use of these soluble catalysts has variable drawbacks such as purification of the final product (s) from the reaction mixture and further catalyst recyclability which offer considerable complexity to the reaction that may render it industrially unacceptable. Thus, the heterogenous catalyst are a logical step to avoid these problems. The recoverability and reusability offered by heterogeneous systems, to give high yields in short times and sometimes without the need for organic material, lead to green chemistry [1] In the present work, alkyl amino pyridin-functionalized NaY zeolite has been prepared.

### 2. Experimental

Organic modification of NaY zeolite with 3-chloro propyltriethoxysilane (3-CIPTES) was performed by stirring 0.1 g of porous materials with 3-CPTES (0.10 g, 0.45 mmol) in 20 mL dry toluene at 110 °C for 24 h. The solid was filtered and washed with ethanol and acetone, and air dried at room temperature and 2-amino pyridine (1g) was added to it and refluxed . The powder separated and washed with ethanol. The elemental analysis of modified compounds shows the molar ratio that confirmed immobilized amine on the porous material structure.

### 3. Results and discussion

The FT-IR spectra of hybrid materials indicate an intense band about ca.1022 cm<sup>-1</sup> attributable to the asymmetric stretching of Al–O–Si chain of zeolite. The symmetric stretching and bending frequency bands of Al–O–Si framework of zeolite appear at ca.791 and 463 cm<sup>-1</sup>, respectively .

The FT-IR spectrum of Alkyl amino pyridines/zeolite (Fig. 1) shows the C-H and N-H vibration bands in the 2800-3500 cm<sup>-1</sup> and 1500-1650 cm<sup>-1</sup> regions. These bands are surely absent in the case of NaY zeolite, showing that Alkyl amino pyridines has been attached on zeolite matrix.

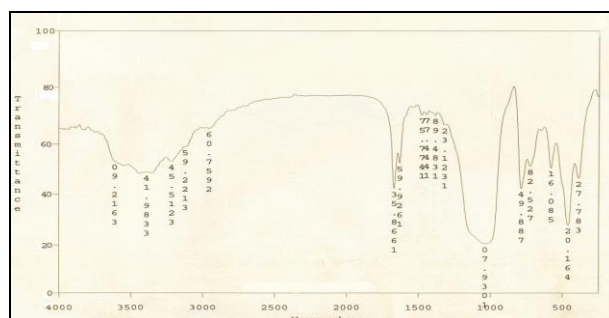


Figure 1. FT-IR spectrum of Alkyl amino pyridines/zeolite



4<sup>th</sup> Iran National Zeolite Conference  
Golpayegan University of Technology, Golpayegan, Iran  
August 23-24, 2017



In Fig. 2 we have seen the FESEM micrograph of Alkyl amino pyridines/zeolite sample with a wide range of shapes and sizes of particles. It indicates the presence of well-defined zeolite crystals with some shadow of modification presence on its external surface. The particle sizes are around 300 nm and this decrease of size for modified zeolite is due to the amine formation on the support [2].

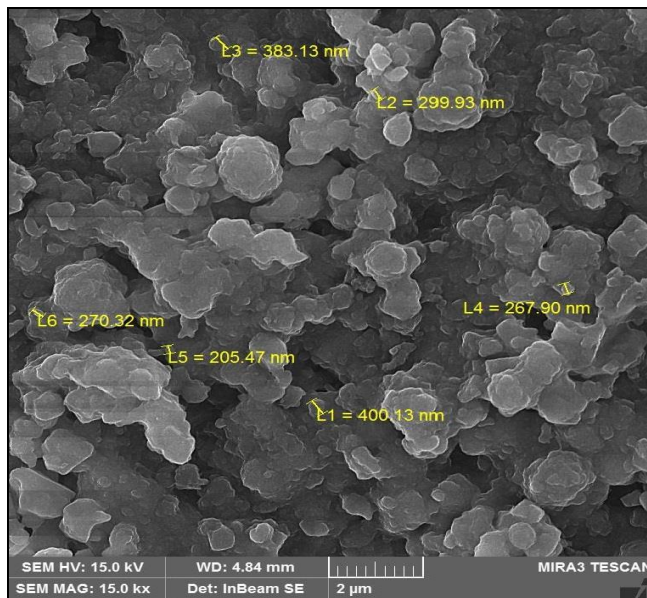


Figure 2. FESEM micrograph of Alkyl amino pyridines/zeolite

The immobilized catalysts were also characterized by means of powder X-ray diffraction. The patterns for NaY, Cl/Y and Alkyl amino pyridines /Y are shown in Fig. 3 (a-c). While the XRD analysis is not quantitative, the diffraction patterns after the binding of organic molecule are similar to that of the native zeolite support. According to similar studies, in the present study no changes were detected in the crystalline structure and morphology of zeolite during the immobilization procedures, also the percentage of amorphous phase is very small [3,4].

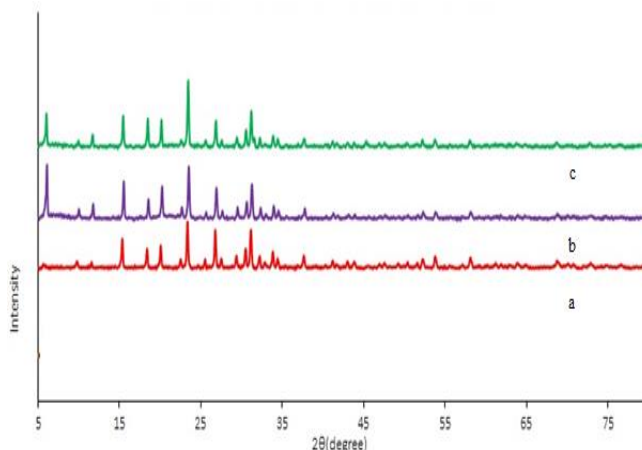


Figure 3. The XRD patterns for NaY (a), Cl/Y (b) and Alkyl amino pyridines /Y (c)



# 4<sup>th</sup> Iran National Zeolite Conference

## Golpayegan University of Technology, Golpayegan, Iran

### August 23-24, 2017



#### 4. Conclusions

The alkyl amino pyridin-functionalized NaY zeolite has been prepared and characterized.

#### Acknowledgments

Thanks are due to the Iranian Nanotechnology Initiative and the Research Council of Arak University of Technology and Center of Excellence in the Chemistry Department of Arak University of Technology for supporting of this work.

#### References

- [1] E. B. Mubofu, J. H. Clark and D. Macquarrie, *Green Chem.* 3 (2001) 23-25.
- [2] K. Li, J. Valla and J. Garcia-Martinez, *Chem. Cat. Chem.* 6 (2014) 46-66.
- [3] S. Mandal, D. Roy, R. V. Chaudhari, and M. Sastry, *Chem. Mater.* 16 (2004) 3714-3724.
- [4] M. R. Didgikar, D. Roy, S. P. Gupte, S. S. Joshi, and R. V. Chaudhari, *Ind. Eng. Chem. Res.* 2010, 49, 1027-1032.

## Synthesis and Characterization of Mesoporous silica clay by bentonite

Mahboobeh Mangoli, Saeedeh Hashemian\*

Department of chemistry, Islamic Azad University, Yazd Branch, , Yazd, Iran

\*Email; Sa\_hashemian@iauyazd.ac.ir

#### 1. Introduction

Nano-holes are a regular part of organic or inorganic porous structure jointly with pore sizes ranging from  $1 \times 10^{-7}$  -  $2 \times 10^{-9}$ . Nano-holes are especially useful in filtration. Nanoporous materials by IUPAC are divided into three categories: Micro porous materials: 0.2 – 2 nm, Meso porous materials: 2 – 50 nm, Macro porous materials: 50 – 100 nm. Silica based mesoporous materials have attracted the attention of material scientists due to their high surface area. They have different applications such as adsorbents, separation process, heterogeneous catalysts, host guest chemistry, separation of large biological molecules, environmental pollution control etc. Silica based materials structures have been synthesized by making use of several sources of silica, such as silicon alkoxides (e.g., TEOS, TMOS), sodium silicate, Ludox, fumed silica, water glass etc [1-3]. bentonite, one kind of widely used clay mineral, is composed with silicate layers[4]. In this study silica based material has been synthesized from natural bentonite.

#### 2. Experimental

All of compounds were analytical reagents grade and were used as received, without any further purification. Distilled water was used in all of the reactions.

Necessary purity analytical chemistry in co Merck were purchased. Purity and analytical materials were used without purification. Of bentonite was used for the preparation of materials hole. Bentonite with NaOH was ground for 4h. Cetyltrimethyl ammonium bromide and polyethylene glycol have been employed as surfactants.



4<sup>th</sup> Iran National Zeolite Conference  
Golpayegan University of Technology, Golpayegan, Iran  
August 23-24, 2017



The FTIR spectra were obtained in KBr pellets using a Bruker, Tensor 27 spectrometer in the range of 400-4000 cm<sup>-1</sup>, and all spectra were collected at room temperature. The powder X-ray diffraction studies were made on Siemens D5000 (Germany) X-ray diffractometer by using Fe-K $\alpha$  radiation of wave length 1.936 Å. Scanning Electron Microscopy was performed using a Philips SEM model XL30 electron microscope.

### 3. Results and discussion

The mesoporous silica clay of bentonite (MSC) was characterized by infrared spectroscopic analysis and results are shown in Figure 1. The results shown broad band around 3400 cm<sup>-1</sup> of bentonite is assigned to -OH stretching band for interlayer water. The bands at 3650 cm<sup>-1</sup> are due to -OH band stretch for Al-OH and Si-OH.

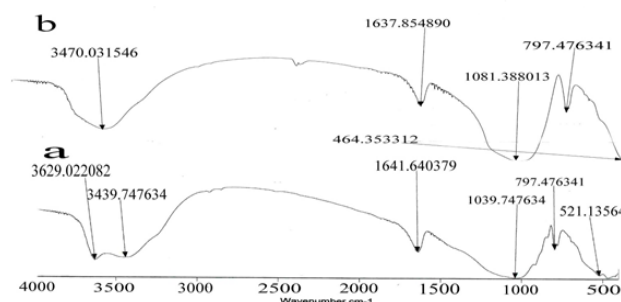


Figure 1. FTIR pattern of a-bentonite and b- MSC

The phase structures of samples were investigated by XRD. X-ray diffraction patterns of MSC is shown in Figure 2. The appearance the patterns of MSC at  $2\theta=33^\circ$ ,  $38^\circ$  and  $55^\circ$  confirmed the formation of silica clay.

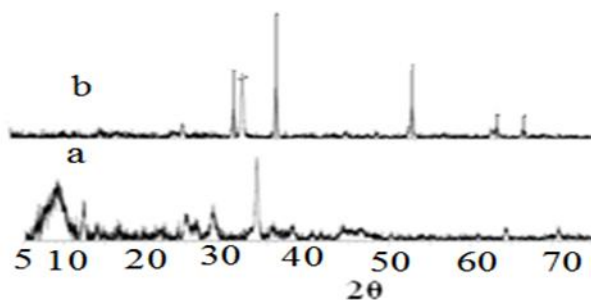


Figure 2. XRD pattern of a-bentonite and b- MSC

To review the material composition of the hole picture was taken SEM ( Figure3). It can be seen that uniform and spherical particles composed of a porous structure with an average size is 25nm. The images also confirm the existence of mesopores in MSC. The approval for the formation of particles with silica is Mesoporous.



# 4<sup>th</sup> Iran National Zeolite Conference

## Golpayegan University of Technology, Golpayegan, Iran

### August 23-24, 2017

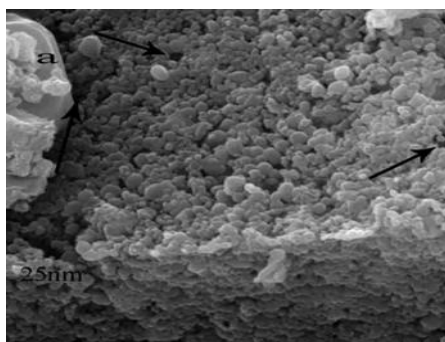


Figure 3. SEM image of MSC

#### 4. Conclusions

Mesoporous silica clay MSC has been synthesized successfully. The Mesoporous silica clay particles was characterized by FTIR, XRD and SEM. FTIR analysis reveals the substantial combination between clay layer and the amorphous hydrolysate of TEOS. SEM and XRD results were confirmed the formation of nano size silica clays from bentonite.

#### Acknowledgments

The authors wish to thank Islamic Azad University of Yazd (IAUY) for the financial support of this work. Also, thank co-workers and technical staff in the chemical department help during various stages of this work.

#### References

- 1). P. Feng, X. Bu, D. J. Pine, Control of pore sizes in the mesoporous silica calcinations by liquid crystals in block copolymer-surfactant-water system, *Langmuir* 2000, 16, 5304-5310.
- 2). J. M. Kim, Y.J. Han, B.F. Chmelka, G.D. Stucky, One-step synthesis of ordered mesocomposites with non-ionic amphiphilic block copolymers: implications of isoelectric point, hydrolysis rate and fluoride, *Chem Commun* 2000, 3, 2437-2438.
- 3). S. Hashemian, Study of adsorption of acid dye from aqueous solutions using bentonite, *Main Group Chemistry* 2007, 6, 97-107.
- 4). S. Hashemian, M. Salimi, Nano composite a potential low cost adsorbent for removal of cyanine, *Chem. Eng. J* 2012, 188, 57-63.

## K<sup>+</sup>-Enriched Clinoptilolite as a Slow Release Fertilizer

Mahboubeh Eslami<sup>a</sup>, Reza Khorassani <sup>\*a</sup>, Amir Fotovat<sup>a</sup>, Akram Halajnia<sup>a</sup>

<sup>a</sup>Ferdowsi University of Mashhad, Faculty of Agriculture, Department of Soil Science, Mashhad, Iran.

\*Email:khorasani@um.ac.ir

#### 1. Introduction

Clinoptilolite is an abundant and inexpensive natural zeolite with unique chemical features for adsorption of monovalents such as K<sup>+</sup> which makes it a suitable candidate for production of slow release fertilizers<sup>1</sup>. Zeolites can be applied to soil both in natural and pre-charged forms. Pre-charging zeolite with nutrients can be done by soaking them in chemical solutions, swine liquids, or melted fertilizers<sup>2,3,4</sup>. The adsorption and desorption (ion exchange) properties



# 4<sup>th</sup> Iran National Zeolite Conference

## Golpayegan University of Technology, Golpayegan, Iran

### August 23-24, 2017



of the zeolites is highly influenced by their crystal chemistry and geochemical behaviour of the adsorbate<sup>5</sup>. Preparation of K<sup>+</sup>-enriched zeolite through soaking method, investigation of the mechanism of saturation, and finally evaluation of this newly prepared K source as a slow release fertilizer via column experiment are the main objectives of this research.

## 2. Experimental Part or Theoretical Details

Zeolite sample came from a mine in Semnan, Iran (Table 1). Soaking method was employed to enriched zeolite with K<sup>+</sup>. Zeolite particles of 0.5-1 mm were soaked in 1 M KCl at zeolite:solution ratio of 1:5. The amount of the adsorbed K<sup>+</sup> was then determined by flame photometrically, at days 1, 3, 5, 7, 10, 15, 20, and 25 after saturation. Five kinetic models were used to study the mechanism of K<sup>+</sup> adsorption onto zeolite: pseudo-first order, pseudo-second order, power function simplified Elovich and parabolic diffusion.

A column leaching test was conducted to evaluate the quality and leaching properties of the prepared potassium zeolitic fertilizer and compare it with K<sub>2</sub>SO<sub>4</sub> fertilizer.

**Table 1.** Chemical composition of the Clinoptilolite

Zeolite	SiO <sub>2</sub>	Al <sub>2</sub> O <sub>3</sub>	K <sub>2</sub> O	Na <sub>2</sub> O	pH <sup>a</sup>	EC <sup>a</sup>
clinoptilolite	%					dS/m
	69.4	6.43	2.57	5.54	9.07	0.37

<sup>a</sup> in 1:2 zeolite:water extract

## 3. Results and Discussion

The results of saturation experiment revealed that preparation of K<sup>+</sup>-enriched zeolite is a time consuming process which took place after 15 days (Figure 1). As shown in Figure 1, approximately 56% of the saturation occurred at the first day of the saturation experiment. This might be due to the abundance of uncovered and readily accessible sites on zeolite at initial time of study<sup>6</sup>.

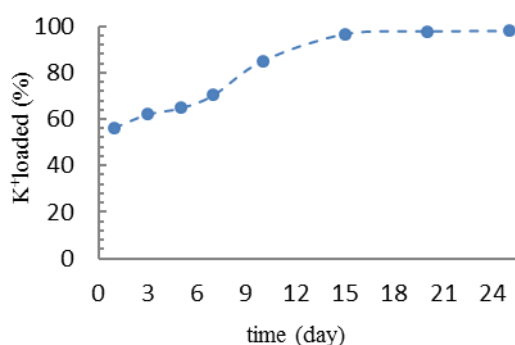


**Figure 1.** K<sup>+</sup> loading onto natural zeolite vs. time

The R<sup>2</sup> and RMSE values obtained from kinetics studies revealed that the pseudo-second order gives the best estimation performance for saturation mechanism, followed by the pseudo-first order model (Table 3). The satisfactory conformity of the experimental data to pseudo-second order and pseudo-first order models suggest that the chemisorption and physisorption control the process of K<sup>+</sup> adsorption onto clinoptilolite, respectively<sup>7</sup>. Jaskunas et al. 2015<sup>8</sup>, in their research paper on kinetics of K<sup>+</sup> adsorption onto clinoptilolite reported that the diffusion is the rate limiting step of K<sup>+</sup> adsorption on zeolite which leads to a maximum adsorption time of more than 1000 hr.



# 4<sup>th</sup> Iran National Zeolite Conference

## Golpayegan University of Technology, Golpayegan, Iran

### August 23-24, 2017



**Table 3.** Kinetic parameters for the adsorption of K<sup>+</sup> onto clinoptilolite

Kinetic	Formula	Parameter	K <sup>+</sup>
Pseudo-first-order	$\ln(q_e - q_t) = a - bt^{\dagger}$	$q_e$ (mg g <sup>-1</sup> )	25.53
		$k$ (min <sup>-1</sup> )	0.13
		R <sup>2</sup>	0.86
		RMSE	0.15
Pseudo-second-order	$\frac{t}{q_t} = a + bt^*$	$q_e$ (mg kg <sup>-1</sup> )	55.55
		$k$ (kg mg <sup>-1</sup> hr <sup>-1</sup> )	0.007
		R <sup>2</sup>	0.989
		RMSE	0.14

<sup>†</sup>a = ln(qe), b is the rate constant (k)

\*a = 1/kqe<sup>2</sup>, b = 1/qe

Chemical and physical characteristics of the soils used in column leaching test is presented in Table 2. Application of K<sup>+</sup> in the form of K<sup>+</sup>-enriched zeolite to sandy soils significantly decreased the potassium leaching rate (Figure. 1). While, a great majority of the K added to the soil amended with chemical fertilizer was leached out at initial time of the experiment. It seems that the retention

of K<sup>+</sup> on exchangeable sites of zeolite can effectively control its release behavior and decrease the K loss through leaching. This zeolitic K sources can be suitable for soilless container media and zeoponic systems.

**Table 2.** Chemical and physical characteristics of the soils used in column leaching test

Soil	Sand	Silt	Clay	OM	pH <sup>a</sup>	EC <sup>a</sup>
	%					dS/m
Column	92.5	5.2	2.3	2.76	7.67	0.74

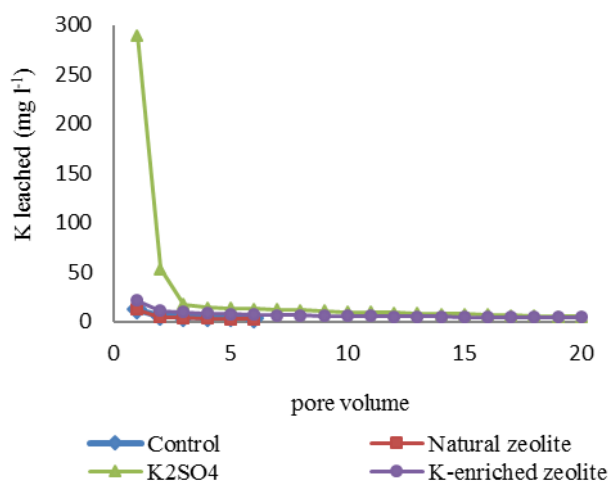


**Figure 2.** Leaching behavior of potassium from different K sources

#### 4. Conclusions

Based on the results of this study, the following 3 major conclusions can be drawn:

- 1- The complete saturation of zeolite by K<sup>+</sup> lasted approximately 15 days. A large proportion of the adsorption (>50%) occurred at the first day of the experiment.
- 2- Chemisorptions and physisorption are the main rate limiting steps of K<sup>+</sup> adsorption process onto clinoptilolite, respectively.
- 3- The K leached from K<sup>+</sup>-enriched zeolite significantly was lower than chemical fertilizer suggesting the slow release characteristics of this zeolitic K fertilizer.





# 4<sup>th</sup> Iran National Zeolite Conference

## Golpayegan University of Technology, Golpayegan, Iran

### August 23-24, 2017



#### Acknowledgment

The authors would like to thank Ferdowsi University of Mashhad (FUM) for financial support of this research project (No: 31201).

#### References

- 1) A. Manikandan, K. S. Subramanian, Fabrication and characterization of nanoporous zeolite based N fertilizer. *Afr J agric res* **2014**, 9(2): 276-284.
- 2) M. Y. Guo, M. Z. Liu, F. L. Zhan, L. Wu, Preparation and properties of a slow-release membrane-encapsulated urea fertilizer with superabsorbent and moisture preservation. *Ind Eng Chem Res* **2005**, 44: 4206-4211.
- 3) T. S. Perrin, D. T. Drost, J. L. Boettinger, J. M. Norton, Ammonium loaded clinoptilolite A slow-release nitrogen fertilizer for sweet corn. *J Plant Nutr* **1998**, 21 :515-530.
- 4) B. Faccini, D. Di Giuseppe, N. Colombani, M. Mastrocicco, D. Malferrari, M. Coltorti, G. Ferretti. Column leaching experiments on ammonium charged zeolite. *Environmental quality* **2014**, 14:43-52.
- 5) S. Wang, Y. Peng, Natural zeolites as effective adsorbents in water and wastewater treatment. *Chemical Engineering Journal* **2010**, 156: 11-24.
- 6) K. Dajana, M. Marinko, B. Felicita., Ammonium Adsorption on Natural Zeolite (clinoptilolite): adsorption isotherm and kinetics modeling. *The Holistic Approach to Environment* **2012**, 2: 145-158.
- 7) D. Wen, Y. S. Ho, S. Xie, X. Tang, Mechanism of the Adsorption of Ammonium Ions from Aqueous Solution by a Chinese Natural Zeolite. *Separ. Sci. Technol.* **2006**, 41: 3485-3498.
- 8) A. Jaskunas, B. Subasius, R. Slinksienė, Adsorption of K<sup>+</sup> ions on natural zeolite: kinetic and equilibrium studies. *Chemija* **2015**, 26 (2): 69-78.

## An Efficient Mesoporous MnCo<sub>2</sub>O<sub>4</sub> Catalyst with peroxidase-like activity

Zeinab Moradi Shoeili<sup>a\*</sup>, Fahime Vetr<sup>a</sup>, Maryam Zare<sup>b\*</sup>

<sup>a</sup> Department of Chemistry, Faculty of Sciences, University of Guilan, P.O. Box 41335-1914, Rasht, Iran

<sup>b</sup> Materials Science & Engineering Department, Golpayegan University of Technology, P.O. Box 8771765651, Golpayegan, Iran

\*Email: zmoradi@guilan.ac.ir (Z. Moradi-Shoeili)

\*Email: m\_zare@gut.ac.ir (M. Zare)

### 1. Introduction

Mesoporous materials have either organic or inorganic framework that create an arranged porous structure. The size of the pores of mesoporous materials have been reported between 2-50 nm. High specific surface area, size and shape selectivity are the most important properties of the porous materials that cause many catalytic, filtration, separation, ion exchanger and sensor applications. Pores have different shapes, such as spherical, cylindrical, groove, funnel-shaped or hexagonal. The porosity can be flat or curved or with turns and twists. Therefore, mesoporous materials play important roles in nano technology [1, 2].

Recently, catalysts with enzyme-like characteristics have attracted great interests. While many kinds of peroxidase-like catalysts have been actively developed recently, improving their catalytic efficiency is significant too. The



4<sup>th</sup> Iran National Zeolite Conference  
Golpayegan University of Technology, Golpayegan, Iran  
August 23-24, 2017



application of materials as artificial enzymes has attracted considerable interest due to the unique properties of these materials and interesting surface chemistry [3].

In this work, we synthesized a mesoporous  $\text{MnCo}_2\text{O}_4$  nanocatalyst by using a simple co-precipitation method. The structure of the prepared  $\text{MnCo}_2\text{O}_4$  was characterized by physico-chemical and spectroscopic techniques.

## 2. Experimental Part

**Synthesis of  $\text{MnCo}_2\text{O}_4$ :** 1 gr  $\text{CoCl}_2 \cdot 6\text{H}_2\text{O}$  and 0.48 gr  $\text{MnCl}_2 \cdot 4\text{H}_2\text{O}$  were dissolved in 20 ml ethanol and stirred for 30 minutes. The KOH solution was added under vigorous stirring into the ethanol solution containing mixture of Co and Mn ions. Upon the addition of KOH, precipitation was formed immediately. The reaction mixture was stirred vigorously for 20 minutes. The obtained precipitation was centrifuged, washed repeatedly with water until  $\text{Cl}^-$  was not detected and dried at 100 °C. Washing the precipitation with water removes KCl and creates mesopore structure of  $\text{MnCo}_2\text{O}_4$  nanocatalyst [2].

**Catalytic oxidation of *o*-phenylenediamine (OPD):** The oxidation reaction with as prepared mesoporous  $\text{MnCo}_2\text{O}_4$  was investigated in 10 ml OPD solution in the range of 5 to 25 mM, catalyst (0.06 gr/l) and  $\text{H}_2\text{O}_2$  (30%). The main product i.e. 2,3-diaminophenazine was detected by the UV-Vis spectral analysis.

## 3. Results and discussion

The FT-IR spectrum of mesoporous  $\text{MnCo}_2\text{O}_4$  nanocatalyst has been shown in Figure 1. Two strong bands observed at 649 and 559  $\text{cm}^{-1}$  that are characteristic to stretching vibrations of tetrahedral and octahedral sites of spinel  $\text{MnCo}_2\text{O}_4$ .

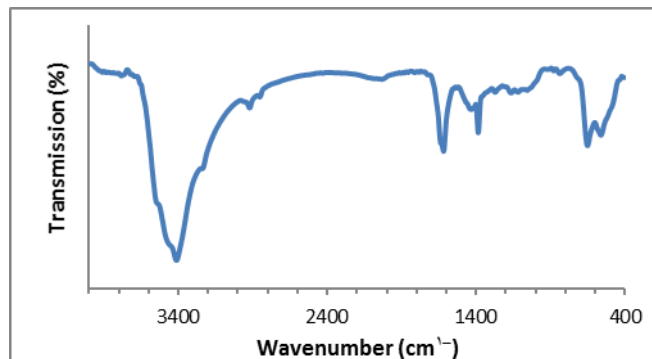


Figure 1. FT-IR spectra of mesoporous  $\text{MnCo}_2\text{O}_4$  nanocatalyst.

In UV-vis spectrum, maximum absorption appeared in 415-420 nm corresponds to the formation of 2,3-diaminophenazine during a 20 min period (Figure 2).

Rate of reaction depends on both the concentration of *o*-phenylenediamine as well as the amount of  $\text{MnCo}_2\text{O}_4$ , while the concentration of hydrogen peroxide in an optimum concentration is constant (Figure 3).



4<sup>th</sup> Iran National Zeolite Conference  
Golpayegan University of Technology, Golpayegan, Iran  
August 23-24, 2017

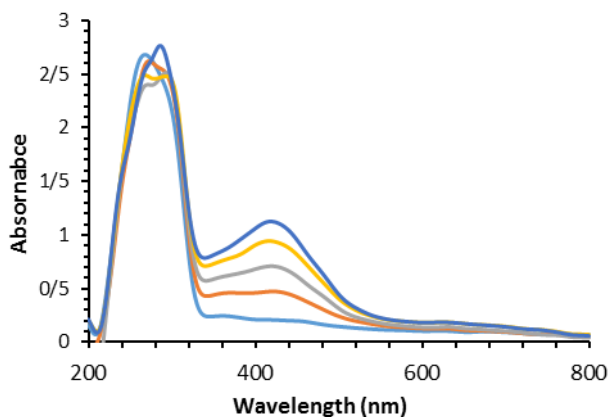


**Figure 2.** Time dependent UV-Visible spectral changes for the oxidation of OPD catalyzed by the  $MnCo_2O_4$  nanoparticles at room temperature for 10 min.

The results have been fitted with a non-linear function of the Michaelis–Menten equation [4, 5]. Therefore, the Michaelis–Menten constant ( $K_m$ ) and maximum reaction velocity ( $V_{max}$ ) can be calculated from the double-reciprocal or Lineweaver–Burk plots according to equation (1) :

$$\frac{1}{v_o} = \frac{K_m}{v_{max}} \frac{1}{[S]} + \frac{1}{v_{max}} \quad (1)$$

The apparent  $V_{max}$  and  $K_m$  values mesoporous  $MnCo_2O_4$  nano catalyst were found to be  $0.25\mu M$  and  $50\text{ mM}$ , respectively.

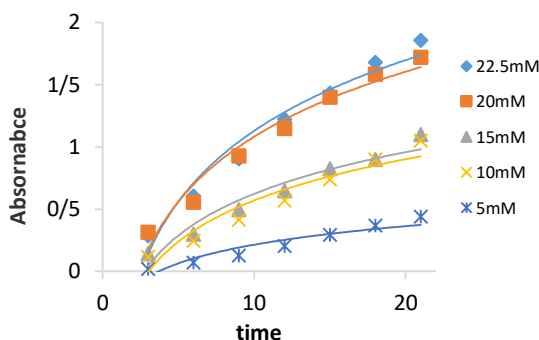


**Figure 3.** Effect of chromogenic substrate concentration on the reaction rate catalyzed by  $MnCo_2O_4$ .

#### 4. Conclusions

In summary, we have successfully synthesized mesoporous  $MnCo_2O_4$  nano catalyst which was found to possess peroxidase-like activity and could catalytically oxidize o-phenylenediamine in the presence of  $H_2O_2$ . The oxidation process of o-phenylenediamine is a second order reaction and  $MnCo_2O_4$  exhibit Michaelis–Menten kinetics.

#### Acknowledgments

The authors are grateful to the University of Guilan and the Golpayegan University of Technology for financial support.

#### References

- 1) A. A. Vernekar, T. Das, S. Gosh, G. Mugesh, *chemistry-An Asian Journal*, **2016**, 11(1), 72-76



4<sup>th</sup> Iran National Zeolite Conference  
Golpayegan University of Technology, Golpayegan, Iran  
August 23-24, 2017



- 2) T. Y. Ma, Y. Zheng, S. Dai, M. Jaroniec, S. Z. Qiao, *Journal of Materials Chemistry A*, **2014**, 2, 8676-8682  
3) H. Jia, D. Yang, X. Han, J. Cia, H. Liu, W. He, *Nanoscale*, **2016**, 8, 5938-5945  
[4] J. Mu, Y. Wang, M. Zhao, L. Zhang, *Chem Commun*, **2012**, 48, 2540-2542.  
[5] H. Jia, D. Yang, X. Han, J. Cai, H. Liu, W. He, *Nanoscale*, **2016**, 8, 5938-5945.

**Heterogenization of peracid onto the SBA-16 mesoporous silica for  
the epoxidation of cyclooctene**

Mahsa Niakan, Majid Masteri-Farahani\*

Faculty of Chemistry, Kharazmi University, Tehran, Islamic Republic of Iran

\*E-mail : mfarahany@yahoo.com

## 1. Introduction

Epoxidation of olefins is an important process in organic synthesis. Organic peracids can react with olefins to give the corresponding epoxides. This process is a convenient and useful method which does not involve any catalyst. However, the use of peracids is not environmentally friendly as considerable amount of carboxylic acid waste are formed. Separation of the produced carboxylic acid from the reaction mixture and regeneration of the peracid is one way to reduce the chemical wastage. To solve this problem, we report our attempt to immobilization of the organic peracid on the surface of inorganic solid support(SBA-16). activity of the obtained supported peracid as well as its recyclability are investigated in the epoxidation of cyclooctene.

## 2. Experimental

### 2.1. Synthesis of supported peracid

First, dried support ( 1g of SBA-16) was dispersed in 50 ml dry toluene. After addition of 3-cyanopropyltrichlorosilane (1 ml), the mixture was refluxed under nitrogen atmosphere for 8 hours. The resulted solid was filtered off and soxhlet extracted with methanol to remove the excess of silylating reagent. Then, The cyanopropyl-functionalized support (1 g) was hydrolyzed by heating in 80 ml aqueous sulfuric acid 50% (v/v) at 120°C for 3 hours and stirred at room temperature for additional 20 hours. The solid was filtered and washed with excess of doubly distilled water. Finally, the supported peracids were achieved by treatment of the supported carboxylic acids with 30% hydrogen peroxide in acidic medium.

### 2.2. Epoxidation experiment

In a typical experiment for the epoxidation of cyclooctene, a 25 ml round bottom flask was charged with the supported peracid (containing 0.4-1.2 mmol of peracid), cyclooctene (0.4 mmol) and solvent (5 ml). The mixture was stirred at room temperature under nitrogen atmosphere. The product of the reaction was collected at various time periods and was analyzed by utilization of a gas chromatograph.



### 3. Results and discussion

A new supported peracid onto the pores of SBA-16 was prepared (Figure 1) and fully characterized by FT-IR, TGA, XRD, TEM, BET and elemental analysis.

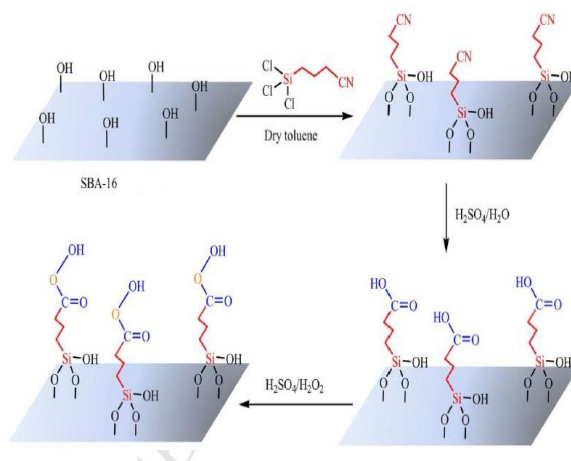


Figure 1. Schematic illustration of the preparation of supported peracid.

Surface functionalization of SBA-16 support was confirmed by investigating the nitrogen adsorption-desorption analysis of the materials. SBA-16 and SBA-COOOH materials showed type IV isotherms with H2 hysteresis loop characteristic of cubic cage like mesoporous materials (Figure 2). It can be inferred that the mesoporous character of the support was preserved during the functionalization processes in spite of the decrease in nitrogen adsorption.

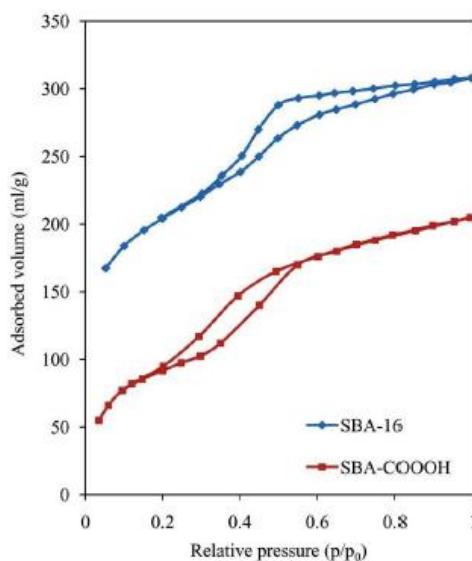


Figure 2. Nitrogen sorption isotherms SBA-16 and SBA-COOOH.

The changes in the textural properties of the support after functionalization with peracid groups were investigated by XRD analysis and the patterns were shown in Figure 3. A decrease in the intensity of the (110) reflection and shift to lower angles can be seen in the XRD pattern of SBA-COOOH in comparison with pristine SBA-16.



4<sup>th</sup> Iran National Zeolite Conference  
Golpayegan University of Technology, Golpayegan, Iran  
August 23-24, 2017

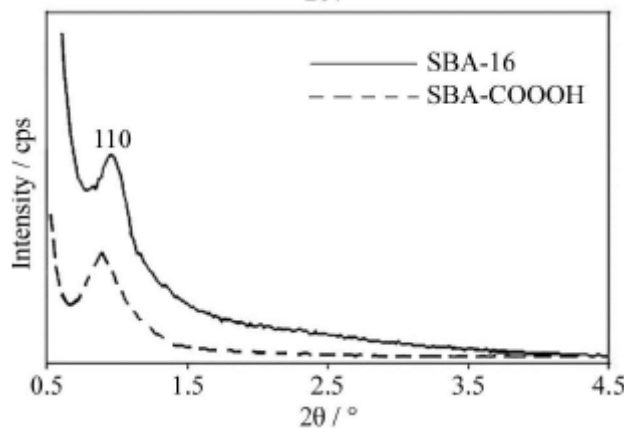


Figure 3. XRD patterns of SBA-16 and SBA-COOH.

The microstructure and pore size of the supported peracid were explored more precisely with transmission electron microscopy (TEM). The TEM image of SBA-COOH (Figure 4) demonstrates that the ordered mesoporous structure of SBA-16 support was preserved with mesopores of diameter  $\sim 3.5$  nm.

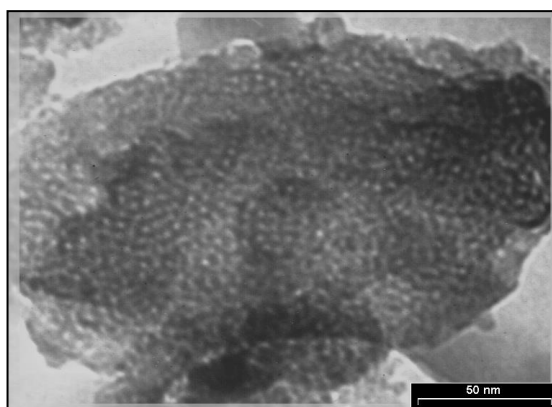


Figure 4. TEM image of SBA-COOH.

The results of the epoxidation of cyclooctene are given in Table 1. It was found that SBA-16 supported peracid has high activity in the epoxidation of cyclooctene. The effect of the type of solvent and catalyst amounts on the conversion of the cyclo-octene was also investigated. Results showed that the highest conversion of cyclooctene was obtained in dichloromethane as solvent. Moreover, SBA-16 supported peracid can be recovered easily and reused in the epoxidation reaction without considerable loss of activity and selectivity.

Table 1. The results of epoxidation of cyclooctene with peracid.

solvent	Time (h)	Conversion%	Selectivity%
CH <sub>2</sub> Cl <sub>2</sub>	8	85	99
CH <sub>3</sub> CN	8	45	99
n-Hexne	8	35	99

Reaction conditions: peracid (1.2 mmol), cyclooctene (0.4 mmol), solvent (5 ml), room temperature.



# 4<sup>th</sup> Iran National Zeolite Conference

## Golpayegan University of Technology, Golpayegan, Iran

### August 23-24, 2017



#### 4. Conclusions

In summary, we have succeeded in designing a new supported peracid using SBA-16 as solid support. The supported peracid was found to be efficient in the selective epoxidation of cyclooctene. The results show that the supported peracid was converted into supported carboxylic acid under the reaction conditions and can be easily recovered and regenerated after simple treatment.

#### Acknowledgments

We acknowledge the financial support from Kharazmi University.

#### References

- 1) M. Masteri-Farahani, M. Niakan, *Materials Chemistry and Physics* **2017**, 195, 74-81.

## Detection of inorganic anions by the immobilized Schiff-base receptor on zeolite-Y

Saba Mahdavi Hezaveh, Mojgan Zendehtel, Hamid Khanmohammadi \*

Department of Chemistry, Faculty of science, Arak University, Arak 38156-8-8349, Iran

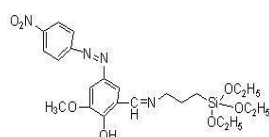
\*Email : h-khanmohammadi@araku.ac.ir

#### 1. Introduction:

Research on design and synthesise of molecular sensors for detection anions is very important, because of the present anions in biological, agriculture, environmental, pharmacologic and industrial [1-4]. Among variety important anions, hydrogen sulfate anion takes more attention; this anion may be exist in sewage industrial and agriculture fertilizer so can pollute surface water and ground water [5-6]. The PH water was made decrease dramatically by anion bisulfate, so presence of  $\text{HSO}_4^-$  anion in water causing irritation skin and eyes [7]. Already most of the molecular sensor works in organic solvent or blend of organic solvent and water. In other hand many studies reported to detect of  $\text{HSO}_4^-$  by free molecular sensor based on hydrogen band that has low sensitivity [8-9]. In this paper we synthesise a molecular sensor was immobilized on the zeolite, that can detection mention anion in aqueous solvent and mechanism detection is based on break band Schiff base [11].

#### 2. Experimental:

The Molecular sensor was synthesized by reaction between azo based on ortovaniline and APTE, then was immobilized over zeolite.



Free molecular sensor



zeolite



# 4<sup>th</sup> Iran National Zeolite Conference

## Golpayegan University of Technology, Golpayegan, Iran

### August 23-24, 2017



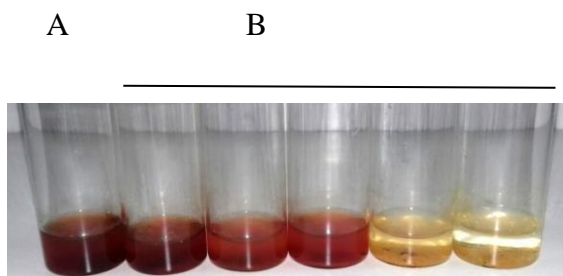
### 3. Results and discussion:

Figure (1) demonstrated that anion  $\text{HSO}_4^-$  was detected by Schiff base receptor on the zeolite among other anions. Such as  $\text{F}^-$ ,  $\text{OAC}^-$ ,  $\text{HSO}_4^-$ ,  $\text{CN}^-$ ,  $\text{N}_3^-$ ,  $\text{NO}_3^-$ ,  $\text{PO}_4^{2-}$



**Figure 1:** Left to right regularly ligand over zeolite without anions (blank) and ligand over zeolite in present different anions  $\text{F}^-$ ,  $\text{OAC}^-$ ,  $\text{HSO}_4^-$ ,  $\text{CN}^-$ ,  $\text{N}_3^-$ ,  $\text{NO}_3^-$ ,  $\text{PO}_4^{2-}$ , respectively ( $5 \times 10^{-3}$  M)

As can be seen in fig (2), Indicated that variety concentrations of anion bisulfate were supplied in rang of ( $1.10^{-5}$  –  $5.10^{-5}$ ) in present Schiff base receptor on the zeolite. The lowest concentration of anion was detected  $4.10^{-5}$ .



**Figure 2:** left to right (a) ligand over zeolite without anion, (b) ligand over zeolite with different concentration regularly  $1.10^{-5}$ ,  $2.10^{-5}$ ,  $3.10^{-5}$ ,  $4.10^{-5}$ ,  $5.10^{-5}$

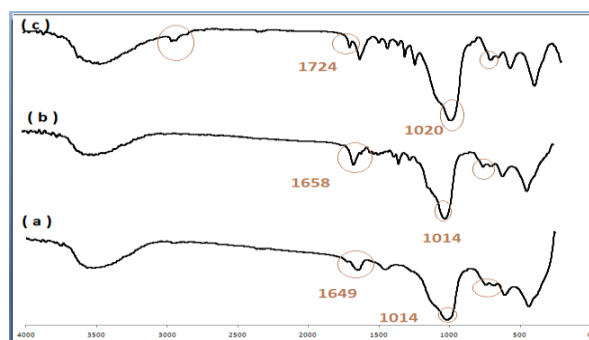


**Figure 3:** IR spectroscopy of (a) zeolite.(b) ligand over zeolite (c) ligand over zeolite in present bisulfate

### IR Spectroscopy:

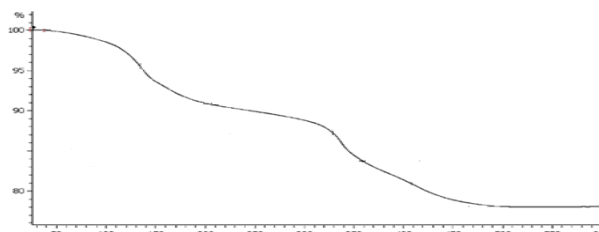
Figures (3) showed spectrum FT-IR of ligand was immobilized over zeolite. In fig (3a) depicts of zeolite, and it can be seen index peaks related to zeolite such as peak at  $1014 \text{ cm}^{-1}$  attribute to asymmetric stretch ( $\text{Si} - \text{O} - \text{Si}$ )  $\text{SiO}_4$  tetrahedral in zeolite. and fig (3b) show that ligand was immobilized over zeolite, the peak at  $1658 \text{ cm}^{-1}$  related to ( $\text{C}=\text{N}$ ) that prove ligand based on zeolite. and fig (3c) indicate ligand on the zeolite was exposed with anion  $\text{HSO}_4^-$ , so peak at  $1658 \text{ cm}^{-1}$  missing and a new peak at  $1724 \text{ cm}^{-1}$  related to ( $\text{C}=\text{O}$ ) appears because of break band of Schiff base in present of mention anion.

### TGA:

As seen from this figure (5), the weight loss of 9.31 % between the temperature intervals of  $25\text{-}200 \text{ }^\circ\text{C}$  is related to desorption of physical and chemical water molecules present in the zeolite of, respectively. Above this temperature make multiple steps in the temperature range  $325\text{-}600 \text{ }^\circ\text{C}$ . attribute to ligand over zeolite. The second step with 8.05% weight loss is assigned to decomposition of Schiff base for zeolite.

In the last step, the structure of zeoliet is changed. These results confirmed the immobilization of organic compound on the zeolite.

**Figure 4:** TGA of zeolite







4<sup>th</sup> Iran National Zeolite Conference  
Golpayegan University of Technology, Golpayegan, Iran  
August 23-24, 2017



**XRD:**

Figure (5) implied that XRD of zeolite and molecular sensor over the zeolite is almost identical, because of most of the Schiff base receptor are in pore zeolite and a amount of them are on the zeolite surface and it is important to know the crystal structure zeolite was kept. Also Structure of ligand over zeolite after heating was changed of amorphous to crystal but peaks of zeolite and ligand was collapsed.

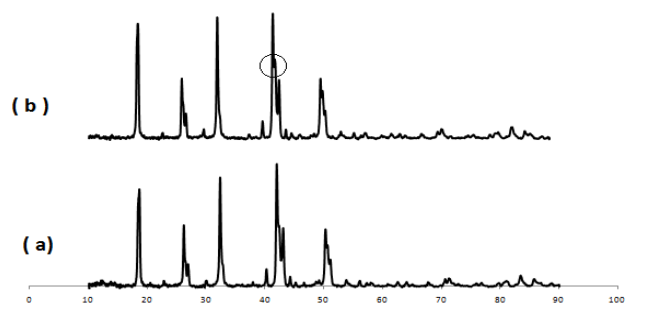


**Figure 5:** (a) XRD pattern of zeolite (b) XRD of ligand over zeolite

**Conclusions:**

We can synthesize a portable sensor for detection anion  $\text{HSO}_4^-$ . This sensor is usable in aqueous environment, and without use any expensive equipment just based on colorimetric.

**References:**

- [1]: L. Wang, J. Ou, Guipo .Fang, D. Cao, Sensors and Actuators B 222 (2016) 1184–1192
- [2]: J. Shao, H. Lin, H.K. Lin, Talanta 75 (2008) 1015–1020.
- [3]: H. Khanmohammadi, K. Rezaeian, RSC Adv. 4 (2014) 1032–1038.
- [4]: A.K. Mahapatra, R. Maji, K. Maiti, S.S. Adhhikari, C.D. Mukhopadhyay, D.Mandal, Analyst 139 (2014) 309–317.
- [5]: B.A. Moyer, L.H. Delmau, C.J. Fowler, A. Ruas, D.A. Bostick, J.L. Sessler, E. Katayeu, G.D. Pantos, J.M. Llinares, M.A. Hossain, S.O. Kang, K. Bowman-James, in: R.V. Eldik, K. Bowman-James (Eds.), Advances in Inorganic Chemistry, Academic Press, New York, 2006, pp. 175–204.
- [6]: P. Li, You-Ming Zhang, Q.Lin, J.Li, T.Wei, Spectrochimica Acta Part A 90 (2012) 152– 157
- [7]: L.Wang, J.Ou, G. Fang, D. Cao, Sensors and Actuators B 222 (2016) 1184–1192
- [8]: M. Alfonso, A. Tárraga, P. Molina, Org. Lett. 13 (2011) 6432–6435.
- [9]: H.M. Chawla, S.N. Sahu, R. Shrivastava, Tetrahedron Lett. 48 (2007)6054–6058.
- [11]: L.E. Santos-Figueroa, M.E. Moragues, E. Climent, A. Agostini, R.Martínez-Máñez, F. Sancenón, Chem. Soc. Rev. 42 (2013) 3489–3613



4<sup>th</sup> Iran National Zeolite Conference  
Golpayegan University of Technology, Golpayegan, Iran  
August 23-24, 2017



## Synthesis of beta-zeolite for applying in the ring-opening reaction

Mahsa Eskandarzade, Aliakbar Tarlani\*

*Inorganic Nanostructures and Catalysts Research Lab., Chemistry & Chemical Engineering Research Center of Iran, Pajooresh Blvd., km 17, Karaj Hwy, Tehran 14968-13151, Iran*

\*Email: Tarlani@ccerci.ac.ir

### 1. Introduction

Zeolites have a wide area of applications as catalyst, adsorbent and ion exchanger [1, 2]. Of the more than 200 known zeolite topologies with a framework code assigned by the Structure Commission of the International Zeolite Association [3]. Beta zeolite is one of the useful compounds that constitute the majority of the commercial zeolite catalyst production [4]. Zeolite Beta, with its intriguing framework architecture and 3-dimensional pore system, displays superior performance in refinery applications, environmental catalysis and a variety of organic reactions because of its vastly accessible pore volume, high adsorption capacity, strong acid sites and shape/size selectivity [5].

The opening of epoxides with alcohols is one of the important transformations for the synthesis of  $\beta$ -alkoxy alcohols which are mainly used as valuable organic solvents, versatile synthons and intermediates [6].

In this report, the prepared heterogeneous acidic nanocatalyst has been applied in the ring opening of styrene oxide by alcohols under ambient temperature.

### 2. Experimental

#### 1) Synthesis of zeolite beta

Synthesis process of zeolite beta was as follows: 14.7 mL tetraethylammonium hydroxide (25 wt.% aqueous solution) and 2.25 mL of 3.70 mol/L HCl were mixed in a glass vessel, then 2.5 g of fumed silica was added under vigorous stirring. After 30 min, NaAlO<sub>2</sub> solution (0.1906 g sodium aluminate dissolved in 2.9 mL water) was added, and the reaction mixture was stirred until a homogeneous gel was obtained. The gel was transferred into a teflon-lined stainless steel autoclave and aged at 140 °C for 168 h under static conditions, yielding the zeolite beta precursor.

Then 9 mL 19.28 wt.% aqueous solution of cetyltrimethylammonium bromide and 1.12 mL of 3.70 mol/L HCl were added to the zeolite beta precursor. After stirring for 1 h, the reagent mixture was transferred into a teflon-lined stainless steel autoclave and aged at 140 °C for 24 h under static conditions. After cooling down to room temperature, the products were filtered, washed with deionized water and dried in air at ambient temperature. The template of as-synthesized zeolite beta was eliminated by calcination at 540 °C (1 °C min<sup>-1</sup>) for 10 h in flowing air for 8 h. The proton form of zeolite beta was obtained from ion-exchange of NH<sub>4</sub>NO<sub>3</sub>, followed by calcination at 540 °C for 4 h [7].

#### 2) Catalytic reactions

In a typical reaction, zeolite beta (0.01 g) was added to the solution of styrene oxide (0.12 g) in alcohols (methanol, ethanol, 1-propanol, 2-butanol)(5mL). The mixture was stirred until full conversion. After filtration through a short pad of alumina and evaporation, chromatography on silica eluted with petroleum ether/ethylacetate (85:15) of the residue led to the product (Figure 1) [8].



# 4<sup>th</sup> Iran National Zeolite Conference

## Golpayegan University of Technology, Golpayegan, Iran

### August 23-24, 2017

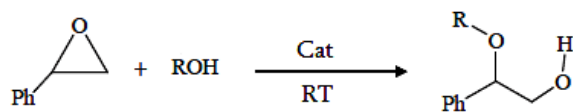


Figure 1

### 3. Results and discussion

Analysis of the powder XRD-pattern of zeolite Beta reveals two significant features. During the first crystallization step of zeolite beta, we investigated the crystallization kinetics of zeolite beta shown in Figure 2. The nitrogen adsorption-desorption isotherms of the calcinated zeolite beta is illustrated in Figure 3. The pore size distribution of zeolite beta has uniform mesoporous channels. The pore diameter (1.8 nm), cumulative pore volume (0.273 cm<sup>3</sup> g<sup>-1</sup>) and BET surface area (607.9 m<sup>2</sup> g<sup>-1</sup>) of zeolite beta has obtained.

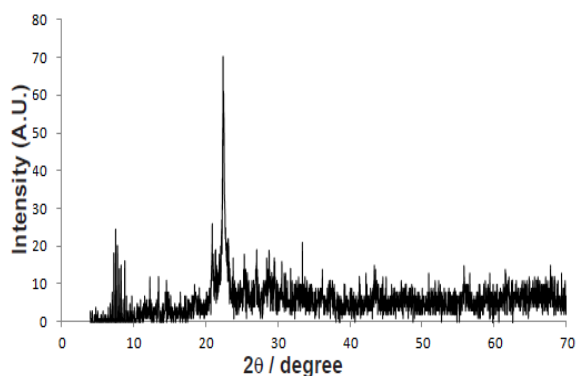


Figure 2. XRD patterns of zeolite beta treated at 140 °C

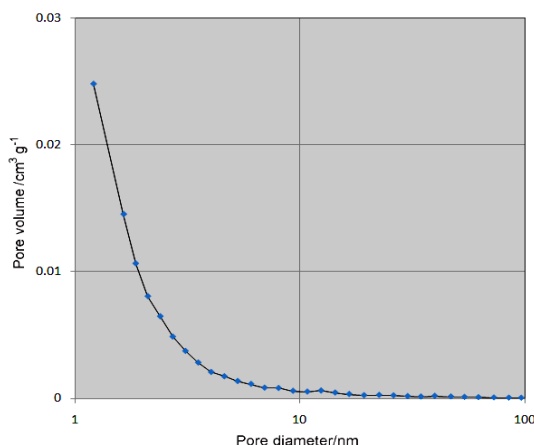


Figure 3. N<sub>2</sub> Adsorption-desorption isotherms of zeolite beta; pore size distribution of zeolite beta.

In the ring-opening process, in the best result, conversion of styrene oxide with methanol completed at 6 h to form its regioselective product with the selectivity of 100%.

### 4. Conclusions

Through a two-step crystallization procedure, an ordered mesoporous aluminosilicate has been synthesized from the assembly of preformed zeolite beta precursors, utilizing (CTAB) as a template. The catalyst was used for epoxide alcoholysis and conversion was obtained under mild conditions. The result with methanol showed 100% conversion after 6 h to its stable regioselective product.

### Acknowledgments

We thank Chemistry & Chemical Engineering Research Center of Iran (CCERCI) for the support of these studies.

### References

- 1) D.W. Breck, *Zeolite Molecular Sieves: Structure, Chemistry and Use*, Wiley, New York, **1974**, p. 771.
- 2) J. Weitkamp, *Solid State Ionics*, **2000**, 131, 175.
- 3) De Baerdemaeker, Trees, et al. "Catalytic applications of OSDA-free Beta zeolite." *J. Catal.*, **2013**, 308, 30873-81.



4<sup>th</sup> Iran National Zeolite Conference  
Golpayegan University of Technology, Golpayegan, Iran  
August 23-24, 2017



- 4) S. Zones, *Micropor. Mesopor. Mater.* **2011**, 144, 1.
- 5) Yilmaz, Bilge, et al. "A new catalyst platform: zeolite Beta from template-free synthesis." *Catal. Sci. & Tech.*, **2013**, 3.10, 2580-2586.
- 6) R.A. Vaibhav, et al. "An epoxide ring-opening reaction by using sol-gel-synthesized palladium supported on a strontium hydroxyl fluoride catalyst." *Comptes Rendus Chimie*, **2016**, 19.10, 1237-1246.
- 7) J. Huang, et al. "Synthesis, characterization and catalytic activity of cubic Ia 3 d and hexagonal p 6 mm mesoporous aluminosilicates with enhanced acidity." *J. mater. Chem.*, **2005**, 15.10, 1055-1060.
- 8) A. Tarlani, et al. "Grafted chromium 13-membered dioxo-macrocyclic complex into aminopropyl-based nanoporous SBA-15." *J. Solid State Chem.*, **2013**, 203, 255-259.

## Synthesis and Characterization of Nano Clinoptilolite/Ag/ZnO zeolite

S. Hatamzadeh<sup>a</sup>, M. Mehdipour Ghazi<sup>\*b</sup>, N. Keramati<sup>a</sup>

<sup>a</sup> Faculty of Nanotechnology, Semnan University, 35131-19111, Semnan, Iran

<sup>b</sup> Faculty of Chemical, Petroleum, and Gas Engineering, Semnan University, 35131-19111, Semnan, Iran

\*E-mail: mohsenmehdipour@yahoo.com

### 1. Introduction

Nano semiconductors especially nanoparticles of ZnO is the most commonly used photocatalyst for a wide range of organic compounds. ZnO, with a direct band gap energy of 3.37 eV is an attractive material for fundamental research and industrial application. Due to its unique optical and electrical properties, it is very useful for solar cells, gas sensors, nanolasers, etc. [1].

Recently, researches have been devoted in searching for the suitable substrates to support ZnO in order to improve the recovery efficiency of ZnO. Many materials have been used as photocatalyst supports; among them zeolites are very important. Properties such as high surface area, individual micropores, a variety of channels and high resistance make zeolites as very useful materials in industrial applications and academic research [2].

There have been substantial interests in the metal ion doped semiconductors as promising materials for potential applications in various fields. It has been recognized that metal ion doping not only facilitate inter facial charge-transfer reaction and enhances their photocatalytic activities, but also modify the absorption spectrum of the metal oxide nanomaterials. Doping of ZnO with Ag<sup>+</sup> into its lattice has been found enhanced the light absorption ability of ZnO nanomaterial as well as improved its gas sensing properties [3].

In this paper, natural zeolite supported Ag doped ZnO photocatalysts were synthesized. Based on this goal, XRD, FT-IR, DRS, SEM and BET are employed to investigate the composition, configuration and morphology of the photocatalysts..



# 4<sup>th</sup> Iran National Zeolite Conference

## Golpayegan University of Technology, Golpayegan, Iran

### August 23-24, 2017



## 2. Experimental

At the first, natural zeolite (clinoptilolite) powders were Purification with distilled water and  $H_2SO_4$  (0.1M) solution. To prepare the ZnO/Clinoptilolite (ZnO/CP), an appropriate amount of CP powder and ZnO was added to decuple of distilled water to form a solution and stirred for 15 min. Then, an appropriate amount of  $NaCO_3$  in aqueous solutions was added to the mixed solutions and was magnetically stirred. The sample was filtered off, washed and dried at  $120^\circ C$  and then calcinated at  $500^\circ C$  for 2 h. To prepare Ag-doped ZnO/CP, the above procedure was repeated. ZnO,  $AgNO_3$  and natural zeolite (CP) were dissolved in distilled water to form a solution. The mixed solutions were stirred continuously and Then, an appropriate amount of  $NaCO_3$  in aqueous solutions was added to the mixed solutions. The resulting solution was magnetically stirred and finally was centrifuged and washed. The final product was dried in oven at  $120^\circ C$  for 4 h and calcinated at  $500^\circ C$  for 2 h.

## 3. Results and discussion

The XRD patterns of the synthesized samples are shown in figure 1. The average crystallite size of the nanocrystale was calculated using the Debye- Scherer Equation from the major diffraction peaks. The average crystallite size of the samples was about 20-40 nm.

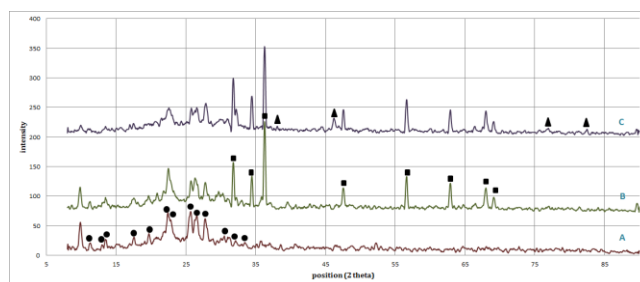


Figure 1. XRD patterns of A) CP, B) ZnO/CP, and C) Ag-ZnO/CP

The FTIR spectra of CP, ZnO/CP and Ag-doped ZnO modified by natural zeolite are shown in Figure 2. The absorption peaks in the range of  $400-800\text{ cm}^{-1}$  were attributed to ZnO stretching modes [5]. The board peak around  $3427\text{ cm}^{-1}$  and  $1627\text{ cm}^{-1}$  can be assigned to the O–H stretching and flexural vibration of adsorbed water, respectively. As shown in the spectrum of zeolite, the peak at  $1060.77\text{ cm}^{-1}$  corresponds to the Si–O–R (Si or Al) stretching vibration. The weak peaks between  $400-800\text{ cm}^{-1}$  correspond to Si–O–Si flexural vibration [6] and the closely spaced bands  $646.1\text{ cm}^{-1}$  are presents in the spectrum evidence of Ag–O–Zn tensional tremble.

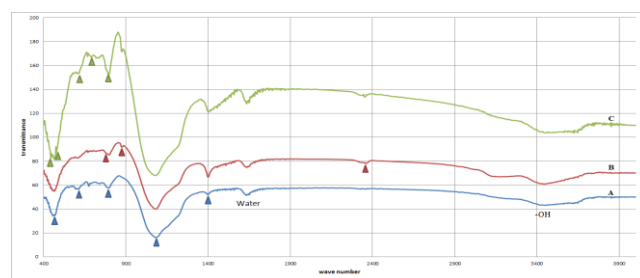


Figure 2. FT-IR patterns of A)CP, B) ZnO/CP, and C) Ag-ZnO/CP



4<sup>th</sup> Iran National Zeolite Conference  
 Golpayegan University of Technology, Golpayegan, Iran  
 August 23-24, 2017



Optical properties of the samples were investigated using DRS technique and the results are shown in Figure 3. The band gap energy ( $E_g$ ) of Ag–ZnO/CP reduce from 3.3 eV to 2.95 eV in comparison with that of ZnO. The reflectance data are presented as  $F(R)$ , obtained by the application of Kubelka-Munk algorithm that are shown at the right on above the figure. The reduction in the band gap of Ag–ZnO /zeolite could give ZnO/CP the capacity to absorb light at lower energy levels.

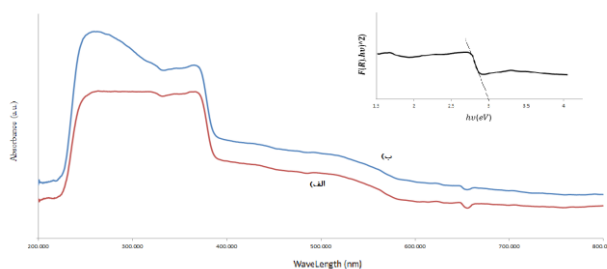


Figure 3. DRS patterns of A) CP, B) ZnO/CP, and C) Ag-ZnO/CP

Surface morphology of ZnO/CP and Ag–ZnO/CP was studied by SEM and the corresponding SEM images are shown in Figure 4(A) and (B), respectively. Images (A) and (B) show that the grinding of sample crystals was well to the spherical grains and the size of these particles is about 46–55 nm.

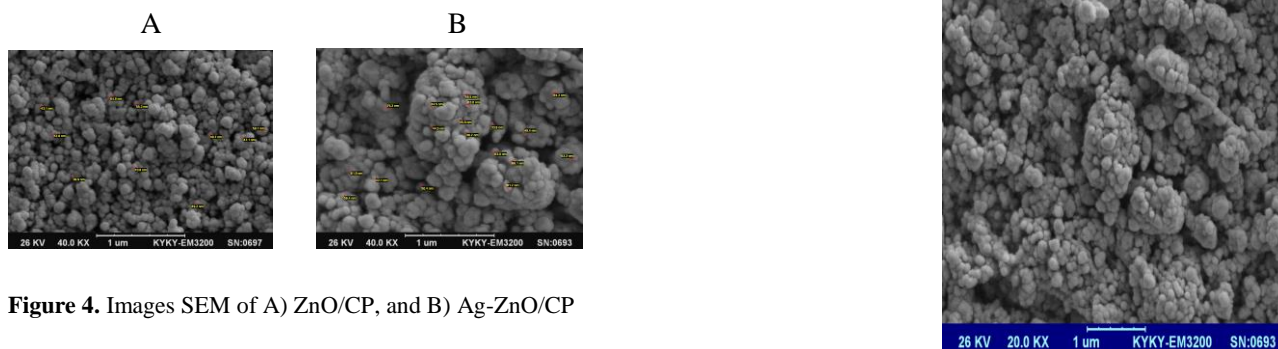


Figure 4. Images SEM of A) ZnO/CP, and B) Ag-ZnO/CP

Table 1. Mean pore diameter (D) and specific surface area (S) of the CP, ZnO/CP and Ag-ZnO/CP.

samples	D(nm)	S(m <sup>2</sup> /g)
CP	---	42.3
ZnO/CP	68	45.51
Ag-ZnO/CP	28.73	47

The BET analysis was carried out to determine the specific surface area of the nanoparticles. As can be seen at the table 1 , Ag–ZnO nanoparticles have higher BET surface area than undoped ZnO/CP and pure zeolite.

#### 4. Conclusions

In this study Natural zeolite supported Ag–ZnO photocatalysts were successfully prepared by co-precipitation method. It is shown that natural zeolite played an important role in the enhancement of photocatalytic properties at the Ag-ZnO nanoparticles. Which give a higher surface area to the synthesized product.



# 4<sup>th</sup> Iran National Zeolite Conference

## Golpayegan University of Technology, Golpayegan, Iran

### August 23-24, 2017



#### References

- 1) M. Bahrami, A. Nezamzadeh-Ejhih, *Materials Science in Semiconductor Processing* 30 (2015): 275-284.
- 2) J.-Ch. Sin, S.-M. Lam, K.-T. Lee, Abdul R. Mohamed, *Mater. Sci. Semicond. Process.* 16 (2013) 1542-1550.
- 3) A. Nezamzadeh-Ejhih, M. Karimi-Shamsabadi, *Appl. Catal. A: Gen.* 477 (2014) 83-92.
- 4) R. Kumar, D. Rana, et al, *Talanta* 137 (2015): 204-213.
- 5) A. Noorhidayati, et al, *Materials Science Forum.* Vol. 827. (2015) 43-48.
- 6) D.I. Petkowicz, R. Brambilla, et al, *Appl. Catal., A* 357 (2009) 125-134.

## Calculation of binding energies and radial distribution functions for diffusion of carbon disulfide in ITQ-7 zeolite

Mohammad Mohsen Loghavi,<sup>a,b</sup> Hossein Mohammadi-Manesh<sup>a,\*</sup>

<sup>a</sup> Department of Chemistry, Yazd University, Yazd, 89195-741, Iran

<sup>b</sup> Iranian space research center, Institute of Mechanics, Shiraz 71555-414, Iran

\*Email: mohammadimanesh@yazd.ac.ir

### 1. Introduction

Nanoporous materials have general applications in chemical industry, but the pathway from laboratory synthesis and testing to practical use of nanoporous materials is noticeably challenging and requires fundamental understanding from the bottom up. With ever-growing computational resources, molecular simulations have become an essential tool for material characterization, screening and design. It is demonstrated that molecular-level studies can bridge the gap between physical and engineering sciences, unravel microscopic insights that are otherwise experimentally unreachable, and assist in the rational design of new materials<sup>1</sup>.

Zeolites are multipurpose materials which are vital for a wide range of industries, because of their unique structural and chemical properties, which are the basis of applications in gas separation, ion exchange, and catalysis<sup>2</sup>. Zeolite as a nanoporous material consist of crystalline three-dimensionally connected SiO<sub>4</sub> and AlO<sub>4</sub> tetrahedra, which encompass cavities comprising exchangeable cations and water molecules. The cations compensate the negative charges of the AlO<sub>4</sub> components. In this study, diffusion of carbon disulfide in all-Siliceous zeolite (ITQ-7) have been simulated and quantities such as binding energy and radial distribution function have been calculated. ITQ-7 (structure type ISV) has a three-dimensional system of large pores. defined by windows containing 12 member rings of about 6 Å in diameter<sup>3</sup>. CS<sub>2</sub>, is very toxic and is harmful by inhalation of the vapor, skin absorption of the liquid, or ingestion<sup>4</sup>.

### 2. Theoretical Details

In the simulation of nanoporous crystal-like materials, the coordinates of basis atoms are generally adopted from experimental crystallographic information. Most studies use rigid frameworks with atomic sites fixed. This has two benefits: first, there is no necessity to estimate intra-framework interactions; second, the interactions among framework and guest can be pre-tabulated and simulation can be faster. Such a simplified action is acceptable, mainly for small guest molecules in nanoporous materials. The ordered crystal structures are mimicked using periodic boundary conditions, in which the simulation box is surrounded by its replicated images. By the way, the simulation system can be considered as extremely large. Simulation should run for sufficiently long to assure equilibration or



# 4<sup>th</sup> Iran National Zeolite Conference

## Golpayegan University of Technology, Golpayegan, Iran

### August 23-24, 2017



steady state is reached, and then ensemble averages can be calculated. All interatomic interactions between the atoms in the simulation box and the nearest image sites were calculated within a cutoff distance of  $R_{\text{cut-off}}=13\text{\AA}$  for all simulated systems. The electrostatic interactions were evaluated using the Ewald method with a precision of  $1\times 10^{-6}$ . Molecular dynamics simulations were performed on the periodic  $3\times 3\times 3$  replica of the ITQ-7 unit cell at loadings of 2, 4, 6, 8, 10, 12, 14 and 16 molecules per unit cell and different temperatures-200 K, 298 K, 400 K, 500 K, 600 K and 700 K via the DL\_POLY program version 2.18. Periodic boundary conditions were applied and the time-step and pressure in all simulations were 1 fs and 1 bar respectively. Each MD simulation started with an equilibration (300000 time-steps in the NVT ensemble) followed by MD runs (500000 time-steps) in the NVE ensemble for data collecting. The trajectory was recorded every 200 steps during the production stage, and radial distribution functions were recorded every 500 steps<sup>5</sup>.

### 3. Results and discussion

The binding energy for the ITQ-7 with  $n\text{CS}_2$  molecules per unit cell is calculated as,<sup>6</sup>  
 $E_{\text{binding}}=E(\text{ITQ+guests}) - E(\text{ITQ}) - nE(\text{guests})$

Amounts of  $E(\text{ITQ+guests})$  and  $E(\text{ITQ})$  can be obtained from simulation run. We assumed  $\text{CS}_2$  as a triatomic ideal gas and  $E(\text{guests})$  calculated via ideal gas law. The binding energies as a function of the number of guest molecules per ITQ-7 zeolite and temperature are plotted in Figure 1. By and large, the binding energies of  $\text{CS}_2$  at lower temperatures are stronger than higher temperatures, regardless of the guest population in the unit cell. Motion ability of the guest molecules diminish with decreasing temperature thus framework-guest interactions become stronger and the guests can escape from binding sites hardly. Besides, binding energies increase with loading because at high loadings there are limited spaces for motion of guests and thus guest molecules encounter with framework atoms increasingly. So, the number of binding sites increase that follow raising the chance of  $\text{CS}_2$  adsorption.

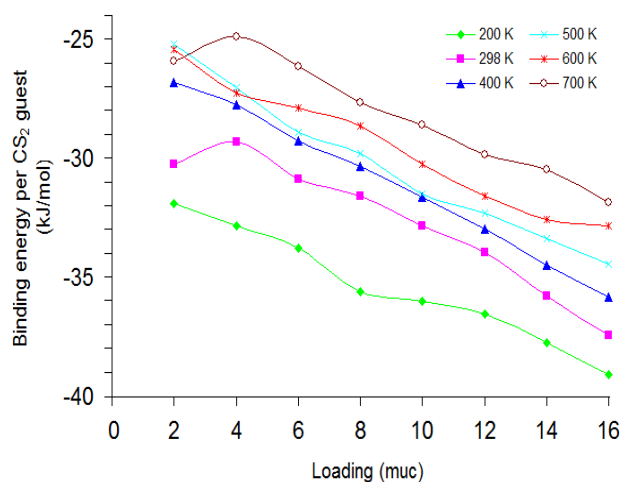


Figure 1. Calculated binding energies as a function of  $\text{CS}_2$  loadings.

Radial distribution function or  $g_{ab}(r)$  specifies the local arrangement of the b-type atoms in the compound as you move radially away from the central a-type atom. For a random distribution of molecules,  $g_{ab}(r)$  would equal one<sup>7</sup>.

Figure 2 shows the carbon-carbon radial distribution functions at 500 K for all loadings. Figure 3 illustrates the carbon-carbon RDFs at loading of 8 muc for all temperatures. As seen, at constant temperature and with increasing loading, first peak appears in smaller distance with higher intensity. Also, at constant loading and with increasing temperature, carbon atoms can be dispersed much more freely and so, first peak begins to broaden and lessen in intensity at larger distance.





4<sup>th</sup> Iran National Zeolite Conference  
Golpayegan University of Technology, Golpayegan, Iran  
August 23-24, 2017

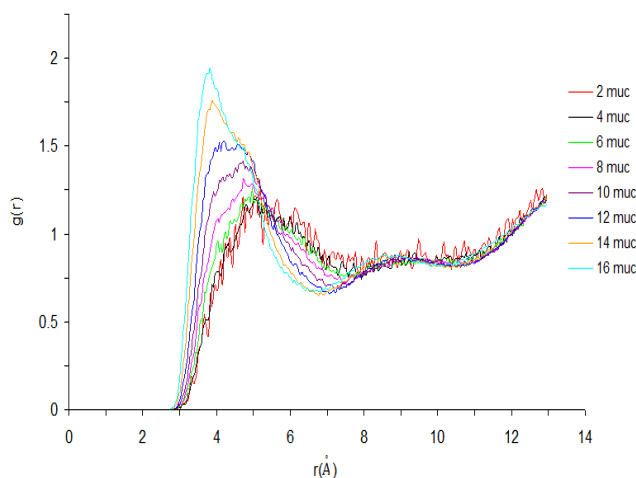


Figure 2. The C-C Radial distribution functions at 500 K and all loadings.

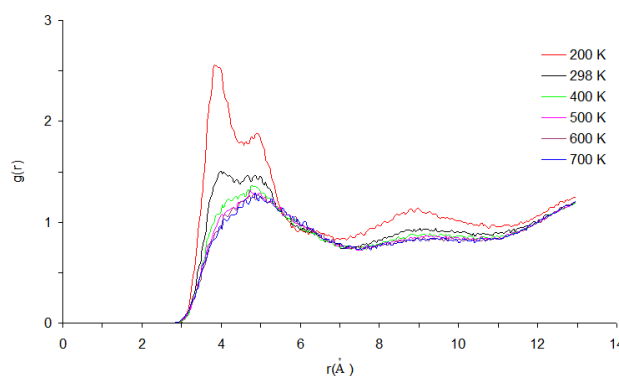


Figure 3. The C-C Radial distribution functions at 8 muc and all temperatures.

#### 4. Conclusions

Diffusion of carbon disulfide molecules in ISV-type zeolite was studied via the molecular dynamics simulation. Some properties such as RDFs and adsorption energies were calculated at different loadings and temperatures. Binding energies were calculated at different conditions of temperature and loading. In general, the binding energies of CS<sub>2</sub> at lower temperatures are stronger. Also, binding energies increase as a function of loading. The C-C RDF plots show at constant temperature and with increasing loading, first peak appears in lesser distance with higher intensity. Also, at constant loading and with increasing temperature, first peak begins to widen and lessen in intensity at longer distance.

#### References

- 1) J. Jiang, R. Babarao, z. Hu, *Chem Soc Rev.* **2011**, 40, 3599-3612.
- 2) A. Abdelrasoul, H. Zhang, C.-H. Cheng, H. Doan, *Microporous and Mesoporous Materials* **2017**, 42, 294-348
- 3) D. Selassie, D. Davis, J. Dahlin, E. Feise, G. Haman, D. S. Sholl, D. Kohen, *J. Phys. Chem. C.* **2008**, 42, 112.
- 4) H. F. Mark, D. F. Othmer, C. G. Overberger, G. T. Seaborg, *Encyclopedia of chemical technology*, John Wiley & Sons, New York, **1978**.
- 5) D. F. Plant, G. Maurin, R. G. Bell, *J. Phys. Chem. B.* **2007**, 11, 111.
- 6) Sirjoosingh, A.; Alavi, S.; Woo, T. K. *J. Phys. Chem. C* **2010**, 114, 2171–2178.
- 7) O.F. Speer, B. C. Wengerter, R. Taylor, *J. Chem. Educ.*, **2004**, 81, 1330-1332.



4<sup>th</sup> Iran National Zeolite Conference  
Golpayegan University of Technology, Golpayegan, Iran  
August 23-24, 2017



**Catalytic activity and electrochemical properties of zeolite encapsulated  
Copper(II)-Schiff-base Complexes for green oxidation of sulfides**

Saeed Rayati\*, Elham Khodaei

Department of Chemistry, K.N. Toosi University of Technology, P.O. Box 16315-1618, Tehran 15418, Iran

\*Email: rayati@kntu.ac.ir

## 1. Introduction

One of the major drawbacks of homogeneous catalysis is the need to separate the catalysts from the reaction mixture at the end of the reaction. In addition, contamination by the metal catalysts restricts their use in industry. Nowadays, many researchers use different techniques to recover the homogeneous catalysts. Among all supports, zeolite is an excellent material to use in a transition metal ion exchange because of its low cost and an intra-crystalline cavity [1-4]. In this study to perform selective oxidation of sulfides to sulfoxides, copper(II) Schiff-base complexes encapsulated in Na-Y zeolite under various reaction conditions have been investigated [5-7].

## 2. Experimental

### 2.1. Preparation of the Schiff base ligands

The Schiff base ligands (Fig. 1) were prepared by the reported methods [8].

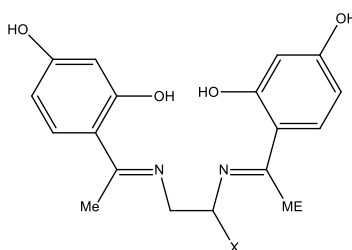


Fig. 1. General structure of the Schiff base ligand

### 2.2 Preparation of the CuL<sub>1</sub>-Y and CuL<sub>2</sub>-Y

Encapsulation of metal complexes was performed with the flexible ligand method. Cu-Y (0.7 g) and 1.25 g of the Schiff base ligands were mixed in 50 mL of methanol, and the reaction mixture was refluxed for 17 h in an oil bath with stirring. The resulting material was separated by filtration and then extracted with methanol using Soxhlet extractor for 72 h to remove unreacted ligands from the cavities of the zeolite as well as those located on the surface of the zeolite along with neat complexes. The unreacted metal ions present in the zeolite were removed by stirring with aqueous 0.01 M NaCl solution. The resulting solid was filtered and washed with distilled water until free from chloride ions.



4<sup>th</sup> Iran National Zeolite Conference  
Golpayegan University of Technology, Golpayegan, Iran  
August 23-24, 2017



### 3. Results and discussion

#### 3.1. Characterization of the catalysts

The Cu-content of the encapsulated catalysts determined by atomic absorption spectroscopy revealed that the metal content of the catalysts is 2.86% and 2.56% for CuL<sub>1</sub> and CuL<sub>2</sub>, respectively.

Table 1 summarizes the BET surface area ( $S_{BET}$ ), the total pore volume and the average pore size of the Cu-Y, CuL<sub>1</sub>-Y and CuL<sub>2</sub>-Y.

**Table 1.** Textural properties of Cu-Y and its complexes-encapsulated analogue.

sample	$S_{BET}$ (m <sup>2</sup> g <sup>-1</sup> )	Average pore size (Å)	Pore volume (cm <sup>3</sup> g <sup>-1</sup> )
Cu-Y	427.9644	102.1748	1.093179
CuL <sub>1</sub> -Y	418.3000	88.2604	0.922983
CuL <sub>2</sub> -Y	413.5092	20.2978	0.209834

The IR spectrum of the ligands and exhibit a sharp band at 1630 (H<sub>2</sub>L<sub>1</sub>) or 1632 cm<sup>-1</sup> (H<sub>2</sub>L<sub>2</sub>) which is characteristic of azomethine group. Copper Schiff base complexes (CuL<sub>1</sub> and CuL<sub>2</sub>) showed sharp bands at lower frequency in 1605 or 1614.43 cm<sup>-1</sup> respectively which indicated the coordination of ligands to copper center.

Typical scanning electron micrographs obtained for the parent Na-Y, CuL<sub>1</sub>-Y, CuL<sub>2</sub>-Y are shown in Fig 2.

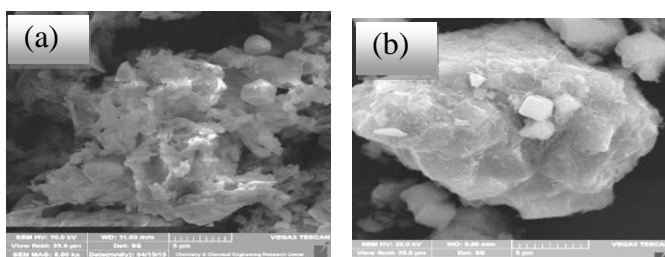


**Fig. 2.** SEM Photographs of (a) CuL<sub>1</sub>-Y and (b) CuL<sub>2</sub>-Y

Comparison the cyclic voltammograms of two catalysts exhibited the catalytic activity of CuL<sub>1</sub>-Y is higher than CuL<sub>2</sub>-Y. Cyclic voltammograms of GC/CuL<sub>1</sub>-Y and GC/CuL<sub>2</sub>-Y in the presence of 80 mmol methyl phenyl sulfide using 880 mmol H<sub>2</sub>O<sub>2</sub> at various scan rates are displayed in Fig 3. The oxidation or reduction peaks became broader with increasing scan rate. In addition, in higher scan rates, the oxidation peaks shifted to more positive potentials for sulfide oxidation which indicates that the electro-oxidation of copper species to higher valance state is much faster than the catalytic oxidation of substrates. This reveals that an increase in scan rate decreases the rate of sulfide oxidation. Furthermore, the anodic peak currents that are linearly proportional to the square root of scan rate suggest that the overall oxidation of sulfide at this electrode is controlled by the diffusion of sulfide to the surface redox sites.



4<sup>th</sup> Iran National Zeolite Conference  
Golpayegan University of Technology, Golpayegan, Iran  
August 23-24, 2017

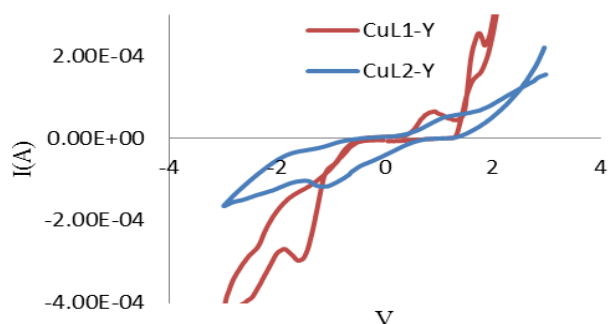


Fig 3. The voltammetric behavior of CuL<sub>1</sub>-Y and CuL<sub>2</sub>-Y at 100 mV/s. Reaction conditions: catalyst (mmol): sulfide: H<sub>2</sub>O<sub>2</sub>: is 1:80:880 at room temperature between -3 and 3 V in acetonitrile solution containing 0.1 M TBAH as supporting electrolyte.

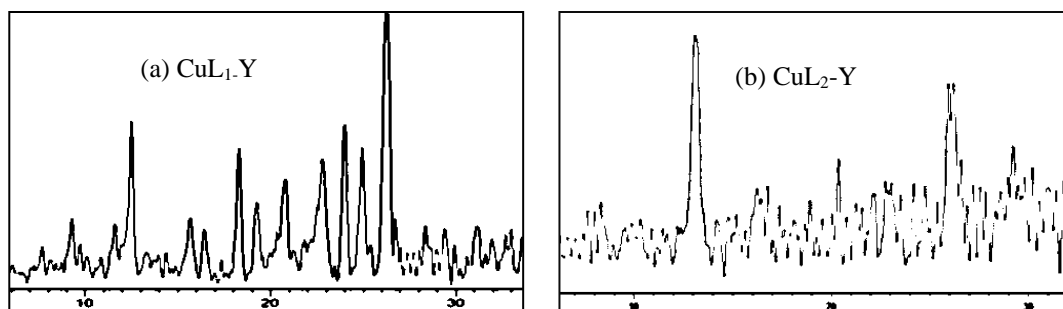


Fig 4. XRD patterns of (a) CuL<sub>1</sub>-Y and (b) CuL<sub>2</sub>-Y

Comparison of the XRD pattern of zeolite Na-Y and the encapsulated Cu complexes indicated no new crystalline pattern for the lattice. Therefore, the crystallinity of the Cu-Y is almost intact after encapsulation of the complexes (Fig 4). These results further suggest that the reduction in surface area of the encapsulated complexes is not due to any collapse of the crystalline structure.

### 3.2. Catalytic activity

The catalytic activity of the heterogeneous catalysts was investigated in the oxidation of various sulfides with hydrogen peroxide as green oxidant in ethanol. We first examined the oxidation of methyl phenyl sulfide as the representative substrate for the optimization of reaction conditions with CuL<sub>1</sub>-Y in the oxidation of sulfides. In this study several parameters, such as reaction time, temperature, molar ratios of the oxidant and the concentration of the catalyst were investigated during the optimization of the reaction.

Under the optimized conditions, the catalysts were used for oxidation of a wide range of sulfides (Table 2). The performance of these catalysts was excellent for the oxidation of sulfides to corresponding sulfoxide products during 20 min at 50 °C.



4<sup>th</sup> Iran National Zeolite Conference  
 Golpayegan University of Technology, Golpayegan, Iran  
 August 23-24, 2017



Table 2. Oxidation of various sulfides by CuL<sub>1</sub>-Y and CuL<sub>2</sub>-Y.

Substrates	Conversion % CuL <sub>1</sub> -Y	Conversion % CuL <sub>2</sub> -Y
	100	91
	98	94
	100	92
	94	86
	51	44
	100	100
	100	96
	95	90
	100	99
	100	97

<sup>a</sup>Reaction conditions: catalyst: sulfide: H<sub>2</sub>O<sub>2</sub> is 1:80:880 at 50 °C for a 20 min reaction time.

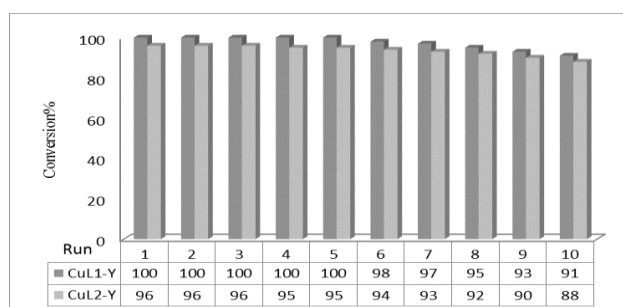


Fig 5. Reuse of the heterogeneous catalysts in the oxidation of thioanisole. Reaction conditions: catalyst: sulfide: H<sub>2</sub>O<sub>2</sub> is 1:80:880 at 50 °C for a 20 min reaction time.



# 4<sup>th</sup> Iran National Zeolite Conference

## Golpayegan University of Technology, Golpayegan, Iran

### August 23-24, 2017



The heterogeneous catalysts can be recovered quantitatively by simple filtration and reused several times without significant loss of activity. The catalysts could be reused at least ten times without appreciable loss of their catalytic performance (Fig. 5).

#### 4. Conclusions

In summary, a tetradentate Schiff base ( $N_2O_2$ ) ligands and their corresponding copper(II) complexes  $CuL_1$  and  $CuL_2$  as homogeneous catalysts synthesized and characterized. In addition, copper was loaded in to zeolite-Y which led to the formation of Cu-Y. The selective oxidation of sulfides to their corresponding products is found to enhance in the presence of the encapsulated complexes using  $H_2O_2$  as green oxidant in ethanol by approaching to the green chemistry. Also the electrochemical behavior of  $CuL_1$ -Y and  $CuL_2$ -Y were investigated in different condition by cyclic voltammetry and chronoamperometry techniques.

Comparison the catalytic activity of homogeneous catalyst in optimum conditions (catalyst: sulfide:  $H_2O_2$  is 1:80:880 at  $50^\circ C$  for a 20 min reaction time) indicated the lower oxidation activity (97% and 94%) of neat  $CuL_1$  and  $CuL_2$  as unsupported catalysts in the oxidation of thioanisole compared with heterogeneous catalysts.

#### References

- [1] J. Hagen, Economic Importance of Catalysts, in Industrial Catalysis: A Practical Approach, Wiley-VCH Verlag GmbH & Co. KGaA, Weinheim, Germany, 2015.
- [2] Y.G. Nazarova, E. N. Ivashkina, E. D. Ivanchina, V. I. Stebeneva, *Pet Coal.*, 2016; 58,709-714.
- [3] B.Yilmaz, U. Müller, *Top Catal.*, 2009, 52, 888.
- L. Lopez, J. Velasco, V. Montes, A. Marinas, S.Cabrera, M. Boutonnet and S. Järås, *Catalysts.*, 2015, 5, 1737-1755.
- [4] D. Friedmann, A. Hakki, H. Kim, W. Choi, D. Bahnemann. *Green Chem.* **2016**, 18, 5391-5411.
- [5] A. Primo, H. Garcia. *Chem. Soc. Rev.* **2014**, 43, 7548-7561.
- [6] Z. Jin, Y. Luan, M. Yang, J. Tang, J. Wang, J. Gao, H. Lu; Y. Wang. *RSC Adv.* **2015**, 5, 78962-78970.
- [7] G. Huang, F. Pan, G. Fan, G. Liu, *J. Environ. Sci Health.* **2016**, 51, 626-633.
- 7, 3364-3369.
- [8] N. Sathya, P. Muthusamy, N. Padmapriya, G. Rajaa, K. Deivasigamani, C. Jayabalakrishnan, *J. Coord. Chem.*, **62**, 3532 (2009).



# 4<sup>th</sup> Iran National Zeolite Conference

## Golpayegan University of Technology, Golpayegan, Iran

### August 23-24, 2017



## A Comparison on Lead Adsorption from Wastewater by Natural, Modified, and Synthetic Zeolites: A review

Somayeh Amiri Zare<sup>a</sup>, Fereshteh Raouf<sup>a\*</sup>, Leila Mivehei<sup>b</sup>

<sup>a</sup> Department of Chemical Engineering, University of Guilan, 4163513769, Rasht, Iran

<sup>b</sup> Department of Textile Engineering, University of Guilan, 4163513769, Rasht, Iran

\*Email: f.raouf@guilan.ac.ir

### 1. Introduction

The water pollution caused by organic and inorganic compounds is a world problem originated by natural or anthropogenic sources[1]. According to the list of priority pollutants of the US Environmental Protection Agency (EPA), arsenic, chromium, cobalt, nickel, copper, zinc, silver, cadmium, mercury, titanium, selenium and lead represent a serious problem for the human health because they are not biodegradable and tend to accumulate in living organisms causing several diseases [2]. Additionally, in the wastewater of paints and pigments industries, heavy metals are also present with dyes and, considering that some dyes are toxic, non-degradable, stable and even carcinogenic, the treatment of these wastewaters is very difficult and mostly ineffective when using traditional purification processes[3]. The most commonly used methods for removing heavy metals are chemical or electrochemical precipitation, both of which pose a significant problem in terms of the disposal of precipitated wastes. Further, ion-exchange treatments are also available, which do not appear to be economical. It has been reported that some aquatic plants, wood materials, agricultural by-products, clay, natural zeolite, microorganisms and other low-cost adsorbents have the capacity to adsorb and accumulate heavy metals[4]. Lead has been found to be acute toxic to human beings when present in high amounts (e.g. >15 µg).

Therefore, the removal of excess lead ions from wastewater is essential. Treatment processes usually include chemical precipitation, adsorption, solvent extraction, ultrafiltration and ion exchange. Zeolites are inexpensive natural materials with a high and selective cation exchange capacity[5]. Natural zeolites have ion exchange and removal capacity. Clinoptilolite has high removal capacity of metal ions  $Pb^{+2}$ ,  $Cu^{+2}$ ,  $Zn^{+2}$ ,  $Cd^{+2}$ ,  $Ni^{+2}$ ,  $Fe^{+2}$  and  $Mn^{+2}$ .

### 2. Experimental Part

#### 2.1 Pb Adsorption on Zeolites

Leppert et al, reported that zeolites, clinoptilolite in particular, demonstrate strong affinity for Pb and other heavy metals [6]. Zeolites are naturally occurring silicate minerals, which can also be produced synthetically. Clinoptilolite is probably the most abundant of more than 40 natural zeolite species[7]. Deposits of this mineral occur in abundance making it readily available and inexpensive. The adsorption properties of zeolites result from their ion-exchange capabilities. Three-dimensional structure of zeolite possesses large channels containing negatively charged sites resulting from  $Al^{3+}$  replacement of  $Si^{4+}$  in the tetrahedra. Sodium, calcium, potassium and other positively charged exchangeable ions occupy the channels within the structure, and can be replaced with heavy metals. Leppert reported that the overall adsorption capacity for zeolites varies for different species, but tends to be around 1.5 meq/g (155.4 mg Pb/g zeolite).



4<sup>th</sup> Iran National Zeolite Conference  
Golpayegan University of Technology, Golpayegan, Iran  
August 23-24, 2017



### 3. Results and discussion

#### 3.1 Effect of pH

The pH value of the solution has a significant impact on the removal of heavy metals, because it determines degree of ionization of metal ions in aqueous solution and the charge on the surface of adsorbents. Kabwadza-Corner et al indicated that precipitation of Pb was only noticeable at  $\text{pH} > 6.5$  [8].

of the amount adsorbed and equilibrium pH at initial concentration of  $600 \mu\text{mol}\cdot\text{L}^{-1}$ . It also highlighted the high dependence on pH, of the adsorption of Pb within this pH region. In the pH range of 2 - 6, the sorption percentage increases gradually with increasing pH. Adsorption is mainly dominated by ion exchange as  $\text{H}^+$  ions are competitive to Pb ions for ion exchange sites.

Pandey et al investigated the effect of pH on sorption of Pb(II) on Zeolite-NaX at 303K by varying the pH from 4.0 to 7.0 for equilibrium adsorption at initial concentrations of 10, 15, 20, 25 and 30 mg/L. It observed that the removal of Pb(II) increased with increasing pH and recorded its minimum values at 4.0 [9]. Effect of pH on the adsorption of Pb(II) by the clinoptilolite was investigated with the changing pH values from 3.0 to 9.0 by Dursun et al [10]. The results depicting the dependence of the Pb (II) removal as a function of pH shows that maximum removal efficiencies have been achieved to be 86 % at pH 5.0.

Argun et al represented at different pH values Pb ions may present in different forms. For this reason,  $\text{Pb}^{+2}$  ions dominate at  $\text{pH} < 6$  and  $\text{Pb}(\text{OH})_2$  dominates at  $\text{pH} > 5$  [11]. The behavior at lower pH values can be explained on the following basis that the  $\text{H}^+$  ions compete with the metal cation for the adsorption sites on the adsorbent, which in turn leads to partial release of the metal cation. The heavy metal cations are completely released under extreme acidic conditions. At higher pH level the concentration of the  $\text{H}^+$  ions as competing ion decreases and that results in an increase in the amount of the adsorbed metals. The amount of complex hydrated forms of the metals increases with increasing pH that intensifies adsorption. Thus, it is possible to manage metal ion uptake from aqueous solution by changing the pH value.

#### 3.2 Effect of Zeolite Modification

Kragovi et al showed that significantly higher sorption of lead was achieved with modification of the natural zeolite with Fe(III) ions under basic conditions [5]. Sorption experiments as well as characterization of both the natural and Fe(III) modified zeolite before and after sorption of lead confirmed complex lead sorption mechanism including ion exchange as well as chemisorption and precipitation of lead at the zeolitic surface. Based on the obtained results by Anari-Anaraket al, modification of clinoptilolite Nano particles with HDTMA and DTZ significantly increased the removal of Pb(II) cations with respect to raw micronized and nanoparticles of clinoptilolite. In the modified Pb-exchanged forms due to occupying of free electrons of nitrogen and sulfur atoms by Pb(II) cations, less tendency of this sorbent was observed towards Pb(II) cations with respect to the corresponding modified raw nano particles [12].

### 4. Conclusions

The results presented in this study show that a more efficient sorbent for Pb removal from aqueous solution was obtained through the modification of a natural zeolitic samples. Although operating conditions such as pH, initial concentration of Pb and contact time had important effect depends to Zeolite types.

### References





4<sup>th</sup> Iran National Zeolite Conference  
Golpayegan University of Technology, Golpayegan, Iran  
August 23-24, 2017



- 1) N. M. Mubarak , J.N.S., E. C. Abdullah and N. S. Jayakumar, Removal of Heavy Metals from Wastewater Using Carbon Nanotubes. Separation & Purification Reviews, **2013**, 43, 311-338.
- 2) D. W. O'Connell, C.B., T. F. O'Dwyer, heavy metal adsorbents prepared from the modification of cellulose: A review. Bioresource Technology **2008** ,99 , 6709–6724.
- 3) Lakherwal, D., Adsorption of Heavy Metals: A Review. International Journal of Environmental Research and Development, **2014**, 4, 41-48.
- 4) S. E. Bailey , T.J.O., R. M. Brick and D. D Adriani, A Review of Potentially Low-Cost Sorbent for Heavy Metals Pergamon, **1999**,33, 2469-2479.
- 5) M. Kragovi, A.D., M, Markovi, Characterization of lead sorption by the natural and Fe(III)-modified zeolite. Applied Surface Science, **2013**. 283, 764-774.
- 6) A. Al-Haj Ali, R.E.-B., Removal of Lead and Nickel Ions Using Zeolite Tuff. J. Chem. Tech. Biotechnol, **1997**, 69, 27-34.
- 7) D. W. Ming, J.B.D., Quantitative Determination of Clinoptilolite in Soils by a Cation-Exchange Capacity Method. Clays and Clay Minerals **1987**, 35, 463-468.
- 8) P. Kabwadza-Corner, E.J., N. Matsue, pH Dependence of Lead Adsorption on Zeolites. Journal of Environmental Protection, **2015**,6, 45-53.
- 9) P. K. Pandey, S.K.S., S.S. Sambhi, Removal of lead(II) from waste water on zeolite-NaX. Journal of Environmental Chemical Engineering, **2015**. 3, 2604–2610.
- 10) S. Dursun, A.P., Lead pollution removal from water using a natural zeolite. urnal of International Environmental Application & Science, **2007**, 2,11-19.
- 11) M. E. Argun, D.Ö., Heavy metal adsorption by modified oak sawdust: thermodynamics and kinetics. Hazard. Materials. In Press., **2007**,141, 77-85.
- 12) M. Anari-Anaraki, A.N.-E., Modification of an Iranian clinoptilolite nano-particles by hexadecyltrimethyl ammonium cationic surfactant and dithizone for removal of Pb(II) from aqueous solution. J. of Colloid and Interface Science **2015**, 44, 272–281.

## Synthesis of Inorganic-organic Hybrid Nano Structures based on Zeolite / Fe<sub>3</sub>O<sub>4</sub>

Zohreh Mortezaei<sup>a</sup> , Mojgan Zendehtdel<sup>\*a</sup> , Mohammad Ali Bodaghi Fard<sup>a</sup>

<sup>a</sup> Department of Chemistry, Faculty of Science, Arak University, Arak 38156-8- 8349; Iran

\*Email: [m-zendehtdel@araku.ac.ir](mailto:m-zendehtdel@araku.ac.ir)

### 1. Introduction

The zeolites are a crystalline aluminosilicates with well defined channel and cavity that these cavities contain metal cations and removable water. One of the good pores structure is Y zeolite consist almost spherical 12 Å° cavities [1] Some articles published report to synthesize magnetic zeolites, such as Horikawa et al., that synthesized magnetic zeolites by nickel ion exchanging sodium ion in the synthesis process. Nah prepared magnetic-modified zeolite (MMZ) was by urethane coating, and other investigators synthesized magnetic carrier by magnetic tetroxide iron (Fe<sub>3</sub>O<sub>4</sub>) modifying zeolites to separate metallic contaminants from water. Because the Fe<sub>3</sub>O<sub>4</sub> particles contacting with zeolite were naked and then oxidized, they easily lost magnetic.

### 2. Experimental

#### Synthesis of Fe<sub>3</sub>O<sub>4</sub>



# 4<sup>th</sup> Iran National Zeolite Conference

## Golpayegan University of Technology, Golpayegan, Iran

### August 23-24, 2017



Fe<sub>3</sub>O<sub>4</sub> nanoparticles were synthesized by coprecipitation of FeCl<sub>3</sub>.6H<sub>2</sub>O and FeCl<sub>2</sub>.4H<sub>2</sub>O at the molar ratio of following condition (Fe<sup>3+</sup> : Fe<sup>2+</sup> = 2:1), and they were dissolved in deionized water. After stirring for 30 min, NH<sub>3</sub> was added to the solution. The Fe<sub>3</sub>O<sub>4</sub> nanoparticle filtered and washed five times with deionized water [2].

### Fe<sub>3</sub>O<sub>4</sub>/NaP composites

Different amount of Fe<sub>3</sub>O<sub>4</sub> was added to a fresh NaP gel with the molar composition of 320 H<sub>2</sub>O : 16 NaOH : 1 Al(OH)<sub>3</sub> : 15 SiO<sub>2</sub> and mixed with agitation to form a Fe<sub>3</sub>O<sub>4</sub>/NaP gel, and finally placed in an autoclave at 100 °C for 24 h. After cooling the reaction mixture to room temperature, filtering, washing with water, and drying in air, the solid product Fe<sub>3</sub>O<sub>4</sub>/NaP composite was recovered from the mixture [3-6].

### Synthesis of Inorg-Org Hybrids

Organic modification of Fe<sub>3</sub>O<sub>4</sub>/NaP composites with 3-chloro propyltriethoxysilane (3-CIPTES) was performed by stirring 0.1 g of porous materials with 3-CPTES (0.10 g, 0.45 mmol) in 20 mL dry toluene at 110 °C for 24 h. The solid was filtered and washed with ethanol and acetone, and air dried at room temperature and 2-amino pyridine (1g) was added to it and refluxed. The powder separated and washed with ethanol. The elemental analysis of modified compounds shows the molar ratio that confirmed immobilized amine on the porous material structure.

### 3. Results and discussion

Fe<sub>3</sub>O<sub>4</sub>/NaP Zeolite nanocomposite with different molar ratio were successfully synthesized and characterized using FT-IR, XRD, TGA, SEM and VSM techniques. The SEM graphs showed that much of Fe<sub>3</sub>O<sub>4</sub> was successfully coated by the NaP zeolite layer. Also, the results show that the magnetism of the products is stable with added zeolite. These particles show perfectly uniform sphere and the average size of Fe<sub>3</sub>O<sub>4</sub> is about 20 nm, and the aggregation of the nanoparticles can be discerned clearly.

The FT-IR spectrum of Fe<sub>3</sub>O<sub>4</sub> shows the three vibration bands in the 388, 577 and 1622 cm<sup>-1</sup> regions.

The FT-IR spectra of hybrid materials indicate an intense band about ca.1000-1030 cm<sup>-1</sup> attributable to the asymmetric stretching of Al–O–Si chain of zeolite. The symmetric stretching and bending frequency bands of Al–O–Si framework of zeolite appear at ca.791 and 463 cm<sup>-1</sup>, respectively

Fig .1 represents the X-ray diffractogram of amino functionalized Fe<sub>3</sub>O<sub>4</sub>@NaP nano composite. The data obtained confirmed the presence of Fe<sub>3</sub>O<sub>4</sub> and NaP. According to similar studies, in the present study no changes were detected in the crystalline structure and morphology of zeolite during the immobilization procedures, also the percentage of amorphous phase is very small.



4<sup>th</sup> Iran National Zeolite Conference  
Golpayegan University of Technology, Golpayegan, Iran  
August 23-24, 2017

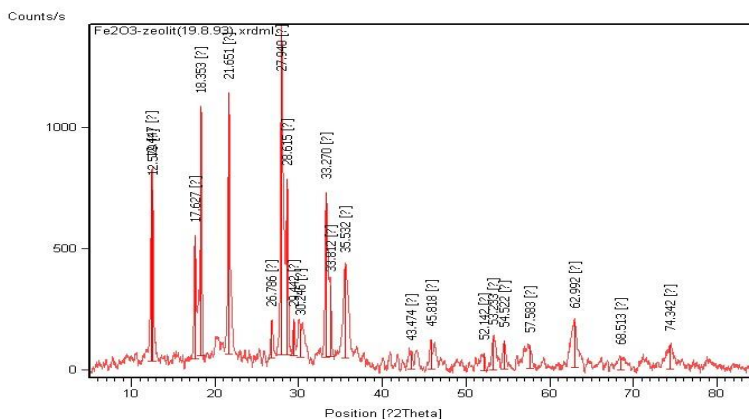


Figure 1. The XRD of amino functionalized  $\text{Fe}_3\text{O}_4@\text{NaP}$

The morphology and structural features of amino functionalized  $\text{Fe}_3\text{O}_4@\text{NaP}$  were observed using SEM and the images are shown in Fig. 2.

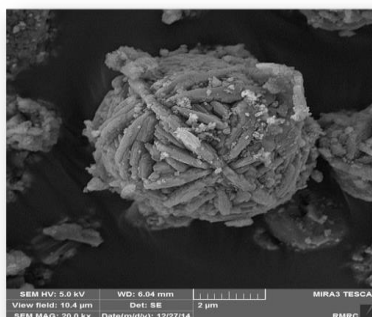


Figure 2. SEM of amino functionalized  $\text{Fe}_3\text{O}_4@\text{NaP}$

#### 4. Conclusions

The alkyl amino pyridin-functionalized  $\text{Fe}_3\text{O}_4@\text{NaP}$  nano composite has been prepared and characterized.

#### Acknowledgments

Thanks are due to the Iranian Nanotechnology Initiative and the Research Council of Arak University of Technology and Center of Excellence in the Chemistry Department of Arak University of Technology for supporting of this work.

#### References

1. M. Zendehtdel, A. Mobinikhaledi, Z. Mortezaei, J. Iran. Chem. Soc. 12 (2015)283-292.
2. Abdullah, M. in AIP Conference Proceedings. 2014.
3. Nassar, N.N., A. Hassan, and P. Pereira-Almao, Energy & Fuels, 2011. 25(3): p. 1017-1023.
4. Nugraha, M.I., et al. in Materials Science Forum. 2013. Trans Tech Publ.
5. Silver, S. Microbes EnViron. 1998, 13, 177.
6. Kazakov, S. A.; Hecht, S. M. In Encyclopedia of Inorganic Chemistry; King, R. B., Ed.; Wiley Interscience: Chichester, U.K., 1994; Vol. 5, p 2697.



# 4<sup>th</sup> Iran National Zeolite Conference

## Golpayegan University of Technology, Golpayegan, Iran

### August 23-24, 2017



## Molecular simulation of gas adsorption on LTA zeolite

Daniel Lotfi moghadam <sup>\*a</sup>, Behruz Bayati <sup>b</sup>, Mona Khodai Pour <sup>c</sup>

<sup>a</sup> Daniel Lotfi moqdm, Department of Chemical Engineering, University of Ilam, Ilam, Iran

<sup>b</sup> Department of Chemical Engineering, University of Ilam, Ilam, Iran

<sup>c</sup> Chemical Engineering faculty, sahand University of technology, Tabriz, Iran

\*Email: [lotfi.dani70@yahoo.com](mailto:lotfi.dani70@yahoo.com)

### abstract

Zeolites, as a sorbent, have a good loading capacity and stable structure to remove contaminants. In this study, using molecular simulation of adsorption of gases, ammonia, carbon dioxide and water vapor were investigated using LTA zeolite. The simulated LTA zeolite contains 96 silicates, 96 aluminum and 384 oxygen atoms, which is an attachment between Si and Al and is considered as three-dimensional. To create a load balance in zeolite, 96 sodium atoms are placed in the structure of LTA, and then placed on zeolite LTA, 14 calcium atoms and 29 sodium atoms. And simulate their rate of absorption of pollutants during simulation. The potential used in this work includes Columbic, Lennard Jones and Buckingham, and its effects on simulation have been studied. Additionally, the effect of pressure and temperature on the absorption rate in the pressure range of 0.0001 to 100 kPa examined. And the simulation results are compared with the laboratory data available in the references. The absorption tendency of zeolite LTA compounds is  $H_2O \gg NH_3 > CO_2$ .

**Keywords:** LTA zeolite, molecular simulation, adsorption, Monte Carlo

### 1. Introduction

This Fossil fuels provide more than 98 percent of the world's energy needs, However, combustion of fossil fuels is one of the main sources of pollutants and greenhouse gases. Today, increasing the concentration of CO<sub>2</sub> in the air due to the problems that it creates Which has recently been named as the cause of global warming and reported 7% of CO<sub>2</sub> emissions from coal combustion [1-2-3]. Ammonia (NH<sub>3</sub>) is the third most nitrogenous compound after alkaline gas in the atmosphere, Which reacts with acidic and neutral species in the atmosphere, The effects of ammonia and ammonium in the environment cause acid rain, corrosion, acidification of water cisterns, changes in the global radiation balance in the atmosphere, and reduced atmospheric visibility through light scattering, Due to the complex role of ammonia, removal of this pollutant is a significant and necessary task in the field of air pollution [4-5]. Various methods are available to eliminate contaminants, including the use of catalysts, activated carbon and separation methods such as solvent (physical and chemical) adsorption, the process of absorption, membrane cooling process. In the meanwhile, adsorption is very important due to high efficiency and simplicity of operation [5-7]. Absorption of NH<sub>3</sub> -CO<sub>2</sub> -H<sub>2</sub>O was carried out using absorbent types such as metal oxide, activated carbon, clays (natural and synthetic), nanotubes, metal oxides, ceramics and zeolites, Zeolites exhibited a very good function in separating these gases [7-8]. Zeolite, as an adsorbent, has a good absorption capacity and a stable structure to remove pollutants Which are available in natural and artificial form and have unique structural properties, high surface to volume ratio and high porosity. It also has important applications in various fields, such as ion exchange, separation, decomposition, biologic and pure biologic molecules, and sensors [12-13-14]. The zeolite LTA is hydrophilic and is considered as an appropriate absorber for gas removal. This zeolite has a high potential for reducing moisture in gas streams, as well as the ability to absorb CO<sub>2</sub>-H<sub>2</sub>O-NH<sub>3</sub> molecules [15-16].

Young investigated the effect of temperature on aluminum oxide on sulfonamide absorption by molecular dynamics simulation. It was concluded that, with increasing temperature, the amount of absorption is reduced to 298 > 293 > 303 Kelvin and the proper matching between absorption isotherm calculated with experimental data Obtained [17].

the molecular simulation of modern research fields in today's science is a direct way of providing the microscopic properties of a system (the mass of their interacting atoms, the molecular structure) to the macroscopic and experimental properties (state equations, transfer coefficients, structural order parameters) We will put. In this way, it



# 4<sup>th</sup> Iran National Zeolite Conference

## Golpayegan University of Technology, Golpayegan, Iran

### August 23-24, 2017



is hoped that the simulator provides a better solution to empirical experiments that will help describe new results. In this study, using molecular simulation of adsorption of gases, ammonia, carbon dioxide, hydrogen sulfide and water vapor on zeolite LTA were investigated and the effect of important parameters such as adsorption molecular structure, temperature and pressure has been evaluated.

## 2. Simulation details

This research has been done using Monte Carlo simulation. Monte Carlo is a random and probabilistic method that can be used to simulate liquids, gases, transitions between surfaces or structures:

- 1- Create a structure for random testing
- 2- Evaluation of an acceptance criterion by calculating the energy change and other properties of the test case
- 3- Comparison with a criterion for rejecting or accepting simulated testing [21].

All interactions between carbon dioxide and zeolite, carbon dioxide, carbon dioxide, ammonia and zeolite, ammonia and ammonia, water and zeolite, water and water, hydrogen sulfide and zeolite, hydrogen sulfide and hydrogen sulfide are utilized in the field of coated modeling force. All of the atoms and molecules in the structure are affected by the potential energy. The equilibrium and electrostatic energy of the Ewald method used to calculate the precision of energy balance. It is often used in the simulation of adsorption isotherm, which is particularly suited for simulating a mixed system and a homogeneous system [22-23]. The pressure required to evaluate the chemical potential of the adsorbed molecules is calculated using the ideal gas law. The calculated energy of the atoms based on van der Waals is 1.3 nm, and the Ewald method is used with an accuracy of 0.0001 for electrostatic potential energy. To achieve the equilibrium in simulation and required properties, data analysis with a precision of  $106 * 2.5$  steps has been used [21-23]. Zeolite is identical to the experimental data used by Fox et al. [26-28]. A unit cell of LTA zeolite contains 96 Si, 96 Al and 384 O atoms, which is a bond between Si and Al. Also, to create a load balance in zeolite, 96 sodium atoms are placed in the structure of LTA, Then put on zeolite LTA 14 calcium atoms and 29 sodium atoms And simulate the rate of their performance in absorbing pollutants during simulation.

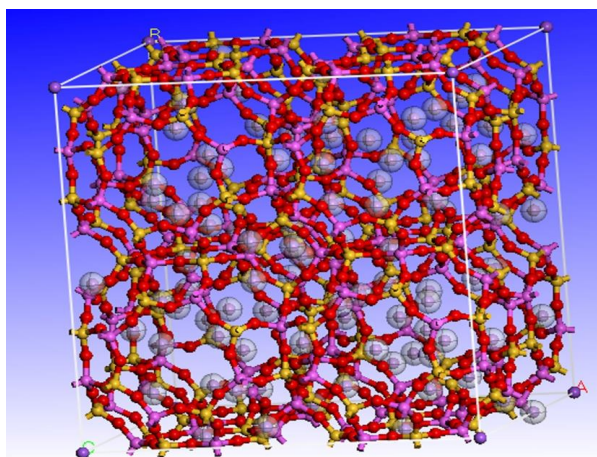


**Figure 1(a).** Schematic diagram of zeolite 4A with silicon atoms shown in yellow, aluminum in purple, oxygen in red, and sodium in Brown.



4<sup>th</sup> Iran National Zeolite Conference  
 Golpayegan University of Technology, Golpayegan, Iran  
 August 23-24, 2017

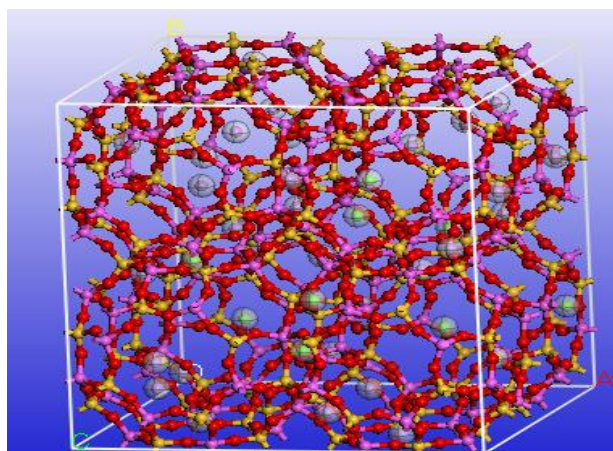


Figure1(b). Schematic diagram of zeolite 5A with silicon atoms shown in yellow, aluminum in purple, oxygen in red, Calcium in green, and sodium in Brown.

The potential used in this work include coulombic, lanard jones and buckingham capable of the following general form:

$$V_{ij} = \frac{q_i q_j}{r_{ij}} + A e^{-\frac{r}{\rho}} - C r_{ij}^{-6} + 4 \epsilon_{ij} \left[ \left( \frac{\sigma_{ij}}{r_{ij}} \right)^m - \left( \frac{\sigma_{ij}}{r_{ij}} \right)^n \right] : \text{Equation 1}$$

Different sets of force fields are used to simulate NH<sub>3</sub> -CO<sub>2</sub>-H<sub>2</sub>O, which allows particles to move, change the volume of the box, and transfer particles between the boxes. All the answers and parameters are obtained using the error test, and their review and matching of the data with the experimental results are available.

Table (1) the partial load used in equation (1)[ 26-28 ]

atom	charge (e)
$O_z$	-1.86875
Si	3.700
AL	2.775
Na	1.000
N	-1.020
$H_N$	0.340
C	0.8000
$O_c$	-0.400
$O_w$	-0.8476
$H_w$	0.4238

TABLE 2: Potential Parameters for NH<sub>3</sub> Isotherms[28-26]

species	$\epsilon_{ij}(\text{kcal. mol}^{-1})$	$\sigma_{ij}(\text{Å})$
$O_z - N$	0.208	3.230
$O_z - H_N$	0.087	2.770
Na-N	0.082	3.310
Na- $H_N$	0.035	2.850
N-N	0.170	3.420
N- $H_N$	0.071	2.960
$H_N H_N^-$	0.000	0.000



4<sup>th</sup> Iran National Zeolite Conference  
 Golpayegan University of Technology, Golpayegan, Iran  
 August 23-24, 2017



TABLE 3: Potential Parameters for CO<sub>2</sub> Isotherms [28-26]

species	$\epsilon_{ij}(\text{kcal. mol}^{-1})$	$\sigma_{ij}(\text{\AA})$
$O_z - C$	0.122	2.897
$O_z - O_C$	0.236	3.255
Na - C	0.048	2.977
Na - $O_C$	0.094	3.335
C - C	0.058	2.753
C - $O_C$	0.113	3.112
$O_C O_C$	0.219	3.470

TABLE 4: Potential Parameters for H<sub>2</sub>O Isotherms [28-26]

species	$\epsilon_{ij}(\text{kcal. mol}^{-1})$	$\sigma_{ij}(\text{\AA})$
$O_W O_z$	0.560	2.495
Si - $O_W$	0.186	1.621
Al - $O_W$	0.118	1.692
$O_z - H_W$	0.255	2.227
Si - $H_W$	0.085	1.354
Al - $H_W$	0.054	1.425
$O_W O_W$	0.155	3.166
$O_W - H_W$	0.000	0.000
$H_W - H_W$	0.000	0.000

### 3. Results and discussion

#### 3-1 Ammonia adsorption on LTA zeolite

As described in the previous section, selecting a model and potential function is one of the fundamental problems in molecular simulation. The potency of Lennard Jones (L-J) is usually used to calculate the thermodynamic properties of a gas [31-39], The NH<sub>3</sub> adsorption isotherm is used to compass the field. Figure 2 Simulated NH<sub>3</sub> adsorption isotherm on LTA zeolite at different temperatures from 273 to 298,332 K. The simulation results are compared with the experimental results conducted by Hilmini et al. [24-25]. As seen, there is a conformity between simulation results and experimental data, and the error in the simulation is negligible, And this affects the proper simulation accuracy.

The simulation in Fig. 2 is carried out in the compression range from 0.02 to 100 kPa And as shown in the figure, the increase in the pressure increases the adsorption. At high pressures, the effect of pressure is adjusted due to the adsorption close to saturation. From the pressure of kpa40, the gradient has fallen sharply, due to the filling of the



# 4<sup>th</sup> Iran National Zeolite Conference

## Golpayegan University of Technology, Golpayegan, Iran

### August 23-24, 2017



cavity capacity at high pressure. In Fig. 3, the graphs show that with increasing temperature, we decrease the adsorption rate and this template is visible. By

comparing the adsorption isotherm ammonia to zeolite, we find that ammonia adsorption is higher in LTA (NA + CA2 +) zeolite. It can be obtained that given the release of CA2 + ion on the adsorbant, the ion diffusion in zeolite due to the small size of calcium ion, the size of the cavity is larger than that of sodium calcium and this process of calcium ion increases the adsorption of ammonia in the surface of zeolite.

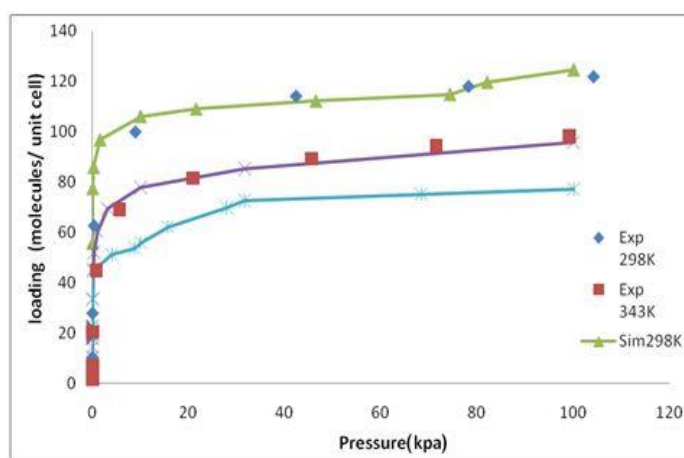


**Figure 2:** Experimental adsorption isotherms (25-25) and simulations for ammonia in LTA zeolite (4A) at temperatures in the range of 273-273 K

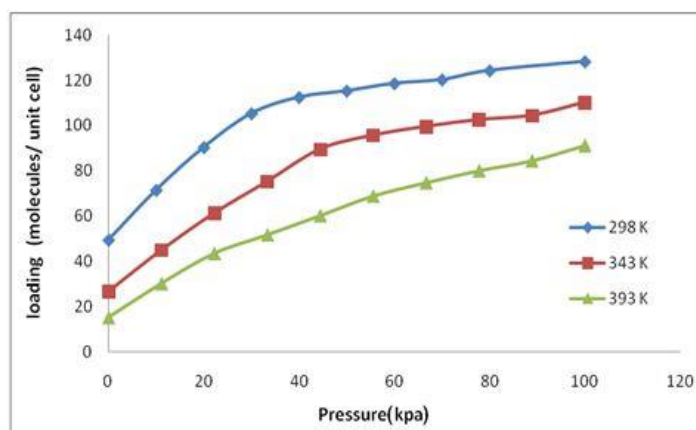


**Figure 3:** Simulation adsorption isotherms for ammonia in zeolite (CA2 + -NA +) LTA At temperatures in the range of 298-323-273 K

### 3-2. Adsorption of carbon dioxide oxide on zeolite LTA

CO<sub>2</sub> adsorption in LTA zeolite is calculated at different temperatures from 323 to 343K. In Figure 3, the isotherm of CO<sub>2</sub> adsorption in LTA zeolite shows a temperature of 273-298 and compares it with the experimental results obtained by Yusl et al. [27]. As seen, there is a conformity between simulation results and experimental data, and the error in simulation is negligible, which indicates the proper simulation accuracy. The simulation in Fig. 4 has been performed in the compression range from 0.0001 to 100 kPa. In the figure, it is clear that the increase in temperature has reduced the amount of adsorption. At high pressures, the dependence of adsorption on the pressure is reduced when adsorption close to saturation and this is valid for all temperature range. The adsorption rate not only depends on pressure but also depends on other parameters, including the structure of the zeolite pore size, can have an effect on





# 4<sup>th</sup> Iran National Zeolite Conference

## Golpayegan University of Technology, Golpayegan, Iran

### August 23-24, 2017



the adsorption rate. Figure 5 shows the adsorption isotherm charts of carbon dioxide simulations on zeolite. Points out that the effect of temperature on adsorption. By comparing the zeolite adsorption isotherm, we find that carbon dioxide adsorption is higher in LTA (NA + CA<sup>2+</sup>) zeolite can be expressed. Which is due to the release of CA<sup>2+</sup> ion on the adsorbent Proliferation of ions in zeolite cavities and due to the small size of calcium ion Increases the diameter of the LTA zeolite cavities, This action accelerates the adsorption of carbon dioxide molecules because it provides more levels for penetration and this process of calcium ion increases the adsorption of carbon dioxide at the zeolite level.

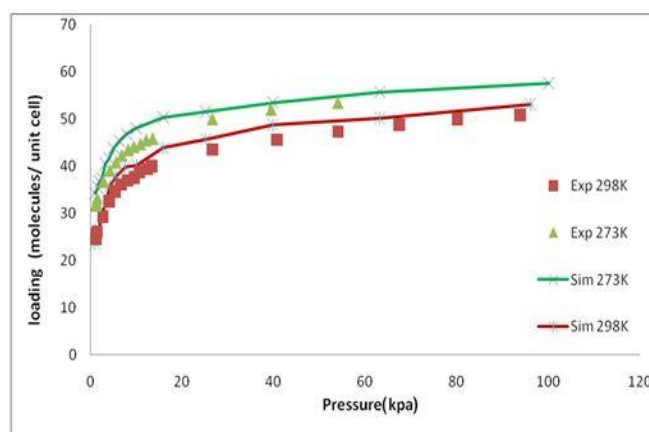


**Figure 4:** Experimental absorption isotherm graph [27] and simulation for CO<sub>2</sub> in LTA zeolite (A4) at temperatures in the range of 278-298 K

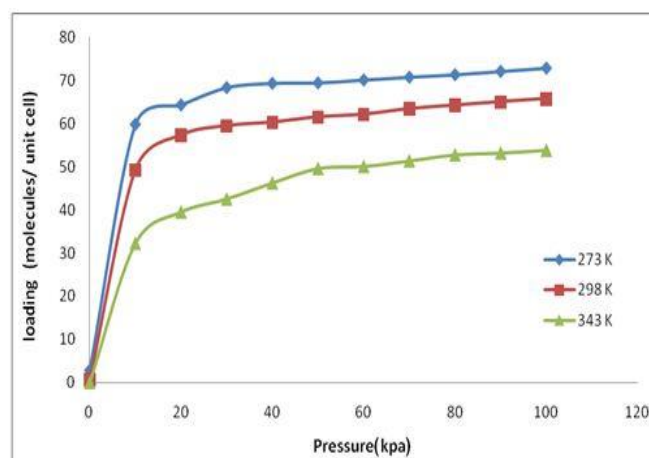


**Figure 5:** Simulation absorption isotherm for CO<sub>2</sub> in zeolite (CA<sub>2</sub> + -NA +) LTA at temperatures in the range of 273-298 -343 K

### 3-3. Water adsorption on zeolite LTA

COMPASS potential for review H<sub>2</sub>O adsorption isotherm has been used, This potential was used to calculate isotherm at 298-323-373 k temperatures. In Figure 4, the adsorption isotherm for H<sub>2</sub>O is shown in LTA zeolite and compares it with the experimental results obtained by Jarmiello and his colleagues [28]. Monte Carlo simulation results are in good agreement with the available experimental results. Simulation using Monte Carlo has been performed in the compression range from 0.0001 to 100 kpa And the increase in pressure increases the adsorption, The greatest impact of the increase in pressure is the same as in the figure, up to a pressure of 10 kpa And then the effect of increasing the pressure decreases as adsorption approaches the saturation state And it's almost a straight line. The water adsorption isotherm has been simulated for zeolite at 3 temperatures from 298 to 343 K and a pressure of 0.001 K to 500 kPa and are presented in Fig. 7. It is evident from the diagrams that, with increasing temperature, we



# 4<sup>th</sup> Iran National Zeolite Conference

## Golpayegan University of Technology, Golpayegan, Iran

### August 23-24, 2017



decrease the adsorption rate. By comparing the zeolite adsorption isotherm, we find that the adsorption of water in the A4 zeolite is more pronounced, Due to the water friendly nature of the active surface, sodium ion contains water molecules and increases the adsorption of water molecules relative to calcium ions.

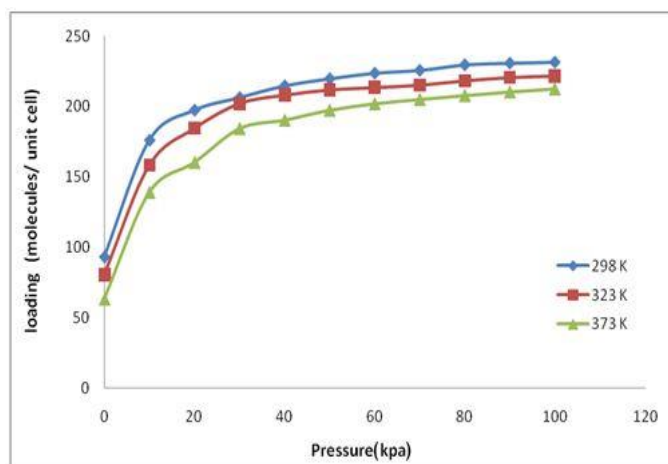


Figure 6;. Experimental absorption isotherm graph [28] and simulation for H2O in LTA zeolite (A4) at temperatures from 373-298-323 k

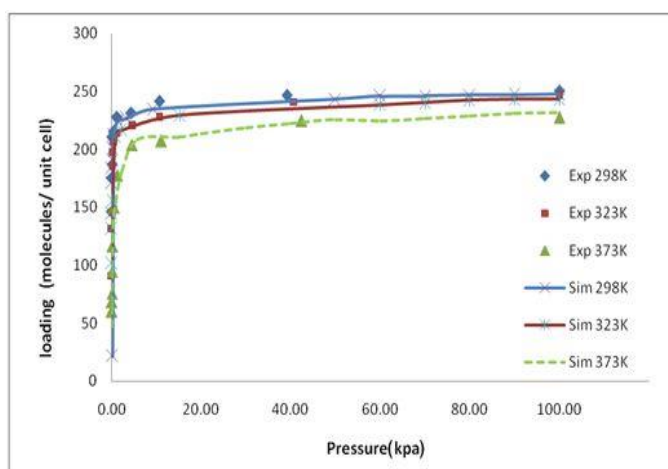


Fig. 7:. Experimental absorption isotherm graph [28] and simulation for H2O in zeolite (CA2 + -NA +) LTA at temperatures of 373-298-323 k

#### 4. Conclusions

The adsorption process has been highly regarded by researchers in recent years as one of the most effective methods for eliminating gaseous pollutants. Zeolites are considered to be an attractive adsorbent because of their unique properties. In this research, using molecular simulation systems, the molecular scavenger-adsorbing behavior was studied, And the effect of process parameters for adsorption of NH<sub>3</sub>-CO<sub>2</sub>-H<sub>2</sub>O in LTA zeolite was investigated by GCMC method. Using the proper force field has led to a good agreement between simulation and experimental results. In this regard, the role of cation was shown in adsorption and selection at different temperatures and pressures and the results obtained from the Monte-Cullu simulation show that increasing the pressure increases the adsorption capacity and decreases the adsorption by increasing the temperature And this result is constant for all simulators and it is



# 4<sup>th</sup> Iran National Zeolite Conference

## Golpayegan University of Technology, Golpayegan, Iran

### August 23-24, 2017



possible to determine the optimum points for pressure in adsorption of pollutants. Future work involves expanding models for simulating and analyzing the effects of different ions, binary mixtures, triples in different zeolites.

#### References

- [1] Yiwei Luo, Hans H. Funke, John L. Falconer, Richard D. Noble; Adsorption of CO<sub>2</sub>, CH<sub>4</sub>, C<sub>3</sub>H<sub>8</sub>, and H<sub>2</sub>O in SSZ-13, SAPO-34, and TType Zeolites ; *Ind. Eng. Chem. Res.* 55 (36), pp 9749–9757; 2016.
- [2] Paolo Cosoli, Marco Ferrone, Sabrina Pricl, Maurizio Fermeglia. “Hydrogen sulphide removal from biogas by zeolite adsorption Part I. GCMC molecular simulations” . *Chemical Engineering Journal*.,vol 145, pp86–92,2008.
- [3] Mehtap Ozekmekci \*, Gozde Salkic \*, Mehmet Ferdi Fellah, “Use of zeolites for the removal of H<sub>2</sub>S: A mini-review “. *Fuel Processing Technology*.,vol.139,pp.49-60, 2015
- [4] Cristina Reche . Mar Viana . Marco Pandolfi . Andrés Alastuey . Teresa Moreno a, Fulvio Amato . “Urban NH<sub>3</sub> levels and sources in a Mediterranean environment” . *Atmospheric Environment*.,vol.57,pp.153-164, 2012.
- [5] Haiming Huang, Dean Xiao, Qingrui Zhang, Li Ding; "Removal of ammonia from landfill leachate by struvite precipitation with the use of low-cost phosphate and magnesium sources"; *Journal of Environmental Management*; Volume 145, Pages 191–198, 2014.
- [6] Ponnivalavan Babu , Praveen Linga ,Rajnish Kumar , Peter Englezos ; A review of the hydrate based gas separation (HBGS) process for carbon dioxide pre-combustion capture ; *Energy Volume 85*, Pages 261– 279, 2015.
- [7] F.J.A.L. Cruz, I.A.A.C. Esteves,. “ Adsorption of light alkanes and alkenes onto single-walled carbon nanotube bundles: Langmuirian analysis and molecular simulations .J.P.B. Mota, *Colloids Surf. A*” .,vol.357,pp. 43–52,2010.
- [8] Y. Zeng, S. Ju, “ Adsorption of thiophene and benzene in sodium-exchanged MFI- and MOR-type zeolites: A molecular simulation study ”. *Purif. Technol.*,vol. 67,pp. 71–78, 2009.
- [9] C. Baerlocher, L.B. McCusker, D.H. Olson , “ Atlas of Zeolite Framework Types, sixth ed” , Elsevier , Amsterdam, 2007.
- [10] J.A. Rabo, M.W. Schoonover, “ Early discoveries in zeolite chemistry and catalysis at Union Carbide, and follow-up in industrial catalysis” . *Appl. Catal. A: General*.,vol.222 ,pp. 261-275, 2001.
- [11] J. Liu, S. Keskin, D. Sholl, K. Johnson “Molecular Simulations and Theoretical Predictions for Adsorption and Diffusion of CH<sub>4</sub>/H<sub>2</sub> and CO<sub>2</sub>/CH<sub>4</sub> Mixtures in ZIFs” . *J. Phys. Chem. C*.,vol.115,pp. 12560–12566, 2011.
- [12] M. Jeffroy , G. Weber , S. Hostachy , J.P. Bellat , A.H. Fuchs A. Boutin “Structural Changes in Nanoporous MFI Zeolites Induced by Tetrachloroethene Adsorption: A Joint Experimental and Simulation Study” . *J. Phys.Chem. C*.,vol. 115 ,pp. 3854–3865 , 2011
- [13] J. Liu, S. Keskin, D. Sholl, K. Johnson , “ Molecular Simulations and Theoretical Predictions for Adsorption and Diffusion of CH<sub>4</sub>/H<sub>2</sub> and CO<sub>2</sub>/CH<sub>4</sub> Mixtures in ZIFs” . *J. Phys. Chem. C*.,vol.115 ,pp. 12560–12566, 2011.
- [14] M. Jeffroy , G. Weber , S. Hostachy , J.P. Bellat , A.H. Fuchs , A. Boutin, “ Structural Changes in Nanoporous MFI Zeolites Induced by Tetrachloroethene Adsorption: A Joint Experimental and Simulation Study” . *J. Phys.Chem. C*.,vol. 115 ,pp. 3854–3865,2011.
- [15] M. Rahmati, H. Modarress, “Grand canonical Monte Carlo simulation of isotherm for hydrogen adsorption on nanoporous siliceous zeolites at room temperature” . *Appl. Surf. Sci.*.,vol. 255 (2009) ,pp. 4773–4778, 2009.
- [16] M. Rahmati, H. Modarress, “ Nitrogen adsorption on nanoporous zeolites studied by Grand Canonical Monte Carlo simulation ”. *J. Mol. Struct. (Theochem.)* .,vol. 901,pp. 110–116,2009.
- [17] Ying- xue Ji . Feng - he Wang . Lun - chao Duan . Fan Zhang . Xue-dong Gong . “Effect of temperature on the adsorption of sulfanilamide onto aluminum oxide and its molecular dynamics simulations” *Applied Surface Science*.,vol. 285,pp. 403-408, 2013
- [18] A. GORBACH, M. STEGMAIER AND G. EIGENBERGER. “ Measurement and Modeling of Water Vapor Adsorption on Zeolite 4A—Equilibria and Kinetics” *Institut f’ur Chemische Verfahrenstechnik*, .,vol. 10 ,pp. 29-46, 2004.
- [19] Honghong Yi, Hua Deng, Xiaolong Tang\*, Qiongfeng Yu, Xuan Zhou, Haiyan Liu . “Adsorption equilibrium and kinetics for SO<sub>2</sub>, NO, CO<sub>2</sub> on zeolites FAU and LTA” . *Journal of Hazardous Materials* .,vol. 203-204,pp. 111-117, 2012.
- [20] Mahmoud Rahmati, Hamid Modarress. “Grand canonical Monte Carlo simulation of isotherm for hydrogen adsorption on nanoporous siliceous zeolites at room temperature”. *Applied Surface Science*, .,vol. 255,pp. 4773–4778, 2009
- [21] Mahmoud Rahmati, Hamid Modarress. “Selectivity of new siliceous zeolites for separation of methane and carbon dioxide by Monte Carlo simulation ”. *Microporous and Mesoporous Materials*.,vol. 176,pp.168–177, 2013
- [22] P.P. Ewald, *Ann. Phys.* . “Die Berechnung optischer und elektrostatischer Gitterpotentiale ”.,vol. 64 ,pp.253–287,1921.
- [23] S. Agnihotri, P. Kim, Y. Zheng, J.P.B. Mota, L. Yang . “ Regioselective Competitive Adsorption of Water and Organic Vapor Mixtures on Pristine Single-Walled Carbon Nanotube Bundles”. *Langmuir*.,vol. 24 ,pp.5746–5754, 2008.
- [24] Helminen, J.; Helenius, J.; Paatero, E.; Turunen, I. . “ Adsorption Equilibria of Ammonia Gas on Inorganic and Organic Sorbents at 298.15 K” . *AIChE J.*,vol. 46,pp. 1541-1549, 2000.
- [25] Helminen, J.; Helenius, J.; Paatero, E.; Turunen, I. “ Adsorption Equilibria of Ammonia Gas on Inorganic and Organic Sorbents at 298.15 K” . *J. Chem. Eng. Data*.,vol. 46,pp.391-399,2001.
- [26] Faux, D. A.; Smith, W.; Forester, T. R. “Molecular Dynamics Studies of Hydrated and Dehydrated Na<sup>+</sup>-Zeolite-4A *J. Phys. Chem. B* 1997, 101, 1762.
- [27] Faux, D. A. Monte Carlo Simulation of Single- and Binary-Component Adsorption of CO<sub>2</sub>, N<sub>2</sub>, and H<sub>2</sub> in Zeolite Na-4A *J. Phys. Chem. B* .,vol. 102,pp.10658-, 1998.
- [28] Faux, D. A. J. “Molecular Dynamics Studies of Hydrated Zeolite 4A” *Phys. Chem.*.,vol. 103,pp. 7803-7811, 1999.



4<sup>th</sup> Iran National Zeolite Conference  
Golpayegan University of Technology, Golpayegan, Iran  
August 23-24, 2017



- [29] Yucel, H.; Ruthven, D. M. J. “ Adsorption of ethyldithiocarbonate ion on Ni clusters and oxygen effect on its system” Colloid Interface Sci., vol. 74, pp. 186-192, 1980.
- [30] E. Jaramillo and M. Chandross . “Adsorption of Small Molecules in LTA Zeolites ”. J. Phys. Chem., vol. 108, pp. 20155-20159, 2004.
- [31] C. Herdes, Z. Lin, A. Valente, J.A.P. Coutinho, L.F. Vega, “Nitrogen and Water Adsorption in Aluminum Methylphosphonate  $\alpha$ : A Molecular Simulation Study” Langmuir., vol. 22, pp. 3097-3104, 2006.
- [32] S. Furmaniak, A.P. Terzyk, P.A. Gauden, K. Lota, E. Frackowiak, F. Beguin, P. “ Determination of the space between closed multiwalled carbon nanotubes by GCMC simulation of nitrogen adsorption”. Journal of Colloid and Interface Science ., vol. 317, pp. 442-448, 2007 .
- [33] X. Zhang, W. Wang, J. Chen, Z. Shen, “ Characterization of a Sample of Single-Walled Carbon Nanotube Array by Nitrogen Adsorption Isotherm and Density Functional Theory” Langmuir ., vol. 19 , pp. 6088-6096, 2003.
- [34] J. Jiang, S.I. Sandler, “ Nitrogen and Oxygen Mixture Adsorption on Carbon Nanotube Bundles from Molecular Simulation” Langmuir., vol. 20 , pp. 10910-10918, 2004.
- [35] Y.F. Yin, T. Mays, B. McEnaney, “ Adsorption of Nitrogen in Carbon Nanotube Arrays” Langmuir., vol. 15 , pp. 8714-8718, 1999.
- [36] J. Pikunic, P. Llewellyn, R. Pellenq, K.E. Gubbins, “ Argon and Nitrogen Adsorption in Disordered Nanoporous Carbons: Simulation and Experiment” Langmuir., vol. 21 , pp. 4431-4440, 2005.
- [37] S. Gavalda, K.E. Gubbins, Y. Hanzawa, K. Kaneko, K.T. Thomson, “ Nitrogen Adsorption in Carbon Aerogels: A Molecular Simulation Study” Langmuir., vol. 18 , pp. 2141, 2002.
- [38] N.D. Hutson, B.A. Reisner, R.T. Yang, B.H. Toby, “Influence of Residual Water on the Adsorption of Atmospheric Gases in Li-X Zeolite: Experiment and Simulation” Chem. Mater ., vol. 39, pp. 1775-1780, 2000.
- [39] A. Heyden, T. Douren, F.J. Keil, “Study of molecular shape and non-ideality effects on mixture adsorption isotherms of small molecules in carbon nanotubes: A grand canonical Monte Carlo simulation study” Chem. Eng. Sci., vol. 57 , pp. 2439-2448, 2002.



# 4<sup>th</sup> Iran National Zeolite Conference

## Golpayegan University of Technology, Golpayegan, Iran

### August 23-24, 2017



## Alkaline-treated titanium dioxide: Modification of its textural and morphological properties

Mahdieh Rajabpour Nikfam, M. A. Zanjanchi\*, A. Ghanadzadeh

*Department of Chemistry, Faculty of Science, University of guilan, Rasht, P.O. Box 41335-1914, Iran*

*\*Corresponding author: zanjanchi@guilan.ac.ir*

### 1. Introduction

Modification of titanium dioxide by incorporating certain species in its structure, immobilizing it onto a support or reducing its crystallite size generally improves its photocatalytic ability. Evonik P-25, which is a mixture of anatase–rutile crystalline structures, is the commercial TiO<sub>2</sub> powder with high photocatalytic activity and it is the one most widely used as standard photocatalyst [1]. Some studies have suggested that addition of polyoxometallates to the synthesis gel might lead to the formation of a surface complex between the POM and TiO<sub>2</sub> [2, 3], in this work, the impregnation of Evonik P-25 nanoparticles and alkaline-treated P-25 nanotube with tungstophosphoric acid (TPA) is reported. The prepared materials are characterized with standard structural and chemical analysis systems such as XRD, FTIR, SEM, PZC etc. Their photocatalytic activity will be evaluated by studying the degradation of methylene blue (MB) solutions.

### 2. Experimental

In a typical preparation procedure, 2 g P25 TiO<sub>2</sub> white power was placed into a Teflon-lined autoclave of 100 ml capacity. Then, the autoclave was filled with 80 ml 10 mol L<sup>-1</sup> NaOH aqueous solution, sealed into a stainless tank and maintained at 130 °C for 24 h. After the autoclave was naturally cooled to room temperature, the obtained sample was filtered, washed with distilled water for several times. Then, the obtained products were collected and washed with HCl aqueous solution (pH 1.6) for 24 h, and washed with distilled water for several times until the pH value turned to 7. At last, the products were annealed at 400 °C in air for 2h. We call this sample as P25(AT)-400.

For Impregnation of tungstophosphoric acid on Evonik P-25 nanoparticles, First, 2.4 g of tungsto-phosphoric acid (TPA) (H<sub>3</sub>PW<sub>12</sub>O<sub>40</sub> × H<sub>2</sub>O, Merck, corresponding to 1.83 g of tungsten) was dissolved in 50 mL of a solution (70% absolute ethanol, 30% distilled water) at pH 1.5 (by adding HCl) in order to avoid the partial degradation of TPA Keggin anion. Then, 4 g of Evonik P-25 nanoparticles was added to reach a TPA concentration of 30% (w/w). This suspension was left until the solvent was completely dried. The solid was washed three times with distilled water in order to remove weakly bonded TPA.

### 3. Results and discussion

We studied the degradation of methylene blue (MB) as a model reaction to investigate the photocatalytic activities of our prepared P25-TPA, P25(AT)-400 and P25(AT)-TPA-400 samples. In an optimized test, 10 mg of the catalyst was added to 50 mL solution of MB (20 mg L<sup>-1</sup>) placed in darkness. There was no noticeable decrease in the MB concentration after 15 min. This indicates that this time is enough for adsorption–desorption equilibrium. Exposing the MB solution to UV irradiation will initiate the degradation and elimination of MB. The photocatalytic efficiency is



# 4<sup>th</sup> Iran National Zeolite Conference

## Golpayegan University of Technology, Golpayegan, Iran

### August 23-24, 2017



highest for 30%(w/w) P25(AT)-TPA-400 which eliminates nearly 84% of the dye within 45 min. FESEM micrographs (Fig. 1) revealed that consists of P25(AT) small particles and agglomerates.

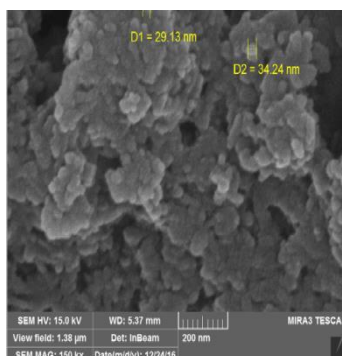


**Figure 1.** FESEM image of P25(AT)

#### 4. Conclusions

P25 can be converted to nanotube forms by an controlled alkaline treatment. we found a remarkable improvement in the photocatalytic degradation of methylene blue using 30% of TPA incorporation into P25(AT)-TPA-400. This finding may show that Incorporation of TPA into TiO<sub>2</sub> results in a synergistic effect, namely, electron transfer from TiO<sub>2</sub> to TPA and consequent retardation of the electron–hole recombination.

#### Acknowledgments

We gratefully acknowledge the Research Department of University of Guilan for supporting this work.

#### References

- 1) J.A. Rengifo-Herrera, M.N. Blanco, M.M. Fidalgo de Cortalezzi, L.R. Pizzio / Materials Research Bulletin 83 (2016) 360.
- 2) J.A. Rengifo-Herrera, M.N. Blanco, L.R. Pizzio, Mater. Res. Bull. 49 (2014) 618.
- 3) D. Wang, B. Yu, F. Zhou, C. Wang, W. Liu / Materials Chemistry and Physics 113 (2009) 602.

## Synthesis and characterization of zeolite Y via ultrasonic method

Modarres Dehghani<sup>a</sup>, Azadeh Tajarodi<sup>a\*</sup>

<sup>a</sup>Department of Chemistry, Iran University of Science and Technology, Tehran, 13114-16846, Iran.

\*Email: [tajarodi@iust.ac.ir](mailto:tajarodi@iust.ac.ir)

#### 1. Introduction

Zeolites and related materials (molecular sieves) have gained enormous importance in many industrial applications



# 4<sup>th</sup> Iran National Zeolite Conference

## Golpayegan University of Technology, Golpayegan, Iran

### August 23-24, 2017



, particularly in selective adsorption, catalysis and ion exchange processes [1]. Among them, Zeolite Y is applied extensively for fluid catalytic cracking, hydrocracking, and petrochemical synthesis. Although mesopores Y has been prepared by special templating techniques [2, 3] dealumination treatment by steaming and acid leaching is still main method to prepare mesopores zeolite Y [4, 5].

In the recent years, microwave irradiation and sonochemical assisted techniques have been reported as a promising method to reduce the synthesis duration of zeolites and mesoporous silicas materials [6]. Ultrasonic irradiation has been proven as a potential tool for generating novel materials like various inorganic materials and fine ceramic powders [7]. For preparation of nano materials, sonochemical methods can lead to homogeneous nucleation and a substantial reduction in crystallization time at room temperature compared to conventional chemical methods [8]. In this paper an efficient ultrasonic procedure for the synthesis of zeolite Y is reported, in which the crystallization temperature is lower and synthesis time is shortened sharply. The physicochemical properties of the resulting sample was characterized using FT-IR (Fourier transform infrared), XRD (X-ray diffraction), and SEM (Scanning microscopy electron)

## 2. Experimental

### 2.1. Materials

Sodium hydroxide (NaOH, 99% wt., Merck), sodium aluminate ( $\text{NaAlO}_2$ , [ $\text{Na}_2\text{O}$ , 40-45 % wt +  $\text{Al}_2\text{O}_3$ , 50-55 % wt.] (Aldrich),  $\text{NaSiO}_2$  (Aldrich) and deionized water were used as received.

### 2.2. Synthesis of zeolite Y via sonochemical method

Zeolite Y was prepared from a starting aluminosilicate gel with molar ratio 1  $\text{Al}_2\text{O}_3$ :4  $\text{Na}_2\text{O}$ :9  $\text{SiO}_2$ :170  $\text{H}_2\text{O}$ . In a typical preparation,  $\text{NaAlO}_2$  (1.409 g),  $\text{H}_2\text{O}$  (18.1 mL), NaOH (5.0776 g), and  $\text{SiO}_2$  (17.3 mL) at room temperature for 24–36 h were mixed by stirring. Then the mixture was subjected to conventional heating, ultrasound radiation. The crystallization experiment was carried out using an ultrasonic processor (FAPAN, 400R) with standard probe for sonicating under atmospheric pressure. The delivered power of ultrasound wave was 150W. During sonication, the temperature of mixture raised from ambient temperature to a steady state of 90 °C within 5 min. Using a circulating oil bath, the reactor temperature was kept constant at 90 °C ( $\pm 1$  °C). After 3.5 h the resultant product was filtered, washed, and dried overnight at 80 °C.

## 3. Results and discussion

The FT-IR spectrum of the synthesized zeolite Y is shown in Fig. 1. There are the strong vibrations at 1002, 719, 567 and 460  $\text{cm}^{-1}$  in this spectrum. The characteristics band at 460, 567 and 1002 were assigned to T–O (T = Si, Al) bending and Si–O, Al–O tetrahedral vibration, respectively [8].

The XRD pattern of zeolite Y has been shown in Fig 2. After crystallization, product shows sharp diffraction peaks at 2 theta of 6.05°, 10.02°, 11.7°, 15.4°, 20.1°, 23.3°, 26.7° and 30.9° and confirms the formation of zeolite Y [9].

The SEM images of zeolite Y were recorded after sonochemical method and given in Fig. 3. The small cavities on the external surface of zeolite-Y were observed.



# 4<sup>th</sup> Iran National Zeolite Conference

## Golpayegan University of Technology, Golpayegan, Iran

### August 23-24, 2017

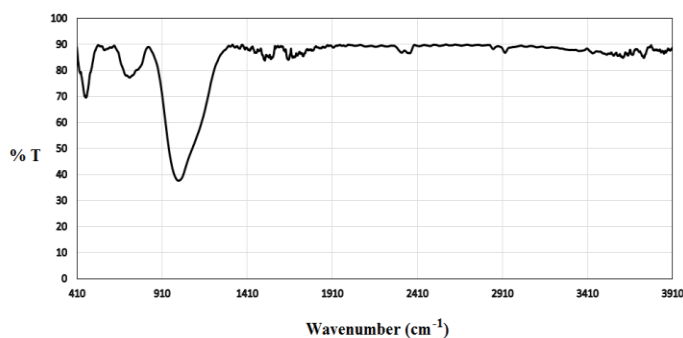


Figure 1. FT-IR spectrum of zeolite Y.

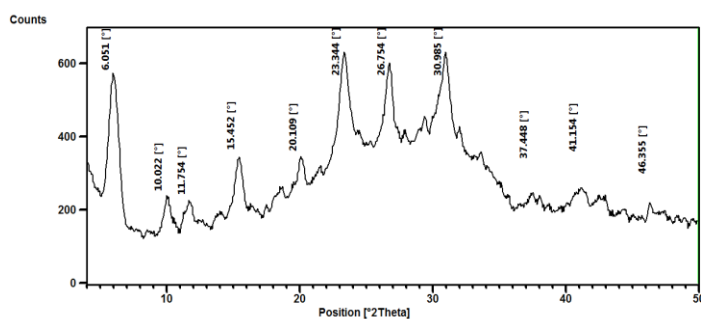


Figure 2. XRD pattern of zeolite Y.

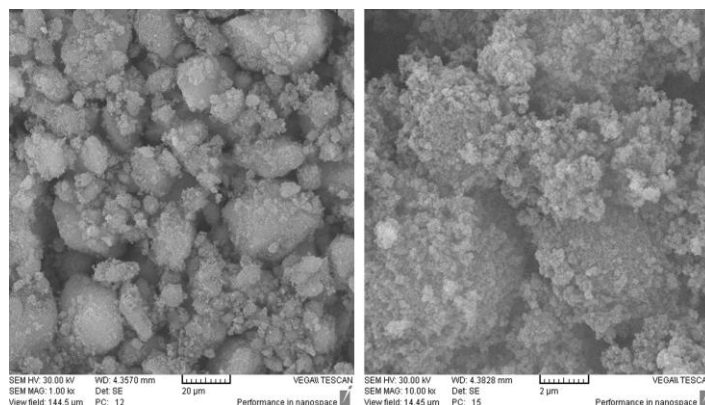


Figure 3. SEM images of zeolite Y.

#### 4. Conclusions

In summary, we demonstrated a simple approach for the synthesis of zeolite Y by ultrasonic method. In comparison to other methods, this strategy is an easy and inexpensive method with having a time of reaction is very short for synthesis of zeolite Y. Also, there are nanoporous cavities with more regular and more uniform structure that these are advantages using of ultrasonic for synthesis.

#### Acknowledgments

We thank Iran University of Science and Technology for financial support.





# 4<sup>th</sup> Iran National Zeolite Conference

## Golpayegan University of Technology, Golpayegan, Iran

### August 23-24, 2017



#### References

- [1] J.C. Scaiano, H. García, *Acc. Chem. Res.*, **1999**, 32, 783.
- [2] Y. Tao, H. Kanoh, K. J. Kaneko, *Phys. Chem. B.*, **2003**, 107, 10974.
- [3] W. Fu, L. Zhang, T. Tang, Q. Ke, Sh. Wang, J. Hu, G. Fang, J. Li, F. Xiao, *J. Am. Chem. Soc.*, **2011**, 133, 15346.
- [4] R. Chal, C. Gérardin, M. Bulut, S. van Donk, *Chem Cat Chem.*, **2011**, 3, 67.
- [5] S. Mi, T. Wei, J. Sun, P. Liu, X. Li, Q. Zheng, K. Gong, X. Liu, X. Gao, B. Wangc, H. Zhao, H. Liu, B. Shen, *Journal of Catalysis.*, **2017**, 347, 116.
- [6] [19] R. Zhou, S. Zhong, X. Lin, N. Xu, *Microporous Mesoporous Mater.*, **2009**, 124, 117.
- [7] J. H. Bang, K. S. Suslick, *Adv. Mater.*, **2010**, 22, 1039.
- [8] P. Pal, J. K. Das, N. Das, S. Bandyopadhyay, *Ultrasonics Sonochemistry.*, **2013**, 20, 314.
- [9] C. N. Desai, A. J. Chudasama, J. T. Karkar, Y. B. Patel, A. K. Jadeja, R. D. Godhani, P. J. Mehta, *Journal of Molecular Catalysis A: Chemical.*, **2016**, 424, 203.

## Nano-Ni@zeolite-Y: preparation and application as a mild and efficient catalyst for green synthesis of pyridopyrazine and quinoxaline derivatives under solvent-free conditions

Mehdi Kalhor <sup>a\*</sup>, Zahra Seyedzade<sup>a</sup>

<sup>a</sup> Department of Chemistry, Payame Noor University, 19395-4697, Tehran, Iran

\* E-mail: [mekalhor@pnu.ac.ir](mailto:mekalhor@pnu.ac.ir)

### 1. Introduction

Recently, the zeolites have attracted a growing interest due to their proper acidity, thermal stability and low cost. The acidity and catalytic activity of zeolite can be dependent on the Lewis and Bronsted acid sites. The dehydration reaction, can decrease the number of proton sites and increase the number of Lewis acid sites. As well as, exchange or relocation of monovalent cations with polyvalent ion creates strong Bronsted centers using the hydrolysis phenomena. These processes can be useful for catalytic reactions such as alcohol dehydration, acylation, esterification, Oxidation, desulfurization and cyclization. Also, nano-zeolites doped with transition metals, with the size of less than 100 nm has attracted a lot of attention of many chemists and activists chemical industry, because of their great applications not only in catalysis, but also in a variety of new applications inclusive chemical sensing, medicine, optoelectronics and *etc.* [1,2]. On the other hands, quinoxalines [3] and pyrido[2,3-b]pyrazines [4] are an important class of benzo-heterocyclic pyrazine compounds and have been widely used in dyes, pharmaceuticals and electrical/photochemical materials. Looking at the above facts, In this study, we report use of nano-Ni(II)/Y-



4<sup>th</sup> Iran National Zeolite Conference  
Golpayegan University of Technology, Golpayegan, Iran  
August 23-24, 2017



zeolite (NNZ) as catalyst for the synthesis of quinoxalines and pyrido[2,3-b]pyrazines under very mild reaction conditions. The present methodology offers several advantages than other procedures such as high yields, short reaction times, solvent free conditions and use of a green, reusable, and thermal stability catalyst.

## 2. Experimental

### Preparation of nano Ni@zeolite Y

A solution of  $\text{NiCl}_2 \cdot 2\text{H}_2\text{O}$  (0.01 M, 200 mL) was added to 2.0 g NaY zeolite in a 150-mL flask. The mixture was stirred for 24 h and filtered. The solid obtained was washed with water until the filtrate was colorless. The Ni-Y zeolite (0.2 g) was then treated with ultrasound for 1 h to furnish nano size particles. The catalyst was then used without further purification.

### Typical procedure for preparation of compounds 3a-o

A mixture of 1,2-arylenediamine, or 2,3-diamino pyridine, (0.1 mmol) and the corresponding 1,2-diketones, in the presence of catalytic amount (5 or 10%, w/w) of nano Ni(II)/Zeolite-Y was heated at 80°C under solvent-free conditions. reaction progress was monitored by TLC. After completion of the reaction, the used catalyst was collected by filtration and cold water was added to the filtrate to give the product.

**2,3-Diphenyl pyrido[2,3-b]pyrazine (3d):** yellow solid. IR (KBr,  $\nu_{\text{max}}$ ): 3056 (C-H), 1544 (C=N), 1430, 1384, 1332 (C=C), 1068, 1019, 780, 697  $\text{cm}^{-1}$ ;  $^1\text{H}$  NMR (500 MHz,  $\text{DMSO-}d_6$ )  $\delta_{\text{H}}$ : 9.15 (d,  $J = 3.52$  Hz, 1H, H-Ar), 8.57 (dd,  $J = 1.32, 6.90$  Hz, 1H, H-Ar), 7.87 (q,  $J = 4.14$  Hz, 1H, H-Ar), 7.49-7.31 (m, 10H, H-Ar) ppm;  $^{13}\text{C}$  NMR (125 MHz,  $\text{DMSO-}d_6$ )  $\delta_{\text{C}}$ : 156.5, 155.3, 154.9, 150.0, 139.1, 138.7, 136.5, 130.6, 130.6, 130.0, 129.9, 128.9, 126.8 ppm.

## 3. Results and discussion

First, the Ni-Y zeolites were produced under ultrasound Based on previous methods reported [5,6] to obtain nano-size. The scanning electron microscopy (SEM) image of the Ni-Y zeolite nano-particles is shown in (Fig. 1, a). The particles size was mainly about 54-272 nm.

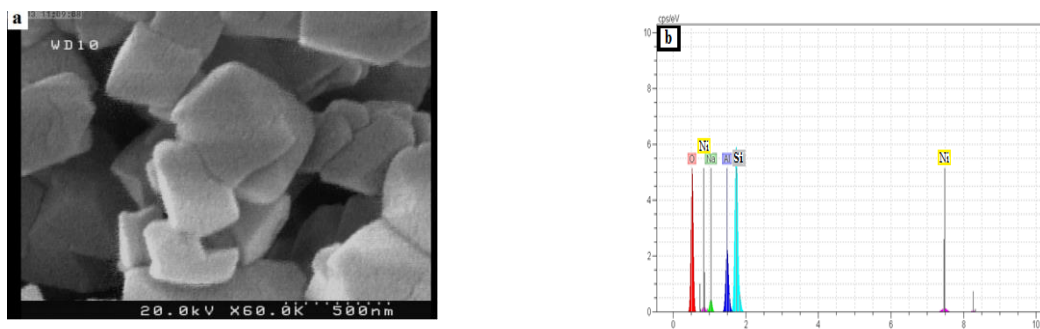


Figure 1. SEM image (a) and EDX spectrum (b) of Ni(II)/Zeolite-Y nanoparticles



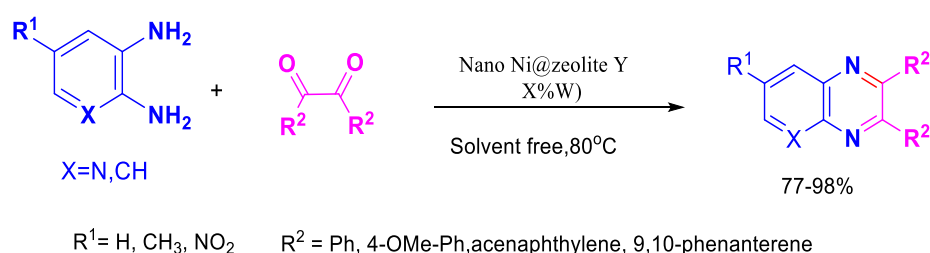
4<sup>th</sup> Iran National Zeolite Conference  
Golpayegan University of Technology, Golpayegan, Iran  
August 23-24, 2017



In the Energy dispersive X-ray (EDX), Peak appeared in the region of 7.5 eV confirmed the presence of nickel metal deposited on zeolite, respectively (Fig. 1, b). In the next step, to obtain the optimal method conditions, the effect of temperature, the amount of efficient catalyst on the yield of the reaction were examined. 5 and 10W% of NNZ as the best catalyst, made the highest yield (83-95%) in a model reaction of benzene-1,2-diamine or pyridine-2,3-diamine with benzil under solvent-free conditions. By generality of this method, the Some quinoxaline and pyrido[2,3-*b*]pyrazine **3a-o** were prepared *via* one-pot reaction by employing aryl-1,2-diamines and 1,2-diketones under the same conditions.

#### 4. Conclusions

In summary, we successfully used nano-Ni(II)/Y zeolite as environmental friendly catalyst for easy synthesis quinoxalines and pyrido[2,3-*b*]pyrazines derived from a one-pot condensation reaction aryl-1,2-diamines and 1,2-diketones. The attractive features of this procedure are its good conversions, easy workup, inexpensive and recyclable catalyst and short reaction times, making it a useful practical method for the synthesis pyrido[2,3-*b*]pyrazines and quinoxalines.



**Scheme 2.** Synthetic method for compounds **3a-o**.

#### Acknowledgments:

We gratefully acknowledge the financial support from the Research Council of Payame Noor University.

#### References

1. L. Tosheva, V.P. Valtchev, *Chem. Mater* **2005**, 17, 2494.
2. A. Corma, *Chem. Rev.* **1997**, 97, 2373.
3. V.A. Mamedov, *Quinoxalines*. 1 ed. Springer, AG Switzerland, **2016**.
4. Guillon, J.; Philippe, G.; Labaied, M.; Sonnet, P.; Le`ger, J. M.; Poulain, P.D.; Bares, I.F.; Dallemagne, P.; Lemaitre, N.; Pehourcq, F.; Rochette, J.; Sergheraert, C.; Christian, J. *J. Med. Chem.* **2004**, 47, 1997.
5. M. Zendehtel, A. Mobinikhaledi, J.F. Hasanvand, *J. Incl. Phenom. Macrocycl. Chem.* **2007**, 59, 41.
6. M. Kalhor, N. Khodaparast, *Res. Chem. Intermed.* **2015**, 41, 3235.



4<sup>th</sup> Iran National Zeolite Conference  
Golpayegan University of Technology, Golpayegan, Iran  
August 23-24, 2017



**Sorption and solidification studies of cesium by a natural zeolite  
(clinoptilolite, sabzevar)**

Parisa Sedighi<sup>a</sup>, Reza Davarkhah<sup>b</sup>, Armen Avanes<sup>a</sup>, Hamid Sepehrian<sup>b,\*</sup>

<sup>a</sup>Department of Chemistry, University of Maragheh, Maragheh, 5518183111, Iran

<sup>b</sup>Nuclear Science and technology Research Institute, P. O. Box 11365-8486, Tehran, Iran

\*Email: [hsepehrian@aeoi.org.ir](mailto:hsepehrian@aeoi.org.ir)

### Abstract

In this study, at first was determined the structure of the natural clinoptilolite of the sabzevar region and investigate the adsorption properties of this absorbent towards Cs<sup>+</sup> ion from aqueous solution. The effects of various parameters like pH, contact time, initial metal ion concentration and temperature were studied in batch operation. The results show that maximum adsorption capacity of cesium on to clinoptilolite adsorbent was found to be 172.4 mg.g<sup>-1</sup>. Then, the cesium-loaded adsorbents were heated at different temperature and the leach test carried out on all the heat-treated samples. Leaching results show that immobilization ability of ion cesium in the heated-treated materials increased as the treatment temperature was increased.

### 1. Introduction

The presence of long-lived radionuclides like strontium-90 and cesium-137 is challenge to the management of radioactive waste. Low and intermediate-level radioactive waste effluents must suitably be treated to reduce radionuclide concentration before disposal [1]. Liquid waste management in nuclear facilities is usually carried out with the aim of (i) decrease the volume of more comfortable storage and (ii) immobilizing radioactive elements therein to avoid leaching. A new strategy is sorption and stabilization them respectively in a natural or synthetic zeolite framework [2]. These materials have been analyzed for their ion-exchange properties with cesium for decades. The interest in zeolites revolves around their low costs, and theoretical high capacities [3, 4].

Stabilization-inertization of the sludge in cement matrix is usually a successful procedure to safely and irreversibly entrap the cation. This technique has proven to be suitable to remove and safely dispose cesium either using natural or synthetic zeolites [5]. The aim of this paper is to evaluate the uptake capacity of cesium, using a natural clinoptilolite zeolite (sabzevar) as adsorbent. The effect of various parameter like the pH, contact time, temperature and initial concentration of the metal ion cesium adsorption efficiencies of zeolite has been studied systematically by batch experiments. Then, the cesium-loaded adsorbents were heated at different temperature and the leach test carried out on all the heat-treated samples.

### Experimental

#### 2.1. Reagents

All the chemical used were of analytical grade from merk (Darmstadt, Germany), expect cesium nitrate (CsNO<sub>3</sub>) which was supplied by (Sigma Aldrich, USA).

#### 2.2. Adsorbent



# 4<sup>th</sup> Iran National Zeolite Conference

## Golpayegan University of Technology, Golpayegan, Iran

### August 23-24, 2017



Clinoptilolite sample used in this work was obtained from the sabzevar . prior to adsorption experiments, clinoptilolite was washed with distilled water, dried at 200 °C at 3 h.

### 2.3. Procedure for sorption studies

The adsorption studies of the cesium ion on the NiHCF-Clino adsorbent were carried out using batch method [6]. In this procedure, 20 mg of adsorbent was dispersed in 20 mL solution of 50 mg.L<sup>-1</sup> cesium ion. The mixture was shaken (~150 rpm) for a preselected period of time using a water shaker bath. Then, it was filtered and the amount of the cesium ion was measured using an atomic absorption spectrometer (AAS). The sorption capacity ( $q$ , mg.g<sup>-1</sup>) was calculated using the equation (1).

$$q = (C_i - C_f) \times \frac{V}{m} \quad (1)$$

where  $C_i$  and  $C_f$ , are the initial and final concentrations (mg.L<sup>-1</sup>) of cesium,  $V$  is the volume of the initial solution (mL), and  $m$  is the mass of the adsorbent (g).

### 1.4. Procedure for immobilization and leach test

For cesium immobilization studies, 0.4 g pellets of the Cs-sorbed NiHCF-Clino were prepared using a hydraulic press and a stainless steel extruder at 400 g.cm<sup>-2</sup> load pressure. The pellets were successively heated at 60, 300, 600, 900 and 1200 °C for 6 h. To describe the leaching of cesium from heat-treated samples, two procedures were used.

## 2. Results and discussion

### 3.1. Characterization of the Natural zeolite (clinoptilolite)

The FT-IR spectrum of the natural zeolite (clinoptilolite) was recorded over the range 400-4000 cm<sup>-1</sup> (Figure 1). Zeolites are significantly hydrated materials, and water absorption bands at 1630 cm<sup>-1</sup> and in the range 3000-3600 cm<sup>-1</sup> confirmed it. The bands at 1120 cm<sup>-1</sup>, 574 cm<sup>-1</sup>, and 468 cm<sup>-1</sup> are assigned to TO<sub>4</sub>, doable ring and T-O bending, respectively (T= Si, and Al). Another band near 645 cm<sup>-1</sup> is due to Si-O-Na bond [7].

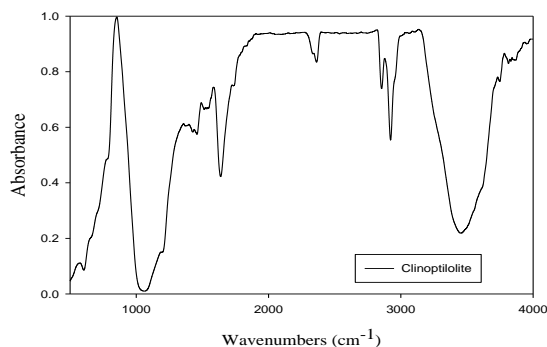


Figure1. FT-IR spectra of natural zeolite (clinoptilolite).



# 4<sup>th</sup> Iran National Zeolite Conference

## Golpayegan University of Technology, Golpayegan, Iran

### August 23-24, 2017



### 3.2. pH effects on the sorption of cesium

The pH is an important parameter to be considered in sorption processes because it may effect both the properties of the adsorbent and the composition of the solution [8]. The effect of solution pH was studied in the rang 1.0-9.0 Such pH values were adjusted by adding small amounts of 0.1 M HCl or NaOH to the Cs solution as required. Figure 2 shows the dependence of the adsorption capacity of the zeolite on initial pH of cesium solution. Cesium sorption on to zeolite was low in pH less than 4.0, that shows a significant competition of H<sup>+</sup> ions with cesium ions for the same site binding of sorbent, since that ion exchange is the main mechanism of cesium adsorption. Significantly less Cs<sup>+</sup> sorbed by the studied zeolite at pH 9.0. A possible formation of carbonate or hydroxide species at this high pH is likely to caused. Complexation of Cs<sup>+</sup> ions resulting to lower Cs amount available for sorption [9]. According to the results of this initial experiment, further adsorption investigation were performed at natural pH value of 6.5 as optimal value.

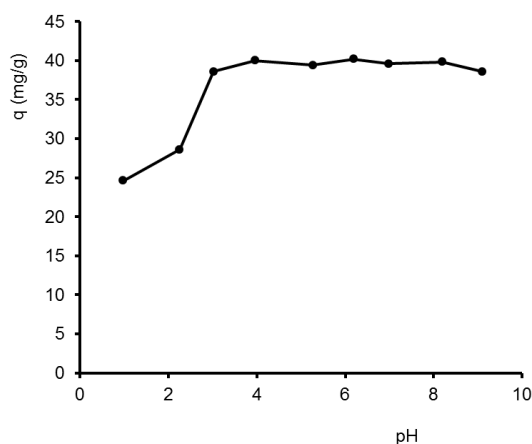


Figure 2. Effect of pH on cesium adsorption onto natural zeolite (clinoptilolite).

### 3.3. Temperature effect on the sorption of cesium

The effects of temperature on cesium sorption onto the zeolite were studied at different temperatures (25, 35, 45, 55 and 65°C). The results show that temperature doesn't have significant effect on cesium sorption.

### 2.4. Effect of contact time and kinetics of sorption

Kinetics of cesium ion sorption governs the residence time and it is one of the important characteristics defining the efficiency of a sorbent. The study of kinetics of a sorbate uptake is required for obtaining essential information, to evaluate the suitability of the sorbent to be used in practical treatment systems, and selecting optimum operating conditions for the full-scale batch process. Therefore, the effect of equilibration time on the sorption of cesium ions, from aqueous solutions, was also studied. The sorption increases with increase in contact time. As seen in Figure 3, the removal of cesium ions from aqueous solution by the natural zeolite as a function of contact time showed that 60 min was sufficient for the sorption equilibrium to be achieved.

Two models for metal ion sorption kinetics, namely (i) the pseudo first-order model (Lagergren) and (ii) the pseudo second-order model was used to fit the experimental results, to determine kinetic parameters for sorption of cesium



# 4<sup>th</sup> Iran National Zeolite Conference

## Golpayegan University of Technology, Golpayegan, Iran

### August 23-24, 2017



ions into the clinoptilolite, and identify the steps involved in the sorption mechanism. The pseudo-first-order kinetic and the pseudo-second-order kinetics are expressed by Equations (2) and (3), respectively [10].

$$\log(q_e - q_t) = \log q_e - \frac{k_1}{2.303} t \quad (2)$$

$$\frac{t}{q_t} = \frac{1}{k_2 q_e^2} + \frac{t}{q_e} \quad (3)$$

where  $q_e$  and  $q_t$  are the sorbed metal in  $\text{mg.g}^{-1}$  on the sorbent at equilibrium and time  $t$ , respectively,  $k_1$  is the constant of first-order sorption in  $\text{min}^{-1}$  and  $k_2$  is the rate constant of second-order sorption in  $\text{g.mg}^{-1}.\text{min}^{-1}$ .

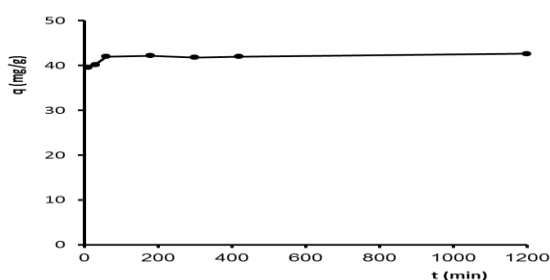


Figure 3. Sorption kinetics of cesium onto natural zeolite.

The parameters of the kinetic models and the regression correlation coefficients ( $R^2$ ) are listed in Table 1. The poor linear fitting of the plots of  $\log(q_e - q_t)$  versus time suggests that the process of cesium ion sorption does not follow the first-order kinetics. Moreover, the values of  $q_e$  obtained from the equation differ substantially from those measured experimentally, further supporting the above conclusion. The higher  $R^2$  value in the case of pseudo first-order plots confirm that the sorption data is well represented by the pseudo second-order kinetic model. The confirmation of pseudo-second-order kinetics indicates that the concentrations of both sorbate (cesium ions) and sorbent (natural zeolite) are involved in the rate determining step of the sorption process [11].

Table 1. Kinetic adsorption parameters obtained using pseudo-first-order and pseudo-second-order models (initial concentration of cesium ion  $50 \text{ mg.L}^{-1}$ )

Pseudo-first-order			Pseudo-second-order		
$k_1$	$q_e$ ( $\text{mg.g}^{-1}$ )	$R^2$	$k_2$	$q_e$ ( $\text{mg.g}^{-1}$ )	$R^2$
0.003	1.6	0.36	0.009	42.6	1

### 2.5. Sorption isotherm

The adsorption isotherm is mainly used to describe sorption equilibrium, which reflects the degree of interaction between the amounts of adsorbate on the adsorbent several theoretical and empirical correlations have been reported in literature for modeling the adsorption isotherm. The most frequently used models are: Langmuir and Freundlich. The Langmuir adsorption isotherm model assumes that adsorption takes place at specific homogeneous sites within the adsorbent. This model can be applied successfully in many monolayer adsorption processes. The linear equation of the Langmuir isotherm model is [12]:

$$\frac{1}{q_e} = \frac{1}{q_m} + \frac{1}{q_m K_L C_e} \quad (4)$$



4<sup>th</sup> Iran National Zeolite Conference  
 Golpayegan University of Technology, Golpayegan, Iran  
 August 23-24, 2017



Where,  $q_m$  is the monolayer adsorption capacity of the adsorbent ( $\text{mg.g}^{-1}$ ) and  $k_l$  is the Langmuir constant ( $\text{L.mg}^{-1}$ ) and related to the free energy of adsorption. The empirical Freundlich model can be applied for non-ideal sorption on heterogeneous surfaces and multilayer sorption. The Freundlich model in linear form is given as follows [13]:

$$\log q_e = \log K_f + \left(\frac{1}{n}\right) \log C_e \quad (5)$$

Where  $k_f$  is related to the adsorption capacity and  $1/n$  is an empirical parameter related to the adsorption intensity, which varies with the heterogeneity of material. The experimental, Langmuir and Freundlich model isotherms were shown in Figure 4. The parameters for the Langmuir and Freundlich isotherms were evaluated based on the data from present experimental system (Table 2), with the Langmuir fitting the data better than the Freundlich as seen, the calculated maximum sorption capacity ( $q_{max}$ ) was  $172.4 \text{ mg.g}^{-1}$ .

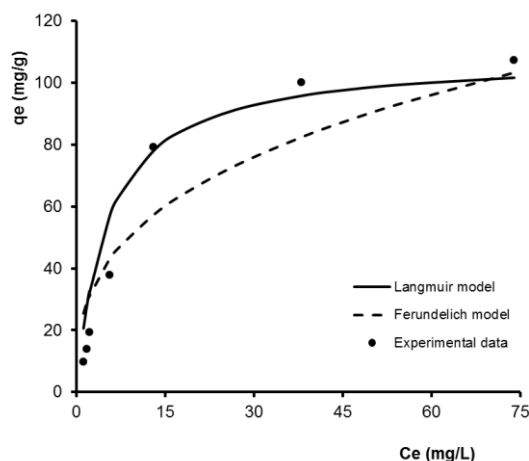


Figure 4. Adsorption isotherms of natural zeolite for cesium adsorption.

Table 2. Langmuir and Freundlich isotherm model fitting parameters for cesium.

Models	Fitting parameters		
	Langmuir	$R^2$	$K_l (\text{L.mg}^{-1})$
0.99		0.05	172.4
Freundlich	$R^2$	$K_f (\text{mg.g}^{-1}.\text{mg}^{-m}.\text{L}^m)$	$m$
	0.93	11.15	0.60

## Conclusion

A natural zeolite sorbent (clinoptilolite, sabzevar) showed high efficiency for the removal of cesium ions from aqueous solutions.

The kinetics of cesium adsorption onto natural zeolite reveals that cesium ions are adsorbed satisfactorily according to the pseudo-second-order equation and the concentrations of both sorbate and sorbent are involved in the rate determining step of the adsorption process. The Langmuir isotherm fitted the equilibrium data better than the Freundlich isotherm that demonstrated homogeneous surfaces with identical binding sites for natural zeolite. The maximum adsorption capacity of cesium onto natural zeolite was found to be  $172.4 \text{ mg.g}^{-1}$ . The immobilization and leach test results show that immobilization ability was increased with increase of the treatment temperature.

## Acknowledgments

The authors are thankful to the staff of material and nuclear fuel research school for providing research facilities.





# 4<sup>th</sup> Iran National Zeolite Conference

## Golpayegan University of Technology, Golpayegan, Iran

### August 23-24, 2017



#### References

- 1) B. L, D. C, F. I, P. A, B. G, *J. Nucl. Mater* **2013**, 435, 196–201.
- 2) P. B, D. C, B. L, C. C, *J. Nucl. Mater* **2004**, 324, 183–188.
- 3) S.A. S, Y. C.H, S. K, *Appl. Clay Sci* **2006**, 31, 306-313.
- 4) E.H. B, R. H, L. M, D. P, *J. Hazard. Mater* **2009**, 172, 416-422.
- 5) B. L, A. C, C. C, *J. Hazard. Mater* **2006**, 137, 1206-1210.
- 6) S. V, H. T, R. C, H. S. *Desalination water treat* **2015**, 55, 1220-1228.
- 7) H. F, M. M, A. F, M. I, *Clay clay miner* **2013**, 61, 193-203.
- 8) A. S, M. T, D. C, M. S, *J. Hazard. Mater* **2007**, 148, 387-394.
- 9) F. G, C. H, A. C, D. G, *J. Hazard. Mater* **2009**, 161, 499-509.
- 10) N. B, S. K, *Sep.Purif. Technol*, **2004**, 39, 189-200.
- 11) C. C. L, M. K.W, Y. S.L, *Ind. Eng. Chem. Res* **2005**, 44,1438-1445.
- 12) A. S, O. G, A. O, *J. Hazard. Mater* **2009**, 161, 499-509.
- 13) M. A, M. K, M. D, O. D. *J. Colloid Interface Sci* **2005**, 291, 309-318.

## Evaluating thermal shock effect on the size of zeolite particles

Azadeh Nademi\*,<sup>a</sup> Amir Hossein Meysami,<sup>a</sup> Reza Amini<sup>a</sup>

<sup>a</sup>Tehran,665-3245-87865, Irain

\*Email : azade199nademi@gmail.com

#### Abstract

In this research, the effect of thermal shock on the dimensions of zeolite particles was investigated[1]. The results showed that thermal shock reduced the zeolite particles. According to SEM images, applying thermal shock to the particles reduced their size to 1/4 of the initial size[2]. Here, a model for the effect of thermal shock mechanism on the size of zeolite particles was proposed and a criterion for fragmentation of fragile materials was also considered. The proposed model and criterion fully explains why the diameter of the zeolite particles decreased by about a quarter of the initial particle diameter after thermal shock[3],[4],[5].

#### 1.Introduction

Zeolites are consistent with each other in terms of composition and appearance[6]. These minerals contain a lot of water and their hardness varies from 3.5 to 5.5 and their volumetric mass is from 2 to 2.4 g per cubic centimeter[7]. Zeolites form the largest group of tectosilicates, and 35 different types of topologies are identified, which may be more likely to exist[8]. Up to now, more than 40 types of natural zeolite and more than 150 types of synthetic zeolites have been identified or made. In general, in the tectosilicate structure[9],[10], all SiO<sub>4</sub> tetrahedrons share all their corners with each other and have a Si:O ratio of 1:2. In this structure, a tetravalent silicon atom is balanced by two



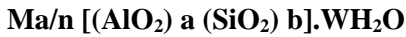
# 4<sup>th</sup> Iran National Zeolite Conference

## Golpayegan University of Technology, Golpayegan, Iran

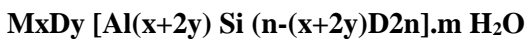
### August 23-24, 2017



divalent oxygen atoms. In this type of silicates, some part of the silicon atoms is replaced by aluminum and is like (Si,Al)O<sub>2</sub>. The general chemical formula for zeolites is:



M is a cation with valence n, W is the number of water molecules and (a + b) summation is the total number of tetraheders per zeolite unitcell[11]. A and b are small numbers. The structure of zeolites consists of three parts: the aluminosilicate framework, the empty spaces through the framework, which contain various cations (M), and typically water molecules assume them as a trapped and confiscated phase[12]. The other general chemical formula for zeolites is:



Where M is the monovalent cations of K and Na and D is the divalent cations of Br, Sr, Ca, Mg and etc[13]. The purpose of this project is to develop a simple mathematical model to explain the effect of thermal shock on zeolite particle size, as well as a fracture criterion for brittle materials[14],[15]. For example, a qualitative model that explains why a thermal shock produces smaller particle?

Progressing previous activities, the thermal activation of zeolite is considered as a goal, which is in fact the thermal shock zeolite is being used. The average diameter of the particles is measured in different directions. After that, the particles are milled in different periods of time resulting in smaller zeolite particles[16],[17]. The zeolite particles obtained from the milling process are heated after being placed in an alumina crucible. Finally, the before heating, after heating with standard cycles[18], and after heating with thermal shock, the particle size was measured and then analyzed using appropriate electron microscopes (XRD, SEM) and then modeled with related software[19].

## 2. Experimental

We used a commercial zeolite that is usually utilized for water filtration. The average grain diameter was  $(10.64 \pm 0.21)$  mm[20]. Measurements were conducted directly by using a micrometer screw, and the diameter was taken as an average of measurements at various orientations[21]. The grain was then milled using a mechanical mortar at different time periods to produce smaller zeolite particles of different average diameters. The zeolite particles obtained from the milling process were then put in alumina crucibles and heated in atmospheric condition. Two routes of heating were carried out: standard heating, as shown in Fig. 1(a), and standard heating with the addition of a thermal shock phase, as shown in Fig. 1(b). Scanning electron microscopy (SEM JEOL JSM-6510LA) was used to observe the particle size before heating, after heating by the standard route, and after heating with the addition of the thermal shock phase[22],[23].

## 3. Results and discussion

### 3.1. Experimental results

Fig. 2 shows SEM images of zeolite particles: (a) before the heating process, (b) after heating through the standard route, as shown in Fig. 1(a), and (c) after heating through the standard route with the addition of thermal shock phase as in Fig. 1(b). The average diameter of zeolite particles prior to heating process was  $(17.66 \pm 0.13)$  μm[29]. A significant change in particle size appeared after the heating process with the additional thermal shock phase. By measuring the diameters of the particles in the SEM images, we obtained the diameter distribution, as shown in Fig. 3. The diameter of the particle was taken as the average value of the width of the particle in the vertical and horizontal directions[30]. Fig. 3(a) shows the diameter distribution for the particles without suffering the heating process; Fig. 3(b) shows the distribution after heating through the standard route; and Fig. 3(c) shows the distribution after heating through the standard route with the addition of the thermal shock phase. By fitting to a log-normal distribution function, we estimated the average diameters of the particles in Fig. 2(a), (b) and (c) to be  $(17.66 \pm 0.13)$  μm,  $(16.59 \pm 0.14)$  μm, and  $(4.58 \pm 0.44)$  μm, respectively. Given the significant changes of the particle sizes, we sought to explain the underlying mechanisms[31]. Moreover, another interesting phenomenon was observed: the particle diameter of fragmentation was approximately 1/4 the diameter of the initial particle. This result also needs to be



# 4<sup>th</sup> Iran National Zeolite Conference

## Golpayegan University of Technology, Golpayegan, Iran

### August 23-24, 2017



explained, at least qualitatively. The breakage phenomenon of zeolite was also not caused by an increase of gas pressure in the pores of zeolite, because the heating temperature was not sufficiently high at only 225 °C. Zeolites have pores and channels of molecular dimensions[24], [25]. The ideal gas equation indicates that the gas pressure in the zeolite pores when heated at 225 °C is only  $1 \text{ atm} \times (275+225) \text{ K} / 300 \text{ K} = 1.66 \text{ atm} = 0.17 \text{ GPa}$ . This pressure is not high enough to make the zeolite rupture. Surface fracturing of the zeolite was observed with a stress of several hundreds of MPa (tens of GPa) [26]; the maximum compressive stress of zeolite thin films is 2.51 GPa [27]. A similar phenomenon also occurred on a zeolite particle that was heated through the standard route. Because the heating temperature was 225 °C, the pressure increase was only 0.17 GPa, not high enough to cause zeolite breakage[28].

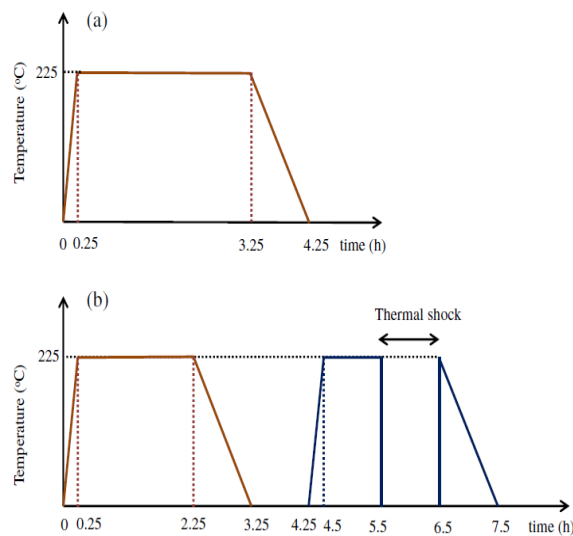


Fig. 1. Two routes of heating processes were used in the experiment: (a) thermal activation using the standard route and (b) thermal activation with the addition of a thermal shock phase.

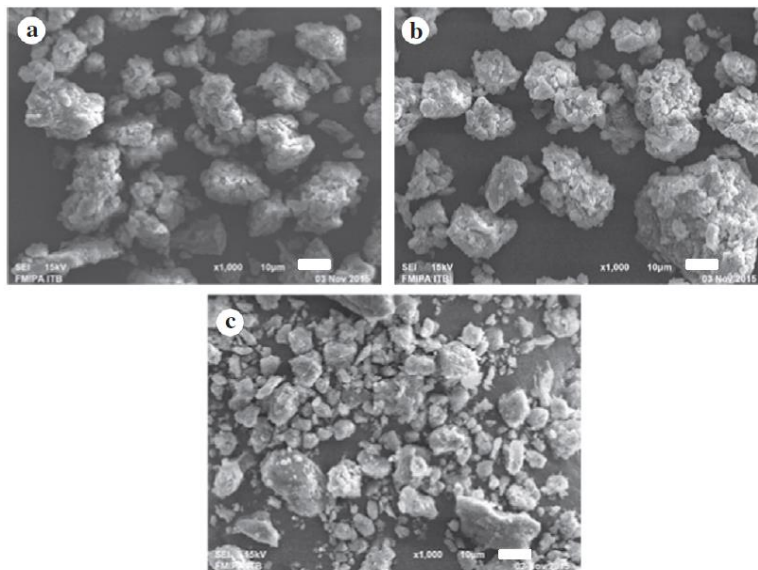


Fig. 2. SEM images of zeolite particles: (a) before the heating process (b), after heating through the standard route [Fig. 1(a)], and (c) after heating through the standard route with the addition of thermal shock phase [Fig. 1(b)].



4<sup>th</sup> Iran National Zeolite Conference  
 Golpayegan University of Technology, Golpayegan, Iran  
 August 23-24, 2017

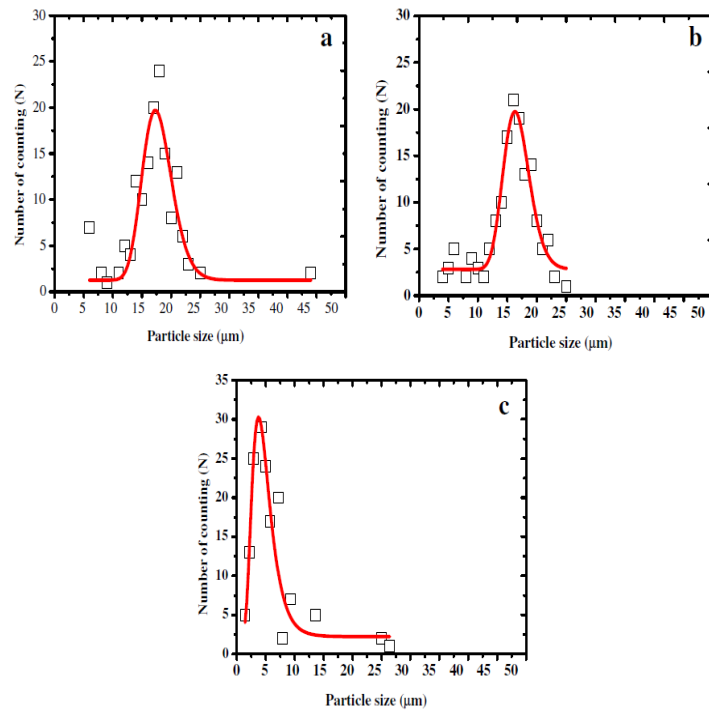


Fig. 3. Size distribution of zeolite particles: (a) before suffering the heating process, (b) after heating through the standard route (Fig. 1 (a)), and (c) after heating through the standard route with the addition of thermal shock phase (Fig. 1 (b)). Symbols are measurement data while the curve is the log-normal function with the closest fit to the measurement data.

### 3.2. Modeling

To further prove the above predictions, we have conducted thermal shock processes on other zeolite samples with different initial sizes[32]. All parameters of the heating process have been maintained as before. Fig. 4 is SEM images of zeolite samples prior to thermal shock (left) and after thermal shock (right) processes. Zeolite particle size distributions before and after the thermal shock processes are shown in Fig. 5[33]. The curves in the figure are the results of fitting by using the log-normal distribution function. The fitting results have produced average diameters as shown in Table 1[34]. The third column in the table shows the ratio of initial diameter with the final diameter. It is proven very strongly that the diameter of the resulting particles is roughly a quarter of the diameter of the initial particles[35].

Indeed, we can make further predictions from the curve in Fig.6, although experimental confirmation has not yet been carried out[36]. From the shape of the curve of  $j_1$ , it appears that  $j_1$  will be smaller if  $r$  moves toward  $R$  from the inside. In other words,  $j_1(R-\delta R)$  becomes smaller if  $\delta R$  is also smaller. (11), we see that if  $\Delta T_0$  becomes greater, the right side will be smaller, so that  $j_1(R-\delta R)$  is also smaller. As a result, the value of  $\delta R$  will be smaller (Fig. 4). The smaller value of  $\delta R$  suggests that the thickness of the outside layer of particle that causes the fragmentation of the layer will be smaller if  $\Delta T_0$  is larger. The size of the resulting particle is approximately equal to the thickness of From the inequality the initial layer that undergoes fragmentation. Thus, we can conclude that if  $\Delta T_0$  increases, the size of the resulting particles decreases.

If the size of the initial particle subjected to thermal shock is large enough that the requirement condition of  $\alpha\pi c / R^2 \ll 1$  is satisfied, we obtain an approximation:

$$j_1\left(\frac{\pi(R-\delta R)}{R}\right) \geq \frac{\xi R}{2\pi^2\gamma a_0 \Delta T_0} \quad 1$$

It can be observed from Eq. (12) that if the size of the initial particle increases, the  $j_1$  value also increases. This also occurs if  $\delta R$  increases (see Fig. 10). These results show that the larger size of the initial particle that suffers thermal shock will also produce a new particle with a larger size.



4<sup>th</sup> Iran National Zeolite Conference  
 Golpayegan University of Technology, Golpayegan, Iran  
 August 23-24, 2017



A similar conclusion has been reported by Saastamoinen [15] for fragmentation of limestone particles during thermal shock and calcinations in a fluidized bed. Generally, the authors have concluded that the final average diameter is proportional to the initial diameter, although their data distribution was quite scattered. In our study, a near linear relationship between the size of the produced particles with the size of the initial particle can be roughly estimated from Eq. (12). From Eq. (12) we can write where  $j_1^{-1}(x)$  is the inverse of  $j_1(x)$ . In general,  $\delta R$  is directly proportional to  $R$ . However, it is not absolutely linear because there is one factor in the bracket that is a function of  $R$  [36].

$$\pi \left( 1 - \frac{\delta R}{R} \right) \approx j_1^{-1} \left( \frac{\xi R}{2\pi^2 \gamma a_0 \Delta T_0} \right)$$

or

$$\delta R \approx R \left[ 1 - \frac{1}{\pi} j_1^{-1} \left( \frac{\xi R}{2\pi^2 \gamma a_0 \Delta T_0} \right) \right] \quad 2$$

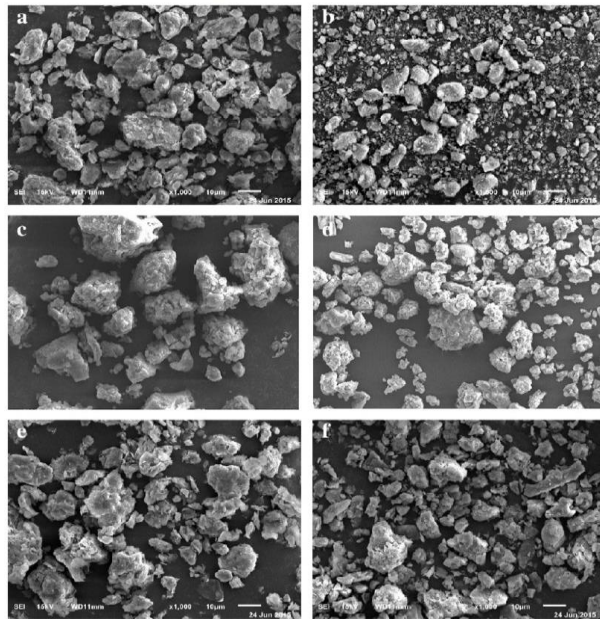


Fig. 4. SEM images of zeolite particles with different size distribution: left side [(a), (c) and (e)] is initial size before the heating process; right side [(b), (d) and (f)] is final size after heating through the standard route with the addition of thermal shock phase

#### 4. Conclusion

From the above discussion, we conclude that thermal shock causes zeolite particles to be transformed into smaller particles. The particle would be broken if the expansion difference of the adjacent layers exceeds a certain fraction of the atomic distance and occurs in a time interval that exceeds the characteristic value. For the zeolite particles that we used, the diameter of the produced particles was approximately 1/4 of the initial particle diameter. The proposed model qualitatively explains why thermal shock causes fragmentation of zeolite particles and why the diameters of zeolite particles as a result of thermal shock are approximately 1/4 the initial particle diameter. The proposed criterion of zeolite particle fragmentation may be used as a reference for explaining the breakage phenomenon of other brittle materials.



4<sup>th</sup> Iran National Zeolite Conference  
 Golpayegan University of Technology, Golpayegan, Iran  
 August 23-24, 2017

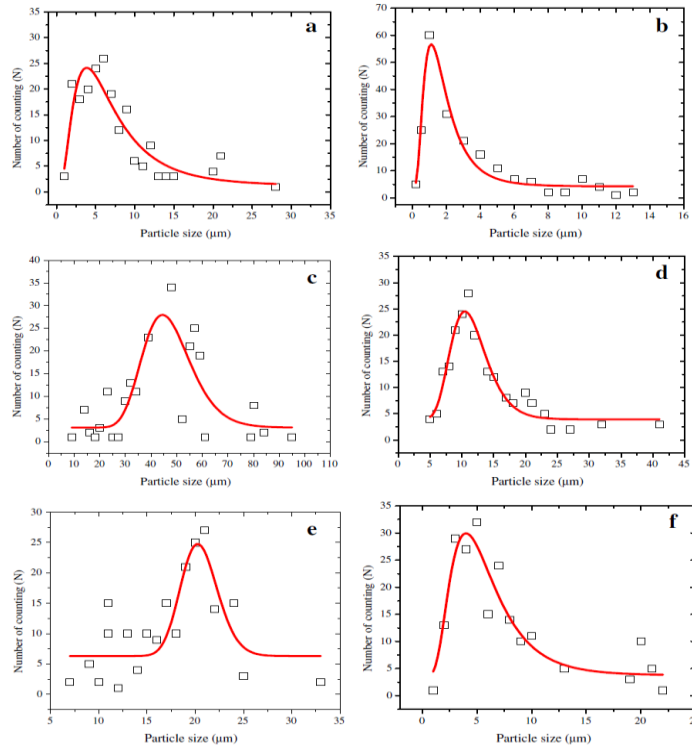


Fig. 5. Size distribution of zeolite particles: left side [(a), (c) and (e)] is initial size before the heating process; right side [(b), (d) and (f)] is final size after heating through the standard route with the addition of thermal shock phase.

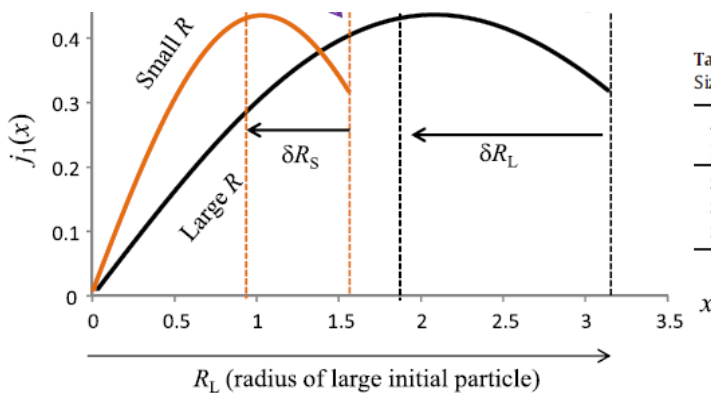


Fig. 6 The plot of  $j_1(x)$  function for two different values of radius

List of symbols

- $a_0$  atomic spacing on the reference temperature [m]
- $j_n(x)$  spherical Bessel function of order  $n$  [-]
- $j_1^{-1}(x)$  inverse of  $j_1(x)$  [-]
- $\delta R$  thickness of outside layer of particle [m]
- $\gamma$  thermal expansion coefficient [ $K^{-1}$ ]
- $\Delta T = T_1 - T$  temperature differences [K]
- $\xi$  fraction of atomic distance [-]

Table 1

Size distribution of zeolite particles before and after suffering the thermal shock process.

Average particles diameter prior to thermal shock ( $\mu m$ )	Average particles diameter after thermal shock ( $\mu m$ )	Ratio of initial and final diameter
Sample a ( $6.19 \pm 0.69$ )	Sample b ( $1.63 \pm 0.62$ )	3.8
Sample c ( $46.38 \pm 0.21$ )	Sample d ( $11.22 \pm 0.26$ )	4.1
Sample e ( $20.42 \pm 0.09$ )	Sample f ( $5.22 \pm 0.51$ )	3.9



# 4<sup>th</sup> Iran National Zeolite Conference

## Golpayegan University of Technology, Golpayegan, Iran

### August 23-24, 2017



#### Acknowledgement

This work was financially supported by the Ministry of Research and Higher Education, Republic of Indonesia (Grant No. 310y/I1.C01/PL/2015).

#### References

- [1] S. Balci, Effect of heating and acid pre-treatment on pore size distribution of sepiolite, *Clay Miner.* 34 (1999) 647–655.
- [2] M. Lenarda, M. Da Ros, M. Casagrade, L. Storaro, R. Ganzerla, Post-synthetic thermal and chemical treatments of H-BEA zeolite: effects on the catalytic activity, *Inorg.Chem. Acta.* 349 (2003) 195–202.
- [3] E. Wibowo, M. Rokhmat, Sutisna, R. Murniati, Khairurrijal, M. Abdullaha, Thermally activated clay to compete zeolite for seawater desalination, *Adv. Mater. Res.* 1112 (2015) 154–157.
- [4] V.J. Inglezakis, M.K. Doula, V. Aggelatou, A.A. Zorpas, Removal of iron and manganese from underground water by use of natural minerals in batch mode treatment, *Desalin. Water Treat.* 18 (2010) 341–346.
- [5] Z. Li, H.K. Jones, P. Zhang, R.S. Bowman, Chromate transport through columns packed with surfactant-modified zeolite/zero valent iron pellets, *Chemosphere* 68 (2007) 1861–1866.
- [6] Z. Li, J.S. Jean, W.T. Jiang, P.H. Chang, C.J. Chen, L. Liao, Removal of arsenic from water using Fe-exchanged natural zeolite, *J. Hazard. Mater.* 187 (2011) 318–323.
- [7] N. Widiastuti, H. Wu, H. Ming Ang, D. Zhang, Removal of ammonium from greywater using natural zeolite, *Desalination* 277 (2011) 15–23.
- [8] M. Gougazeh, J.-C. Buhl, Synthesis and characterization of zeolite A by hydrothermal transformation of natural Jordanian kaolin, *J. Assoc. Arab Univ. Basic Appl. Sci.* 15 (2014) 35–42.
- [9] A.M. Akimkhan, Structural and Ion-Exchange Properties of Natural Zeolites. InTech, 2012, <http://dx.doi.org/10.5772/51682> (Chapter 10).
- [10] V.H. Bekkum, E.M. Flanigen, P.A. Jacobs, J.C., Introduction to Zeolite Science and Practice, 2nd revised ed. Elsevier, Amsterdam, 1991.
- [11] E. Monteverde, L. Scatteia, Resistance to thermal shock and to oxidation of metal diborides-SiC ceramics for aerospace application, *J. Am. Ceram. Soc.* 90 (2007) 1130–1138.
- [12] G. Li and H. Chen. Effect of repeated thermal shock on mechanical properties of ZrB<sub>2</sub>-SiC-Bn ceramic composites. *Sci. World J.* <http://dx.doi.org/10.1155/2014/419386>.
- [13] A.L. Leanos, P. Prabhakar, Experimental investigation of thermal shock effects on carbon-carbon composites, *Compos. Struct.* 132 (2015) 372–383.
- [14] F.W. Nyongesa, N. Rahbar, S. K. Obwoya, J. Zimba, B. O. Aduda and W. O. Soboyejo. An investigation of thermal shock in porous clay ceramics. <http://dx.doi.org/10.5402/2011/816853> *ISRN Mech. Eng.*
- [15] J. Saastamoinen, T. Pikkariainen, A. Tourunen, M. Räsänen, T. Jäntti, Model of fragmentation of limestone particles during thermal shock and calcination in fluidized beds, *Powder Technol.* 187 (2008) 244–251.
- [16] V.V. Murashov, M.A. White, Thermal properties of zeolites: effective thermal conductivity of dehydrated powdered zeolite 4 A, *Mater. Chem. Phys.* 75 (2002) 178–180.
- [17] S. Narayanan, X. Li, S. Yang, I. McKay, H. Kim, E.N. Wang Design, Optimization of high performance adsorption-based thermal battery, ASME, Heat Transfer Summer Conference, 2013, <http://dx.doi.org/10.1115/HT2013-17472>.
- [18] S.K. Schnee, T.J.H. Vlugt, Thermal conductivity in zeolites studied by non-equilibrium molecular dynamics simulations, *Int. J. Thermophys.* 34 (2013) 1197–1213.
- [19] W.F. Krupke, M.D. Shinn, J.A. Caird, S.E. Stokowski, Spectroscopic, optical, and thermomechanical properties of neodymium- and chromium-doped gadolinium scandium gallium garnet, *JOSAB* 3 (1986) 102–114.
- [20] S.H. Park, R.-W. Große Kunstleve, H. Graetsch, H. Gies, The thermal expansion of the zeolites MFI, AFI, DOH, DDR, and MTN in their calcined and as synthesized forms, *Stud. Surf. Sci. Catal.* 105 (1997) 1989–1994.
- [21] J. Felsche, S. Luger, C.H. Baerlocher, Crystal structures of the hydro-sodalite Na<sub>6</sub>[AlSiO<sub>4</sub>]<sub>6</sub> 8H<sub>2</sub>O and of the anhydrous sodalite Na<sub>6</sub>[AlSiO<sub>4</sub>]<sub>6</sub>, *Zeolites* 6 (1986) 367.
- [22] J.J. Williams, R.I. Walton, K.E. Evans, J.D. Bass, Negative Poisson's ratios in siliceous zeolite MFI-silicalite, *J. Chem. Phys.* 128 (2008) 184503.
- [23] T.J. Lu, N.A. Fleck, The thermal shock resistance of solids, *Acta Mater.* 46 (1998) 4755–4768.
- [24] K. Okuyama, I.W. Lenggoro, Preparation of nanoparticles via spray route, *Chem. Eng.Sci.* 58 (2003) 537–547.
- [25] C. Sanchez-valle, S.V. Sinogeikin, Z.A.D. Lethbridge, R.I. Walton, C.W. Smith, J.K.E. Evans, D. Bass, *J. Appl. Phys.* 98 (2005) 053508.
- [26] D. Song, L. Lamberson, D. Casem, J. Kimberley (Eds.), *Dynamic Behavior of Materials*, Vol. 1, Proceeding of the 2015 Annual Conference on Experimental and Applied Mechanics, Springer, Heidelberg, 2016.
- [27] L. Hu, J. Wang, Z. Li, S. Li, Y. Yan, Interfacial adhesion of nanoporous zeolite thin films, ASME 2004 International Mechanical Engineering Congress and Exposition, Anaheim, California, USA November 13–19, 2004, pp. 199–203.
- [28] Z. Malou, M. Hamidouche, N. Bouaouadja, J. Chevalier, G. Fantozzi, Thermal shock resistance of a soda lime glass, *Ceramics-Silikáty* 57 (2013) 39–44.
- [29] M. Karel, D.B. Lund, *Physical Principles of Food Preservation*, Marcel Dekker, New York, 2003.
- [30] D.-W. Oh, S. Kim, J.A. Rogers, D.G. Cahill, S. Sinha, Interfacial thermal conductance of transfer-printed metal films, *Adv. Mater.* 23 (2011) 5028–5033.
- [31] M. Abrarowitz, I.A. Stegun, *Handbook of Mathematical Functions: With Formulas, Graphs, and Mathematical Tables*, Dover Publications, Inc., New York, 1964.
- [32] M.D. Mikhailov, M.N. Ozisik, *Unified Analysis and Solutions of Heat and Mass Diffusion*, Dover Publications, Inc., New York, 1994.



4<sup>th</sup> Iran National Zeolite Conference  
Golpayegan University of Technology, Golpayegan, Iran  
August 23-24, 2017



- [33] P.R. Couchman, The Lindemann hypothesis and the size dependence of melting temperature. II, *Philos. Mag.* 40 (1979) 637–643.  
[34] J.J. Gilvarry, The Lindemann and Grüneisen Laws, *Phys. Rev.* 102 (1956) 308.  
[35] A.C. Lawson, D.P. Butt, J.W. Richardson, J. Li, Thermal expansion and atomic vibrations of zirconium carbide to 1600 K, *Philos. Mag.* 87 (2007) 2507–2519.  
[36] F.D. Stacey, R.D. Irvine, Theory of melting: thermodynamic basis of Lindemann's law, *Aust. J. Phys.* 30 (1977) 631–640.

Fig. 10. The plot of  $j_1(x)$  function for two different values of radius.

## Synthesis and characterization of Zeolite / Graphene oxide nanocomposite

Sara Javanmardi<sup>\*a</sup>, B. Divband<sup>b</sup>, F. Farahmand-zahed

<sup>a</sup>Department of Clinical Sciences, Faculty of Veterinary Medicine, University of Tabriz, C.P. 51666, Tabriz, Iran

<sup>b</sup>Inorganic Chemistry Department, Faculty of Chemistry, University of Tabriz, C.P. 51664, Tabriz, Iran

\*Email: Sarahjavanmardi@yahoo.com

### 1. Introduction

Graphene is a sheet of two-dimensional (2D) single layer  $sp^2$  hybridized carbon atoms with exceptional electrical, mechanical and thermal properties [1]. Geim and co-workers discovered graphene, the thinnest known material, in 2004 and received Noble Prize in Physics for this discovery. It has special properties which make it suitable for many applications. Graphene oxide (GO) is oxidized form of graphene that has carboxylic, hydroxide and epoxy groups. But there are some concerns about toxicity of graphene and its derivatives. Recent researches have shown that different forms of graphene will affect differently on cells. A lot of factors are important, some of them are rigidity, lateral dimensions and etc [2,3]. Additionally, large surface area of graphene,  $\pi$ - $\pi$  stacking and electrostatic or hydrophobic interactions of graphene, hydrophilic interaction of graphene oxide allows it to achieve high drug loading capacity.

Zeolites, porous aluminosilicates, have found many uses because of their special architecture. They have been used widely as absorbants, catalysts, and detergent builders. Recently their uses in biomedical applications have attracted a lot of attention. For example, they have been used in biosensors, magnetic resonance imaging and drug delivery systems. As mentioned before, different forms of graphene will effect on cells differently and preparing safe composites of it has got a lot of interest so adding zeolite not only improves its biocompatibility but also doesn't decrease surface area of nanocomposite so much because of high surface area of zeolite [4].

Herein we synthesized zeolite/GO nanocomposite and as prepared samples were characterized by X-ray diffraction (XRD) and Scanning electron microscopy (SEM). Moreover, drug (Curcumin) loading capacity of nanocomposite was investigated.





# 4<sup>th</sup> Iran National Zeolite Conference

## Golpayegan University of Technology, Golpayegan, Iran

### August 23-24, 2017



## 2. Experimental

GO was synthesized using widely reported modified Hummers method starting from graphite. GO and Zeolite (mass ratio of 1:1) were dispersed in water by using ultrasonic irradiation, then NaBH<sub>4</sub> was added and treated under reflux at 80 °C for 8 hours. Then obtained powder was filtered, washed with distilled water, dried at 60 °C.

## 3. Results and discussion

In XRD pattern Zeolite/GO, all of zeolite peaks were clearly observed and it was highly crystalized and the peak at  $2\theta=11.33$  is related to GO (figure1).

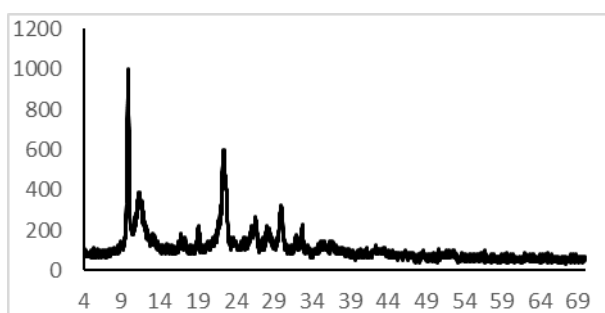


Figure 1. XRD pattern Zeolite/GO

Figure 2 showed SEM image of zeolite/GO nanocomposite. It is obvious that cubical Zeolite particles were randomly placed on graphene plates and graphene acted like a substrate for Zeolite particles. Thin films of graphene with thickness of 30-45 nm is clearly observed.

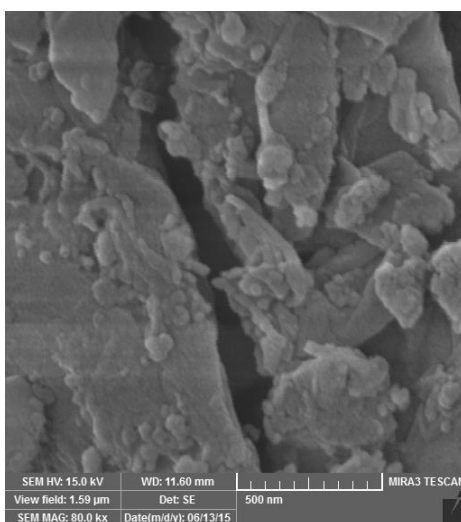


Figure 2. Image of Zeolite/GO nanocomposite



4<sup>th</sup> Iran National Zeolite Conference  
Golpayegan University of Technology, Golpayegan, Iran  
August 23-24, 2017

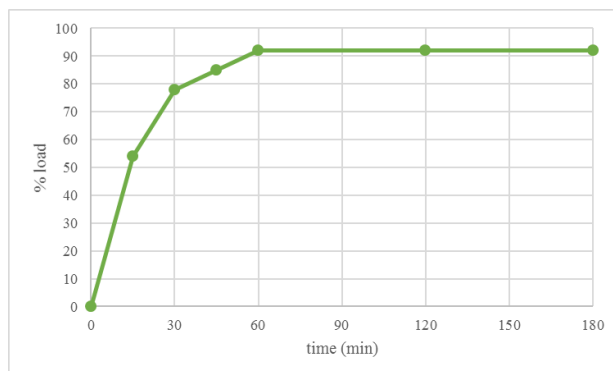


Figure 3. drug loading capacity of zeolite/GO nanocomposite

#### 4. Conclusions

Herein we successfully synthesized zeolite/GO nanocomposite and XRD pattern and SEM image confirmed it. This nanocomposite showed a high drug loading capacity. Which gives the idea of studying it more for medical uses.

#### References

- 1) K. S. Novoselov, A. K. Geim, S. V. Morozov, D. Jiang, Y. Zhang, S. V. Dubonos, I. V. Grigorieva and A. A. Firsov, *Science*, **2004**, 306, 666-669.
- 2) J. Liu, L. Cui, D. Losic, , *Acta Biomater.*, **2013**, 9, 9243.
- 3) X. Zhang, M. Li, Y. B. Wang, Y. Cheng, Y. F. Zheng, T. F. Xi, S. C. Wei, *J. Biomed. Mater. Res. A*, **2014**, 102 732-742.
- 4) A. M. Cardoso, M. B. Horn, L. S. Ferret, C. M.N. Azevedo, M. Pires, *J. Hazard. Mat.* **2015**, 287, 69-77.



4<sup>th</sup> Iran National Zeolite Conference  
Golpayegan University of Technology, Golpayegan, Iran  
August 23-24, 2017



**Sulfamic acid-functionalized NaY zeolite as a reusable solid catalyst for  
formylation of amines**

Fatemeh Tavakoli<sup>a\*</sup>, Mojgan Zندهدل<sup>a</sup>

<sup>a</sup>Department of Chemistry, Faculty of science, Arak university, Arak, 38156-8-8349, Iran

\*Email : f.tavakoli20@yahoo.com

### 1. Introduction

Formamides are considered as valuable intermediates in the production of various pharmaceuticals [1,2,3]. The transformation of primary and secondary amines leads to useful products that are applicable as polar solvents [4,5]. The reported methods have several disadvantages such as expensive and toxic formylating reagents and catalysts, long reaction times, high temperature, low yields, production of side products, environmental pollution caused by using non green solvents, tedious work up, complex isolation and recovery procedures. Here in we assume immobilization of sulfamic acid on the outside of NaY zeolite surface can increase catalyst activity. So, in continuation of our recent studies on application of heterogeneous catalysts [8] we hereby report a new protocol for preparation of sulfamic acid-functionalized NaY zeolite (SA-NaY) for the first time and its application in synthesis of N-formylamines as an efficient and reusable heterogeneous catalyst.

### 2. Experimental Part or Theoretical Details

*Preparation of the SA-NaY:*

To a mixture of NaY zeolite in toluene (20 mL), trimethoxysilyl propylamine (2 mL) was added and stirred for 24 hours in reflux condition. Then catalyst was filtered and dried at 60°C. For solfonation, chlorosulfonic acid (2 mL) and triethylamine (0.2 mL) were added to a mixture of functionalized zeolite (1 g) in toluene (20 mL) and it was stirred at reflux condition for 24 hours. Then, solfonated zeolite was filtrated and dried.

*General procedure for formylation of amines:* To mixture of aniline (1 mmol) and 0.02 catalyst in ethyl acetate (1 mL), formic acid (2 mmol) was added and stirred at room temperature for appropriate time. The progress of reaction was followed by TLC. After completion the reaction, products were extracted by ethyl acetate (4 mL) and catalyst was filtrated, washed and dried for reuse.

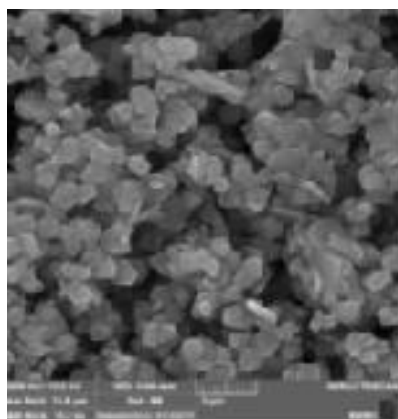
### 3. Results and discussion

*Characterization of SA-NaY:*

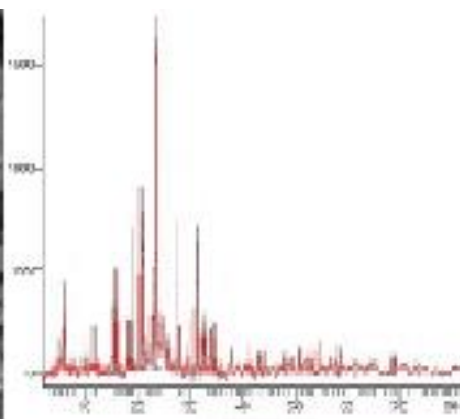
we prepared and characterized Sulfamic acid-functionalized NaY zeolite (SA-NaY) by FTIR, XRD, SEM, BET and TGA.



4<sup>th</sup> Iran National Zeolite Conference  
 Golpayegan University of Technology, Golpayegan, Iran  
 August 23-24, 2017



SEM of (SA-NaY)



XRD of (SA-NaY)

**Table 1.** Formylation of different amines

Substrate	Product	Time (min)	Yields (%) <sup>b</sup>
Anilin	N-Phenylformamide	3	99
4-Nitroaniline	N-4-Nitrophenylformamide	60	48
4-Methylaniline	N-Paratolylformamid	3	99
1-Naphtylamine	N-Naphtalene2ylformamide	7	99
4-Chloroaniline	N-4-Chloro phenylformamide	35	86
4-Bromoaniline	N-4-Bromo phenylformamide	40	74
Ortophenylenedi amine	N,N'-(1,2-Phenylene) Diformamide	47	69

**Table 2.** Studying efficiency of the present protocol over some reported .catalysts

Catalyst	Solvent	Temperature (°C)	Time (min)	Yield (%)	Ref
SA-NaY	Ethyl acetate	rt	3	99	present
$\alpha$ -Fe <sub>2</sub> O <sub>3</sub> @HAp-SO <sub>3</sub> H	Solvent free	rt	20	97	9
ZnO	Solvent free	70	10	99	10
Nano basic Al <sub>2</sub> O <sub>3</sub>	Solvent free	40	5	98	11
Iodine	Solvent free	70	240	96	12
Sulfated titania	MeCN	rt	30	99	13
HClO <sub>4</sub> -SiO <sub>2</sub>	THF	rt	15	96	14
Natrolite zeolite	Solvent free	rt	20	89	1
PEG-400	Solvent free	rt	240	91	15



# 4<sup>th</sup> Iran National Zeolite Conference

## Golpayegan University of Technology, Golpayegan, Iran

### August 23-24, 2017



*Catalytic studies:* At first, aniline has been selected as a test compound to determine the optimal reaction conditions. best yields and reaction times were obtained using 10 mol % of catalyst loading in ethylacetate as the solvent. So, in this optimized condition, several aniline derivatives have been *N*-formylated to corresponding formamides in good yields and short reaction times (Table 1). Finally, this protocol for formylation of aniline has been compared with some other reported methods in (Table 2).

According to this table, this methodology improved in yields, reaction times or reaction conditions. *Recyclability of catalyst:* To investigate the catalytic efficiency of the recycled catalyst, successive cycles of the model reaction were run under the optimal reaction conditions using recycled SA-NaY from the previous run. The recovered catalyst could be reused without any significant loss of activity up to seven cycles for *N*-formylation (Figure 1).

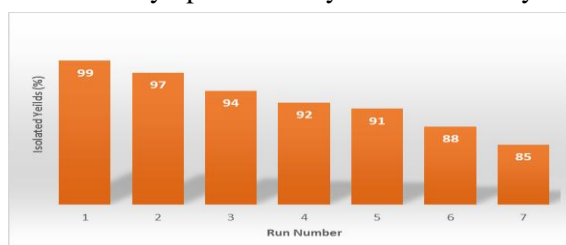


Figure 1. Catalytic efficiency of the recycled catalyst

#### 4. Conclusions

In conclusion, we have carried out a new, mild, novel, clean and fast methodology for synthesis of formamide derivatives using formic acid in the presence of SA-NaY zeolite as a new, heterogeneous, highly efficient and environmentally friendly catalyst at room temperature by easy work-up in which the separation techniques are not necessary to get the pure compounds.

#### Acknowledgments

The authors thank Arak University for the scientific and instrumental support.

#### References

- 1) D. Habibi, M. Nasrollahzadeh, H. Sahebkhari, J. Mol. Catal. A: Chem **2013**, 378,148.
- 2) K. Kobayashi, S. Nagato, M. Kawakita, O. Morikawa, H. Konishi, Chem. Lett **1995**, 24, 575.
- 3) B.C. Chen, M.S. Bednarz, R. Zhao, J.E. Sundeen, P. Chen, Z. Shen, A.P. Skoumbourdis, J.C. Barrish, Tetrahedron. Lett **2000**, 41, 5453.
- 4) J. Deutsch, R. Eckelt, A. Ko'ckritz, A. Martin, Tetrahedron **2009**, 65, 10365.
- 5) M. Hosseini-Sarvari, H. Sharghi, J. Org. Chem **2006**, 71, 6652.
- 6) L.M. Payawan Jr, J.A. Damasco, K.W.E. Sy Piecco, Philippine Journal of Science **2010**, 139, 105.
- 7) M.R. Didgikar, D. Roy, S.P. Gupte, S.S. Joshi, R.V. Chaudhari, Ind. Eng. Chem. Res **2010**, 49, 1027.
- 8) M. Zendehei, A. Mobinikhaledi, F. Hasanvand Jamshidi, J. Incl. Phenom. Macrocycl. Chem **2007**, 59, 41.
- 9) L. Ma'mani, M. Sheykhani, A. Heydari, M. Faraji, Y. Yamini, Appl. Catal. A: **2010**, 377, 64–69.
- 10) M. Hosseini-Sarvari, H. Sharghi. J. Org. Chem **2006**, 71, 6652.
- 11) V.K. Das, R.R. Devi, P.K. Raul, A.J. Thakur, Green. Chem **2012**, 14, 847.
- 12) J.-G. Kim, D.O. Jang, Synlett **2010**, 2093.
- 13) B. Krishnakumar, M. Swaminathan, J. Mol. Catal. A: Chem **2011**, 334, 98.
- 14) M.I. Ansari, M.K. Hussain, N. Yadav, P.K. Gupta, K. Hajela, Tetrahedron. Lett **2012**, 53, 2063.
- 15) B. Das, K. Meddeboina, P. Balasubramanayam, V.D. Boyapati, K.D. Nandan Tetrahedron. Lett **2008**, 49, 2225.



4<sup>th</sup> Iran National Zeolite Conference  
Golpayegan University of Technology, Golpayegan, Iran  
August 23-24, 2017



Catalytic conversion of ethylbenzene to styrene by K-chromosilicate/Fe<sub>2</sub>O<sub>3</sub> composites through CO<sub>2</sub>

Maasoumeh Khatamian<sup>\*a</sup>, Ebrahim Sadegi<sup>a</sup>, Maryam Saket<sup>a</sup>, Sara Fazli Shokouhi<sup>b</sup>

<sup>a</sup>Department of Inorganic Chemistry, Faculty of Chemistry, University of Tabriz, Tabriz, Iran.

<sup>b</sup>Research centre for Advanced Materials and Minerals Processing, Department of Material Engineering, Sahand University of Technology, Tabriz.

\*Email: Khatamian@tabrizu.ac.ir

### Abstract

Styrene is one of the most precious basic materials which its demands and applications are currently increasingly growing all over the world. Mostly styrene is produced by catalytic dehydrogenation of ethylbenzene at high temperatures in the presence of excess steam. This paper introduces novel composites of K-chromosilicate/Fe<sub>2</sub>O<sub>3</sub> with high performance in oxidative dehydrogenation (ODH) of ethylbenzene to produce styrene with CO<sub>2</sub>. Regarding K-chromosilicate as catalyst support, various amounts of iron oxide nanoparticles ( $\gamma$ -Fe<sub>2</sub>O<sub>3</sub>) were introduced into porous support by solid-stated dispersion (SSD) in order to enhance catalytic activity. The prepared samples were characterized by X-ray diffraction (XRD), scanning electron microscopy (SEM) coupled with the energy dispersive analysis-EDX, and N<sub>2</sub> physical adsorption analysis. According to the GC results of prepared nanocomposites in ODH reaction, the highest styrene yield, 46.95% with the selectivity of 92.40% belongs to 5F/KCS catalyst (potassium chromosilicate/5% Fe<sub>2</sub>O<sub>3</sub>). The relatively high performance of catalytic activity of the samples in ethylbenzene dehydrogenation process can be attributed to the synergistic effect of Cr<sub>2</sub>O<sub>3</sub> and potassium K<sup>+</sup> and iron Fe<sup>3+</sup> ions in the structure of catalysts.



4<sup>th</sup> Iran National Zeolite Conference  
Golpayegan University of Technology, Golpayegan, Iran  
August 23-24, 2017



**Synthesis and characterization of Mn-incorporated ZSM-5 type zeolite  
in the presence of K<sup>+</sup> as an alkaline system**

Maasoumeh Khatamian<sup>\*a</sup>, Sima Heidari<sup>a</sup>, Mohammad Mahdi Najafpour<sup>b</sup>, Sara Fazli Shokouhi<sup>c</sup>

<sup>a</sup>Department of Inorganic Chemistry, Faculty of Chemistry, University of Tabriz, Tabriz, Iran

<sup>b</sup>Department of Chemistry, Institute for Advanced Studies in Basic Science, Zanjan, Iran

<sup>c</sup>Research centre for Advanced Materials and Minerals Processing, Department of Material Engineering, Sahand University of Technology, Tabriz

\*Email: mkhatamian@yahoo.com

### 1. Introduction

Zeolites are crystalline aluminosilicates with regular and uniform porous structures. In these materials, Si/Al atomic ratio can be varied from 1 to  $\infty$ ; so highly hydrophobic aluminum-free synthetic zeolites can also be attainable [1]. Thanks to the development of the synthetic techniques, there are graded many synthetic zeolites with different compositional elements and frameworks [2]. Other elements, especially transition metals, can incorporate into the zeolite framework.

Following our previous reports in synthesis of Al [3], Cr [4] or Fe [5] containing MFI type zeolites, we were prepared Mn-incorporated ZSM-5 type zeolite by means of MnCl<sub>2</sub>.4H<sub>2</sub>O in aqueous basic solution as manganese source, silicic acid as silica source and potassium carbonate as alkaline system with a facile “one-step” hydrothermal method. Because of cost saving effects, “one-step” methods have great significance in industrial approaches in contrast to “multi-step” methods. The samples were characterized by N<sub>2</sub> adsorption analysis, XRD, SEM, and FTIR. Aforementioned techniques confirmed successfully synthesis of pure ZSM-5 type manganosilicates and evidences were achieved for incorporation of Mn ions into zeolite lattice.

### 2. Experimental

The manganosilicate sample was prepared in a non-stirred autoclave by hydrothermal procedure from silicic acid (Merck), MnCl<sub>2</sub>.4H<sub>2</sub>O (Merck), potassium carbonate (Panreac, 99.8%) sulfuric acid (Scharlau), and tetrapropylammonium bromide (TPABr, Merck) as template. Firstly the solution of silicic acid and sodium carbonate in distilled water was added slowly to the solution of MnCl<sub>2</sub>.4H<sub>2</sub>O and sulfuric acid in water with pH=0.5. The obtained mixture was stirred for 4 h at a relatively high pH (~9), and then TPABr was added. All the mixture components were transferred in to Teflon-lined stainless-steel autoclave. The sample was obtained after about 48 h of hydrothermal treatment of the mixtures at 180 °C. The synthesized sample was filtered, washed with distilled water, and dried overnight in air at about 120 °C. The template was removed with calcining the sample in the air at 550 °C for 5 h.

### 3. Results and discussion

XRD is a good method for identification of purity, crystallinity and phase identity of solid materials. As presented in Fig. 1, XRD pattern of the calcined KMS-180 sample well accordance to ZSM-5-type structure with orthorhombic symmetry. With comparison of the manganosilicate sample and the all silica ZSM-5 zeolite, a slight shift to lower 2 $\theta$



4<sup>th</sup> Iran National Zeolite Conference  
Golpayegan University of Technology, Golpayegan, Iran  
August 23-24, 2017



is observed for the Mn incorporated sample. The larger size of the Mn ions than tetrahedrally coordinated Si atoms terminates to an increasing in the crystal lattice parameters. This shift is a good evidence for incorporation of manganese ions into the zeolite lattice. No peaks related to crystalline extra-framework manganese oxides are visible in the XRD patterns of the manganosilicate sample, which suggests amorphous phase of the extra-lattice oxides phase.

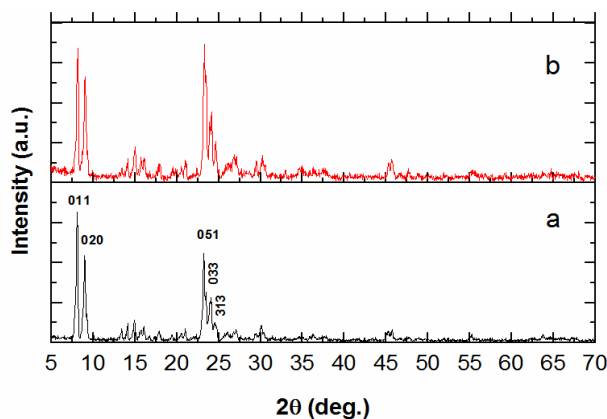


Figure 1. XRD patterns of: all silica zeolite (a), KMS-180 (b).

As it is shown in Fig. 2, Peaks related to Si-O-Si symmetric stretching are assigned in around  $800\text{ cm}^{-1}$ . Broad asymmetric stretching bond of T-O-T as a doublet broad peak is appeared in around  $1053\text{ cm}^{-1}$ . The presence of this band could be good evidence for Mn substitution in the zeolite framework and the presence of Mn-O-Si linkage in the structures. It should be noted that the T-O-T vibration peak is a singlet in the all silica ZSM-5 zeolite (Fig. 3).

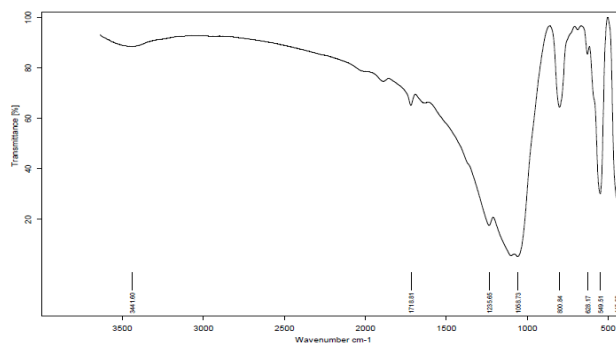


Figure 2. FTIR spectrum of KMS-180 sample.

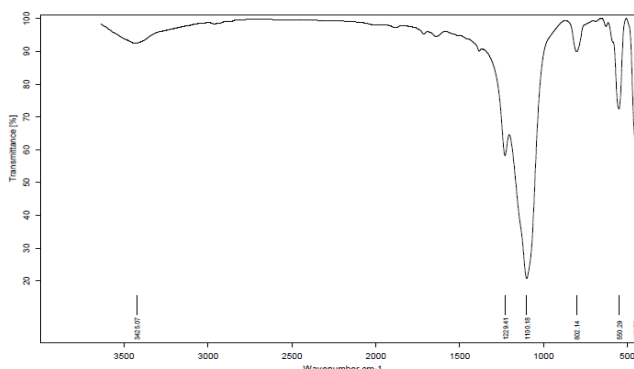


Figure 3. FTIR spectrum of all silica ZSM-5 zeolite.





4<sup>th</sup> Iran National Zeolite Conference  
Golpayegan University of Technology, Golpayegan, Iran  
August 23-24, 2017



The SEM images of the manganosilicate sample show micro-scale zeolite particles with some plate-like structures on them which could be related to extra-framework species.

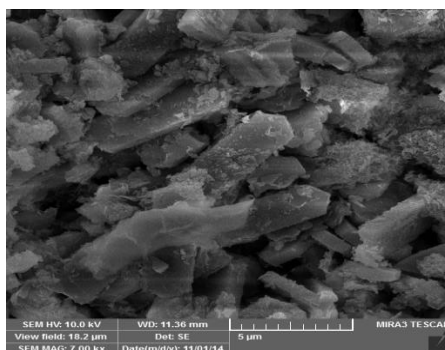


Figure 4. SEM image of KMS-180 sample.

#### 4. Conclusions

We demonstrated the hydrothermal synthesis of aluminum-free MFI-type manganosilicate. The XRD results of calcined manganosilicate sample showed a pure MFI phase. The crystallization of the ZSM-5 type manganosilicate was performed at 180 °C for 48 h while the final pH of the reaction mixture was 9. The evidences such as: i) increasing cell parameters after insertion of Mn into the zeolite lattice, ii) shift of the zeolite pentasil peaks at ~550  $\text{cm}^{-1}$  to lower wavenumbers in the FT-IR spectra of manganosilicate sample confirmed that Mn ions were successfully incorporated into the zeolite framework.

#### Acknowledgments

The authors would like to thank the University of Tabriz and Iran Nanotechnology Initiative Council.

#### References

- 1) C.S. Cundy, P.A. Cox, *Chem. Rev.* **2003**, 103, 663.
- 2) M.E. Davis, R.F. Lobo, *Chem. Mater.* **1992**, 4, 756.
- 3) M. Khatamian, M. Irani, *J IRAN CHEM SOC* **2009**, 6, 187.
- 4) M. Khatamian, M.S. Oskoui, M. Darbandi, *Microporous Mesoporous Mater.* **2013**, 182, 50.
- 5) M. Khatamian, A. Khandar, M. Haghighi, M. Ghadiri, M. Darbandi, *Powder Technol.* **2010**, 203, 503.



# 4<sup>th</sup> Iran National Zeolite Conference

## Golpayegan University of Technology, Golpayegan, Iran

### August 23-24, 2017



## Natural gas dehydration process simulation using zeolite adsorbents

Amirhossein Behroozibakhsh<sup>a\*</sup>, Mohammad Samipoorgiri<sup>b</sup>

<sup>a</sup> Islamic Azad University North Tehran Branch, Tehran, 1969633651 Zip code, Iran

<sup>b</sup> Islamic Azad University North Tehran Branch, Tehran, 1969633651 Zip code, Iran

\*Email: behroozibakhsh@gmail.com

### 1. Introduction

Dehydration operation is one of the most important operations at the gas refinery that can be set through the gas dew point. Absorbent material in terms of business groups, bauxite, alumina, gels, activated carbon and molecular sieves are divided.

Zeolites in this category because of the reasonable prices, good thermal stability, good chemical stability, mechanical stability is acceptable, high specific surface area and acidity levels in the oil and gas industry can be used as absorbent. Zeolite crystals that have good thermal stability, are very active.

The simulation using the Aspen Hysys software performance molecular sieve zeolite Dehydration unit 104 refinery in South Pars Phase 19 was carried out. In order to collect field data simulation process and the influence of various parameters on the performance of zeolites were investigated.

### 2. Theoretical Details

Adsorption isotherm, thermo-physical properties and absorption profile, the data needed to model is an adsorption process. Due to commercial considerations, industrial absorbents adsorption isotherm data are rarely available in published sources and data to specific conditions and limited appeal. Dehydration of molecular sieve adsorbent used in absorbent substrates 4A Zeolite, which is provided from the Swiss company Zeochem. The water vapor adsorption isotherm data on the absorption of the company were taken.

In Aspen Adsim software Langmuir developed model for molecular sieve 4A included in the form you can see in below:

To take advantage of this isotherms, empirical data on this model has been adapted. The isotherm parameters for use in simulation developed as Table is obtained (Table 1).

$$w_i = \frac{q_i}{\rho_s} = 2.0 + \frac{A \exp\left(\frac{B}{T}\right) P_i}{1 + C \exp\left(\frac{D}{T}\right) P_i}$$

**Table 1.** Langmuir developed model parameters to absorb water vapor on zeolite molecular sieve adsorbent 4A

Parameter	Value	Unit
A	7.4220*10 <sup>-6</sup>	Kmol/kg.bar
B	5.0414*10 <sup>3</sup>	K
C	3.0603*10 <sup>-3</sup>	1/bar
D	4.5731*10 <sup>3</sup>	K
W	Loading	Kmol H <sub>2</sub> O/100kg solid
P <sub>i</sub>	Partial pressure	Bar
T	Temperature	K



# 4<sup>th</sup> Iran National Zeolite Conference

## Golpayegan University of Technology, Golpayegan, Iran

### August 23-24, 2017



### 3. Results and discussion

Dehydration process using zeolite adsorbents with the Aspen Hysys software simulation and verification of field data sent using simulated data. Results showed that 8.5% of the errors are. Thermo-physical properties of zeolite adsorbent bed it has been shown (Table 2).

### 4. Conclusions

After verification of the bed in a regenerative cycle and were absorbed in the process and litter moisture absorption was calculated over the bed. The restoration process gas inlet temperature and flow rate were studied. The results showed that by changing the flow rate and temperature of the gas somewhat reduced operating costs. To optimize the process of resuscitation procedure was used response surface. Optimization results showed that gas at a temperature of 170 ° C and flow rate 6500 kg mol per hour can be restored bed at the time was 500 minutes.(Figure 1)

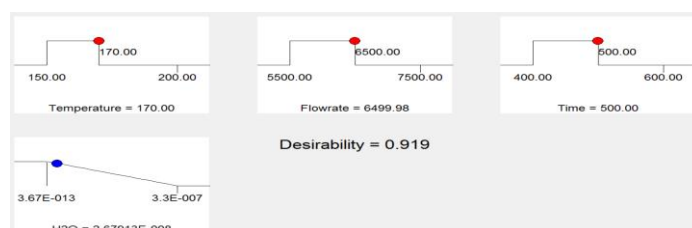


Figure 1 . Optimized parameters

Table 2. Thermo-physical properties of zeolite adsorbent bed

Parameter	Symbol	Unit	Value
Internal diameter of adsorbent layer	$D_b$	M	3.5
Gas phase thermal conductivity	$K_g$	W/m/K	0.042226
Heat of water adsorption	$H_r$	J/kmol	-75600
Adsorbent thermal conductivity	$K_s$	W/m/K	0.128
Inter-particle voidage	$\epsilon$	$m^3 \text{ void}/m^3 \text{ bed}$	0.34
Intra-particle voidage	$p^e$	$m^3 \text{ void}/m^3 \text{ bed}$	0.28
Tortuosity	$\tau_p$	-----	0.36
Height of desiccant	L	M	6.8
Bulk solid density of adsorbent	$\rho_s$	$kg / m^3$	746
Adsorbent particle diameter	$d_p$	Mm	3.175
Specific surface area of adsorbent	$a_p$	$m^2 / m^3$	623



# 4<sup>th</sup> Iran National Zeolite Conference

## Golpayegan University of Technology, Golpayegan, Iran

### August 23-24, 2017



#### Acknowledgments

We acknowledge the science support from Society of Petroleum Engineers International (SPE) and the technical support from Pars Oil and Gas Company (POGC).

#### References

1. Moharir, A.S., kunzru, D., saraf, D.N., effect of adsorption particle size distribution on breakthrough curve for molecular sieve column, chemical engineerin science, 35 (1980) 1795-1801
2. Grandi, S.C., Grande, A., Rodrigues, A.E., separation of methane and nitrogen by adsorption of carbon molecular sieve, chemical engineerin science, 61 (2013) 3893-3906
3. Restrepo, M.L., Mosquera, M.A., Accurate correlation thermochemistry and structural interpretation of equilibrium adsorption isotherm of water vapor in zeolite 3A by means of a generalized statistical thermodynamic adsorption model, Fluid Phase equilibrium, 283 (2014) 73-88
4. Elizondo, T., Molecular sieve dehydration operation, Problems and solutions. British petroleum. Huston, 2015
5. Wu, Zhang, H., Sun, D., Mathematical simulation and experimental study of a modifield zeolite 13X-water adsorption refrigeration module, applied thermal engineering, 29 (2015) 645-651
6. Mayer, M., Adsorption Engineering, Tokyo: Kodansha Ltd, 1990

## In vitro, the comparison of Natural Zeolite and Nano – zeolite to absorb ammonia to rainbow trout (*Oncorhynchus mykiss*)

Mahan Salamroodi <sup>a</sup>, Mohammad Farhangi \* <sup>b</sup>

<sup>a</sup>, *Guilan University, Iran.*

<sup>b</sup> *Departments of Natural Resources and Agriculture, Gonbad Kavous, Gonbad Kavous University, Iran.*

\*Email: s.farhangi@yahoo.com

#### 1. Introduction

One of the best materials for removing of ammonia compounds from water ambient is zeolite Natural resins, such as zeolite, are used in removing ammonia from wastewater culture systems. They are further characterized by ability to loss and gain water reversibly and to exchange some of their constituent elements like Na<sup>+</sup> and K<sup>+</sup> with ammonium ion without major change of structure (Boranic 2001). The adsorption characteristics of any zeolite are dependent upon the detailed chemical-structural makeup of the adsorbent (Ackley, 2003). Recently, application of Nano- zeolite is important. The Nano- zeolite is a kind of Clinoptilolite that prepared after processing on natural Clinoptilolite. In nature, these charges were satisfied by attraction of cat ions from the surroundings (Keith, 1981). However, the cat ions on Nano -zeolite readily exchange with other cat ions. Recently, it has been used in detergents, aquaculture ponds and nuclear treatment, but it also has large potentials for other applications in liquid waste treatment (James et al.



4<sup>th</sup> Iran National Zeolite Conference  
Golpayegan University of Technology, Golpayegan, Iran  
August 23-24, 2017



2000). This research tried to prevent acute toxicity of ammonia compounds on rainbow trout by Nano- zeolite and Natural Zeolite.

This research tried to prevent acute toxicity of ammonia compounds on rainbow trout by Nano- zeolite and Natural Zeolite.

## 2. Materials and methods

The testing carried out in Ramsar Fish Culturing Center, Iran. Experimental fish was in the weight of  $52 \pm 4$  g and total length of  $21 \pm 3$  cm. Temperature, pH and dissolved oxygen in all experiments was stable at  $20 \pm 0.5$  °C, 8.4 and 9 ppm, respectively. Ammonia Concentration was produced by adding ammonium chloride (NH<sub>4</sub>-Cl) to water (Merck Co., Germany). Total ammonia concentrations were measuring with colorimeter DR/890 (Hach, USA). 15 fishes were placed in basin with 35 liters capacity. All tests were conducted to static water method during 24hours. Lethal concentration of total ammonia was based on initial experimental (reported by Farhangi et al., 2002). So, fish mortality was appeared after 24h. A group of fish was as a control. After 24 hours, Total ammonia (N-NH<sub>4</sub>) was determined with a spectrophotometric method. Air-stone has been used in treatment as an aerator. The Clinoptilolite zeolite was used as Nano – zeolite. Initially the amount of substantial ammonia in the water was measured by photometric method and then each aquarium contained 25 mg/lit ammonia salt according to preliminary test. Nano-Zeolite was applied from Gharehyazi Company. For preparation of Nano zeolite, they were located in 10 % sodium chloride solution at a temperature of 90 °C for 30 minutes and then washed with distilled water, and finally were dried at 60 °C for 1 hour (Wang *et al.* 2005). Nano- zeolites at dosages of 1, 3, 5, 7, 8 g/l were used with three replications. Until the end of study, the amount of ammonia in the water was measured by the 4 hours intervals in each step. A group of fish was placed in lethal concentration as a control. Data were analyzed by one-way analysis of variance (ANOVA) followed by Duncan multiple range test. All data are expressed as mean  $\pm$  SD. The significance of results was at 5%.

## 3. Results and discussion

The mortality rates was observed in lethal concentration (25 mg/lit) after 24 hours. High mortality rates were observed in the early hours of exposure. In first treatment as control treatment no mortality was observed. Ammonia measured in each treatment at the end of the preliminary stage that was equivalent to the initial amount. Nano zeolite used in the main test effectively reduced ammonia in the water. Most absorption of ammonia in the first 4 hours after the start of testing was recorded. Eventually, the absorption rate of ammonia by Nano zeolite treatments with increasing Nano zeolite considerably increased. Most value of ammonia absorbed in the fourth treatment with 7 g/lit zeolite. Results indicate significant differences between treatments with each other and also control ( $p < 0.05$ ). With increasing Nano zeolite amount in each treatment, the survival rate of fish also increased significantly ( $p < 0.05$ ). Fish survival rates were 0, 32, 45, 88 and 100 % in the main test treatments, respectively (fig.1). Figure 2 indicates decreasing ionized ammonium after 24 h in the main test treatments.



4<sup>th</sup> Iran National Zeolite Conference  
Golpayegan University of Technology, Golpayegan, Iran  
August 23-24, 2017

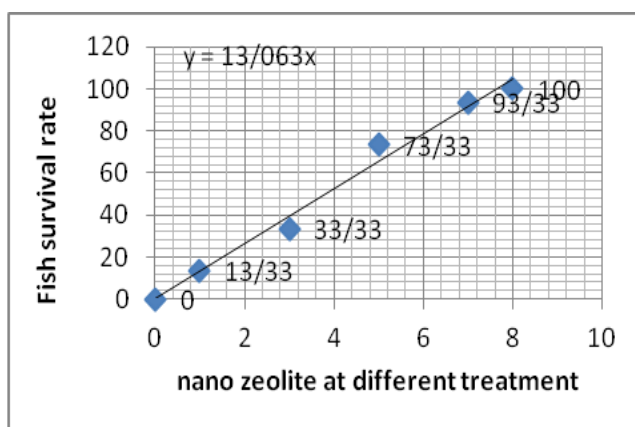


Figure 1. Fish survival rate at different ammonia concentrations

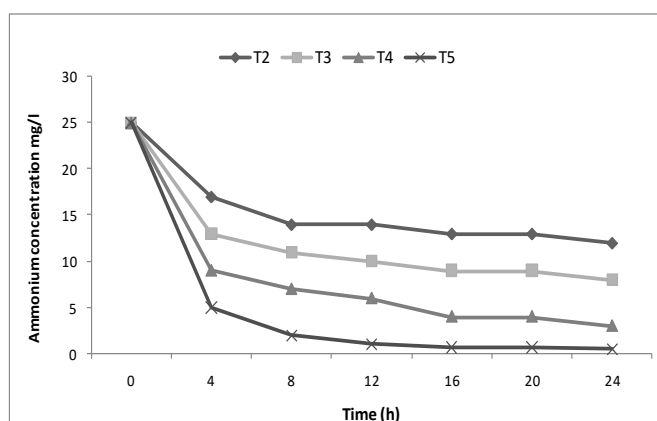


Fig.2-Decreasing the ammonium ( $\text{NH}_4^+$ ) concentration during 24 h

#### 4. Conclusions

In the trial, Nano- zeolite was able to make a considerable reduction of the lethal concentration of ammonia from 25 mg/l to 5.0 mg/l. While about 65 % of total ammonia in first 4 h were removed. Application of Nano-zeolite has directly associated to removal of ammonia compounds. This ability to absorbing ammonia by using the Nano- zeolite after some time depending on the amount of Nano- zeolite for remove ammonia compounds were improved and during decrease ammonia in treatments, the zeolites reached to saturation point and not being able to continue the absorbing of this compounds. Just like in main test (fig. 2). However that was saturated after about 16 h. Absorption speed rate considerably decreased after saturation zeolite. Application of 7g/l Nano- zeolite reduced mortality rate after 24h. So, mortality percentage of fish was 0 after 24h in lethal concentration. Application Nano-zeolite to reduce ammonia toxicity on fish was demonstrated. While, there was application of 15g/l Clinoptilolite zeolite to prevent mortality of rainbow trout by Farhangi *et al*, 2002. This means, Nano- zeolite is more effective. Consequently, using a particular amount of Nano- zeolite for prevention of ammonia compounds could be advisable. Hence, it seems that the zeolite is able to effectively remove the ammonia compounds but this absorption rate is relatively dependent to kind and quantity of Nano zeolite.



# 4<sup>th</sup> Iran National Zeolite Conference

## Golpayegan University of Technology, Golpayegan, Iran

### August 23-24, 2017



#### References

- 1) M.W. Ackley, S.U. Rege and H. Saxena. Application of natural zeolites in the purification and separation of gases. *Micro porous and Meso porous Materials*. **2003**; 61: 25-42.
- 2) M. Boranic. The effect of the zeolite Clinoptilolite on serum chemistry and hematopoietic in mice. *Food and Chemical Toxicology*. **2001**; 39(7):717-727.
- 3) M. Farhangi, A. M. Hajimoradloo and A. Kamali. The efficiency of natural Zeolite to decrease toxicity of ammonia in rainbow trout (*Oncorhynchus mykiss*). *Agriculture Sciences and Natural Resources Journal*. **2002**; 2: 195-203.
- 4) R. James, K. Sampath and P. Selvanami. Effect of Ion-Exchanging Agent, Zeolite on Removal of Copper in Water and Improvement of Growth in *Oreochromis mossambicus*. *Asian Fisheries Science*. **2000**; 13: 317-325.
- 5) F. Keith. The Encyclopedia of mineralogy. Hutchinson Ross publishing company. **1981**; 523-530.
- 6) Y. Wang and P.J. Walsh. High ammonia tolerance in fishes of the family Batrachoididae (Toadfish and Midshipmen). *Aquatic Toxicology*. **2000**; 50: 205-219.

## Increasing of Survival Rate to *Acipenser persicus* by Added Clinoptilolite Zeolite in Acute Toxicity Test of Ammonia

Omid Ehsaniyan <sup>a</sup> , Mohammad Farhangi\*<sup>a</sup> ,

<sup>a</sup> Departments of Natural Resources and Agriculture, Gonbad Kavous, Gonbad Kavous University, Iran.

\*Email: s.farhangi@yahoo.com

### 1. Introduction

Fish production capacity can increase by identifying environmental factors and providing an appropriate environment for the fish (Imanpoor et al, 2011). It has been established that heavy metals have wide spectrum of negative Influence on fish organisms, disrupting endocrine system, and inducing decrease of quantity and quality of offspring (Popek et al, 2009). The two principal methods of removing ammonia in water are: nitrification and ion exchange (Emadi et al, 2001). For nitrification, materials such as oyster shell, rock, sand, activated carbon, etc. are used to prepare a substrate for bacteria. Ion exchange is a process in which ions of an exchange (synthetic or natural resin) are exchanged with certain ions in wastewater. Some natural resins, such as zeolite, are used to removing ammonia (Bergero et al, 1994). One of the best zeolite to remove is Clinoptilolite (Wang and Walsh, 2000). It can be the basis of its use in aquaculture.

### 2. Materials and methods

The experiments were performed in Shahid Marjani Sturgeon Culturing Center, Iran. Temperature in all stages maintained to 26°C and pH were equivalent 8.2. The experiments were done by Water Static Method during 96 hours. Different amounts 0, 5, 15, 25, 35 mg l<sup>-1</sup> of ammonia salt were used. In each basin, 12 fishes with average weight 26±3 g and total length 12±2 cm were placed. Treatments every 12 h were attended from behavior and mortality. Used ammonia was ammonium chloride salt (made by Merck Company; Germany). Total ammonia concentrations were measuring with hack colorimeter DR/890 (made by USA). After determine the lethal concentration of ammonia



# 4<sup>th</sup> Iran National Zeolite Conference

## Golpayegan University of Technology, Golpayegan, Iran

### August 23-24, 2017



(LC96) to *A. persicus*, the main test to measure the efficiency of zeolite was assessed in removal of ammonia lethal concentration. The used zeolite was Clinoptilolite type with 90 % purity. 180 fishes in 12 basins (with 35 liters capacity) were used and in each basin 12 fishes were placed. Granulated zeolite at 3 treatments in 4, 8, 12 g l<sup>-1</sup> with three replications for each treatment and a control treatment was used. Until the end testing, once every 12 hours the amount of ammonia in the water basin was measured. All behavioral activity of fishes was recorded during this process. Air-stone has been used in treatment as an aerator. Samples were taken from gill, kidney and liver of fish and histopathological sections were prepared. The results were compared by ANOVAs (Analysis of Variance).

### 3. Results and discussion

Based on the results in preliminary stage, highest mortality rate in doses of 35 mg l<sup>-1</sup> were observed. Ionized ammonia lethal concentrations were equivalent to 35 mg l<sup>-1</sup> in sturgeon fishes during 96 hours. Mortality percentage of fish was 0, 8.33, 33.33, 75 and 100% respectively in different concentration of ammonia (fig 1). Results revealed mortality percentage of fish increase with increasing of ammonia concentration. The LC<sub>50</sub> (median lethal concentration) was 18.65 mg l<sup>-1</sup> by used of linear regression and relationship between of mortality percentage and ammonia different concentrations (fig 2). Results indicate significant differences between treatments with each other and also control ( $p < 0.05$ ). With increasing zeolite in each treatment, the survival rate of fish also increased significantly ( $p < 0.05$ ). Application of 12g l<sup>-1</sup> granulated zeolite could be prevented the mortality after 96 hours (fig 3). Results The studied of histological samples show that, The common lesions of fish gill, liver and kidney exposed to ammonia lethal concentration were hyperplasia, edema, hyperemia, hemorrhage, expansion of secondary lamella, epithelial cells necrosis of gill and inflammation. In control group and zeolite without ammonia group less hyperplasia in tip of gill filaments and edema observed too (Fig 4, 5).

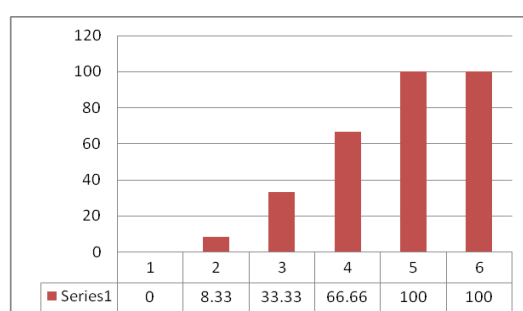


Figure 1. Fish mortality in different dosage of ammonia

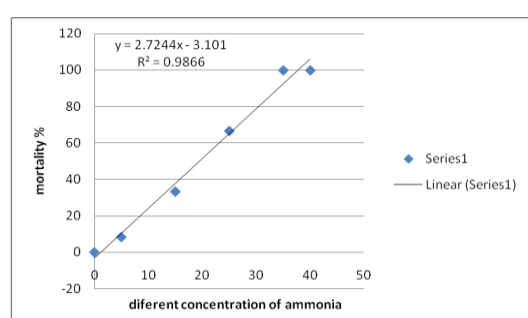


Fig 2. Linear regression of fish mortality to different concentration of ammonia.

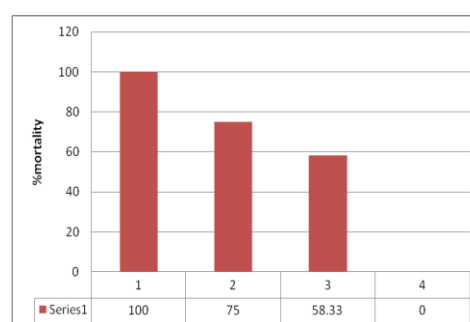
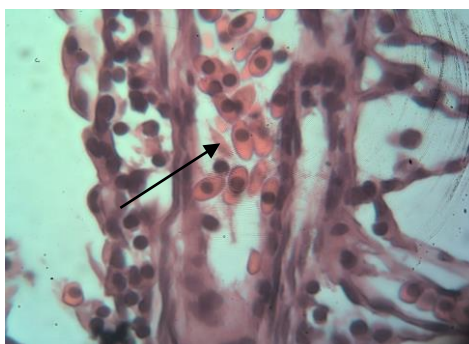


Fig 3. Reduction of mortality rate of the fishes by adding zeolite





4<sup>th</sup> Iran National Zeolite Conference  
Golpayegan University of Technology, Golpayegan, Iran  
August 23-24, 2017



**Fig 4.** Gill histological section that exposure to lethal ammonia toxicity. Arrows show edema and hyperemia (\* 100).

**Fig 5.** Gill histological section that exposure to lethal ammonia toxicity. Arrows show hemorrhage (\* 100).

#### 4. Conclusions

Relevant to using of Zeolite in the main test (Fig. 3), removed faster the ammonia compounds by more adding the zeolites in different treatments. As well, after the specific time zeolites reach to saturation point. Therefore, we should use a particular amount of zeolites due to prevent ammonia compounds. However, Application of 12 g l<sup>-1</sup> of zeolite doesn't seem to be essential on fish ponds, because it is expensive. In second, the present lethal concentration isn't available in fish ponds at all. Therefore I just suggest applying about 2-5 g l<sup>-1</sup> of zeolite to prevent of fish mortality.

#### Acknowledgments

We acknowledge the financial support from our sponsors.

#### References

- 1) Emadi H., Nezhad J.E. Pourbagher H., 2001 *In vitro* Comparison of zeolite (Clinoptilolite) and activated carbon as ammonia absorbents in Fish Culture. Naga, the ICLARM Quarterly, Vol. 24, Nos. 1 & 2, January-June.
- 2) Imanpoor M.R., Ahmadi A.R., Kabir M., 2011 Effects of sub lethal concentration of Chloramines T on growth, survival, haematocrit and some blood biochemical parameters in common carp fry (*Cyprinus carpio*). ACCL Bio flux. 4, 3:280-291.
- 3) Poek W., Kleczar K., Nowak M., Epler P., 2009 Heavy metals concentration in the tissues of perch (*Perca fluviatilis*) and bleak (*Alburnus alburnus*) from Czarna Orawa River, Poland. AACL. 2, 2:205-208.
- 4) Wang Y., Walsh P.J., 2000 High ammonia tolerance in fishes of the family Batrachoididae (Toadfish and Midshipmen). Aquatic Toxicology 50: 205-219



4<sup>th</sup> Iran National Zeolite Conference  
Golpayegan University of Technology, Golpayegan, Iran  
August 23-24, 2017



Pyranoring formation with Alkyl amino pyridine-functionalized NaY zeolite

Zahra Kalateh<sup>a</sup>, Mohammad Ali Bodaghi Fard<sup>a</sup>, Mojgan Zendehei<sup>\*a</sup>

<sup>a</sup> Department of Chemistry, Faculty of Science, Arak University, Arak 38156-8- 8349; Iran

\*Email: [m-zendehei@araku.ac.ir](mailto:m-zendehei@araku.ac.ir)

### 1. Introduction

Homogeneous organic catalyst such as Alkyl amino pyridines have been used as active catalysts for many different organic reactions. The use of these soluble catalysts has variable drawbacks such as purification of the final product (s) from the reaction mixture and further catalyst recyclability which offer considerable complexity to the reaction that may render it industrially unacceptable. Thus, the heterogenous catalyst are a logical step to avoid these problems. The recoverability and reusability offered by heterogeneous systems, to give high yields in short times and sometimes without the need for organic material, lead to green chemistry [1] In the present work, alkyl amino pyridin-functionalized NaY zeolite has been prepared. This catalyst was used in the synthesis of 2-amino-4H-chromene derivatives .

### 2. Experimental

alkyl amino pyridin-functionalized NaY zeolite has been prepared. The structure of the functionalized zeolite was characterized by some techniques such as FT-IR, FE-SEM, XRD, CHN and TGA analysis. The powder separated and washed with ethanol. The elemental analysis of modified compounds shows the molar ratio that confirmed immobilized amine on the porous material structure. This solid basic catalyst was used in the synthesis of 2-amino-4H-chromene derivatives through the multicomponent reactions with aldehydes, malononitrile and  $\beta$ -naphthole under solvent-free condition and the temperature of reaction was 100 °C.

### 3. Results and discussion

The effect of the catalyst on the efficiency of multi component reaction shows in the table 1. High conversion was achieved at moderate temperatures and without solvent. Some of analysis by <sup>1</sup>HNMR shows in the Fig.1a,b.

Table 1. The effect of the catalyst on the efficiency of multi component reaction

Compound	(%)Yield	(°C) M.P	(h) Time
benzaldehyde	85	280	1.40
4-cl-benzaldehyde	95	204	1.30
2-cl-benzaldehyde	94	257.5	1.05
2,4-dichloro benzaldehyde	93	216.5	1.20
4-hydroxy benzaldehyde	90	246	1.15
4-nitro benzaldehyde	94	183.5	1.20
3-nitro benzaldehyde	95	193.5	1.15
4-methoxy-benzaldehyde	88	190	1.30
2-methoxy-benzaldehyde	87	170	1.15
4-methyl-benzaldehyde	92	272.5	1.30
Iso terfetaldehyde	71	199.5	2.30
terfetaldehyde	74	202	2.20

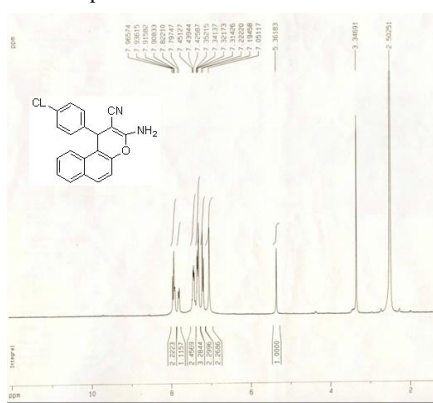


Fig.1 (a) <sup>1</sup>HNMR

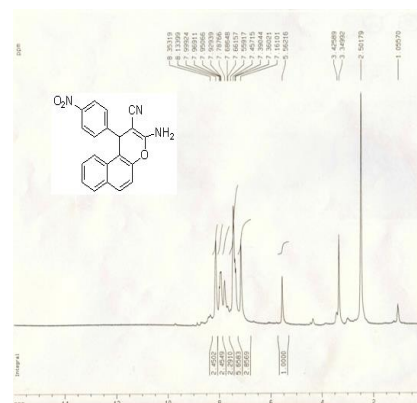


Fig.1 (b) <sup>1</sup>HNMR



4<sup>th</sup> Iran National Zeolite Conference  
Golpayegan University of Technology, Golpayegan, Iran  
August 23-24, 2017



Although, the yield of reactions were good but effort for separation of catalyst of reaction media was difficult. So easy separation of heterogeneous catalyst promoted us to connect homogenous catalyst to the surface and to prepare desirable heterogeneous catalysts. In the following Fig. 2, we can see the proposed mechanism.

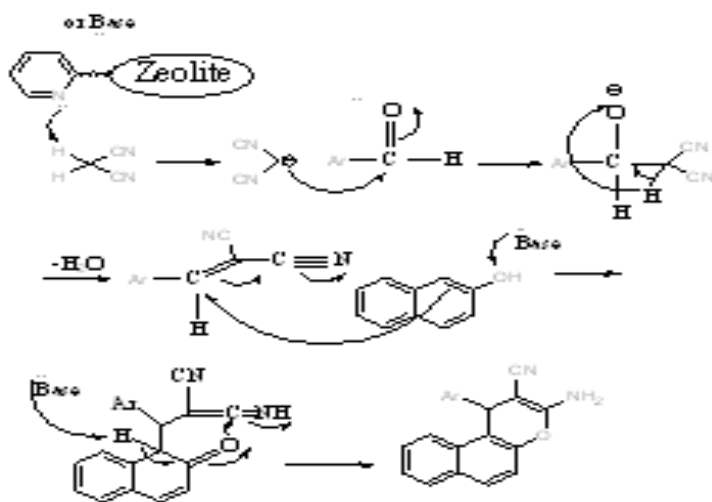


Fig. 2. The proposed mechanism.

#### 4. Conclusions

In summary, the surface of NaY zeolite was modified with various organic functionalities. We showed highly active, selective, and recyclable heterogeneous catalysts in organic transformations and more importantly, the stability of these catalysts was found to be good and easily separated from the liquid phase after reaction.

#### Acknowledgments

Thanks are due to the Iranian Nanotechnology Initiative and the Research Council of Arak University of Technology and Center of Excellence in the Chemistry Department of Arak University of Technology for supporting of this work.

#### References

- [1] E. B. Mubofu, J. H. Clark and D. Macquarrie, *Green Chem.* 3 (2001) 23-25.
- [2] K. Li, J. Valla and J. Garcia-Martinez, *Chem. Cat. Chem.* 6 (2014) 46-66.
- [3] S. Mandal, D. Roy, R. V. Chaudhari, and M. Sastry, *Chem. Mater.* 16 (2004) 3714-3724.
- [4] M. R. Didgikar, D. Roy, S. P. Gupte, S. S. Joshi, and R. V. Chaudhari, *Ind. Eng. Chem. Res.* 2010, 49, 1027-1032.



4<sup>th</sup> Iran National Zeolite Conference  
Golpayegan University of Technology, Golpayegan, Iran  
August 23-24, 2017



**A covalently anchored Pd(II)-Schiff base complex over modified surface of mesoporous silica SBA-16: an efficient and reusable catalyst for Heck-Mizoroki coupling reaction in water**

Mahsa Niakan<sup>a</sup>, Zahra Asadi<sup>\*a</sup>, Majid Masteri-Farahani<sup>b</sup>

<sup>a</sup>Faculty of Sciences, Department of Chemistry, Shiraz University, Shiraz, Shiraz 71454, Islamic Republic of Iran

<sup>b</sup>Faculty of Chemistry, Kharazmi University, Tehran, Islamic Republic of Iran

\*E-mail: zasadi@shirazu.ac.ir

## 1. Introduction

Palladium-mediated Heck-Mizoroki coupling reactions have received considerable attention due to the industrial applications of these reactions in fine chemical fields, such as pharmaceuticals and herbicides. These reactions generally proceed in the presence of a homogeneous palladium catalyst which has two main drawbacks, a tedious work up and recovery process and palladium contamination in products. One way of overcoming these difficulties would be the use of heterogeneous catalyst systems instead of homogeneous counterparts for application in industrial reaction processes.

In this work we wish to report the synthesis of a heterogeneous Pd (II) complex catalyst supported on SBA-16 for application in Heck reaction.

## 2. Experimental

### 2.1. Preparation of the catalyst

Preparation of SBA-16 was performed according to the literature. After calcination and removing of the template, the resulting material was functionalized with amino groups and then reacted with Schiff base ligand. The supported Schiff base ligand was metallated with Pd (II) acetate to produce the final catalyst.

### 2.2. General procedure for Heck reaction

A mixture of alkene (1.2 mmol), iodobenzene (1 mmol), base (2 mmol) and catalyst was added to 3 ml water. The reaction mixture was heated for the required time. The progress of the reaction was monitored by TLC or GC.

## 3. Results and discussion

A new Pd complex supported on SBA-16 was prepared and fully characterized by FT-IR, ICP, TGA, SEM, HR-TEM, XPS, XRD, EDX, BET, UV-VIS and elemental analysis.

The elemental composition of the prepared catalyst was determined by EDX analysis. The results shown in Figure 1 revealed that the Pd catalyst contains Si, Pd, N, C and O. The amount of Pd was estimated to be 1.53 wt%.



4<sup>th</sup> Iran National Zeolite Conference  
Golpayegan University of Technology, Golpayegan, Iran  
August 23-24, 2017

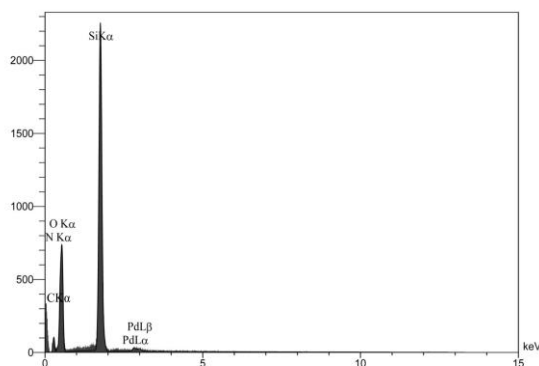


Figure 1. EDS pattern of the catalyst

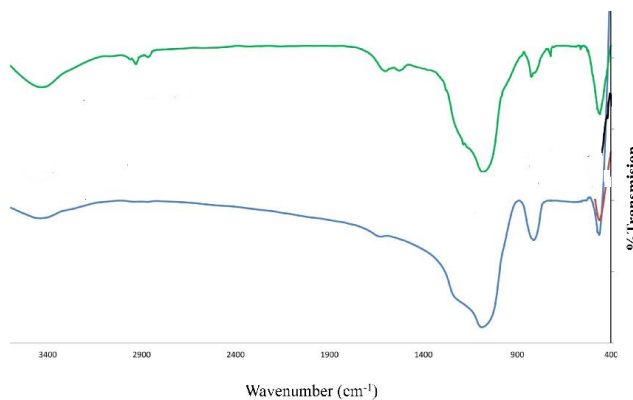


Figure 2. FT-IR spectra of SBA-16 and Pd(II)-SBA-16

The attachment of Pd complex onto the mesoporous support was confirmed by comparison of the FT-IR spectra (Figure 2) of the support before and after loading with Pd complex, both in the mid IR (4000-400  $\text{cm}^{-1}$ ) region. FT-IR spectra of both SBA-16 and Pd(II)-SBA-16 materials revealed bands at around 1086  $\text{cm}^{-1}$  which is due to Si-O-Si linkages of the silica network. The FT-IR spectrum of Pd(II)-SBA-16 showed additional peaks at 563 and 735  $\text{cm}^{-1}$  which can be attributed to the  $\nu(\text{Pd-N})$  and  $\nu(\text{Pd-O})$  vibrations respectively, and confirmed the immobilization of Pd complex on the surface of SBA-16.

To evaluate the activity of the catalyst, the Heck-Mizoroki coupling reaction of alkenes with organic halides was studied. The results are given in Table 1. As can be seen in Table 1, The catalyst exhibited excellent activity in the Heck reaction in water as a green solvent.

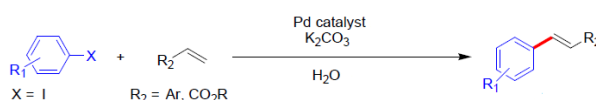


Table 1. Heck reaction of different aryl halides with alkenes.

R <sub>1</sub>	R <sub>2</sub>	Time (h)	Conversion%
OMe	Ar	4	90
CH <sub>3</sub>	Ar	4	98
NO <sub>2</sub>	Ar	3	85

Reaction conditions: aryl halide (1 mmol), alkene (1.2 mmol), K<sub>2</sub>CO<sub>3</sub> (2.0 mmol) in H<sub>2</sub>O (3 ml), 80 °C.

It was found that Pd(II)-SBA-16 heterogeneous catalyst showed no significant loss of activity in recycling experiments. The active sites did not leach out from the support and thus can be reused without appreciable loss of activity, indicating effective anchoring. The reusability of this catalyst was high without significant decrease in its initial activity.

#### 4. Conclusions

In summary, we have synthesized a novel palladium immobilized recyclable catalyst bearing Schiff base ligand anchored on SBA-16. The resulting Pd(II)-SBA-16 catalyst showed good catalytic activity in Heck reaction in water



# 4<sup>th</sup> Iran National Zeolite Conference

## Golpayegan University of Technology, Golpayegan, Iran

### August 23-24, 2017



as green solvent. Moreover, the catalyst can be reused many times with complete conversion and negligible palladium leaching.

#### Acknowledgments

We acknowledge the financial support from Shiraz University.

#### References

- 1) Fahimeh Dehghani Firuzabadi, Zahra Asadi, Farhad Panahi, *RSC Advances* **2016**, 6, 101061.
- 2) Zeinab Mandegani, Mozaffar Asadi, Zahra Asadi, *Green Chemistry* **2015**, 17, 3326.

## Effect of Ca and K promoters on the catalytic activity of Co/zeolite Y for removing of NO<sub>2</sub> as a pollutant gas

Aliakbar Tarlani\*, Sabri Aliarnejad, Mahsa Eskandarzade

*Inorganic Nanostructures and Catalysts Research Lab, Chemistry & Chemical Engineering Research Center of Iran, Pajoohesh Blvd., km 17, Karaj Hwy, Tehran 14968-13151, Iran*

\*Email: [Tarlani@ccerci.ac.ir](mailto:Tarlani@ccerci.ac.ir)

### 1. Introduction

Zeolites have been used mainly as adsorbent, catalyst and support in the last decades. The mentioned applications are because of the unique properties of the zeolites such as high surface area, pore volume and ordered channels in these materials. Primary building units of TO<sub>4</sub> (T = Al or Si) lead to secondary building units which form the zeolite. By increasing the ratio of Al/Si, thermal stability of the zeolite increases. Among these zeolites, the Y type has wide applications in industry as adsorbent, molecular sieve, ion exchanger and catalyst. Y zeolite is made from double six rings and super cages. This low density Y zeolite is active and stable in order to use in petrochemical industry [38]. Y zeolite which has been ion exchanged by Co<sup>+2</sup> was utilized in desulfurization process [51]. The same catalyst was used for the conversion of ethane to acetonitrile [53]. Modification of the Y zeolite with a wide range of the cations will improve and promote its activity in many important processes.

NO<sub>x</sub> is referred to NO and NO<sub>2</sub> which is produced at high temperature. NO<sub>x</sub> is the main pollutant of the air and is very dangerous for the environment. Many attempts devoted for removing NO<sub>x</sub> such as selective non-catalytic reduction (SNCR) and selective catalytic reduction (SCR).

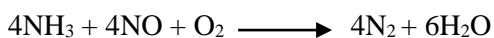
NO is thermodynamically stable because it has high activation energy (364 KJ/mol). Therefore it is better to use a catalyst for its degradation. NO<sub>x</sub> is produced from the vehicles and petrochemical units. Zeolites, metal oxides and perovskites are the main catalytic supports for removing the NO<sub>x</sub>. One of the most effective methods for removing the NO<sub>x</sub> is using NH<sub>3</sub> (SCR-NH<sub>3</sub>/NO<sub>x</sub>). Because this system shows high yield of (96-99%) NO<sub>x</sub> removing.



# 4<sup>th</sup> Iran National Zeolite Conference

## Golpayegan University of Technology, Golpayegan, Iran

### August 23-24, 2017



V/TiO<sub>2</sub>, Pt and zeolites are common catalysts for this process. In this study, Co/Y zeolite promoted by potassium and calcium to be used for NH<sub>3</sub>-SCR process.

## 2. Experimental

### Preparations of the catalyst

5 g Y zeolite was added to the 0.5 M solution of KNO<sub>3</sub>, Ca(NO<sub>3</sub>) and Co(NO<sub>3</sub>) and stirred for 4h at 60 °C. After filtration and rinsing, it was dried at 100 °C. Then it was calcinations at 550 °C for 1h (Table 1). The final catalysts are named K/Co/zeolite Y (N1) and K/Ca/Co/zeolite Y (N2).

### Catatest

A catatest system with a gas inlet and a fixed bed reactor which was equipped with three thermocouples and temperature control was used.

## 3. Results and discussion

FT-IR of the zeolite Y is depicted in Figure 1.

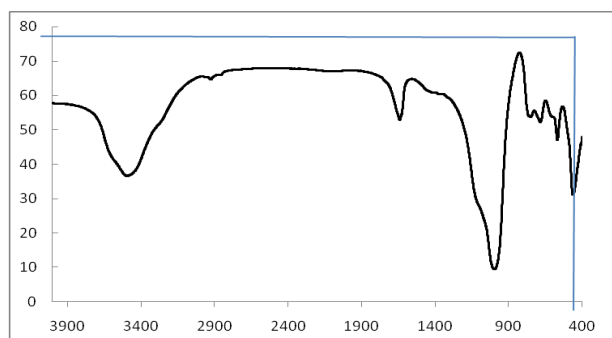


Figure 1. FT-IR of the zeolite Y

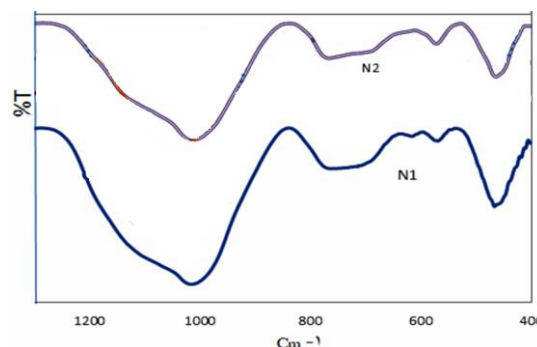


Figure 1. FT-IR of the N1 and N2

The main peaks at 460, 565, 682, 754, 1010 and 1080 cm<sup>-1</sup> are representative of the zeolite Y.

By doping the cobalt, potassium and calcium ions, the Figure 2 obtained. As can be seen, modification of the zeolite did not change the framework of the Y zeolite.

The process of NO<sub>x</sub> reduction carried out by the following composition.

Table 1. reactor conditions

	Gas type	Gas inlet mL/min	Purity
1	NH <sub>3</sub>	53	100
2	NO <sub>2</sub>	19.5	100
3	N <sub>2</sub>	500	100
4	O <sub>2</sub>	27.5	50
5	H <sub>2</sub> O	0.015	--

T: 360 °C



4<sup>th</sup> Iran National Zeolite Conference  
Golpayegan University of Technology, Golpayegan, Iran  
August 23-24, 2017



By heating the reactor to 360 °C, the N1 and N2 could catalyze the reaction. After 1 h, the ppm of the NO<sub>x</sub> was measured for the two catalysts (Table 1). As can be seen, the amount of the NO<sub>x</sub> decreases during the first 45 min of the reaction. But N1 is more active catalyst than N2. In continuous, the both catalysts were slowly deactivate and resulted in increase of the ppm of the NO<sub>2</sub> in the reactor.

In the comparison between the two types of catalysts, N1 and N2, it is clear that K/Co/zeolite Y is more active than K/Ca/Co/zeolite Y. The low activity of K/Ca/Co/zeolite Y is due to occupation of the position 2 in the zeolite Y (Table 2 & Figure 2).

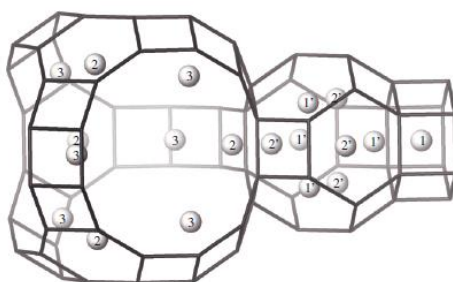


Figure 2. Zeolite Y

As the cobalt is the active catalytic site of the catalyst, both promoters of potassium and calcium ions can facilitate the electron transfer to cobalt. But, potassium ion with larger ionic radius is more active than calcium ion. This reason directly affects and enhances the catalytic activity of N1.

Table 2. Catalyst result

Promoter/Co/Zeolite	10 min	30 min	45 min	60 min
Y				
N1	1025*	591	328	745
N2	660	550	548	592

$$*ppm(NO_2) = (10/69 - VHCL)$$

#### 4. Conclusions

Co/zeolite is an active catalyst for the selective catalytic reduction of NO<sub>2</sub>. Promoter of potassium can activate the catalyst much more than calcium ion.

#### Acknowledgments

We thank Chemistry & Chemical Engineering Research Center of Iran (CCERCI) for the support of these studies.

#### References (Time new roman, 9 pts)

- 1) A.K.S. Clemens et al., *ACS Catal.*, **2015**, 5, 6209–6218
- 2) C. A. Ríos R, J. A. Henao, M. A. Macías, *Catal. Today* 2012, 109, 61-61
- 3) H.G. Karge, H. K. Beyer, Solid-state ion exchange in microporous and mesoporous materials. *Molecular Sieves* **2002**, vol 3, 43-201.
- 4) Y. Li, J. Armor, *Appl. Catal. A: Gen.*, **1999**, 188, 211-217.





4<sup>th</sup> Iran National Zeolite Conference  
Golpayegan University of Technology, Golpayegan, Iran  
August 23-24, 2017



## Sulfonic acid functionalized mesoporous SiO<sub>2</sub> for solvent-free synthesis imidazoles

Sadegh Rostamnia \*

Organic and Nano Group (ONG), Department of Chemistry, Faculty of Science, University of Maragheh, P.O.B 55181-83111, Maragheh, Iran

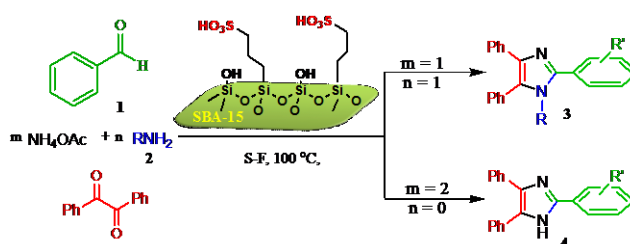
\*Email: srostamnia@gmail.com; rosamnia@maragheh.ac.ir

### 1. Introduction

Multicomponent reactions (MCRs), as a general way to improve synthetic efficiency, by virtue of their convergence, productivity, facile execution, and generally high yields of products, have attracted much attention from the point of combinatorial chemistry [1].

The imidazole, being a core molecule in many biological systems [2] and an active component in several drug molecules has attracted attention in recent years. Different substituted imidazoles show variable biological activities. Despite the availability of wide variety of synthetic routes towards imidazoles, only few studies exist for the synthesis of 1,2,4,5-tetrasubstituted imidazoles, which are most widely performed via multi-step routes or via trisubstituted 1H-imidazole in which the nitrogen is substituted in the final step [3]. A powerful strategy for the rapid introduction of molecular diversity in the construction of 1,2,4,5-tetrasubstituted imidazoles involves multicomponent reactions (MCRs). Supported solid catalysts have received a great deal of attention in recent years and indeed have been proved versatile in several commercial scale processes [4]. Mesoporous silica materials, including MCM-41 and SBA-15, have been some of the most common supports which emerged as high surface, tunable, and stable alternative materials [5]. In other hand, in recent years, the multicomponent reaction over high surface area porous metal oxide material has been studied. In these studies, the researchers have tried to find the optimized conditions for this reaction to increase the selectivity and yield of reaction. The sulfonic acid functionalized mesoporous materials were reported to be efficient catalysts for acid catalyzed reactions [6].

Hybrid mesoporous SBA-15-Pr-SO<sub>3</sub>H with organic propyl groups in the pores of the SiO<sub>2</sub> mesostructure would make the materials hydrothermal stable and hydrophobic and thus provide the materials with improved catalytic properties during applications for organic small molecules [7]. For these reasons and in our continuing interest in the development of environmental friendly protocols and one-pot multi-component reactions, we report herein our results for the synthesis of tri- and tetra-substituted imidazoles using easy producible and affordable SBA-15-Pr-SO<sub>3</sub>H as a suitable, efficient and green catalyst for the multicomponent condensation of an benzil and amines with aldehyde, without any solvent, salts and additives with excellent yields (Scheme 1).



Scheme 1. SBA-15/SO<sub>3</sub>H-catalyzed one-step synthesis of substituted imidazoles via MCRs.



4<sup>th</sup> Iran National Zeolite Conference  
Golpayegan University of Technology, Golpayegan, Iran  
August 23-24, 2017



## 2. Experimental

### Chemicals and apparatus

All reagents were obtained from Merck (Germany) and Fluka (Switzerland) and were used without further purification. Melting points were measured on an Electrothermal 9100 apparatus. Progress of reactions was monitored by Thin Layer Chromatography (TLC). <sup>1</sup>H and <sup>13</sup>C NMR spectra were measured (CDCl<sub>3</sub>) with a Bruker DRX-300 AVANCE spectrometer at 300 and 75 MHz, respectively.

### General procedures

**Synthesis of SBA-15/SO<sub>3</sub>H:** The synthesis of SBA-15-PrSO<sub>3</sub>H has been achieved using three main steps: first step for preparation of the SBA-15 which known procedure described by Zhao *at. al.* Second step is functionalization of the SBA-15 to the SBA-15-Pr-SH. Finally, oxidation of the SBA-15-Pr-SH to SBA-15-Pr-SO<sub>3</sub>H was done by hydrogen peroxide (Figure 1)

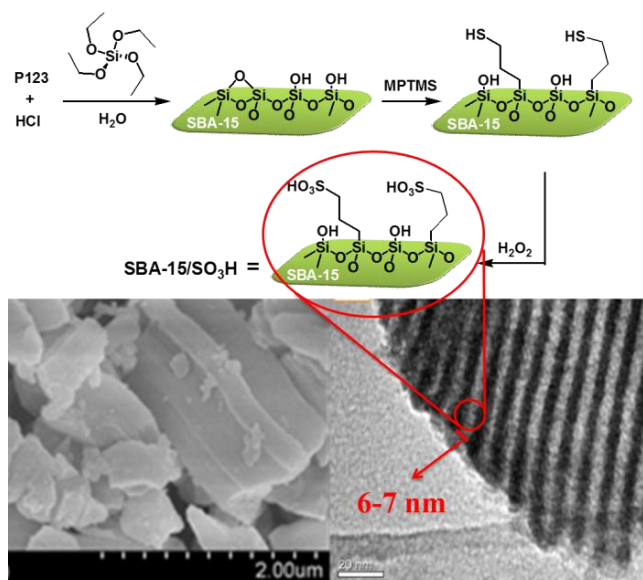


Fig 1. SEM (a) and TEM (b) images of SBA-15/SO<sub>3</sub>H nanoreactor.

**Synthesis of imidazoles 3 and 4:** To a mixture of benzil (1 mmol), aldehyde (1 mmol), amine (1 mmol), and ammonium acetate (1.2 mmol) was added SBA/SO<sub>3</sub>H (2 mol%) and heated (schlenk flask) at 100 °C in solvent free condition. When the reaction was complete as judged by TLC, ethanol (8 mL) was added and the reaction mixture was filtered and the remaining solid was washed with warm ethanol (3 × 5 mL) in order to separate the SBA/SO<sub>3</sub>H solid catalyst. The products were recrystallized from ethanol. For synthesis of the tri-substituted imidazoles, reagents were only (1 mmol), aldehyde (1 mmol) and ammonium acetate (2.2 mmol) in same condition. All the products were previously reported by other method and were characterized by comparing physical and spectroscopic data with those. Spectroscopic data for selected examples are shown below.

**1,2,4,5-tetraphenyl-1H-imidazole (3a):** IR (KBr  $\nu_{\text{max}}$ /cm<sup>-1</sup>): 1443, 1479, 1496, 1601. <sup>1</sup>H NMR (300.1 MHz, CDCl<sub>3</sub>):  $\delta$  = 7.05 (2 H, d, *J* 7.8 Hz), 7.15 (2 H, d, *J* 6.9 Hz), 7.18-7.27 (12 CH, m), 7.44 (2 H, t, *J* 7.5 Hz), 7.62 (2 H, t, *J* 7.5 Hz). <sup>13</sup>C NMR (75.4 MHz, CDCl<sub>3</sub>):  $\delta$  = 126.60, 127.41, 127.95, 128.09, 128.16, 128.24, 128.34, 128.43, 128.96, 129.06, 130.52, 130.65, 130.85, 131.12, 134.43, 137.11, 138.27, 146.93.



4<sup>th</sup> Iran National Zeolite Conference  
Golpayegan University of Technology, Golpayegan, Iran  
August 23-24, 2017



**2,4,5-triphenyl-1H-imidazole (4a):** IR (KBr  $\nu_{\text{max}}/\text{cm}^{-1}$ ): 1441, 1461, 1488, 1587, 1601, 3037  $^1\text{H}$  NMR (300.1 MHz,  $\text{CDCl}_3$ ):  $\delta$  = 7.19-7.46 (9 CH, m), 7.55(4 H, t,  $J$  6.6 Hz), 7.90 (2 H, d,  $J$  8.1 Hz).  $^{13}\text{C}$  NMR (75.4 MHz,  $\text{CDCl}_3$ ):  $\delta$  = 125.31, 127.50, 127.83, 128.60, 128.90, 129.02, 129.91.

### 3. Results and discussion

Herein the condensation of benzil, ammonium acetate and Benzyl amine using benzaldehyde was selected to be the model (Table 1). Initial studies of the influence of reaction conditions were carried out of the model reaction.

Due to the fact that the solvent may play an important role in this process, different types of solvents were screened for this reaction. The model reaction was first examined in ethanol, ethanol/ $\text{H}_2\text{O}$  and water medium by 2 mol% of SBA/ $\text{SO}_3\text{H}$ . When

the reaction was run in solvent-free condition, condensation had 88 % yields in 100 °C during 2 hour (Table 1).

**Table 1** Study of conditions by model reaction. <sup>a</sup>

Solvent	Temp (°C)	Time (h)	% Yield <sup>b</sup>
EtOH	r.t	24	15<
EtOH/ $\text{H}_2\text{O}$	70	24	77
$\text{H}_2\text{O}$	95	14	50
Solvent-free	80	3	65
Solvent-free	100	3	87
Solvent-free	120	2	89
Solvent-free	100	2	86 <sup>c</sup>
Solvent-free	100	2	88 <sup>d</sup>

<sup>a</sup> Benzil (1 mmol), PhCHO (1 mmol), PhCH<sub>2</sub>NH<sub>2</sub> (1.1 mmol), NH<sub>4</sub>OAc (1.1 mmol), SBA/ $\text{SO}_3\text{H}$  (2 mol%), solvent (3mL). <sup>b</sup> Isolated yield. <sup>c, d</sup> SBA/ $\text{SO}_3\text{H}$  (3 and 5 mol%)

These results encouraged us to investigate the scope and the generality of this new SBA/ $\text{SO}_3\text{H}$ -based protocol for various aldehydes and amines under optimized conditions. The results summarized in Table 2.

With these results in hand we decided to explore the scope of this method. The above reaction condition was further explored for the synthesis of 2,4,5-trisubstituted imidazoles by the condensation of aldehyde, with ammonium acetate under similar conditions at 100 °C in high yields. The obtained results are summarized in Table 3.

### Conclusions

In summary, we have described an efficient protocol for multicomponent synthesis of tetra- and tri-substituted imidazoles catalyzed by easy preparable SBA/ $\text{SO}_3\text{H}$  under solvent-free condition. The use of high surface area solid catalyst combining solvent-free condition in the multicomponent condensation brings up the merits like high yields of the products, short reaction times, low pollution and simple experimental procedure. In optimized condition, the recycling performance of SBA/ $\text{SO}_3\text{H}$  in the model reaction was investigated that showed the catalyst could be reused at least six times without significant decrease in catalytic activity.



4<sup>th</sup> Iran National Zeolite Conference  
Golpayegan University of Technology, Golpayegan, Iran  
August 23-24, 2017



Table 2 Synthesis of 1,2,4,5-tetrasubstituted imidazoles in the presence of SBA/SO<sub>3</sub>H.<sup>a</sup>

Entry	3a-j	ArCHO (1)	Imidazole (3)	Yield (%) <sup>b</sup>
1	3a			94
2	3b			92
3	3c			95
4	3d			90
5	3e			93
6	3f			85
7	3g			92
8	3h			94
9	3i			94
10	3j			96

<sup>a</sup> Benzil (1 mmol), aldehyde (1 mmol), amine (1.1 mmol), NH<sub>4</sub>OAc (1.1 mmol), SBA/SO<sub>3</sub>H (2 mol%), 100 °C. <sup>b</sup> Isolated yield <sup>c</sup> Literature data of known compounds.



4<sup>th</sup> Iran National Zeolite Conference  
Golpayegan University of Technology, Golpayegan, Iran  
August 23-24, 2017



Table 3. Synthesis of 2,4,5-tetrasubstituted imidazoles in the presence of SBA/SO<sub>3</sub>H.<sup>a</sup>

Entry	4a-f	ArCHO (1)	Imidazole (4)	Yield (%) <sup>b</sup>
1	4a			95
2	4b			92
3	4c			94
4	4d			92
5	4e			94
6	4f			95

<sup>a</sup> Benzil (1 mmol), aldehyde (1 mmol), NH<sub>4</sub>OAc (2.2 mmol), SBA/SO<sub>3</sub>H (2 mol%), 100 °C. <sup>b</sup> Isolated yield. <sup>c</sup> Literature data of known compounds

## References

- 1) A. Dömling. *Chem. Rev.*, **2006**, 106, 17.
- 2) S. A. Laufer, W. Zimmermann and K. J. Ruff, *J. Med. Chem.*, **2004**, 47, 6311.
- 3) C. Leister, Y. Wang, Z. Zhao and C. W. Lindsley, *Org. Lett.* **2004**, 6, 1453.
- 4) A. Corma and H. Garcia, *Adv. Synth. Catal.*, **2006**, 348: 1391.



# 4<sup>th</sup> Iran National Zeolite Conference

## Golpayegan University of Technology, Golpayegan, Iran

### August 23-24, 2017



### Survey zeolite occurrences in Iran

Mehdi Hashemi \*

Department of Geology, Payame Noor University, PO Box 19395-3697, Tehran, Iran

\*Email : Economic.geology@yahoo.com

#### Abstract:

Most zeolites in Iran are volcanic type, like rest of the world and their host rocks mainly are andesite and tuff. There are sedimentary zeolite deposits in areas of Sartakht Mountain in Semnan. Type of zeolites in Iran primarily are clinoptilolite and secondly are the type of natrolite, mesolite and analcime. Most zeolite deposits of Iran primarily are of Eocene age and secondly are Oligomiocene age and are of hydrothermal origin. Iran has a very high potential in the field of zeolite deposits and zeolite deposits are widespread in the country. The major occurrences of zeolite in Iran are located in the edge of Semnan, Varamin, Mianeh and Kerman and province of Semnan is the most fertile area of the country in zeolite. Zeolite occurrences mainly are observed in areas of Sartakht mountain in Semnan, Semnan After, Varamin Tallhe, Mianeh (Eshlaq Chay and Ney Bagh), Goud Biyabany in Kerman Bardsir, Shahr Babak, Ghale Asgar in Baft, Moghuyeh in Kerman Sarcheshme, Kerman Rayen, Kerman Kalejak, Firuzkuh Afgar, Rudehen, the village of Maryam (Shahin Dej), Kurd Qeshlaq in Zanjan, Qazvin Avaj, Taleqan Shahrak, Dian Robai in Damghan, Arab Abad in Tabas Deyhuk, Natanz Hasanabad, Zahedan Harmak, , Qom Aliabad, Kahrizak, Gardaneh Nal Shekan in Tehran, Chalus and south Damavand. Si/Al average ratio of the zeolites from the Semnan, Varamin, Mianeh, Kerman, Firuzkuh and Rudehen is 0.60. Average values of Na and Ca in mentioned zeolites are 11.13 and 1.93, respectively, therefore zeolites was formed by lake saline fluids.

**Keywords:** Zeolite, Clinoptilolite, Volcanic, Andesite, Tuff, Eocene Oligomiocene, Hydrothermal

Table 1. Representative electron microprobe analyses of zeolites from the Semnan(T3), Varamin(T11), Mianeh (T14), Kerman (T19), Firuzkuh (T23),Rudehen (T29).

Mineral	Natrolite	Natrolite	Thomsonite	Thomsonite	Analcime	Analcime
Sample Number	T3	T11	T14	T19	T23	T29
SiO <sub>2</sub> (wt%)	45.23	47.64	36.66	37.90	58.29	55.55
Al <sub>2</sub> O <sub>3</sub>	27.20	26.15	29.18	28.90	20.11	22.29
Fe <sub>2</sub> O <sub>3</sub>	0.00	0.00	0.21	0.00	0.24	0.19
MgO	0.00	0.00	0.00	0.00	0.00	0.00
Na <sub>2</sub> O	14.59	15.30	3.92	3.96	11.91	13.40
K <sub>2</sub> O	0.11	0.14	0.10	0.19	0.26	0.13
CaO	1.46	0.28	8.74	8.70	0.31	0.13
MnO	0.07	0.00	0.22	0.00	0.00	0.22
BaO	0.25	0.23	0.50	0.12	0.38	0.21
SrO	0.00	0.00	9.12	7.85	0.00	0.00
Total	88.91	89.74	88.65	87.62	91.50	92.12
Si (apfu)	23.42	24.30	20.36	20.94	34.00	32.48
Al	16.60	15.72	19.10	18.82	13.82	15.36



4<sup>th</sup> Iran National Zeolite Conference  
Golpayegan University of Technology, Golpayegan, Iran  
August 23-24, 2017



Fe	0.00	0.00	0.09	0.00	0.11	0.08
Mg	0.00	0.00	0.00	0.00	0.00	0.00
Na	14.65	15.13	4.22	4.24	13.47	15.19
K	0.07	0.09	0.07	0.13	0.19	0.10
Ca	0.81	0.15	5.20	5.15	0.19	0.08
Mn	0.03	0.00	0.10	0.00	0.00	0.11
Ba	0.05	0.05	0.11	0.03	0.09	0.05
Sr	0.00	0.00	2.94	2.52	0.00	0.00
Si /Al	0.59	0.61	0.52	0.53	0.71	0.68

## Synthesis, Characterization and wound healing evaluation of zeolite -based drug delivery nanocomposite for curcumin

Sara Javanmardi<sup>\*a</sup>, B.Divband<sup>b</sup>, M.Karami<sup>c</sup>

<sup>a</sup>Department of Clinical Sciences, Faculty of Veterinary Medicine, University of Tabriz C.P.51666, Tabriz, Iran

<sup>b</sup>Inorganic Chemistry Department, Faculty of Chemistry, University of Tabriz, C.P. 51664, Tabriz, Iran

<sup>c</sup>Under graduate student of Veterinary Medicine, University of Tabriz, C.P.51666, Tabriz, Iran

\*Email: Sarahjavanmardi@yahoo.com

### 1. Introduction

Carrier technology offers an intelligent approach for drug delivery by coupling the drug to a carrier particle such as microspheres, nanoparticles, liposomes, etc, which modulates the release and absorption characteristics of the drug. [2,3] Conventional drug administration does not usually provide rate- controlled release or target specificity. Drug Delivery Strategies for Poorly Water-Soluble Drugs provides a comprehensive overview of currently used formulation strategies for hydrophobic drugs, including liposome formulation, cyclodextrin drug carriers, solid lipid nanoparticles, polymeric drug encapsulation delivery systems, self-microemulsifying drug delivery systems, nanocrystals, microemulsions, solid dispersions, cosolvent use, polymer- drug conjugates, polymeric micelles, and mesoporous silica nanoparticles.[1,2]

### 2. Experimental

The composite was characterized by fourier transform infrared spectroscopy (FT-IR), scanning electron microscopy (SEM) and X-ray diffraction (XRD) techniques.

The composite was characterized by Fourier Transmission Infrared Spectroscopy (FTIR), Scanning Electron Microscopy (SEM), Xray Diffraction (XRD) analysis. In vitro cytocompatibility tests were performed using L929



# 4<sup>th</sup> Iran National Zeolite Conference

## Golpayegan University of Technology, Golpayegan, Iran

### August 23-24, 2017



murine fibroblasts using Mossman's tetrazolium toxicity (MTT) assay Curcumin-loaded zeolite was evaluated for drug release, antimicrobial activities and susceptibility tests in vitro. In vivo wound healing analysis was carried out using an excisional wound model on Sprague Dawley rat.

### 3. Results and discussion

In this study, we synthesized and characterized curcumin /zeolite composite (SEM image in figure 1a) which inhibited in vitro growth of *Staphylococcus aureus* and *Pseudomonas aeruginosa*, and enhanced wound healing in an in vivo rat wound model. Curcumin is a naturally derived substance with innate antimicrobial and wound healing properties. Curcumin's poor aqueous solubility and rapid degradation profile hinder usage; in this study, zeolite encapsulation overcame this pitfall and enables extended topical delivery of curcumin (loading efficiency in figure 1b). In XRD pattern Zeolite/GO, all of zeolite peaks were clearly observed and it was highly crystallized and the peak at  $2\theta=11.33$  is related to GO (figure1).

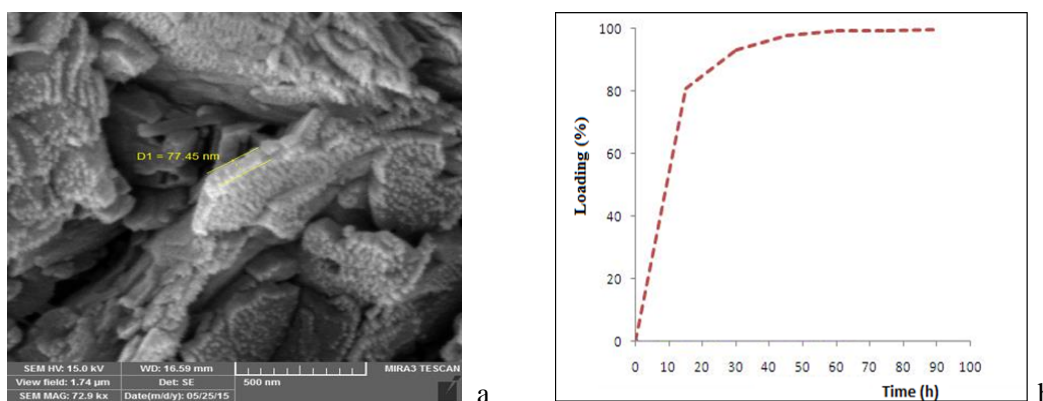


Figure 1: a) SEM image of Curcumin /zeolite composite; b) loading efficiency of the composite

### 4. Conclusions

Herein we successfully synthesized Curcumin /zeolite composite and SEM image confirmed it. This nanocomposite showed a high drug loading capacity. Curcumin /zeolite composite may represent a novel topical antimicrobial and wound healing adjuvant for infected wounds and other cutaneous injuries.

### References

- 1- Matthew McKenzie, David Betts, Amy Suh, Kathryn Bui, London Doyoung Kim and Hyunah Cho. *Molecules* 2015, 20, 20397–20408; doi:10.3390
- 2- Palmira Tավարոա, Silvia Catalanob, Guglielmo Martinoc, Adalgisa Tավարոա. *Applied Surface Science* 380 (2016) 135–140
- 3- Dania Akbik, Maliheh Ghadiri, Wojciech Chrzanowski, Ramin Rohanzadeh. *Life Sciences* 116 (2014) 1–71) K. S. Novoselov, A. K. Geim, S. V. Morozov, D. Jiang, Y. Zhang, S. V. Dubonos, I. V. Grigorieva and A. A. Firsov, *Science*, 2004, 306, 666





4<sup>th</sup> Iran National Zeolite Conference  
Golpayegan University of Technology, Golpayegan, Iran  
August 23-24, 2017



**Amino Functionalize Zeolite: as an efficient catalyst in synthesis of  
5-Substituted 1H-tetrazoles**

Soheila Khaghaninejad\*<sup>a</sup>, Mojgan Zendehtdel<sup>a</sup>

<sup>a</sup>Department of Chemistry, Faculty of Science, Arak University, Arak 38156-8- 8349; Iran

\*Email: [s-khaghani@araku.ac.ir](mailto:s-khaghani@araku.ac.ir)

### 1. Introduction

The recoverability and reusability offered by heterogeneous systems, to give high yields in short times and sometimes without the need for organic material, lead to green chemistry. Zeolites are crystalline aluminosilicates whose internal voids are formed by cavities and channels of strictly regular dimensions and of different sizes and shapes. Also, design of the solventless systems as the relatively green source, has stirred up interest among organic chemists in recent years.

We selected NaY zeolite for immobilization of sulfamic acid. In contrast, the presence of sodium ions in the crystalline matrix of Zeolite Y, gives NaY-NH<sub>2</sub> a strong basic nature even without the grafted organic bases [1].

Tetrazoles with a 5-membered ring of four nitrogen and one carbon atoms are as important class of N-rich heterocycles. Due various applications this poly-aza-heterocyclic compounds have attracted significant attention such as in medicinal chemistry, and in material sciences [2].

A few of them derivatives exhibited biological potencies, such as antibacterial, antiinflammatory, antifungal, antiviral, antituberculous, cyclo-oxygenase inhibitors, antinociceptive, hypoglycemic and anticancer activities [3] and this valuable compounds have always been considered as important synthetic targets [4].

### 2. Experimental

To a mixture of NaY zeolite in toluene (20 mL), trimethoxysilyl propylamine (2 mL) was added and stirred for 24 hours in reflux condition. Then catalyst was filtered and dried at 60°C. Then, this catalyst was used for synthesis 5-Substituted 1H-tetrazoles *via* one-pot three-component reaction of active carbonyl compounds, malononitrile and IL 1-butyl-3-methylimidazolium azide [BMIM]N<sub>3</sub> as a azide source without any solvent at thermal conditions .

### 3. Results and discussion

The FT-IR spectrum of NH<sub>2</sub>Y indicate an intense band about ca.1022 cm<sup>-1</sup> attributable to the asymmetric stretching of Al-O-Si chain of zeolite. The symmetric stretching and bending frequency bands of Al-O-Si framework of zeolite appear at ca.791 and 463 cm<sup>-1</sup>, respectively. Also, the C-H and N-H vibration bands attributed in the 2800-3500 cm<sup>-1</sup> and 1500-1650 cm<sup>-1</sup> regions. These bands are surely absent in the case of NaY zeolite, showing that 3-APTES has been attached on zeolite matrix.

In Fig. 1 we have seen the FESEM micrographs of NH<sub>2</sub>Y sample with a wide range of shapes and sizes of particles. It indicates the presence of well-defined zeolite crystals with some shadow of modification presence on its external surface. The particle sizes are around 200 nm and this decrease of size for modified zeolite is due to the complex formation on the support.



4<sup>th</sup> Iran National Zeolite Conference  
Golpayegan University of Technology, Golpayegan, Iran  
August 23-24, 2017

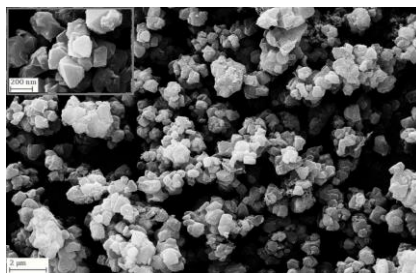


Fig.1. FESEM micrographs of NH<sub>2</sub>Y

**(Z)-2-(2-oxoindolin-3-ylidene)-2-(1H-tetrazole-5-yl) acetonitrile:** mp 211–213 °C, FT-IR (KBr) (cm<sup>-1</sup>): 3261, 3109 (N-H), 2231 (CN), 1730 (C=O), 1635, (C=C), 1585, 1465 (N-H in-plane bending); <sup>1</sup>H NMR (300 MHz, DMSO-*d*<sub>6</sub>, ppm): 5.08 (broad, s, N-H, overlap with solvent), 6.89 (1H, d, <sup>3</sup>J<sub>HH</sub> = 8 Hz, H-Ar.), 6.97 (1H, t, <sup>3</sup>J<sub>HH</sub> = 7.8 Hz, H-Ar.), 7.43 (1H, t, <sup>3</sup>J<sub>HH</sub> = 7.6 Hz, H-Ar.), 8.212 (1H, d, <sup>3</sup>J<sub>HH</sub> = 8 Hz, H-Ar.), 11.09 (1H, s, N-H).

**(E)-3-phenyl-2-(1H-tetrazole-5-yl) acrylonitrile:** mp = 165-167 °C, FT-IR (KBr) (cm<sup>-1</sup>): 3431 (N-H), 3047 (C-H Ar.), 2204 (CN), 1693 (C=C alkene), 1556, 1471 (NH in-plane bending).

**2-(1,3-dioxo-1H-inden-2(3H)-ylidene)-2-(1H-tetrazole-5-yl) acetonitrile (8):** mp = 160-164 °C, FT-IR (KBr) (cm<sup>-1</sup>): 3522, 3447, 3304 (N-H), 3176 (C-H Ar), 2220 (CN), 1710 (C=O), 1641 (C=C Ar.), 1575, 1467 (N-H in-plane bending).

#### 4. Conclusions

In summary, the surface of NaY zeolite was modified with various organic functionalities. We showed highly active, selective, and recyclable heterogeneous catalysts in organic transformations such as the preparation of tetrazoles and more importantly, the stability of these catalysts was found to be good and easily separated from the liquid phase after reaction.

#### Acknowledgments

Thanks are due to the Research Council of Arak University of Technology and Center of Excellence in the Chemistry Department of Arak University of Technology for supporting of this work.

#### References

1. E.B. Mubofu, J.H. Clark, D. Macquarrie, *Green. Chem.* 3 (2001) 23-25.
2. R.J. Herr, *Bioorg. Med. Chem. Lett.* 10 (2002) 3379.
3. P.B. Mohite, V.H. Bhaskar, *Int. J. Pharm. Technol. Res* 3 (2011) 1557.
4. T. Jin, S. Kamijo, Y. Yamamoto, *Tetrahedron Lett.* 45 (2004) 9435.



# 4<sup>th</sup> Iran National Zeolite Conference

## Golpayegan University of Technology, Golpayegan, Iran

### August 23-24, 2017



## Novel hydrothermal synthesis of mesoporous zeolite mordenite

Esmat Koohsaryan, Mansoor Anbia\*, Mohammad Sepehrian

Research Laboratory of Nanoporous Materials, Faculty of Chemistry, Iran University of Science and Technology  
Tehran, P.O. Box 16846-13114, Iran

\*Email :Mansoor Anbia: anbia@iust.ac.ir

### 1. Introduction

Zeolites are microporous three dimensional molecular sieves which have widespread applications in agriculture, water and wastewater treatments, petrochemical industries, oil refinery and so on. In fact, the presence of Al atoms in their structures causes the ion-exchange and acidic properties resulting in extraordinary utilization in different scientific and industrial areas [1-4]. One of the most useful zeolite frameworks is MOR-type (mordenite) which was determined by Meier in 1961. Mordenite usually regarded as a mono-dimensional zeolite utilized in separation, catalysis and purification processes due to its small and uniform pore size, high internal surface area, controlled chemistry and flexible framework [5,6]. There are many routes to introduce mesoporosity into zeolites structures such as dealumination, desilication, hard and soft templating etc. An interesting another way for this purpose is to form microporous zeolitic nanocrystals which connected to each other through larger pores [7]. Several researchers have assessed the synthesis of mesoporous zeolite mordenite via templating and dealumination methods [6,8]. However, in this study, we have investigated the preparation of mesoporous well-defined zeolite mordenite using an easy hydrothermal method and with the aid of commercial available zeolite mordenite microcrystals. The prepared product could have potential to utilize in various industrial applications.

### 2. Experimental

The used reagents for the preparation of mesoporous zeolite mordenite were sodium silicate, sodium hydroxide, sodium aluminate and distilled water. The alumina and silica precursors were transferred into a stain-less autoclave after mixing together in an alkali medium to form a zeolite synthetic gel. The solution was kept in an oven during a period of time under certain temperature. Then the end white power sample was filtered, washed and dried at ca. 100°C. In order to enhance crystallinity of zeolite crystallites and shorten the crystallization time, some commercial zeolite mordenite seeds were added to the gel. Thereafter, as-prepared mesoporous zeolite mordenite was characterized using different standard techniques such as X-ray diffraction pattern (XRD, X-ray diffractometer JEOL-JDX 8030, by Cu-K $\alpha$  radiation operating at 30 kV and 20 Ma), scanning electron microscopy (SEM, VEGA||TESCAN), nitrogen adsorption-desorption analysis (Belsorp-Max equipment, BEL Japan Inc., Japan) and Fourier transform infrared spectroscopy (FT-IR spectrometer, SHIMADZU-8400-s).

### 3. Results and discussion

Fig. 1 represents the X-ray diffraction pattern of as-prepared sample. The characteristic peaks of mesoporous zeolite mordenite are apparent at  $2\theta$ : 10.8, 20.6, 23.2, 26.6 and 27.3 degrees which are in match with them reported in the references [5]. Moreover, the elliptical particles with rough external surface are perceptible for the mesoporous zeolite mordenite in the SEM images (Fig. 2). The average particle size is determined about 500 nm.



4<sup>th</sup> Iran National Zeolite Conference  
Golpayegan University of Technology, Golpayegan, Iran  
August 23-24, 2017

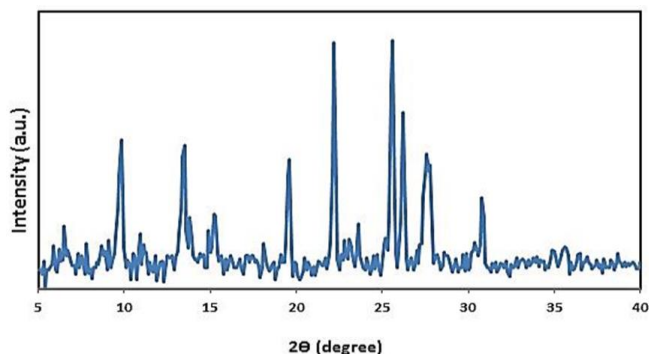


Figure 1. X-ray diffraction pattern of as-synthesized mesoporous zeolite mordenite.

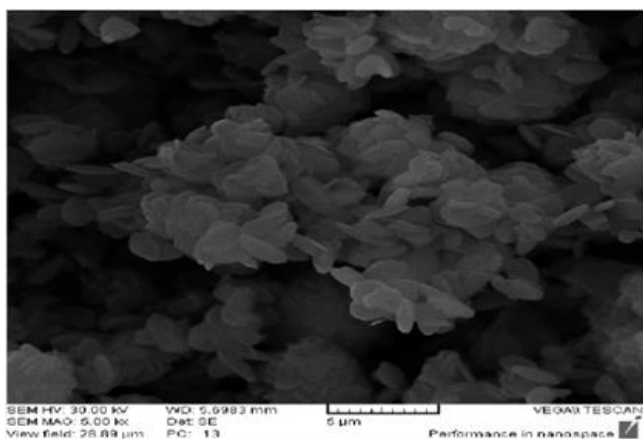


Figure 2. SEM images of as-synthesized mesoporous zeolite mordenite

As can be seen in Fig. 3, the bands assigned to the zeolite mordenite structure is shown in its FT-IR spectra. The bands at wavenumbers of ca. 1200 and 1000  $\text{cm}^{-1}$  belong to the external and internal asymmetric stretching vibration of tetrahedra T-O (T is Al or Si atoms), respectively. Besides, the bands attributed to the double ring are appeared at 580-560  $\text{cm}^{-1}$  and that of T-O bending is observed at wavenumber of 450  $\text{cm}^{-1}$ . The assigned bands to the external and internal symmetric stretching vibration are also present at 800 and 720  $\text{cm}^{-1}$ , respectively [5].

In addition, BET (Brunauer, Emmett, and Teller) specific surface area for the mesoporous zeolite mordenite has been determined more than  $300\text{m}^2/\text{g}$  and the BJH (Barrett-Joyner-Halenda) method was fulfilled to declare the existence of mesopores in the structure which are not exhibited here. It seems that agglomeration of many small crystals made a new porosity in the range of meso-scale (2-50 nm) and conducts the formation of a mesoporous zeolite structure.

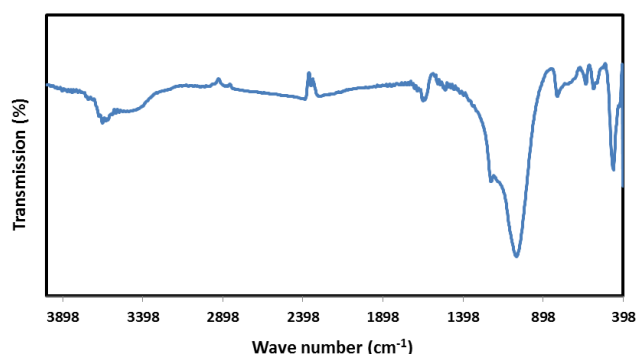


Figure 3. FT-IR spectra of as-synthesized mesoporous zeolite mordenite



# 4<sup>th</sup> Iran National Zeolite Conference

## Golpayegan University of Technology, Golpayegan, Iran

### August 23-24, 2017



#### 4. Conclusions

The preparation of mesoporous zeolite mordenite was carried out successfully via a hydrothermal method and with the aid of commercial zeolite mordenite seeds. The results of characterization techniques demonstrated that elliptical well-crystallized zeolitic crystals with a new porosity system in their structure were formed. It is prospected that the synthesized sample would be an outstanding candidate for adsorptive and catalytic applications in the future.

#### Acknowledgments

We acknowledge the financial support from Iran University of Science and Technology (IUST) and Arvand Petrochemical Company.

#### References

- 1) M. Anbia, F. Mohammadi Nejati, M. Jahangiri, A. Eskandari, V. Garshasbi, *J. Sci. I. R. Iran.* **2015**, 26, 213.
- 2) E. Koohsaryan, M. Anbia, *Chin, J. Catal.* **2016**, 37, 447.
- 3) M. Anbia, E. Koohsaryan, A. Borhani, *Mater. Chem. Phys.* **2017**, 193, 380.
- 4) V. Garshasbi, M. Jahangiri, M. Anbia, *Appl. Surf. Sci.* **2017**, 393, 225.
- 5) B. O. Hincapie, L. J. Garces, Q. Zhang, A. Sacco, S. L. Suib, *Microporous Mesoporous Mater.* **2004**, 67, 19.
- 6) X. Li, R. Prins, J. A. van Bokhoven, *J. Catal.* **2009**, 262, 257.
- 7) K. Möller, T. Bein, *Chem. Soc. Rev.*, **2013**, 42, 3689.
- 8) S. K. Saxena, N. Viswanadham, *Appl. Surf. Sci.* **2017**, 392, 384.

## Investigation of effective factors in adsorption of Cu(II) and Pb(II) in wastewater refinery on bentonite by using box behnken design

Fateme Zamani<sup>a</sup>, Shoeib Jafari<sup>a</sup>, Farideh Bandarchian<sup>\*b</sup>

<sup>a</sup> Department of Chemistry, Science and Research Branch, Islamic Azad University, Tehran, Iran.

<sup>b</sup> Department of Chemistry, Islamic Azad University, Central Tehran Branch, P.O. Box 14169 63316 Tehran, Iran

\*Email: Far.Bandarchian@iauctb.ac.ir

#### 1. Introduction

Eliminating metal ions from wastewater is an important issue that has been researched extensively (1). Methods such as precipitation, membrane separation, ion exchange, solvent extraction, and electrochemical reduction can be used. However, these methods are often ineffective and costly. For instance, when the contaminations are present in trace amounts, precipitation is not practical and also a large amount of sludge is produced. In contrast to most of these methods, adsorption has been proved to be one of the most simple, feasible, and efficient method for elimination of heavy metals from contaminated water. Among the different adsorbents zeolites are effective and inexpensive candidates but, many factors can affect the efficiency of them (2). The Box–Behnken design (BBD), a kind of RSM, is a second-order experimental design method that received widespread application in optimization of experimental conditions (3).



# 4<sup>th</sup> Iran National Zeolite Conference

## Golpayegan University of Technology, Golpayegan, Iran

### August 23-24, 2017



In this study, the elimination of  $Pb^{2+}$  and  $Cu^{2+}$  using bentonite sorbent was reported. The significant factors including pH, time, and sorbent amount were optimized and, also, the interactions were investigated by BBD. The samples and real samples (sea water and wastewater) were analyzed by atomic absorption spectrometry (AAS). The figures of merit under optimized removal conditions were reported.

## 2. Experimental Part or Theoretical Details

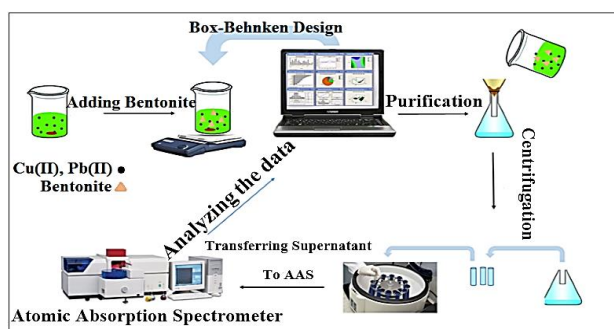


Figure 1. Experimental scheme

## 3. Results and discussion

According to the 15 steps design for each ion from the software, the optimum conditions were determined (table 1).

Table 1. Optimum conditions

ion	pH	Sorbent(g)	Stirring time (min)
Cu	4.2	1.8	49
Pb	4.8	1.9	50

The absorption responses of ions as a function of effective factors are presented in figures 2-7.

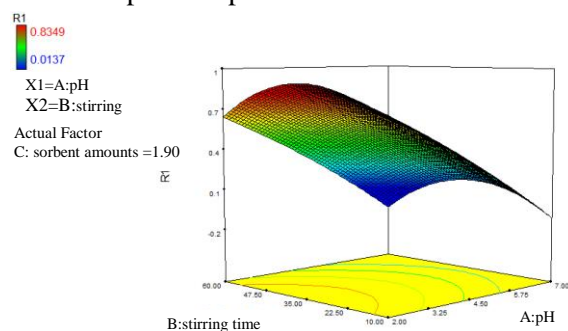


Figure 2. The absorption response of  $Pb^{2+}$  as a function of pH and stirring time.

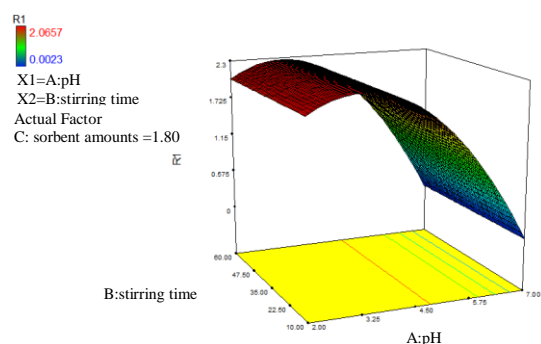


Figure 3. The absorption response of  $Cu^{2+}$  as a function of pH and stirring time.



# 4<sup>th</sup> Iran National Zeolite Conference

## Golpayegan University of Technology, Golpayegan, Iran

August 23-24, 2017

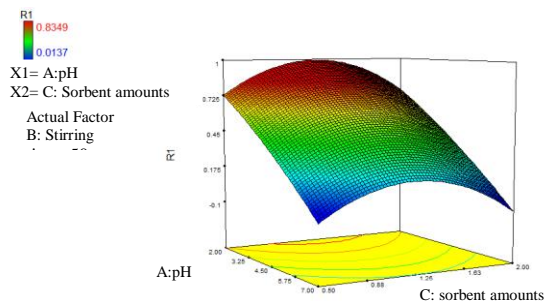


Figure 4. The absorption response of Pb<sup>2+</sup> as a function of pH and sorbent amounts.

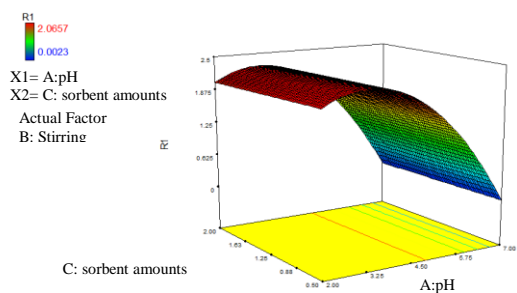


Figure 5. The absorption response of Cu<sup>2+</sup> as a function of pH and sorbent amounts.

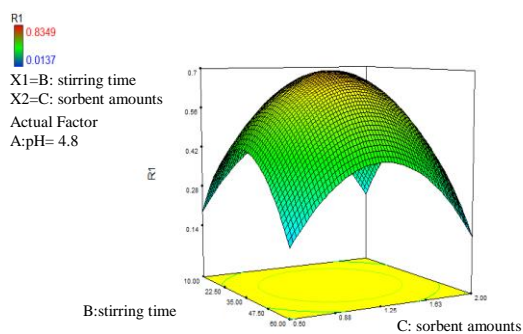


Figure 6. The absorption response of Pb<sup>2+</sup> as a function of stirring time and sorbent amounts.

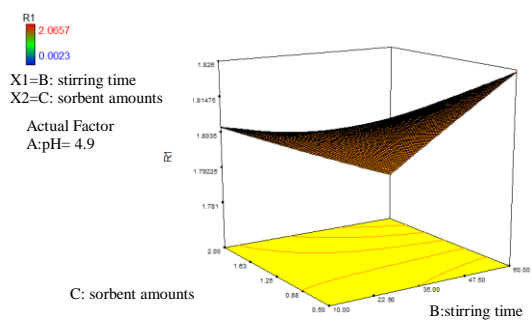


Figure 7. The absorption response of Cu<sup>2+</sup> as a function of Stirring time and Sorbent amounts.



4<sup>th</sup> Iran National Zeolite Conference  
Golpayegan University of Technology, Golpayegan, Iran  
August 23-24, 2017



The adequacy of the model was investigated using the analysis of variances (ANOVA) and the results are shown in Table 2.

Table 2. Results of analysis of variance

ion	Std. Dev	Adeq Precision	Pred R-Squared	Adj R-Squared	R-squared
Cu	0.022	116.574	0.9970	0.9995	0.9998
Pb	0.017	61.674	0.9890	0.9977	0.9992

The results of metals removal under the optimum conditions on real samples are in table 3.

Table 3. Results on real samples

Analite		Initial Conc. (mg/l)	Final Conc. (mg/l)	% adsorption
Cu <sup>2+</sup>	wastwater	7.408	0.27	74.05
	sea water	0.273	0.022	20
Pb <sup>2+</sup>	wastwater	0.56	0.05	47
	seawater	0.69	0.14	49

#### 4. Conclusions

In this research, the removal of Pb<sup>2+</sup> and Cu<sup>2+</sup> ion using bentonite sorbent was successfully performed. The factors were optimized and the interaction was investigated using BBD. The fast time analysis, reduced solvent and sorbent requirement, and simplification of the whole analytical procedure are major advantages using this method.

#### Acknowledgments

The financial support of the Research Council and Central Branch of Islamic Azad University of Iran is gratefully acknowledged.

#### References

- 1) T. K. Sen, D. Gomez, *Desalination* (2011) 267, 286-294
- 2) G. Zeng, Y. Liu, L. Tang., *Chem. Eng. J.* (2015) 259, 153-160
- 3) M.M. Ba-Abbad, et al., *Materials and Design* (2015)
- 4) G. H. Mahdavinia and H. Sepehrian, *Chin. Chem. Lett.*, 2008, 19, 1435.
- 5) G. M-Ziarani, A. R. Badiei, Y. Khaniania and M. Haddadpour, *Iran. J. Chem. Chem. Eng.*, 2010, 29, 1.
- 6) B. Karimi and D. Zareyee, *Org. Lett.*, 2008, 10, 3989.





4<sup>th</sup> Iran National Zeolite Conference  
Golpayegan University of Technology, Golpayegan, Iran  
August 23-24, 2017



**Physical Mixture of ZSM-5 and Mordenite Zeolites as an active catalyst for Catalytic Cracking of *n*-Heptane**

Narges Afroukhteh langroudi<sup>a</sup>, Sara Tarighi<sup>\*b</sup>, Hossein Ali Khonakdar<sup>a</sup>

<sup>a</sup> Department of Chemical Engineering, Faculty of Engineering, Central Tehran Branch, Islamic Azad University, Tehran, Iran

<sup>b</sup> Faculty of Petrochemicals, Iran Polymer and Petrochemical Institute, Tehran, P.O. Box 14965/115, Iran

\*Email: s.tarighi@ippi.ac.ir

### 1. Introduction

Catalytic cracking is of most important conversion processes used in petroleum refineries<sup>1</sup>. The main objective of this process is the conversion of high molecular weight hydrocarbons to more valuable products including light olefins<sup>2</sup>. Zeolites which are crystalline aluminosilicate materials are widely used as shape selective catalysts in this process<sup>3</sup>. They have defined micropores close to molecular diameters of light hydrocarbons, causing a significant molecular sieving effects<sup>4</sup>. Catalytic cracking of pure hydrocarbons is usually used as a model compound of light naphtha to study the behavior of these catalysts in industrial processes<sup>5</sup>. In this study, the performance of ZSM-5, mordenite and ZSM-5/Mordenite mixture (3:1) was investigated in catalytic cracking of *n*-Heptane.

### 2. Experimental

The catalytic behavior of two zeolites, including ZSM-5 ( $\text{SiO}_2/\text{Al}_2\text{O}_3=300$ ) and mordenite as well as a mixture of them with a weight ratio of 3:1 for ZSM-5 and mordenite, respectively were studied in a microactivity test (MAT) unit in accordance with ASTM-D3907. The cracking reactions was operated at temperatures 500, 550 and 600 °C under  $\text{N}_2$  atmospheric pressure. *n*-Heptane (97% purity, Merck), as a model compound for naphtha, was used as feedstock. 4.0 g of pelletized catalyst were packed in a fixed-bed reactor and preheated at 550 °C under dry air for 30 min before each run. The catalyst to oil ratio was 3.0 and the time on stream for all cracking tests was 70 sec. After adjusting the reactor to the desired temperature, the system was purged for 20 min with  $\text{N}_2$  flow of 50 ml/min at the reaction temperature and then *n*-Heptane were fed. The effluent from the reactor was cooled in an ice-bath and separated into liquid and gas products. At the end of the reaction process, the catalyst bed was purged with  $\text{N}_2$  flow for 20 min due to stripping the entrapped hydrocarbons in the catalyst bed. The gaseous products of the reaction were analyzed using Agilent Technology 7890 fast RGA GC instrument.

### 3. Results and discussion

The catalytic performance of ZSM-5, mordenite and a physically mixed ZSM-5/Mordenite catalyst with weight percentage of 75 wt% and 25 wt% of ZSM-5 and mordenite, respectively were evaluated in catalytic cracking of *n*-Heptane according to ASTM-D3907. Conversion of the catalysts together with the distribution of products including light olefins (ethylene, propylene and butenes) and light alkanes (ethane, propane and butane) were investigated. Table 1 shows the conversion of reaction as well as selectivity of the products in reaction temperature 500, 550 and 600°C.



# 4<sup>th</sup> Iran National Zeolite Conference

## Golpayegan University of Technology, Golpayegan, Iran

### August 23-24, 2017



Table1. The catalytic cracking results for ZSM-5, Mordenite and ZSM-5/Mordenite in n-Heptane cracking

Catalyst	T(°C)	Conversion (%)	Selectivity(%)	
			Total olefins	Total alkanes
ZSM-5	50	32.1	39.3	42.9
	55	53.9	44.5	34.9
	60	57.4	45	31.3
Mordenite	50	12.3	56.6	19
	55	12.7	55.8	19.3
	60	12.8	53.4	21.1
ZSM-5/Mordenite	55	37.5	44.8	35.1

According to the results, ZSM-5 exhibited more selectivity to propylene while mordenite is more selective to ethylene. This could be attributed to the larger pore sizes in ZSM-5 zeolite. The conversion of ZSM-5 and mordenite over different reaction temperatures are plotted in Fig. 1. Comparing the conversion values indicates the low conversion value for mordenite which is approximately constant at different reaction temperatures, whereas ZSM-5 has significant conversion values which obeys an ascending trend by temperature.

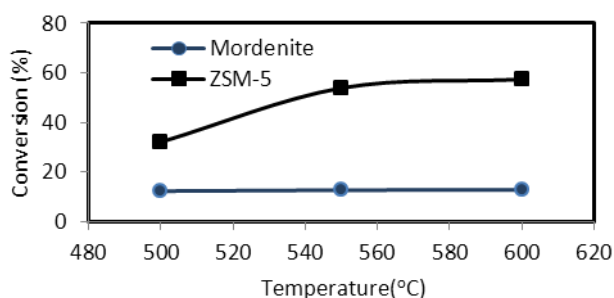


Figure 1. Conversion values for ZSM-5 and Mordenite over temperature

From data presented in table 1, it can be concluded that ZSM-5 shows an ascending correlation with temperature for olefins production while the corresponded trend for alkanes production is descending. However, there is no considerable difference in terms of alkanes and olefins selectivity at different temperatures over mordenite as catalyst. The olefins to alkanes ratios over two zeolites were calculated and plotted in Fig. 2.

This ratio under ZSM-5 is about 1.0 while the ratio under mordenite is about 3 at all reaction temperatures.

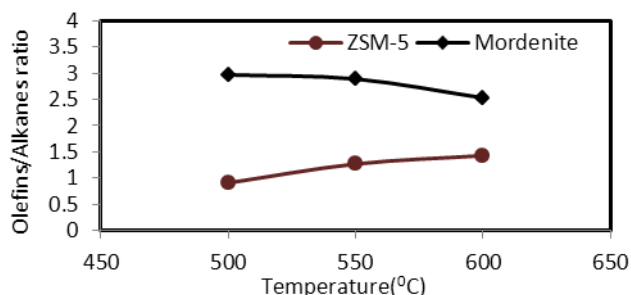


Figure 2. Olefins to alkanes ratio over ZSM-5 and mordenite in n-heptane cracking

Thus, according to higher olefins selectivity of mordenite and high conversion value obtained over ZSM-5 zeolite, ZSM-5/Mordenite mixture catalyst was investigated as catalyst and the catalytic reaction was done at 550 °C. The conversion and olefins selectivity for three examined catalysts in this work are presented in Fig. 3. It indicates that the mixture catalyst shows the characteristics of both zeolites which are proportional with the weight percentage of each component.



4<sup>th</sup> Iran National Zeolite Conference  
Golpayegan University of Technology, Golpayegan, Iran  
August 23-24, 2017

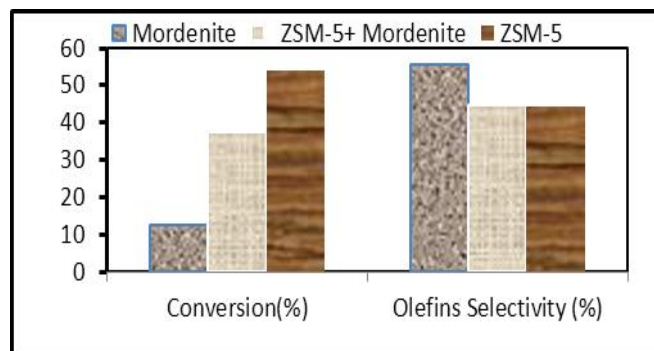


Figure 3. Comparison of conversion and olefins selectivity for pure and the mixture catalysts

#### 4. Conclusions

This study examined the catalytic cracking of n-heptane over ZSM-5, mordenite and a mixture of them as catalyst. The catalysts performance was evaluated at reaction temperatures 500, 550 and 600 °C. The data showed that increasing temperature enhances both conversion and olefins selectivity over ZSM-5 zeolite, while mordenite zeolite follows an approximately constant trend at different reaction temperatures. Mordenite zeolite showed higher olefins to alkanes ratio in comparison with ZSM-5. However, ZSM-5 resulted in higher conversion values. The mixture catalyst indicates the reasonable conversion and suitable olefins selectivity due to both ZSM-5 and mordenite characteristics. In conclusion, zeolite characteristic has significant influence on catalytic cracking. ZSM-5/Mordenite mixed catalyst can be introduced as an appropriate catalyst to fulfil both conversion and light olefins production requirements in catalytic cracking.

#### Acknowledgments

The financial support from Iran Polymer and Petrochemical Institute (IPPI) is acknowledged.

#### References

- 1) M. J. B. Souza, A. O. S. Silva, A. M. G. Pedrosa, A. S. Araujo, *React. Kinet. Catal. Lett.*, **2005**, 84, 287-293.
- 2) A. Janda, A. T. Bell, *J. Am. Chem. Soc.*, **2013**, 135, 19193-19207.
- 3) Y. Nakasaka, T. Okamura, H. Konno, T. Tago, T. Masuda, *Microporous Mesoporous Mater.*, **2013**, 182, 244-249.
- 4) H. Konno, T. Okamura, T. Kawahara, Y. Nakasaka, T. Tago, T. Masuda, *Chem. Eng. J.*, **2012**, 207, 409-496.
- 5) A. Corma, J. Mengual, P. Miguel, *J. Catal.*, **2015**, 330, 520-532.



4<sup>th</sup> Iran National Zeolite Conference  
Golpayegan University of Technology, Golpayegan, Iran  
August 23-24, 2017



**Synthesis and characterization of hydroxypropyl- $\beta$ -cyclodextrin (HP- $\beta$ -CD) conjugated magnetic nanoparticles and its adsorption of crystal and methyl violet dye**

Nina Alizadeh\*<sup>a</sup>, Shohreh Nasiri<sup>a</sup>

<sup>a</sup> Department of Chemistry, Faculty of Science, University of Guilan, Rasht, P.B. 41335-1914, Iran

\*E-mail: n-alizadeh@guilan.ac.ir

## 1. Introduction

Organic dye contaminants have received increased concerns in recent years because of the fast development of industry processing. Hence, removal of the dye contaminants prior to their discharge into the environment is necessary. The most notable feature of CD is its ability to form host-guest complexes with a wide range of molecules including dyes,<sup>1,2</sup> due to its special molecular structure. Because of its low cost, easy regeneration, and effectiveness, adsorption is regarded as a useful technique. Crystal violet and Methyl violet is a family of organic compounds that are mainly used as dyes. In the present study, we used HP- $\beta$ -cyclodextrin conjugated magnetic nanoparticles due to easy and inexpensive synthesis and separation much easier with the use of a magnet is done to remove dye.

## 2. Experimental and Theoretical Details

**2.1. Materials.** Materials were supplied by Merck.

### 2.2. Preparation

#### 2.2.1. Synthesis of Fe<sub>3</sub>O<sub>4</sub> nanoparticles

FeCl<sub>3</sub>·6H<sub>2</sub>O (1.350 gr), PEG 6000 (1.000 gr), anhydrous sodium acetate (3.600 gr) and ethylene glycol solution (40 mL) were mixed in a beaker with constant stirring. After thirty minutes stirring, the mixture was transferred into a stainless steel autoclave and maintained at 200 °C for 8 h. Finally, the black precipitate was obtained by magnetic separation, washed with ethanol three times and dried in vacuum at 60 °C for 6 h. Then the Fe<sub>3</sub>O<sub>4</sub> nanoparticles were obtained.<sup>3</sup>

#### 2.2.2. Synthesis of HP- $\beta$ -cyclodextrin

HP $\beta$ CD is commonly synthesized from  $\beta$ CD and propylene oxide in alkaline conditions.<sup>4</sup>

#### 2.2.3. HP- $\beta$ -cyclodextrin conjugated magnetic nanoparticles

To obtain the Fe/HP $\beta$ CD composite, 0.15 gr Fe<sub>3</sub>O<sub>4</sub> and 0.5 gr HP $\beta$ CD were dispersed in 60 mL deionized water, and then ultrasonicated for 30 min. The mixture was then transferred into an oven and heated at 150 °C for 5 h. The resulting composite was washed several times with deionized water. Finally, the obtained sample was dried in a vacuum oven at 80 °C for 24 h.<sup>3</sup>



# 4<sup>th</sup> Iran National Zeolite Conference

## Golpayegan University of Technology, Golpayegan, Iran

### August 23-24, 2017



### 2.3. Characterization

The absorption Spectra were obtained in a Unico S2100 UV–Vis at  $(25 \pm 0.1)$  °C. The morphology of the obtained fibers was characterized by a field-emission scanning electron microscopy (SEM, LEO-1430 VP). FT-IR spectra were recorded on a (Nicolet protege 460) spectrometer.

### 3. Results and discussion

#### 3.1. FT-IR analysis

The IR spectrum of HP $\beta$ CD (Figure 1) is characterized by prominent peaks at  $3413\text{cm}^{-1}$  (OH),  $2932\text{cm}^{-1}$  (C-H),  $1638\text{cm}^{-1}$  and  $1617\text{cm}^{-1}$  (H-O-H bending),  $1032\text{cm}^{-1}$  (C-O-C) Which is consistent with previous studies.<sup>5</sup>

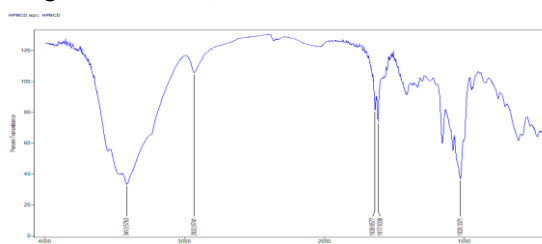


Figure 1. FT-IR spectra of HP $\beta$ CD

#### 3.2. Morphological analysis

SEM is a qualitative technique to visualize changes in the surface morphology of a substance. The SEM microphotograph of HP $\beta$ CD conjugated magnetic nanoparticles is displayed in Figure 2. That Connect nanoparticles  $\text{Fe}_3\text{O}_4$  to HP $\beta$ CD surface in the clear.

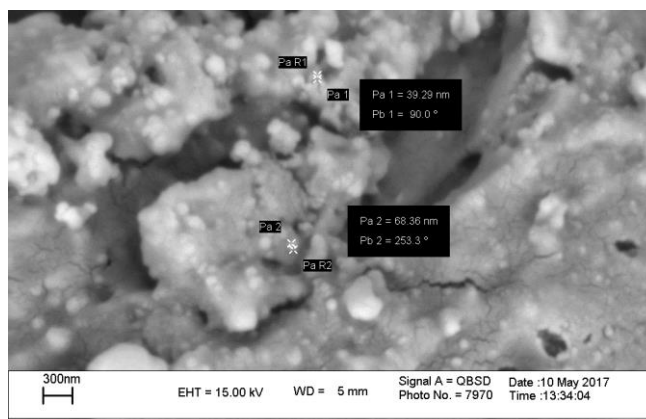


Figure 2. SEM photographs of HP $\beta$ CD conjugated  $\text{Fe}_3\text{O}_4$  nanoparticles

#### 3.3. Optical study

Figure 3 shows the absorption spectrum of the crystal violet in the presence of different concentrations of HP $\beta$ CD/ $\text{Fe}_3\text{O}_4$  (0.001 gr/30ml, 0.002 gr/30ml). We can observe a Reduce the absorption by the addition of the cyclodextrin. We can clearly observe that the addition of HP $\beta$ CD/ $\text{Fe}_3\text{O}_4$  causes a change in the spectral behavior.



4<sup>th</sup> Iran National Zeolite Conference  
Golpayegan University of Technology, Golpayegan, Iran  
August 23-24, 2017

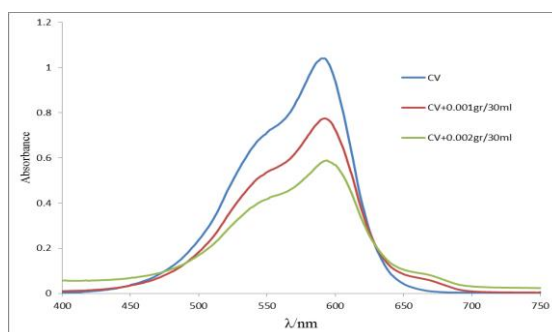


**Figure 3.** Absorption spectrum of the  $[CV] = 1.3 \times 10^{-5}$  M, in the presence of different concentrations of HP $\beta$ CD/Fe $_3$ O $_4$  ranging from (0.001 gr/30ml, 0.002 gr/30ml) T=25 °C.

Figure 4 shows the absorption spectrum of the methyl violet in the presence of different concentrations of HP $\beta$ CD/Fe $_3$ O $_4$  (0.001 gr/30ml, 0.002 gr/30ml). As the Figure is clear reduce the absorption in methyl violet almost double crystal violet.

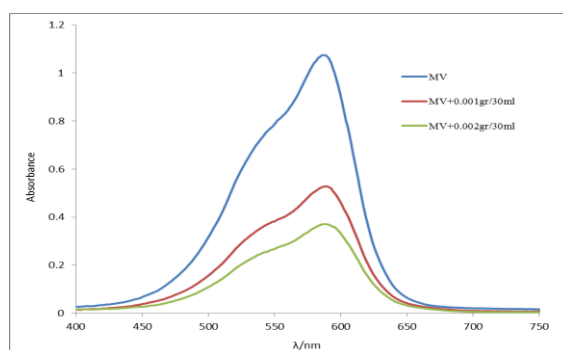


**Figure 4.** Absorption spectrum of the  $[CV] = 1.25 \times 10^{-5}$  M, in the presence of different concentrations of HP $\beta$ CD/Fe $_3$ O $_4$  ranging from (0.001 gr/30ml, 0.002 gr/30ml) T=25 °C.

#### 4. Conclusions

We demonstrated that magnetically tagged HP $\beta$ CD allow efficient handling, trapping, and release of organic dyes model molecule such as crystal violet and methyl violet. Isolation of the immobilized inclusion complex can easily be carried out within a few seconds by magnetic separation. Tagging cyclodextrins with magnetic, stable nanoparticles makes them magneto responsive and may lead to a new generation of adsorbents in separation, intermediate, or contaminant enrichment or drug delivery. The strong magnetization (metal core), easy chemical functionalization open access to highly efficient treatments in large scale applications such as drinking or process water treatment.

#### References

- 1) R. Zhao, Y. Wang, X. Li, ACS Appl. Mater. Interfaces, **2015**, 7 (48), 26649–26657.
- 2) M. Sowmiya, A. K. Tiwari, J. Phys. Chem. C, **2014**, 118 (5), 2735–2748
- 3) W. Hu, X. Wu, F. Jiao, DESALINATION AND WATER TREATMENT **2016**, 4, 1–12.
- 4) M. Malanga, J. Szem, E. Fenyvesi, jpharmsci **2016**, 1-11.
- 5) S. George, D. Vasudevan, Journal of Young Pharmacists **2012**, 4, 220-227.



4<sup>th</sup> Iran National Zeolite Conference  
Golpayegan University of Technology, Golpayegan, Iran  
August 23-24, 2017



**Spectroscopic study and antioxidant activity of host–guest complexes of  $\beta$ -cyclodextrin and  $\gamma$ -cyclodextrin with amlodipine besylate drug**

Nina Alizadeh<sup>\*a,b</sup>, Shokufeh Malakzadeh Rusta<sup>b</sup>

<sup>\*a</sup>Department of Chemistry, Faculty of Science, University of guilan, Rasht, 4193833697, Iran

<sup>b</sup>Department of Chemistry, Faculty of Science, University Campus 2, University of guilan, Rasht, 4144784475, Iran

\*Email: n-alizadeh@guilan.ac.ir

### 1. Introduction

The host–guest interaction of the drug materials with cyclodextrins were improved solubility and properties without outbreak sensitive into body [1]. This point were investigated according in order to papers encapsulation drugs in cyclodextrins [2]. The aim of the study was to synthesize and characterization the host–guest complexes of amlodipine besylate drug with  $\beta$ -cyclodextrin ( $\beta$ -CD) and  $\gamma$ -cyclodextrin ( $\gamma$ -CD) which has antioxidating activity property. The intraction host–guest complex was characterized by Fourier transform infrared (FTIR) and Ultraviolet-visible (UV-vis) spectroscopics. Kinetic studies of 2,2-diphenyl-1-picrylhydrazyl (DPPH<sup>•</sup>) cyclodextrins (CDs) complexes were done.

### 2. Experimental Part or Theoretical Details

The intraction host-guest complexes was characterized by Ultraviolet-visible (UV-vis) spectroscopics as quantitative and Fourier transform infrared (FTIR) as quality spectroscopics.

UV-vis spectra were analysed of  $\beta$ -CD/AML and  $\gamma$ -CD/AML complexes at maximum wavelength 207 nm in comparison with  $\beta$ -CD,  $\gamma$ -CD and AML raw materials. UV-vis absorption spectra of host-guest complexes in presence of increasing with various concentrations (mM) of  $\beta$ -CD and  $\gamma$ -CD were observed.

Job's plot for  $\beta$ -CD/AML host-guest complex and Mole ratio plot for  $\gamma$ -CD/AML host-guest complex from absorbance UV-vis spectra at 207 nm were measured. The formation stability constants were calculated by using amodified Benesi-Hildebrand Equation at 25°C  $1/\Delta A = 1/\Delta \epsilon \cdot [AML] \cdot K \cdot [\beta\text{-CD}] + 1/\Delta \epsilon \cdot [AML]$  and  $1/\Delta A = 1/\Delta \epsilon \cdot [AML] \cdot K \cdot [\gamma\text{-CD}] + 1/\Delta \epsilon \cdot [AML]$ . The rate a stable free radical DPPH<sup>•</sup>-scavenging in presence of  $\beta$ -CD/AML and  $\gamma$ -CD/AML host-guest complexes and AML free were obtained.

### 3. Results and discussion

Besides that, the stoichiometry ratio was also determined to be 1:1 for the host–guest complexes of  $\beta$ -CD and  $\gamma$ -CD with amlodipine besylate (Figure1-2). FTIR spectra were indicated comparison between quality the intensity at the host-guest complexes  $\beta$ -CD/AML,  $\gamma$ -CD/AML and amlodipine besylate free. Fourier Transform infrared spectra show some increase and decrease in intensity changes,  $\Delta\delta$ . This experimental resulted were confirmed the forming of amlodipine besylate complexes with CDs. The increment is due to the insertion of the benzene part ring into the electron rich cavity of  $\beta$ -cyclodextrin and will increase the density of electron cloud, which will lead to the increase in frequency. The decrease in the frequency between the host-guest complex and its constituent molecule is due to the changes in the microenvironment which lead to the formation of hydrogen bonding and the presence of van der Waals



4<sup>th</sup> Iran National Zeolite Conference  
Golpayegan University of Technology, Golpayegan, Iran  
August 23-24, 2017



forces during their interaction to form the host-guest complex. Thus, the FTIR spectra significantly proves imitated the characteristic peaks which can be regarded as a simple superimposition of those host and guest molecules. The formation of the amlodipine besylate/ $\beta$ -CD and the amlodipine besylate/ $\gamma$ -CD host-guest complexes.

The formation constant was calculated by using a modified Benesi-Hildebrand equation at 25°C. The host-guest complexes  $\beta$ -CD/AML and  $\gamma$ -CD/AML stability constant as  $K(M^{-1})$  in order to calculated  $8.45 \times 10^3$  L/mol and  $3.63 \times 10^7$  L/mol (Table 1). This proves the formation of the host-guest complex where the benzyl part of amlodipine besylate has been encapsulated by the hydrophobic cavity of  $\beta$ -CD and  $\gamma$ -CD.

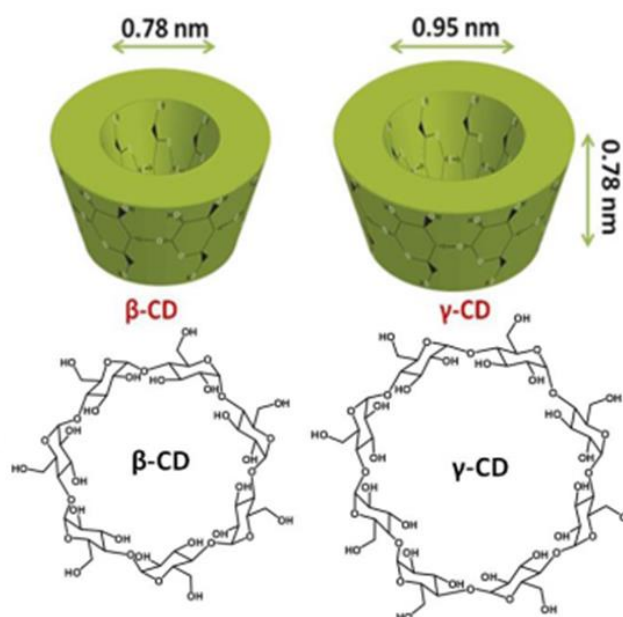


Figure 1. The structure of  $\beta$ -cyclodextrin and  $\gamma$ -cyclodextrin.

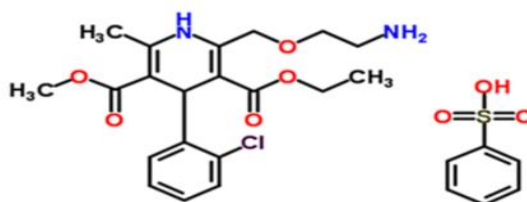


Figure 2. chemical structure of the drug amlodipine and its besylate (AML).

Figure 3 shows UV-vis absorption spectra of elimination a stable free radical DPPH<sup>•</sup> by addition host-guest complexes  $\beta$ -CD/AML,  $\gamma$ -CD/AML and amlodipine besylate free were prepared. The rate a stable free radical DPPH<sup>•</sup>-scavenging in presence of  $\beta$ -CD/AML and  $\gamma$ -CD/AML host-guest complexes and AML free were obtained.





4<sup>th</sup> Iran National Zeolite Conference  
Golpayegan University of Technology, Golpayegan, Iran  
August 23-24, 2017

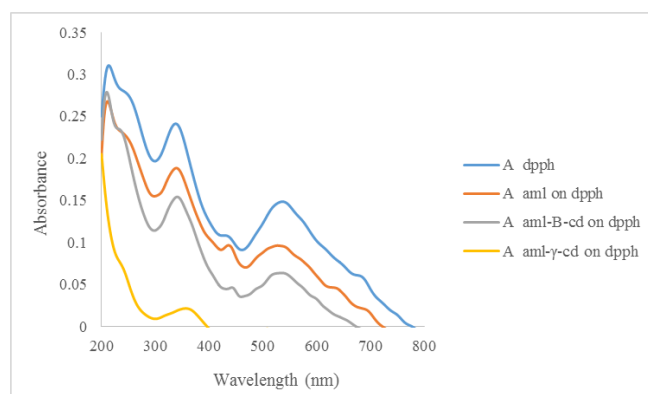


Figure 3. UV-vis absorption spectra of a stable free radical DPPH' by addition AML free, inclusion complex  $\beta$ -CD/AML and  $\gamma$ -CD/AML.

Table 1. Data of Benesi-Hildebrand linear plot for  $1/\Delta A$  against various  $1/[\beta\text{-CD}]$  at 207 nm.

Host-guest	$1/\Delta\epsilon.[\text{AML}]^a$	$1/\Delta\epsilon.[\text{Aml}].K.[\text{CD}]$	$K(\text{M}^{-1})$
AML/ $\beta$ -CD	8.3	0.98	$8.45 \times 10^3$
AML/ $\gamma$ -CD <sup>b</sup>	2.5	$7 \times 10^{-5}$	$3.63 \times 10^7$

<sup>a</sup> Amlodipine besylate at fixed concentration (mM) as intercept

<sup>b</sup> Cavity  $\gamma$ -cyclodextrin is bigger than cavity  $\beta$ -cyclodextrin

#### 4. Conclusions

The results obtained indicated that the amlodipine besylate/ $\beta$ -CD and the amlodipine besylate/ $\gamma$ -CD host-guest complexes was the most reactive than its free form into antioxidant activity.

#### Acknowledgments

We acknowledge the financial support from University Campus 2, University of guilan.

#### References

- 1) S., U. Lucretia, L. Ionut, S. Zoltan, F. Adriana, S. Claudiu, Journal Thermal Analytical Calorimetry **2016**, 123, 2377–2390.
- 2) L. Jinxia, Z. Huizhi, Y. Yanyan, S. Shuman, Journal Inclusion Phenomena Macrocyclic Chemistry **2016**, 84, 115–120.



4<sup>th</sup> Iran National Zeolite Conference  
Golpayegan University of Technology, Golpayegan, Iran  
August 23-24, 2017



Investigation of  $M_xH_{3-x}PW_{12}O_{40}$  (M=K, Cs)/ OMS-2/ MCM-41 nanocomposites  
on esterification reactions

Sedigheh Taheri Mirghaed\*, Nafiseh Mahdi Babaei, Mojgan Zendehtdel

Department of Chemistry, Faculty of Science, Arak University, Arak 38156-8- 8349; Iran

\* E-mail: Sedighetaheri1393@gmail.com

### 1. Introduction

Esterification reactions are used in synthetic organic chemistry. Sulphuric acid or tin octoate which are corrosive and virulent need to be neutralized after the completion of the reaction are used as typical catalysts for this reaction. But in case of metal containing Lewis acid catalysts, the metal needs to be removed carefully after the reaction which can be done, for instance, by adsorption on bleaching earth, which however leads to the formation of large of amounts wastes [1]. These problems can be overcome by using heterogeneous catalyst. Many heterogeneous catalysts reported in the literature for esterification reaction includes ion-exchange resin, H-ZSM-5, zeolite-Y, niobic acid, sulphated oxides and heteropoly acids. Supported heteropoly acid (HPA), which have been proved to be nearly comparable in their efficiency for a series acid catalyzed reactions to  $H_2SO_4$  in liquid phase, their high solubility in the polar media, often made them difficult to separate from the reaction products, that problematic in industrial processes [2]. So the challenge was to replace them by solid acid catalysts such as zeolite or resins. But in case of zeolite, in spite of its high activity, its reaction always gives a variety of undesired by products due to higher reaction temperature [3]. Water-tolerant catalysis will be introduced as new functions of  $Cs_{2.5}H_{0.5}PW_{12}O_{40}$ . Supporting and composite catalysts consist of silica or MCM-41 and  $H_3PW_{12}O_{40}$  or  $H_4SiW_{12}O_{40}$  show excellent catalytic performances. Well-dispersed heteropoly acids showed high catalytic activities in a liquid-phase alkylation of aromatics [4]. Calcination of the precipitates brought about the migration of  $H^+$  and  $Cs^+$  in the solid to form a nearly uniform solid as revealed by solid-state NMR and XRD.

### 2. Experimental

For synthesis of butyl acetate and isobutyl acetate, alcohol (35mmol) with acetic acid (80 mmol) was mixed. After that catalyst was added and reaction mixture was refluxed at  $70^\circ C$ . In order to regenerate the catalyst after 2 h of reaction, it was separated by filtration. Then Diethyl ether (30 ml) was added to mixture and finally  $NaHCO_3$  (10 ml, 10%) was added.

### 3. Results and discussion

Table.1 show various catalysts was investigated at esterification reaction butyle acetate and table.2 show effect of catalysts on iso- butyle acetate reaction.

Table 1. Effect of catalysts at esterification butyle acetate reaction

Catalyst	Yield	Catalyst	Yield
MCM-41	41.91	$K_{1.5}H_{1.5}PA$	40.71
HPA	57.47		
OMS-2	32.54	$K_{1.5}H_{1.5}PA/MCM-41/OMS-2$	51.23
$Cs_{1.5}H_{1.5}PA$	45.24	$Cs_{1.5}H_{1.5}PA/MCM-41/OMS-2$	52.79



4<sup>th</sup> Iran National Zeolite Conference  
Golpayegan University of Technology, Golpayegan, Iran  
August 23-24, 2017



Table 2. Effect of catalysts at esterification iso-butyle acetate reaction

Catalyst	Yield	Catalyst	Yield
MCM-41	41.17	K <sub>1.5</sub> H <sub>1.5</sub> PA	35.9
HPA	32.28		
OMS-2	54.07	K <sub>1.5</sub> H <sub>1.5</sub> PA/MCM-41/OMS-2	41.51
Cs <sub>1.5</sub> H <sub>1.5</sub> PA	55.70	Cs <sub>1.5</sub> H <sub>1.5</sub> PA/MCM-41/OMS-2	79.34

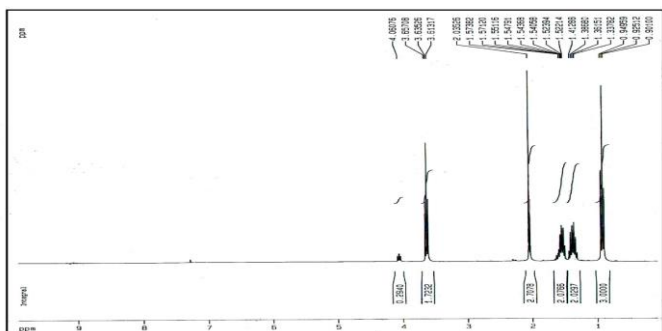


Fig. 1 H-NMR spectra of butyle acetate in CDCl<sub>3</sub> solvent

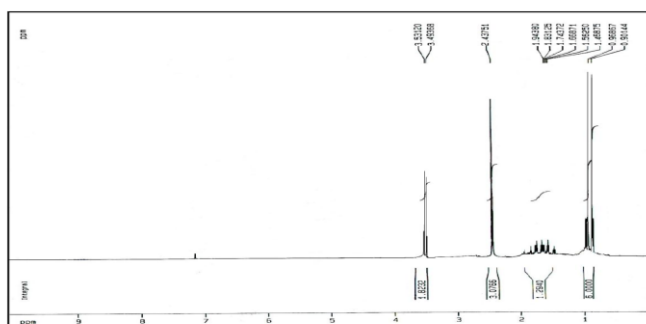


Fig. 2. H-NMR spectra of iso-butyle acetate in CDCl<sub>3</sub> solvent

#### 4. Conclusions

Leaching of the catalyst from the support is a negative property for the catalyst, which makes it unattractive for reusing. So it was necessary to study the stability of Cs salt of phosphotungstic acid promoted MCM-41/OMS-2 in order to reuse the catalyst. SEM, XRD and IR showed that Cs<sub>1.5</sub>H<sub>0.5</sub>PW<sub>12</sub>O<sub>40</sub> was highly dispersed on mesoporous silica. The supported Cs<sub>1.5</sub>H<sub>0.5</sub>PW<sub>12</sub>O<sub>40</sub> on MCM-41/ OMS-2 was highly active for esterification of butyle acetate and iso-butyle acetate. Adsorption analysis demonstrated that Cs<sub>1.5</sub> possesses mesopores and micropores as well as very strong acid sites a high surface area, and hydrophobic surface.

#### References

- 1) T. Okuhara, H. Watanabe, T. Nishimura et al *Chem Mater* **2000**, 12, 2230
- 2) Y. Izumi, *Catal Today* **1997**, 33,371
- 3) AS. Dias, S. Lima, M. Pillinger, *Carbohydr Res*, **2006**, 341, 2946.
- 4) S. Tangestaninejad, V. Mirkhani M., Moghadam et al, *Ultrason Sonochem* **2008**, 15(4), 438.



# 4<sup>th</sup> Iran National Zeolite Conference

## Golpayegan University of Technology, Golpayegan, Iran

### August 23-24, 2017



## Synthesis and Characterization of ZnO/GO Nanocomposite via a Rapid Method

Zahra Karami<sup>a</sup>, Iran Sheikhshoae<sup>\*a</sup>, Hassan Karimi-Maleh<sup>\*b</sup>

<sup>a</sup> Department of Chemistry, Shahid Bahonar University, Kerman, Iran

<sup>b</sup> Department of Chemistry, Tehran University of Iran, Tehran, Iran

\*Email: i\_shoae@yahoo.com

### Abstract

In this method ZnO/GO nanocomposite were synthesized via a direct method (precipitation), and characterized its structure with some normal spectroscopic methods. The prepared ZnO/GO nanocomposite were characterized by X-ray diffraction analysis (XRD), field emission scanning electron microscopy (FESEM), elemental analysis and EDAX spectroscopy.

### 1. Introduction

Graphene is a single atom-thick planar sheet of  $sp^2$ -bonded carbon atoms, and it possesses large theoretical surface areas ( $2600 \text{ m}^2\text{g}^{-1}$ ) and excellent mobility of charge carriers ( $200,000 \text{ cm}^2 \text{ V}^{-1}\text{s}^{-1}$ ). Meanwhile, as a substrate, graphene is also an excellent electron-transport material in the process of photocatalysis. Besides these graphene property, GO also shows semiconductive properties due to its  $\pi$ -conjugated  $sp^2$  domains and an oxygenated  $sp^3$  domain. So compositing the inorganic semiconductor with GO will also increase the photo-catalytic efficiency by increasing surface area. Also ZnO/graphene oxide (ZnO/GO) composite material, in which ZnO nanoparticles were densely coated on the GO nanosheets, was successfully prepared by an improved two-step method and characterized by IR, XRD, TEM and map analysis. In the most recent couple of years, graphene-based composites are being examined for supercapacitor applications. In general, the specific capacitance of graphene is lesser than the expected value due to restacking of the graphene sheets which could be improved by making it as a composite with other materials.

### 2. Experimental Part or Theoretical Details

In this work, we synthesized nano particles of ZnO by a rapid sol-gel method and characterized its by SEM, XRD, TEM, EDAX analysis and Map. Then we prepared a nano composite ZnO-GO by using grapheme oxide.

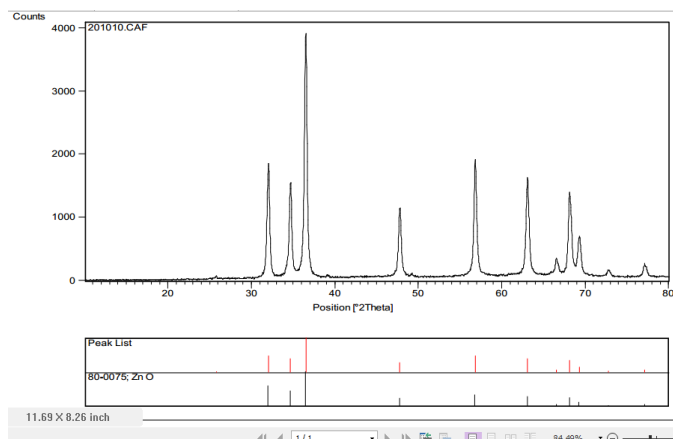


Figure 1. XRD pattern of nano sized ZnO

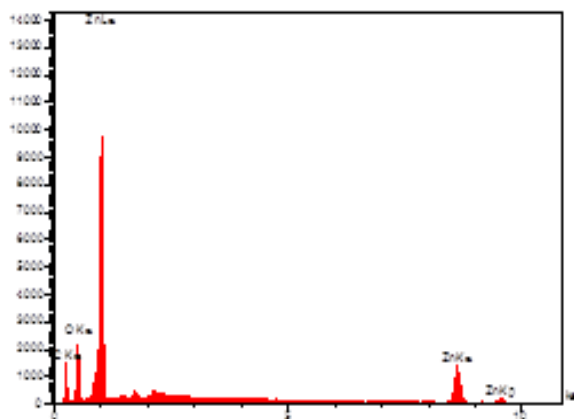


Figure 2. EDX spectra of ZnO/GO nanocomposite



4<sup>th</sup> Iran National Zeolite Conference  
Golpayegan University of Technology, Golpayegan, Iran  
August 23-24, 2017

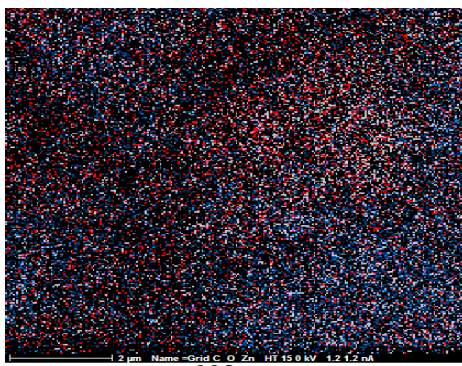


Figure 3. MAP analysis for ZnO/GO nanocomposite

### 3. Results and discussion

Figure 1 shows the the XRD pattern of nanosized ZnO, Figure 2 shows the EDX spectra for this nanocomposite (ZnO/GO) and Figure 3 shows the MAP analysis of ZnO/GO, ZnO/GO nano composite was successfully prepared via an improved two-step method. In the second step of preparing ZnO/GO composite material, the GO sheets are further exfoliated and unfolded.

### 4. Conclusions

In this study we prepared nano sized ZnO with sol-gel rapid method and characterized and confirmed the structure of this nano oxide with some spectroscopic methods such as SEM, MAP, EDAX and XRD. The nano composite (ZnO-GO) was synthesis and characterized by some common analysis.

### References

- 1) F.-H. Wu, G.-C. Zhao, X.-W. Wei, Z.-S. Yang, , *Microchim. Acta*, 2004, 144, 243.
- 2) Q. J. Xiang, J.G. Yu, M. Jaroniec, *Enhanced* , *Nanoscale* 2011, 3670–3679.
- 3) H. Zhang, X. Lv, Y. Li, Y. Wang, J. Li, *ACS Nano*, 2010, 380–387.
- 4) Y.Q. Cao, T. He, Y.M. Chen, *J. Phys. Chem. C*, 2010, 3627–3634.
- 5) J. Choi, H. Park, M.R. Hoffmann, *J. Phys. Chem. C*, 2010, 783–793.
- 6) B.T. Su, Z.Y. Ma, S.X. Min, et al., *Sci. Eng. A*, 2007, 44–47.



4<sup>th</sup> Iran National Zeolite Conference  
Golpayegan University of Technology, Golpayegan, Iran  
August 23-24, 2017



**Availability portland cement for add zeolite in building industry  
(Case study zeolite sangsar cement company-semnan)**

Hossein Bibakian Sangsar<sup>\*a</sup>, Hadi Hamidian Shormasti<sup>b</sup>, Dariush Jamalodin<sup>c</sup>

<sup>a</sup> Mining Engineering phd Student at Qaemshahr Azad University, Mazandaran Iran

<sup>b</sup> Assistant Professor at Qaemshahr Azad University, Mazandaran Iran

<sup>c</sup> Mining Engineering and lab. Sangsar cement company, Semnan, Iran

\*Email : Bibakianh@yahoo.com

**Abstract**

In this paper, the properties of concrete containing zeolite as partial replacements of cement and sand were studied in lab. Sangsar cement company –semnan-Iran. The compressive strength, water absorption, chloride ion diffusion and resistance to acid environments of concretes made with zeolite (clinoptilolite) at proportions of 6%, 10%, 15%, 20% and 25% of zeolite in four mine zeolite and amount 42 cubic 15\*15 cm and different blain and std. aggregate at were investigated. So, results of this study show that the compressive strength of samples with zeolite increased considerably. With the incorporation zeolite, the chloride resistance of specimens was enhanced significantly that zeolitic cement can cause improving mechanical specifications of cement and its durability in

sensitive situations such as marin, acidic, and sulphatic situations. Decreasing hydration temperature of cement. Improving klinker ductility and controlling silica basic reaction are others advantages of zeolitic cement. Also, one must pay attention that zeolite may cause to increasing cement required water for achieving to suitable level. Above advantages about zeolitic cement because of different zeolitic ores with different purity are inaccessible cement. In the other words, as using zeolite cement in sensitive situation, using test and survey with regarding to cement durability are recommended.



4<sup>th</sup> Iran National Zeolite Conference  
Golpayegan University of Technology, Golpayegan, Iran  
August 23-24, 2017



## The effect of pH on the synthesis of MFI-type drug delivery systems

Maasoumeh Khatamian<sup>\*a</sup>, Azin Yavari<sup>a</sup>, Maryam Saket Oskoui<sup>a</sup>, Sara Fazli Shokohi<sup>b</sup>

<sup>a</sup> Department of Inorganic Chemistry, Faculty of Chemistry, University of Tabriz, Tabriz, 5166616471, Iran

<sup>b</sup> Research centre for Advanced Materials and Minerals Processing, Department of Material Engineering, Sahand University of Technology, Tabriz

\*Email: mkhatamian@yahoo.com

### 1. Introduction

Over the past decades, much attention has been devoted to the design of efficient drug delivery systems (DDSs). In this way, zeolites and zeolite composites have been considered as potential DDSs [1, 2]. The drug loading capacity of zeolites can be controlled by variations in the Si/Al ratio of zeolite [2] or by incorporation of heteroatoms into the zeolites framework [3]. The incorporation of heteroatoms into the framework of zeolites has been developed as a suitable method for tailoring the physicochemical properties of zeolites [4]. For an efficient incorporation of heteroatoms into the framework of zeolite, the precise control of synthesis parameters is inevitable.

In this work, we report the effect of synthesis gel pH on the crystallization and morphology of MFI-type borosilicate ([B]-MFI) zeolites. We also consider the efficiency of prepared zeolites as DDSs.

### 2. Experimental Part

[B]-MFI zeolites with Si/B ratio of 11 were synthesized using proper amounts of silicic acid, borax, TPABr and NaOH. The pH of mixture was adjusted to the desired amount using diluted H<sub>2</sub>SO<sub>4</sub> and crystallization was carried out at 160 °C for 44 h. Finally, the products were calcined at 500 °C in air for 3 h and designated as [B]-MFI(x), which x stands for pH value.

The drug loading efficiency of zeolites was examined using an aqueous solution of doxorubicin (0.5 mg/mL) as a test drug. MTT assay was carried out in order to study the cytotoxicity of doxorubicin-loaded zeolites against MDA-MB-231 cell lines.

### 3. Results and discussion

The XRD patterns of [B]-MFI zeolites synthesized at different pH values are shown in Figure 1. It can be seen from XRD patterns that all samples show the characteristic peaks of the MFI structure in the range of  $2\theta = 7-9^\circ$  and  $2\theta = 23-25^\circ$ . No additional peaks due to the presence of crystalline impurities are observed in these patterns. On the other hand, it was revealed that the highly crystalline borosilicate zeolites can be obtained at relatively low pH values (pH=9) using the starting materials and synthesis conditions described here.



# 4<sup>th</sup> Iran National Zeolite Conference Golpayegan University of Technology, Golpayegan, Iran August 23-24, 2017

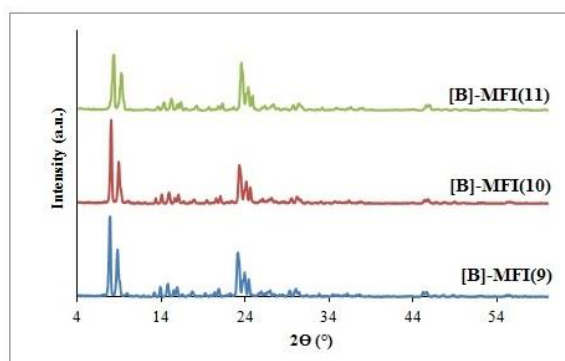


Figure 1. The XRD pattern of [B]-MFI zeolites.

According to the SEM images (Figure 2), all [B]-MFI zeolites have coffin-type crystals which are mainly comprised of the aggregation of small rectangular crystals with different size distribution. It is evident from SEM images that the particle size of zeolites increases by decreasing the pH value and also the crystallization of zeolites takes place at preferential directions at relatively lower pH values according to the literature [5].

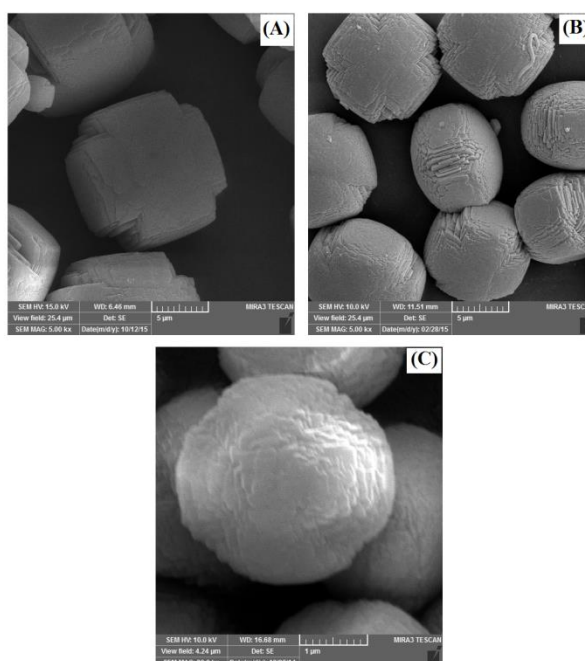


Figure 2. SEM images of (A): [B]-MFI(9), (B): [B]-MFI(10) and (C): [B]-MFI(11).

The doxorubicin loading efficiency was relatively low for all samples (2%, 21% and 27% for samples prepared at pH values of 9, 10 and 11, respectively). It is noteworthy that the size of doxorubicin molecules is larger than the pore diameter of [B]-MFI zeolites, thus the drug molecules cannot enter to the pores and channels of zeolites. The adsorption of drug molecules takes place at external surface of zeolites due to the electrostatic interaction between doxorubicin molecules and zeolite surface.

The highest loading efficiency was reported for [B]-MFI (11) zeolite and this sample was subjected to the MTT assay. The results of cytotoxicity experiments are presented in Figure 3. As can be seen in Figure 3, the unloaded zeolite particles have not significant effect on the cell viability, which confirms the excellent biocompatibility of borosilicate





4<sup>th</sup> Iran National Zeolite Conference  
Golpayegan University of Technology, Golpayegan, Iran  
August 23-24, 2017



zeolites. On the other hand, drug loaded zeolite exhibited increased cytotoxicity and the cell viability decreased to ~14% after incubation for 48h. These results prove that the boron containing MFI- type zeolites can be considered as efficient drug delivery systems.

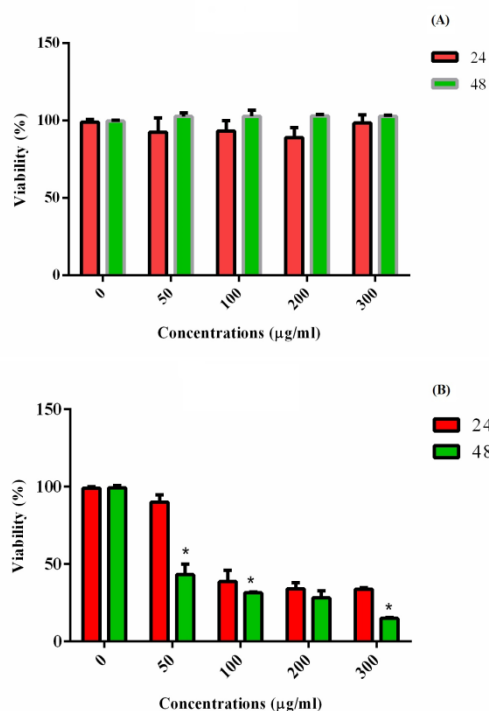


**Figure 3.** In vitro cytotoxicity of (A): [B]-MFI(11) and (B): drug- loaded [B]-MFI(11) against MDA-MB-231 cells.

#### 4. Conclusions

The [B]-MFI zeolites was synthesized by hydrothermal method at different pH values. The SEM images proved the effect of pH value on the morphology and particle size of zeolites. The efficiency of zeolites as DDSs was investigated. The drug-loaded zeolite showed high cytotoxicity against MDA-MB-231 cell lines in spite of low value of loaded drug.

#### Acknowledgments

We would like to thank the University of Tabriz and Iranian Nanotechnology Initiative Council for the financial support of this project.

#### References

- 1) R. Amorim, N.I. Vilaça, O. Martinho, R.M. Reis, M. Sardo, J.o. Rocha, A.n.M. Fonseca, F.t. Baltazar, I.C. Neves, *J. Phys. Chem. C* **2012**, 116(48), 25642-25650.
- 2) A. Datt, E.A. Burns, N.A. Dhuna, S.C. Larsen, *Micropor. Mesopor. Mater.* **2013**, 167, 182-187.
- 3) A. Tavoraro, I.I. Riccio, P. Tavoraro, *Micropor. Mesopor. Mater.* **2013**, 167, 62-70.
- 4) F. Trudu, G. Tabacchi, A. Gamba, E. Fois, *J. Phys. Chem. A* **2007**, 111, 11626-11637.
- 5) N.G. Vargas, S. Stevenson, D.F. Shantz, *Micropor. Mesopor. Mater.* **2013**, 170, 131-140.



# 4<sup>th</sup> Iran National Zeolite Conference

## Golpayegan University of Technology, Golpayegan, Iran

### August 23-24, 2017



## Synthesis and characterization of hierarchically-structured zeolite Na-P

Mohammad Sepehrian, Mansoor Anbia\*, Esmat Koohsaryan

Research Laboratory of Nanoporous Materials, Faculty of Chemistry, Iran University of Science and Technology  
Tehran, P.O. Box 16846-13114, Iran

\*Email :Mansoor Anbia: anbia@iust.ac.ir

### 1. Introduction

Molecular sieves are known as porous materials including carbons, oxides, zeolites and glasses etc. Among these, the most attractive candidates for industrial and agricultural applications could be referred to the zeolitic structures due to their fantastic features such as outstanding chemical and hydrothermal stability, being not toxic materials and eco-friendly compounds as well as high surface area [1-3]. In recent year, there has been many interests in the investigating synthesis strategies of hierarchical zeolites especially low-silica ones like clinoptilolite and faujasite-type zeolites owing to the positive effects of auxiliary porosity introduction into zeolite frameworks on their adsorptive and catalytic applications [4-6]. So far, preparation of zeolite P as one of the low-silica microporous materials has been studied by many authors; because it is a useful zeolitic framework to separate tiny liquid or gas molecules and remove noxious heavy metals from wastewaters. Moreover, it could be utilized in the detergent industries as builders [7,8]. However, to the best of our knowledge, there were few papers investigation the synthesis of hierarchical zeolite Na-P. So, the aim of this study was to evaluate the synthetic conditions of zeolite P formation which could be a novel sorbent in various industries.

### 2. Experimental

The used reagents for the preparation of hierarchical zeolite P were sodium aluminate, sodium silicate, sodium hydroxide and distilled water. The alumina and silica precursors were mixed together in an alkali media to form a gel transferred into a stain-less autoclave and was kept under certain temperature during a period of time. Then the final white power product was filtered, washed and dried in an oven overnight. As-prepared zeolite P was characterized using different standard techniques such as scanning electron microscopy (SEM, VEGA||TESCAN), X-ray diffraction pattern (XRD, X-ray diffractometer JEOL-JDX 8030, by Cu-K $\alpha$  radiation operating at 30 kV and 20 mA), Fourier transform infrared spectroscopy (FT-IR spectrometer, SHIMADZU-8400-s) and nitrogen adsorption-desorption analysis (Belsorp-Max equipment, BEL Japan Inc., Japan).

### 3. Results and discussion

As can be seen in Fig. 1, the characteristic peaks of zeolite P structures have been appeared in the X-ray diffraction pattern of as-prepared sample at  $2\theta$ : 12.4, 17.8, 21.7, 28.2 and 33.3 degrees which are in fit with them reported in the references [5].



4<sup>th</sup> Iran National Zeolite Conference  
Golpayegan University of Technology, Golpayegan, Iran  
August 23-24, 2017

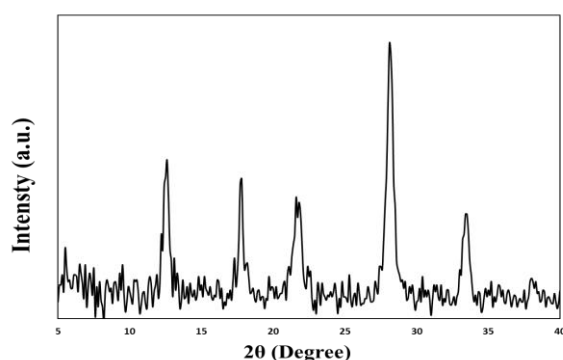


Figure 1. X-ray diffraction pattern of as-synthesized hierarchical zeolite Na-P.

Moreover, from SEM images (Fig. 2), the tennis ball-like crystals with rough external surface are observable for the zeolite P. The average particle size is estimated ca. 2  $\mu\text{m}$ . It seems that each particle is constructed from agglomeration of numerous small individual units while large pores are formed between them.

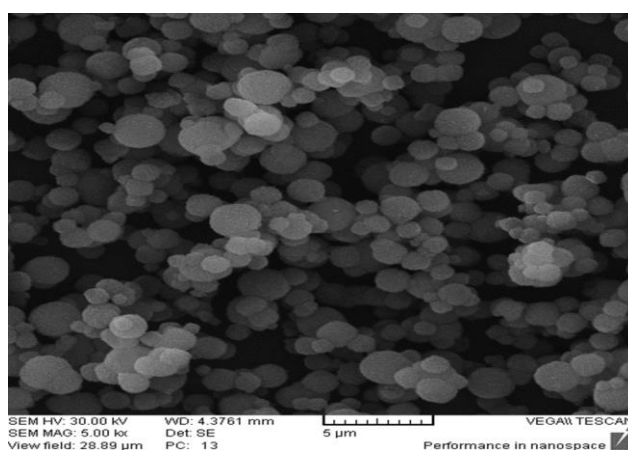


Figure 2. SEM images of as-synthesized hierarchical zeolite Na-P.

Fig. 3 represents the FT-IR spectra of zeolite P. Generally, the bands assigned to the zeolitic structures are present in the wavenumber range of 400-1200  $\text{cm}^{-1}$ .

For example, broad bands at approximately 1000  $\text{cm}^{-1}$  belong to the internal asymmetric stretching vibration of tetrahedra T-O (T is Al or Si atoms). Internal bending vibration of (Si or Al)-O also occurs at 400  $\text{cm}^{-1}$  and peak exhibited at nearly wavenumber of 1650  $\text{cm}^{-1}$  is related to the transfiguring vibration of water molecules bounded in the zeolite channels.

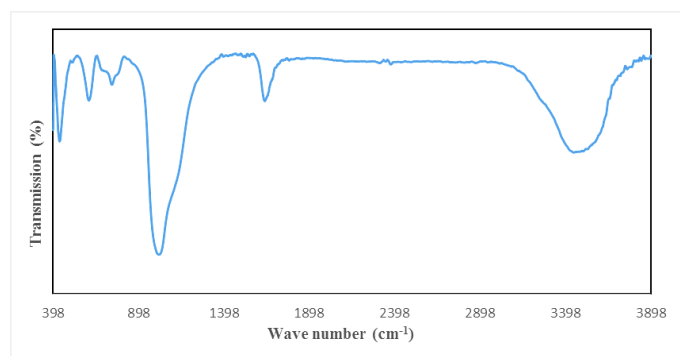


Figure 3. FT-IR spectra of as-synthesized hierarchical zeolite Na-P.



# 4<sup>th</sup> Iran National Zeolite Conference

## Golpayegan University of Technology, Golpayegan, Iran

### August 23-24, 2017



In addition, BET (Brunauer, Emmett, and Teller) specific surface area for the end product was calculated more than 60 m<sup>2</sup>/g and the presence of mesopores in the structure was determined using BJH (Barrett-Joyner-Halenda) method.

#### 4. Conclusions

The preparation of hierarchically-structured zeolite Na-P was performed successfully via a hydrothermal method. The results of characterization techniques confirmed the formation of bi-model porosity system in zeolite P structure with tennis ball-like morphology. It is anticipated the synthesized sample would be a promising materials with enhanced adsorptive properties in different fields of industries.

#### Acknowledgments

We acknowledge the financial support from Iran University of Science and Technology (IUST) and Arvand Petrochemical Company.

#### References

- 1) E. Koohsaryan, M. Anbia, *Chin. J. Catal.* **2016**, 37, 447.
- 2) V. Garshasbi, M. Jahangiri, M. Anbia, *Appl. Surf. Sci.* **2017**, 393, 225.
- 3) M. Anbia, F. Mohammadi Nejati, M. Jahangiri, A. Eskandari, V. Garshasbi, *J. Sci. I. R. Iran.* **2015**, 26, 213.
- 4) M. Anbia, E. Koohsaryan, A. Borhani, *Mater. Chem. Phys.* **2017**, 193, 380.
- 5) S. K. Saxena, N. Viswanadham, *Appl. Surf. Sci.* **2017**, 392, 384.
- 6) K. Möller, T. Bein, *Chem. Soc. Rev.*, **2013**, 42, 3689.
- 7) Z. Huo, X. Xu, Z. Lü, J. Song, M. He, Z. L. Q. Wang, L. Yan, *Microporous Mesoporous Mater.* **2012**, 158, 137.
- 8) J. Behin, H. Kazemian, S. Rohani, *Ultrason. Sonochem.* **2016**, 28, 400.



4<sup>th</sup> Iran National Zeolite Conference  
Golpayegan University of Technology, Golpayegan, Iran  
August 23-24, 2017



**Preparation and characterization of nano hydroxyapatite / Clinoptilolite and the removal of environmental pollutants Fluorine**

S. Jalalvandi Fard<sup>a</sup>, M. Zendehei<sup>a\*</sup>, M.Haddadi<sup>a</sup>

<sup>a</sup> Department of Chemistry, Faculty of Science, Arak University, Arak38156-8- 8349; Iran

\*Email: m-zendehei@araku.ac.ir

### 1. Introduction

The increasing population and urbanization of society caused to increase production and distribution of toxic chemicals, into the environment [1]. One of the known disruptors is Fluoride. Since most types of pollution, water pollution is caused by fluorine, the concentration Fluoride is one of the most important factors in choosing safe drinking water. In the 1930s in America, it was found that the cause of death and paralysis in humans is fluorine. According to one of organizations of Health America in this areas, bone cancer that is caused by fluoride is three times [2]. In this study NaP:HAp nanocomposite was used as an effective adsorbent for removal of fluoride from aqueous solution and Also in this study, Box-Behnken design with three-level and four-factor has been employed determination of effective process parameters. Fluoride uptake quantitatively evaluated using the Langmuir and Freundlich models [3].

### 2. Experimental Part or Theoretical Details

The starting materials used in this study included, calcium nitrate (CNT), potassium dihydrogen phosphate (KPP), ammonia and deionized water. All chemical materials supplied by Merck and aqueous solutions were made dissolving them in deionized water. XRD, FT-IR, TGA,EDX and SEM were used to characterization of obtained product. At first NaP zeolite and hydroxyapatite was prepared separately. Clinoptilolite Natural Zeolite has been developed of Semnan mine. and then nanocomposite of NaP:HAp synthesized with hydrothermal method at 40°C for 24h. Batch experiments were carried out using synthetic NaP:HAp. The effect of solution PH (4-11), temperature (25-55 °C), initial adsorbent dose (1-3 g) and initial fluoride concentration (5-25 mg/L) on removal of fluoride from aqueous solution were also investigated. Fluoride uptake quantitatively evaluated using the Langmuir and Freundlich models.

### 3. Results and discussion

X-ray diffraction pattern of NaP:HAp is shown in Fig.1.a A, Some diffraction peaks such as  $2\theta = 31.03^\circ$ ,  $34.26^\circ$ ,  $27.72^\circ$  and  $25.82^\circ$  can be indexed as the HAp and  $2\theta = 22.34$ ,  $9.90^\circ$ ,  $11.18^\circ$  can be indexed as the NaP. Similar to other observation found in the literature, both cactus-like and diamond like morphology with the 1-2  $\mu\text{m}$  size of each diamond-shape particle were appeared in the SEM image of NaP:HAp nanocomposite. The result in Fig.1.b showed that the synthesized Nanocomposite powder were particle Shape with the diameter of 30-40 nm and were made.



# 4<sup>th</sup> Iran National Zeolite Conference

## Golpayegan University of Technology, Golpayegan, Iran

### August 23-24, 2017

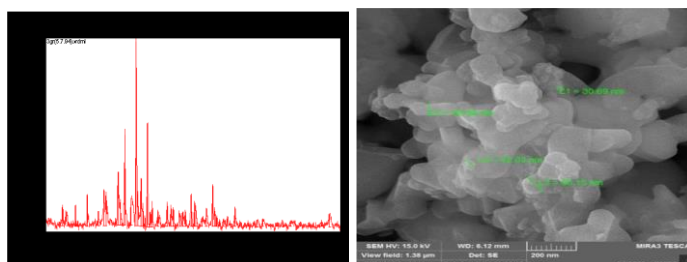


Figure 1. (a) XRD pattern of NaP:HAp nanocomposite, (b) SEM micrograph of NaP:HAp nanocomposite

In the present work, the prediction of total adsorption by NaP:HAp nanocomposite was done by using Box-Behnken design with three-level and four-factor has been employed determination of effective process parameters. Fluoride uptake quantitatively evaluated using the Langmuir and Freundlich models. The rate of adsorption was rapid and followed pseudo-second-order kinetics for this adsorbent. In this study, pH (range 4-11), initial concentration (range of 5-25 ppm), adsorbent dosage (range 1-3 g/L) and temperature (range 25-55 °C) was chosen as an input variable, and percent removal of fluoride from aqueous solution was selected as an output variable. As shown in Fig.2, it was tried to showing correlation between predicted data and experimental data. We can see a high degree of correlation between ANN outputs (predicted data) and the corresponding targets (experimental data). Test outputs showed a very small deviation in efficiency values from the experimental data.

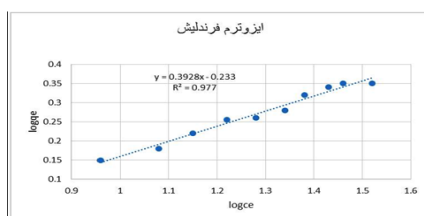


Figure 2. Freundlich Adsorption Isotherm

#### 4. Conclusions

The significant advantages of this nanocomposite are high capacity for adsorption of fluoride, high stability in different PH and temperature and reusability of sorbent makes this method nearly green and environmentally friendly Fluoride uptake quantitatively evaluated using the Langmuir and Freundlich models. The rate of adsorption was rapid and followed pseudo-second-order kinetics for this adsorbent. The fluoride sorption on Clin: HAP. The model and the test data are in perfect match with  $R^2$  value of 0.977.

#### Acknowledgments

Thanks are due to the Iranian Nanotechnology Initiative and the Research Council of Arak University of Technology and Center of Excellence in the Chemistry Department of Arak University of Technology for supporting of this work.

#### References

- [1] D. P. Mohapatra, S. K. Brar, R. D. Tyagi, R. Y. Surampalli, Chemosphere 2010, 78, 923-941.
- [2] S.P. Kamble, P. Dixit, S.S. Rayalu, N.K. Labhsetwar, Defluoridation of drinking water using chemically modified bentonite clay, Desalination 249 (2009) 687-693.
- [3] M.Trigo, J. peric, " interaction of the zeolitic luff with zn-containing simulated, Vol.260,PP.166-175



4<sup>th</sup> Iran National Zeolite Conference  
Golpayegan University of Technology, Golpayegan, Iran  
August 23-24, 2017



**Sorption and immobilization of cesium by natural clinoptilolite zeolite modified with nickel hexacyanoferrate**

Parisa Sedighi<sup>a</sup>, Reza Davarkhah<sup>b</sup>, Armen Avanes<sup>a</sup>, Hamid Sepehrian<sup>\*b</sup>

<sup>a</sup>Department of Chemistry, University of Maragheh, Maragheh, 5518183111, Iran

<sup>b</sup>Nuclear Science and technology Research Institute, P. O. Box 11365-8486, Tehran, Iran

\*Email: hsepehrian@aeoi.org.ir

**Abstract**

In this study, Nickel Hexacyanoferrate-Clinoptilolite composite (NiHCF-Clino) was prepared and used as an ion exchanger for the removal of cesium from aqueous solution. The effect of various parameter like the pH, contact time, temperature and initial concentration of cesium on adsorption efficiencies of NiHCF-Clino has been studied systematically by batch experiments. The results show that maximum adsorption capacity of cesium onto NiHCF-Clino adsorbent was found to be 108.69 mg.g<sup>-1</sup>. Then, the cesium-loaded adsorbents were heated at different temperature and the leach test carried out on all the heat-treated samples. Leaching results show that immobilization ability of ion cesium in the heated-treated materials increased as the treatment temperature was increased.

**1. Introduction**

Advancement of nuclear technology has resulted in large scale release of radioactive cesium isotopes into environment since <sup>137</sup>Cs is among the main fission products in radioactive wastes [1]. Often, the liquid radioactive wastes are managed by a two-step procedures: (1) removal of hazardous radionuclides by ion-exchange resins and (2) subsequent storage of the spent ion-exchanger resins in a cement matrix prior to encapsulation in stainless steel drums. A new strategy is sorption and stabilization them respectively in a natural or synthetic zeolite framework [2]. It was found that among organic and inorganic ion exchangers, the inorganic type has several superior qualities required for the treatment of waste streams compared to organic resins.

These are their higher thermal stability and good compatibility with the final waste forms. Several inorganic ion exchanger such as zeolites, sodium titanates, silicotitanates, metal oxides, and hexacyanoferrates are in use for the treatment of wastes. Hexacyanoferrates have a high selectivity toward cesium [3]. Previous research pointed out that ceramization of zeolitic sludges entrapping polluting cations may be a possible alternative procedure to safely dispose harmful species. In particular, it has proven that pre-formed compacts of zeolitic sludge can be transformed by firing into stable alumino-silicate structures, which are highly resistant to leaching and possibly also of interest as ceramic materials [4].

The aim of this paper is to evaluate the zeolite uptake capacity of cesium, using clinoptilolite zeolite modified by Nickel hexacyanoferrate (NiHCF-Clino) as adsorbent. The effect of various parameter like the pH, contact time, temperature and initial concentration of the metal ion cesium adsorption efficiencies of NiHCF-Clino has been studied systematically by batch experiments. Then, the cesium-loaded adsorbents were heated at different temperature and the leach test carried out on all the heat-treated samples.



# 4<sup>th</sup> Iran National Zeolite Conference

## Golpayegan University of Technology, Golpayegan, Iran

### August 23-24, 2017



## 2. Experimental

### 2.1. Reagents

All the chemical used were of analytical grade from Merk (Darmstadt, Germany), except cesium nitrate ( $\text{CsNO}_3$ ) which was supplied by (Sigma Aldrich, USA).

### 2.2. Preparation of NiHCF- loaded zeolite

Five grams of clinoptilolite zeolite (sabzevar) dried at 200 °C was contacted with a 100 mL solution of 0.5 M  $\text{Ni}(\text{NO}_3)_2$  under reduced pressure 25 °C for 3 hours and then washed with acetone and air- dried at 90 °C for 3 hours. Clinoptilolite impregnated with  $\text{Ni}(\text{NO}_3)_2$  was reacted with a 50 mL solution of 0.5 M  $\text{K}_4[\text{Fe}(\text{CN})_6]$  to form NiHCF precipitates in the surface of clinoptilolite zeolite. Then clinoptilolite was washed with deionized water and acetone, air-dried at 90 °C for 3 hours, and finally stored in a sealed vessel over a saturated NaCl solution, then clinoptilolite was washed deionized water and air- dried at 90 °C for 3 hours.

### 2.3. Procedure for sorption studies

The adsorption studies of the cesium ion on the NiHCF-Cli-no adsorbent were carried out using batch method [5]. In this procedure, 20 mg of adsorbent was dispersed in 20 mL solution of 50  $\text{mg.L}^{-1}$  cesium ion. The mixture was shaken (~150 rpm) for a preselected period of time using a water shaker bath. Then, it was filtered and the amount of the cesium ion was measured using an atomic absorption spectrometer (AAS). The sorption capacity ( $q$ ,  $\text{mg.g}^{-1}$ ) was calculated using the equation (1).

$$q = (C_i - C_f) \times \frac{V}{m} \quad (1)$$

where  $C_i$  and  $C_f$ , are the initial and final concentrations ( $\text{mg.L}^{-1}$ ) of cesium,  $V$  is the volume of the initial solution (mL), and  $m$  is the mass of the adsorbent (g).

### 2.4. Procedure for immobilization and leach test

For cesium immobilization studies, 0.4 g pellets of the Cs-sorbed NiHCF-Cli-no were prepared using a hydraulic press and a stainless steel extruder at 400  $\text{g.cm}^{-2}$  load pressure. The pellets were successively heated at 60, 300, 60, 900 and 1200 °C for 6 h. To describe the leaching of cesium from heat-treated samples, two procedures were used .

## 3. Results and discussion

### 3.1. Characterization of the NiHCF-Cli-no

Infrared spectroscopy was used to check the cyano group in NiHCF on the clinoptilolite. the FT-IR spectra of clinoptilolite and NiHCF-Cli-no are shown in Figure 1. The plot of the NiHCF-Cli-no is similar to that of Cli-no, except the sharp and strange peak at 2092  $\text{cm}^{-1}$  corresponding to the  $\text{C}\equiv\text{N}$  stretching vibration [6]. Which offers the evidence that NiHCF is loaded on the clinoptilolite after carefully isolated from the mentioned preparation system.





4<sup>th</sup> Iran National Zeolite Conference  
Golpayegan University of Technology, Golpayegan, Iran  
August 23-24, 2017

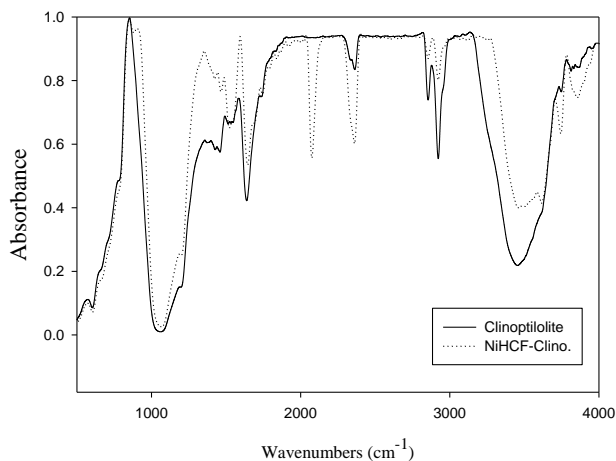


Figure 1. FT-IR spectra of clinoptilolite and NiHCF-Clino

### 3.2. pH effects on the sorption of cesium

The pH solution is a crucial factor in metal sorption. In this study, the effect of pH on cesium adsorption onto NiHCF-Clino was studied in the rang 1.0-9.0. (Figure 2) shows the dependence of the adsorption capacity of the NiHCF-Clino on initial pH of cesium solution. Cesium sorption NiHCF-Clino was low in pH less than 4.0. that shows a significant competition of H<sup>+</sup> ions with cesium ions for the same site binding of sorbent. Significantly less Cs sorbed by the studied NiHCF-Clino at pH 9.0. A possible formation of carbonate or hydroxide species at this high pH is likely to caused. Complexation of Cs<sup>+</sup> ions resulting to lower Cs amount available for sorption [7] . According to the results of this initial experiment, further adsorption investigation were performed at natural pH value of 6.5 as optimal value.

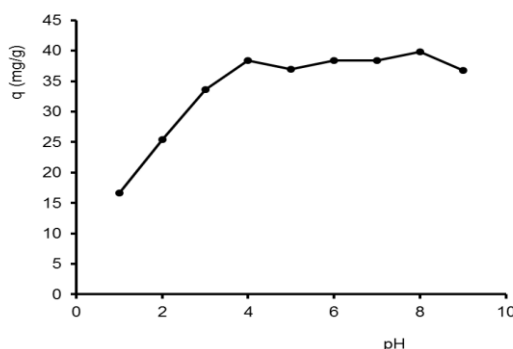


Figure 2. Effect of pH on cesium adsorption onto NiHCF-Clino .

### 3.3. Temperature effect on the sorption of cesium

The effects of temperature on cesium sorption onto the zeolite were studied at different temperatures (25, 35, 45, 55 and 65°C). The results show that temperature doesn't have significant effect on cesium sorption.

### 3.4. Effect of contact time (kinetics of sorption )

In order to investigate the controlling mechanism of adsorption processes such as mass transfer and chemical reaction, the pseudo-first-order and pseudo -second-order equations are to applied to model the kinetics of cesium adsorption onto NiHCF-Clino. the pseudo-first-order kinetic and the pseudo-second-order kinetics are expressed by equations (2) and (3), respectively .



# 4<sup>th</sup> Iran National Zeolite Conference

## Golpayegan University of Technology, Golpayegan, Iran

### August 23-24, 2017



$$\log(q_e - q_t) = \log q_e - \frac{k_1}{2.303} t \quad (2)$$

$$\frac{t}{q_t} = \frac{1}{k_2 q_e^2} + \frac{t}{q_e} \quad (3)$$

where  $q_e$  and  $q_t$  are the sorbed metal in  $\text{mg.g}^{-1}$  on the sorbent at equilibrium and time  $t$ , respectively,  $k_1$  is the constant of first-order sorption in  $\text{min}^{-1}$  and  $k_2$  is the rate constant of second-order sorption in  $\text{g.mg}^{-1}.\text{min}^{-1}$  [8].

As seen in (Figure 3), the removal of cesium ions from aqueous solution by NiHCF-Clino as a function of contact time showed that 180 min was sufficient for the adsorption equilibrium to be achieved. The rate of metal ions adsorption, one of the important characteristics that define the efficiency of sorption, was evaluated by fitting the experimental data to the pseudo-first-order and pseudo-second-order kinetics. The parameters of the kinetic models and the regression correlation coefficients ( $R^2$ ) are listed in (table 1). From the  $R^2$  and the predicted  $q_e$  it was found that the pseudo-second-order kinetic model fitted the kinetic data of the adsorbent NiHCF-Clino better than that of the pseudo-first-order. The confirmation of pseudo-second-order kinetics indicates that the concentrations of both sorbate (cesium ions) and sorbent (NiHCF-Clino) are involved in the rate determining step of the sorption process [9].

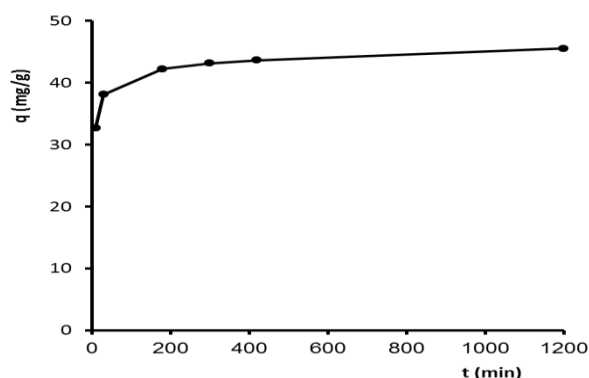


Figure 3. Sorption kinetics of cesium onto NiHCF-Clino.

Table 1. Kinetic adsorption parameters obtained using pseudo-first-order and pseudo-second-order models (initial concentration of cesium ion  $50 \text{ mg.L}^{-1}$ )

Pseudo-first-order			Pseudo-second-order		
$k_1$	$q_e$ ( $\text{mg.g}^{-1}$ )	$R^2$	$k_2$	$q_e$ ( $\text{mg.g}^{-1}$ )	$R^2$
0.004	9.7	0.901	0.002	45.8	0.999

### 3.5. Effect of initial metal ion concentration

In order to determine the relationship between the amount of cesium ions adsorbed on the adsorbent surface and the concentration of remaining metal ions in the aqueous phase, the adsorption isotherm studies were performed. Among various binding models, the Langmuir and Freundlich adsorption isotherm are mathematically expressed in Equations (4) and (5), respectively [10,11].

$$\frac{1}{q_e} = \frac{1}{q_m} + \frac{1}{q_m K_1 C_e} \quad (4)$$



# 4<sup>th</sup> Iran National Zeolite Conference

## Golpayegan University of Technology, Golpayegan, Iran

### August 23-24, 2017



$$\log q_e = \log K_f + \left(\frac{1}{n}\right) \log C_e \quad (5)$$

Where,  $q_m$  is the monolayer adsorption capacity of the adsorbent ( $\text{mg.g}^{-1}$ ) and  $k_l$  is the Langmuir constant,  $C_e$  ( $\text{mg.L}^{-1}$ ) is the equilibrium concentration of the adsorbate in solution,  $k_f$  is the maximum adsorption capacity ( $\text{mg.g}^{-1}$ ),  $k_f$  Freundlich constant for a given adsorbate and adsorbent at a particular temperature. The experimental, Langmuir and Freundlich model isotherms were shown in figure 4. The parameters for the Langmuir and Freundlich isotherms were evaluated based on the data from present experimental system (Table 2), with the Langmuir fitting the data better than the Freundlich as seen, the calculated maximum sorption capacity ( $q_{max}$ ) was  $108.7 \text{ mg.g}^{-1}$ .

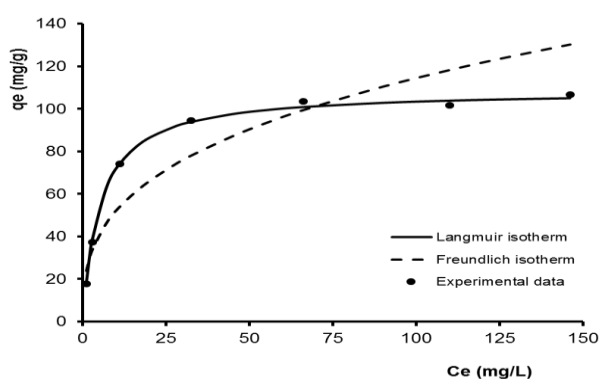


Figure 4. Adsorption isotherms of NiHCF-Clino for cesium adsorption.

Table 2. Langmuir and Freundlich isotherm model fitting parameters for cesium.

Models	Fitting parameters		
	Langmuir	$R^2$	$K_l (\text{L.mg}^{-1})$
Freundlich	0.99	0.19	108.69
	$R^2$	$K_f (\text{mg.g}^{-1}.\text{mg}^{-m}.\text{L}^m)$	m
	0.89	23.93	0.33

## 4. Conclusions

A natural zeolite sorbent (clinoptilolite, sabzevar) was modified with nickel hexacyanoferrate that showed high efficiency for the removal of cesium ions from aqueous solutions. The maximum sorption capacity of cesium onto NiHCF-Clino was found to be  $108.69 \text{ mg.g}^{-1}$  in the optimal conditions. The immobilization and leach test results show that immobilization ability was increased with increase of the treatment temperature .

## Acknowledgments

The authors are thankful to the staff of material and nuclear fuel research school for providing research facilities.

## References

- 14) S. B, L. J. C, *Cem. Conser. Res* **1999**, 29, 479-485.
- 15) P. B, D. C, B. L, C. C, *J. Nucl. Mater* **2004**, 324, 183-188.
- 16) R. S, A. N, R. G, R. Z, *J. Radioanal. Nucl. Chem* **2010**, 284,461-469.
- 17) B. L, A. A. C, C. C, *J. Hazard. Mater* **2006**, 137, 1206-1210.
- 18) S. V, H. T, R. C, H. S, *Desalination water treat* **2015**, 55, 1220-1228.
- 19) A. N, R. S, M. M, H. A, R. Z, *Chem. Eng. J* **2011**, 172, 572-580.
- 20) F. G, C. H, A. C, D. G, *J. Hazard. Mater* **2009**, 161,499-509.
- 21) N. B, S. K, *Sep.Purif. Technol* **2004**, 39, 189-200.
- 22) C.C. L, M. K.W, Y.S. L, *Ind. Eng. Chem. Res* **2005**, 44, 1438-1445.



4<sup>th</sup> Iran National Zeolite Conference  
Golpayegan University of Technology, Golpayegan, Iran  
August 23-24, 2017



- 23) A. S, O. G, A. O, *J. Hazard. Mater* **2009**, 161,499-509.  
24) M. A, M. K, M. D, O. D, *J. Colloid Interface Sci* **2005**, 291,309-318.

## Synthesis and Characterization of a New Metal-Organic Framework (MOF) Nanostructure

Iran Sheikhshoaie<sup>a\*</sup>, Ahmad Khajeh Ebrahimi<sup>a</sup>

<sup>a</sup>*Department of Chemistry faculty of science, Shahid Bahonar University, Kerman, Iran*

<sup>\*</sup>*Email: [i\\_shoaie@yahoo.com](mailto:i_shoaie@yahoo.com)*

### 1. Introduction

Metal organic frameworks (MOFs) due to unique properties like low density, biocompatibility, high surface area, and convenient synthesis use in many applications in gas storage [1], removal of pollutions [2], catalysis [3], imaging [4], optical datum storage[5], and drug carrier[6]. MOFs can be synthesized through a variety of different techniques such as solvothermal [7], ultrasonic [8], microwave [9], interface reaction[10], and mechanochemical method [11] which have been developed for the synthesis of inorganic and organic polymeric structures.

### 2. Experimental Part or Theoretical Details

The Cu-MOF was synthesized by equimolar (0.1 mmol) solutions of Cu (OAc)<sub>4</sub> · 2(H<sub>2</sub>O) and benzene-1,2,4,5-tetracarboxylic acid (H<sub>4</sub>BTEC) were prepared individually in water (10 ml) and Hexane (10 ml), respectively. The solution was stirred for 10 min until a uniform solution obtained. Then the above two solutions were vigorously mixed until a blue precipitate obtained. The stirring continued for about 2 hours, and then the blue precipitate of the MOF was separated by centrifugation for 5 min. The separated Cu-MOF crystals were washed with ethanol and water. Finally obtained product was dried in an oven in the temourature of 70 °C.

### 3. Results and discussion

The prepared MOFs compounds were characterized by some common spectroscopic methods. Fourier transform infrared (FT-IR) spectrum was investigated for study important functional groups of Cu-MOF. A broad adsorption between 3500 cm<sup>-1</sup> to 2800 cm<sup>-1</sup> is related to stretch vibrations of carboxylic groups and solvent molecules in this structure. Also, two stretch peaks are observed at 1573 cm<sup>-1</sup> and 1383 cm<sup>-1</sup> that related to asymmetric stretching vibrations and symmetric stretching vibrations of H<sub>4</sub>BTEC ligand, respectively. Moreover, the absence of the absorption bands from 1670 cm<sup>-1</sup> to 1810 cm<sup>-1</sup> indicates the complete deprotonation of HBTEC ligands [12]. The absorption peak of copper-oxygen in metal organic framework appeared at 590 cm<sup>-1</sup>. It can be concluded that COOH groups coordinates with Cu atoms when the framework forms.



# 4<sup>th</sup> Iran National Zeolite Conference

## Golpayegan University of Technology, Golpayegan, Iran

### August 23-24, 2017



The thermal behavior of the Cu-metal organic framework was investigated by thermogravimetric analysis (TGA) and differential thermal analysis (DTA) methods. The thermal decomposition of Cu-MOF occurs in two steps. The first step, 19% weight loss occurs in 100 °C to 150°C that it is related to the release of solvents in the MOF structure and in the second step, 34.43% weight loss of starting at 325 °C which is due to decomposition of H<sub>4</sub>BTEC from the framework. TGA curve shows that the structure is stable up to approximately 325°C and then, the Cu-MOF structure starts to collapse at a higher temperature of 325°C. The DTA curve displays two phase change that it is in good agreement with TGA analysis.

X-ray diffraction analysis was carried out to approve the phase purity. The XRD pattern showed two peaks at  $2\theta = 27.5$  and  $40.7$  which are equal to the standard patterns for Cu. Also, other observed peaks in the patterns that related to the H<sub>4</sub>BTEC ligand. Also we observed rod morphology for Cu-MOFs at the synthesized procedure.

According to obtained data from nitrogen adsorption (BET), the Cu-MOFs have a surface area of 1222, the pore diameter of and volume pore of 11123 which confirm the mezoporous structure of samples. MOFs with mezoporous structure can be used in several applications. In addition, the photocatalytic degradation process can be explained in terms of the pseudo-first-order kinetic model. Removal of Malachite Green (MG) by Cu-MOF in different synthesis condition at room temperature is accomplished.

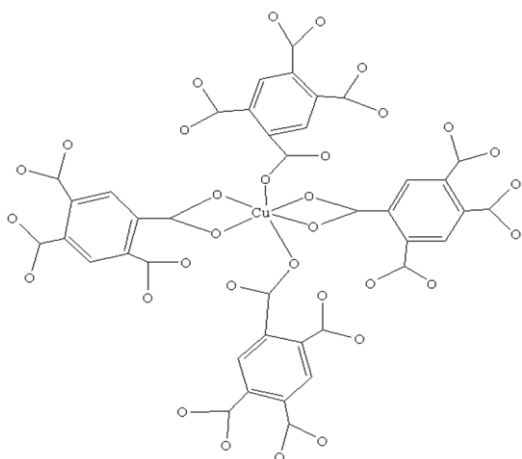


Figure 1. The purpose structure of prepared MOF.

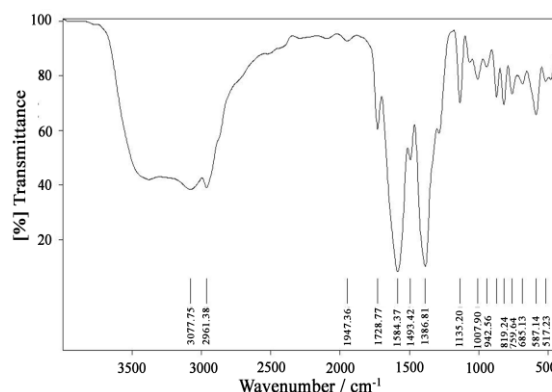


Figure 2. The FT-IR spectra of prepared MOF.

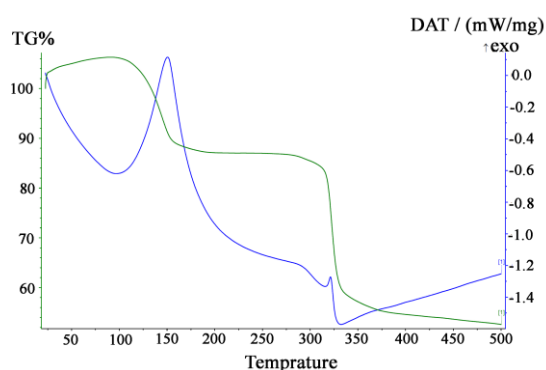


Figure 3. The DTA/TGA spectra of prepared MOF.

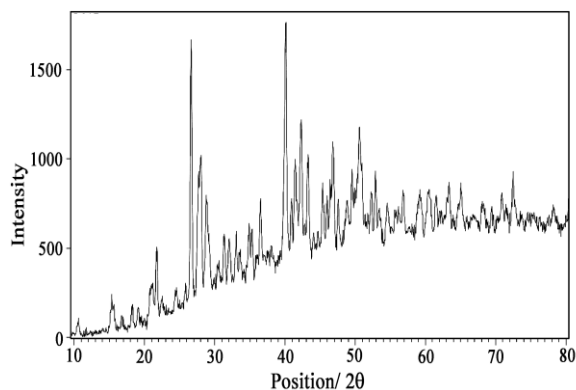


Figure 4. XRD pattern of prepared MOF.



# 4<sup>th</sup> Iran National Zeolite Conference

## Golpayegan University of Technology, Golpayegan, Iran

### August 23-24, 2017



#### 4. Conclusions

In this study, a new Cu (II)-based metal-organic framework (MOF) has been successfully synthesized by using tetracarboxylate ligand under interface reaction method. Morphology of the Cu-MOF was studied by BET, SEM, XRD, DTA/TGA.

#### References

- 1) P. Manna, S.K. Das, *Crystal Growth & Design* 2015, 15, 1407.
- 2) H.F. Clausen, R.D. Poulsen, A.D. Bond, M.-A.S. Chevallier, B.B. 2005, 178, 3342.
- 3) G. Sargazi, D. Afzali, N. Daldosso, H. Kazemian, N. Chauhan, Z. Sadeghian, T. Tajerian, A. Ghafarinazari, M. Mozafari, 2015, 27, 395.
- 4) F. Israr, D. Chun, Y. Kim, D.K. Kim, *Ultrasonics Sonochemistry*, 2016, 31, 93.
- 5) A.D. Katsenis, A. Puškarić, V. Štrukil, C. Mottillo, P.A. Julien, K. Užarević, M.-H. Pham, T.-O. Do, S.A. Kimber, P. Lazić, 2015, 6, 2146.
- 6) M. Pilloni, F. Padella, G. Ennas, S. Lai, M. Bellusci, E. Rombi, F. Sini, M. Pentimalli, C. Delitala, A. Scano, 2015, 213, 14.
- 7) M. Stavola, D.M. Krol, W. Weber, S. Sunshine, A. Jayaraman, G. Kourouklis, R. Cava, E. Rietman, *Physical Review B*, 1987, 36, 850.
- 8) S. Lagergren, About the theory of so-called adsorption of soluble substances, (1898).
- 9) S. Lagergren, Zur theorie der sogenannten absorption gelöster stoffe, PA Norstedt & Söner, 1898.
- 10) Y. Ho, G. McKay, 1998, 76, 313.
- 11) Y.-S. Ho, *Journal of Hazardous Materials*, 2006, 136, 681.
- 12) J. He, Y. Zhang, Q. Pan, J. Yu, H. Ding, R. Xu, *Microporous and Mesoporous Materials*, 2006, 90, 145.

## Thiol-decorated Fe<sub>3</sub>O<sub>4</sub>@SiO<sub>2</sub> magnetic nanoparticle (Fe<sub>3</sub>O<sub>4</sub>@SiO<sub>2</sub>-SH) for water purification from heavy metals of palladium ions

Sadegh Rostammia<sup>a\*</sup>, Moslem Sadeghi<sup>b</sup>, Mahin Abdollahi<sup>b</sup>, Ahmad Sohrabi Noor,<sup>b</sup>

<sup>a</sup> Organic and Nano Group (ONG), Department of Chemistry, Faculty of Science, University of Maragheh, P.O.B 55181-83111, Maragheh, Iran

<sup>b</sup> Maragheh Chemistry Association, University of Maragheh, P.O. Box 55181-83111, Maragheh, Iran

\*Email :srostammia@gmail.com

#### 1. Introduction

Magnetic nanoparticles of Fe<sub>3</sub>O<sub>4</sub>@SiO<sub>2</sub> have been extensively investigated as advanced adsorbents; however, most studies on surface modification of Fe<sub>3</sub>O<sub>4</sub>@SiO<sub>2</sub> substances were of environmentally inefficient grafting methods, especially thiol functional group as adsorption agent for heavy metals [1-3]. Now, we demonstrated that magnetic nanoparticle of Fe<sub>3</sub>O<sub>4</sub> to Fe<sub>3</sub>O<sub>4</sub>@SiO<sub>2</sub> nanomaterials and then preparation of the Fe<sub>3</sub>O<sub>4</sub>@SiO<sub>2</sub>-SH can be facilely prepared by co-condensation of TEOS with Fe<sub>3</sub>O<sub>4</sub> and then adding of propylthiol silane (PrSH).

In order to eliminate heavy metals such as Pd ions in polluted water, various methods have been developed, including chemical precipitation, ion exchange, adsorption, membrane, coagulation and flocculation, flotation, and electrochemical treatment [3].



4<sup>th</sup> Iran National Zeolite Conference  
Golpayegan University of Technology, Golpayegan, Iran  
August 23-24, 2017



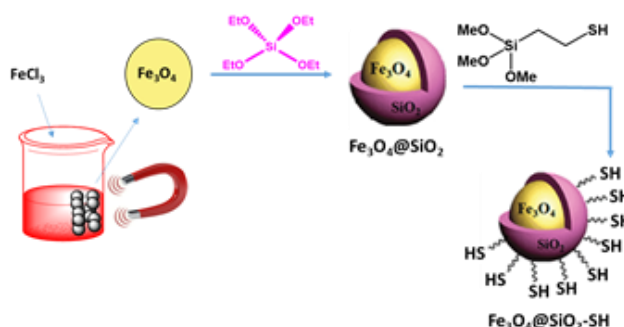
## 2. Experimental

Magnetic  $\text{Fe}_3\text{O}_4$  MNPs were prepared by a solvothermal method as previously reported [3]. Briefly,  $\text{FeCl}_3 \cdot 6\text{H}_2\text{O}$  (1.62 g), NaOAc (14.0 g) and  $\text{Na}_3\text{Cit}$  (15 g) were dissolved in EG (60 mL), after vigorous stirring for 1h, the obtained yellow solution was transferred to controlled Teflonline stainless-steel autoclave, then sealed and heated at 190 °C. After reaction for 12 h, the autoclave was cooled to room temperature. The obtained  $\text{Fe}_3\text{O}_4$  MNPs were washed several times with water and ethanol. Finally, the products were collected with a magnet and then re-dispersed in 80 mL water for further use.

The  $\text{Fe}_3\text{O}_4$  MNPs were then modified sequentially with TEOS and 3-MPTS to introduce thiol groups. Typically, 20 mL magneto-fluid was diluted with 100 mL ethanol, and the mixture was homogenized by ultrasonic for 10 min prior to the addition of 1 mL  $\text{NH}_3$ . After being stirred vigorously for 30 min at 30 °C, 2 mL TEOS was dropped into the solution. The reaction was performed for 45 min and then 1 mL 3-MPTS was introduced and lasted reaction for another 12 h; during the mentioned stages, the amount of 3-MPTS was systematically investigated to correlate the dependence of physicochemical properties of  $\text{Fe}_3\text{O}_4@\text{SiO}_2\text{-SH}$  on the key preparation parameters.

## 3. Results and discussion

The  $\text{Fe}_3\text{O}_4@\text{SiO}_2$  MNPs were directly used for SH-functionalization without any other treatment by an optimized sol-gel process under the following conditions; that is, a mixture of 20 mL magneto-fluid, 100 mL EtOH and 1 mL of  $\text{NH}_3$ , was homogenized by ultrasonic, then 2 mL of TEOS as the hydrolysis precursor was added into the mixture. After the mixture was hydrolyzed, 1 mL 3-MPTS was added to functionalize the MNPs with -SH groups (Scheme 1).



**Scheme 1.** Schematic synthesis of  $\text{Fe}_3\text{O}_4@\text{SiO}_2\text{-SH}$  on the formation of core/shell structures.

Figure 1 shows TEM image of  $\text{Fe}_3\text{O}_4@\text{SiO}_2\text{-SH}$  obtained by a sol-gel modified solvothermal procedure, particles with diameter of about 110 nm are clearly present.



4<sup>th</sup> Iran National Zeolite Conference  
Golpayegan University of Technology, Golpayegan, Iran  
August 23-24, 2017

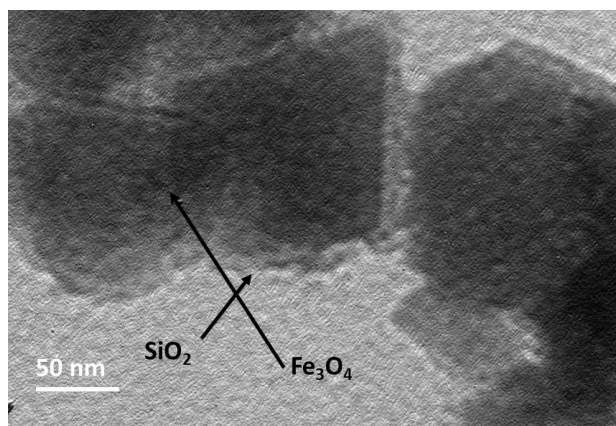


Figure 1. TEM images of Fe<sub>3</sub>O<sub>4</sub>@SiO<sub>2</sub>-SH.

Figure 2 shows the dependence of Fe<sub>3</sub>O<sub>4</sub>@SiO<sub>2</sub>-SH towards PdCl<sub>2</sub> from aqueous solutions. It is clear that with ratio increasing of sulfur to Pd ions based on thiol functionality, the adsorption will have increased. However, MNPs exhibit remarkable PdCl<sub>2</sub> withdrawal capacities. The adsorption results suggest that aqueous PdCl<sub>2</sub> adsorption percentage clearly increases with the SH- group content in the adsorbents, revealing thiol groups worked as efficient chelating sites for PdCl<sub>2</sub> adsorption under performed conditions.

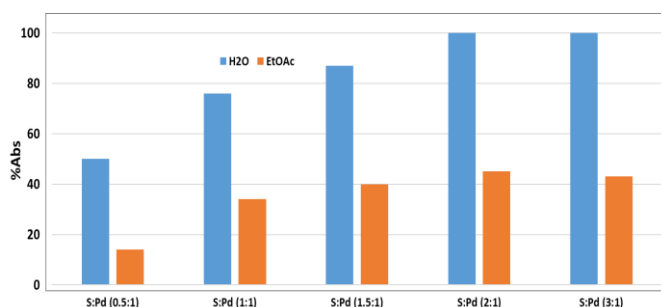


Figure 2. Effect of the Fe<sub>3</sub>O<sub>4</sub>@SiO<sub>2</sub>-SH usage on the adsorption of towards PdCl<sub>2</sub> from aqueous solution.

#### 4. Conclusions

Fe<sub>3</sub>O<sub>4</sub>@SiO<sub>2</sub>-SH with core-shell structure of magnetic nanoparticles of Fe<sub>3</sub>O<sub>4</sub> containing silica core and relatively good loading of SH-functionality were prepared via a proposed sol-gel/hydrothermal modified process. As-synthesized Fe<sub>3</sub>O<sub>4</sub>@SiO<sub>2</sub>-SH were employed in adsorption of PdCl<sub>2</sub> ions from water.

#### Acknowledgments

We acknowledge the financial support from “Vice Chancellor of Socio-Cultural” of University of Maragheh.

#### References

- 1) F. Fu, Q. Wang, *J. Environ. Manage.* **2011**, 92, 407-418.
- 2) J.F. Liu, Z.S. Zhao, G.B. Jiang, *Environ. Sci. Technol.* **2008**, 42, 6949-6954.
- 3) C. Timchalk, M.G. Warner, *Environ. Sci. Technol.* **2007**, 41, 5114-5119.





# 4<sup>th</sup> Iran National Zeolite Conference

## Golpayegan University of Technology, Golpayegan, Iran

### August 23-24, 2017



## Application of Synthesized MIL-101(Cr) Molecular Sieve for Formaldehyde Electrooxidation

Seyed Karim Hassaninejad-Darzi\*, Soheil Gheitani, Masomeh Taherimehr

Department of Chemistry, Faculty of Science, Babol Noshivani University of Technology, Babol, P.O.Box: 47148-71167, Iran.

\*Email: hassaninejad@nit.ac.ir

### 1. Introduction

Metal organic frameworks (MOFs) consist of metal cations or metal-based-clusters linked by organic molecules forming a crystalline network, which after removal of guest species may result in three dimensional structures with permanent porosity [1-2]. MOFs are crystalline materials that can be tailored to specific applications through varying the metals, ligands, and linkers making up the MOF and the number of potential MOFs are virtually limitless. they can be synthesized inexpensively, relatively easily, in high purity, and in a highly crystalline form. these materials cover a much wider range of pore sizes than zeolites, even bridging micro and mesoporous materials. The combination of organic and inorganic building blocks offers an almost infinite number of variations, enormous flexibility in pore size, shape, structure and myriad opportunities for functionalization and grafting [3]. The combination of organic and inorganic building blocks offers an almost infinite number of variations, enormous flexibility in pore size, shape, and structure, and myriad opportunities for functionalization and grafting.

In this study, MIL-101(Cr) was synthesized and characterized by XRD and SEM. Then, this MOFs was applied for modification of CPE and applied for electrocatalytic oxidation of formaldehyde in the alkaline medium.

### 2. Experimental

MIL-101(Cr) was synthesized according to the published method [4]. A mixture containing 4 g of  $\text{Cr}(\text{NO}_3)_3 \cdot 9\text{H}_2\text{O}$  (99%, Sigma-Aldrich), and 1.66 g of terephthalic acid ( $\text{H}_2\text{BDC}$ ) (98%, Aldrich) in 50 mL of distilled water was heated to 210 °C in 10 min (microwave heating at 1000 W) and kept at 210 °C for 40 min. The product was washed with DMF ( $\geq 99\%$  Sigma-Aldrich) followed by drying in an air oven at 60 °C overnight and then soxhlet extraction in ethanol (laboratory type, Chem-Lab) for 48 h and drying in an oven.

MIL-101(Cr) samples were characterized by Elemental analysis, Scanning Electron Microscopy (SEM, Philips XL-30 FEG equipped with a tungsten filament), powder X-ray Diffraction (XRD, STOE StadiP diffractometer in high-throughput transmission mode) [5]. The electrochemical experiments were performed at room temperature using potentiostat/galvanostat electrochemical analyzer (SAMA500, Iran) with a voltammetry cell in a three electrode configuration. The  $\text{Ag}|\text{AgCl}|\text{KCl}$  (3M) and platinum wire were used as reference and auxiliary electrodes, respectively. The bare CPE and MIL-101(Cr) modified carbon paste electrode (MIL-101(Cr)/CPE) were used as working electrodes.

During preparation of the electrodes, diethyl ether was added to a mixture MIL-101(Cr) and graphite powder. After hand mixing with a mortar and pestle, the solvent was evaporated with stirring. Then, paraffin oil was blended with the mixture in a mortar by hand mixing for 30 min until a uniformly wetted paste was obtained. This paste was packed into the end of a glass tube and the copper wire was utilized for electrical contact. The CPE was also prepared in the same way in the absence of MIL-101(Cr) molecular sieves.

### 3. Results and discussion

XRD powder pattern of synthesized MIL-101(Cr) molecular sieves is presented in Fig. 1. The crystallization products matched the characteristic peaks of MIL-101(Cr). The SEM image of crystalline phase provides useful approach to the determination of size and morphology of the obtained crystals. Inset of Fig. 1 illustrates SEM image of synthesized MIL-101(Cr) nanocrystals with spherical morphology.



4<sup>th</sup> Iran National Zeolite Conference  
Golpayegan University of Technology, Golpayegan, Iran  
August 23-24, 2017

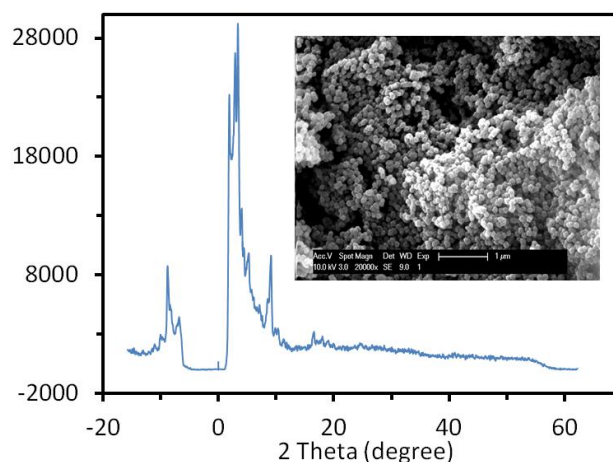


Figure 1. The representation of XRD pattern and SEM image of synthesized MIL-101(Cr) molecular sieves.

Figure 2 shows Cyclic voltammograms (CVs) of the electrochemical oxidation of  $K_4Fe(CN)_6$  at the surface of CPE and MIL-101(Cr)/CPE electrodes. It can be observed that the anodic peak current for MIL-101(Cr)/CPE is higher than that at bare CPE. This is a quasi-reversible system because the peak separation potential,  $\Delta E_p$  is equal to 120 mV and lower than that for CPE (*i.e.* 240 mV).

In the next experiment, the MIL-101(Cr)/CPE were immersed in the 0.1 M  $NiCl_2$  solution with stirring for 20 min at 150 rpm, and then washed completely with distilled water to remove the surface adsorbed species. Figure 3 shows CVs of the Ni-MIL-101(Cr)/CPE (after immersed of ZP/CPE at 0.1 M  $NiCl_2$  solution) in 0.1 M NaOH solution in the absence and presence of 0.02 M formaldehyde. When formaldehyde diffuses from the bulk solution to the electrode surface it is quickly oxidized to produce by the NiOOH species on the electrode surface. Therefore, the amount of NiOOH species decreases due to its chemical reaction with formaldehyde. This behavior is a typical observation expected from the mediated oxidation (EC' mechanism), illustrated in the following equations [6]:

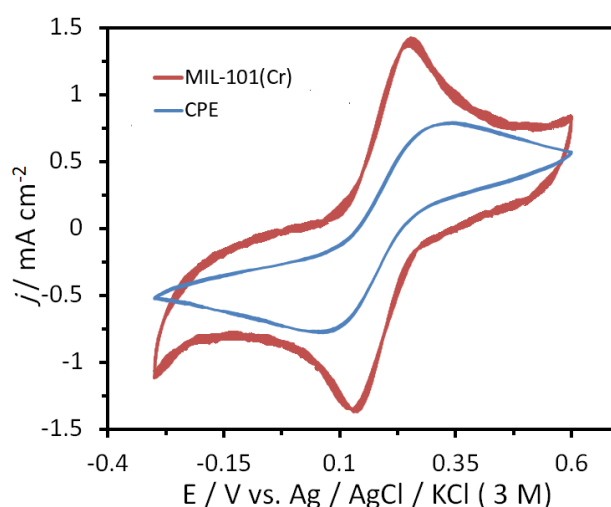
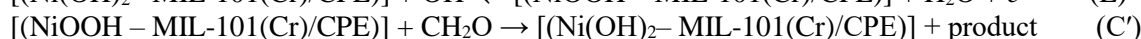


Figure 2. The CVs of bare CPE and MIL-101(Cr)/CPE in the presence of 10 mM  $K_4Fe(CN)_6$  and 0.1 M KCl ( $v = 20 \text{ mV s}^{-1}$ ).



4<sup>th</sup> Iran National Zeolite Conference  
Golpayegan University of Technology, Golpayegan, Iran  
August 23-24, 2017

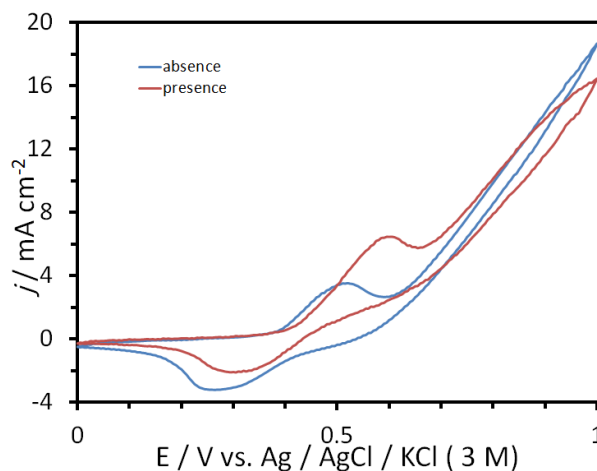


Figure 3. CVs of Ni-MIL-101(Cr)/CPE in the absence and the presence of 0.02 M formaldehyde at scan rate of 20 mV s<sup>-1</sup>.

#### 4. Conclusions

In summary, a novel modified CPE were prepared and developed by loading nickel ions into synthesized MIL-101(Cr) molecular sieves. The Ni-MIL-101(Cr)/CPE has large electrochemical surface area, and exhibit the superior electro catalytic performance in the oxidation of HCOH with decreasing overpotential. Results specified that the NiOOH species formed during the oxidation of the Ni-MIL-101(Cr)/CPE is found to be a good catalyst for oxidation of HCOH and the modified electrode can overcome the kinetic limitation by a catalytic process.

#### References

- 1) O. M. Yaghi, M. O'Keeffe, N. W. Ockwig, H. K. Chae, M. Eddaoudi, J. Kim, J. Reticular, *Nature* **2003**, 423, 705–714.
- 2) Ferey, G. *Chem. Soc. Rev.* **2008**, 37, 191–214.
- 3) L. MacGillivray, *Metal Organic Framework: Design and Application*, John Wiley & Sons, **2010**.
- 4) L. Bromberg, Y. Diao, H. Wu, S. A. Speakman, T. A. Hatton, *Chem. Mater.*, **2012**, 24, 1664–1675.
- 5) L. H. Wee, C. Wiktor, S. Turner, W. Vanderlinden, N. Janssens, S. R. Bajpe, K. Houthoofd, G. Van Tendeloo, S. De Feyter, C. E. A. Kirschhock, *J. Am. Chem. Soc.*, **2012**, 134, 10911–10919.
- 6) S.K. Hassaninejad-Darzi, *J. Electroceram.*, **2014**, 33, 252–263.



4<sup>th</sup> Iran National Zeolite Conference  
Golpayegan University of Technology, Golpayegan, Iran  
August 23-24, 2017



## Synthesis and characterization of MPA (M=K, Cs)/ OMS-2/ MCM-41 nanocomposites

Nafiseh Mahdi Babaei\*, Sedigheh Taheri Mirghaed, Mojgan Zendehtdel

Department of Chemistry, Faculty of Science, Arak University, Arak 38156-8- 8349; Iran

\* E-mail: nmahdibabai@yahoo.com

### 1. Introduction

It has been reported that substitution of large monovalent cations, such as  $\text{NH}_4^+$ ,  $\text{K}^+$ ,  $\text{Cs}^+$ , etc., for  $\text{H}^+$  in  $\text{M}_x\text{H}_{3-x}\text{PW}_{12}\text{O}_{40}$  catalysts improved surface area and thermal stability compared to parent acids. A problem associated with the use of Heteropolyacid salts is that the salt particles disperse as a colloid in water and organic solvents, making it difficult to separate the salt from the reaction products by simple filtration. Therefore they were supported on a carrier. The POMs of the Keggin structure have molecular diameter of around 1.2 nm, it is therefore feasible to insert into the MCM-41. MCM-41 is a promising support because of its large surface area ( $\sim 1000 \text{ m}^2/\text{g}$ ), high thermal stability and large pore size (1.5–8 nm). However, MCM-41 lacks Brønsted acid sites and exhibits only weak hydrogen-bonded type of sites [1]. For MCM-41 to be used as a catalyst or catalyst support in acid catalyzed reactions Brønsted acid sites need to be created and the acid strength must be enhanced. The acidity of MCM-41 can be increased by surface modification, through the introduction of strong acid species such as sulfate ions, sulfated zirconia or heteropolyacids with Keggin-type structures [2], either on the surface or within the inner channels of MCM-41. This can result in creating Brønsted acid sites which can lead to a significant improvement in the acid strength of MCM-41. Here we wish to report the results of a study on the use of MCM-41-supported heteropolyacids salts in esterification reactions. Previously, bulk HPA and carbon-supported HPA have been studied [3] as catalysts in esterification

### 2. Experimental

First MCM-41 was mixed with OMS-2 (1 g) and the mixture was stirred for 30 minutes, after then  $\text{M}_{1.5}\text{H}_{1.5}\text{PW}_{12}\text{O}_{40}$  (M=K, Cs) salts (1 g) was added. Nanocomposite was dried in an oven at  $100^\circ\text{C}$  for 72 h. The residue was filtered and gently washed with deionized water and dried in a vacuum oven at  $50^\circ\text{C}$ . Finally the prepared compounds have been distinguished using FT-IR, XRD, TGA and SEM.

### 3. Results and discussion

The FTIR Cs-PTA-loaded MCM-41 and OMS-2 is shown in Fig. 1 the spectra show a broad band around  $3100\text{--}3600 \text{ cm}^{-1}$ , which is due to adsorbed water molecules. The absorption band due to H–O–H bending vibration in water is at  $1620\text{--}1640 \text{ cm}^{-1}$ . The absorption band around  $1087\text{--}1092 \text{ cm}^{-1}$  is due to Si–O asymmetric stretching vibrations of Si–O–Si bridges. The characteristic signature of the Keggin structure was seen in each case, with dips at 1080, 985, 890, and  $800 \text{ cm}^{-1}$ . The band assignments are available in the literature [4].

Fig. 2 shows SEM micrograph of  $\text{Cs}_{1.5}\text{H}_{1.5}\text{PW}_{12}\text{O}_{40}/\text{MCM-41}/\text{OMS-2}$  nanocrystal recorded.



# 4<sup>th</sup> Iran National Zeolite Conference

## Golpayegan University of Technology, Golpayegan, Iran

### August 23-24, 2017

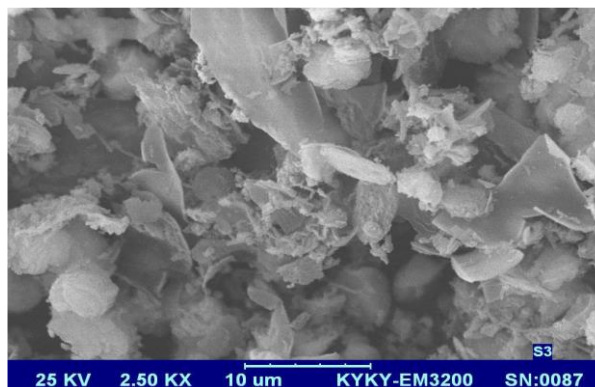
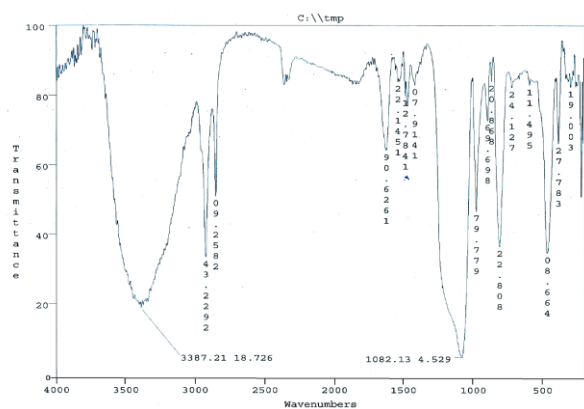


Fig.1. FTIR spectra of Cs<sub>1.5</sub>H<sub>1.5</sub>PW<sub>12</sub>O<sub>40</sub>/MCM-41/OMS-2 sample

Fig.2. SEM micrograph of Cs<sub>1.5</sub>H<sub>1.5</sub>PW<sub>12</sub>O<sub>40</sub>/MCM-41/OMS-2

#### 4. Conclusions

The studies of FT-IR, thermogravimetric analyses (TGA) and X-ray diffraction (XRD) confirmed the presence and high dispersion of HPA salts on MCM-41 mesoporous structure. We also examined the reusability of the supported catalysts.

#### References

- 1) T. Okuhara, H. Watanabe, T. Nishimura et al *Chem Mater* **2000**, 12, 2230
- 2) Y. Izumi, *Catal Today* **1997**, 33,371
- 3) AS. Dias, S. Lima, M. Pillinger, *Carbohydr Res*, **2006**, 341, 2946.
- 4) S. Tangestaninejad, V. Mirkhani M., Moghadam et al, *Ultrason Sonochem* **2008**, 15(4), 438.

## Application of vortex-assisted solid phase extraction for simultaneous preconcentration of Cd(II) and Pb(II) on clinoptilolite nanoparticles modified with 5(p-dimethylaminobenzylidene)rhodanine

Ali Jouki<sup>a</sup>, Saadat Rastegarzadeh<sup>a\*</sup>, Mojgan Zندهدل<sup>b</sup>

<sup>a</sup> Department of Chemistry, Faculty of Science, Shahid Chamran University of Ahvaz, Ahvaz, Iran

<sup>b</sup> Department of Chemistry, Faculty of Science, Arak University, Arak, Iran

\*Email: [rastegarz@scu.ac.ir](mailto:rastegarz@scu.ac.ir)

#### 1. Introduction

Recently, heavy metals pollution is widely considered as a main source of the environmental problems, since they have severe hazardous effects on the ecological systems. Cadmium and lead known as serious hazards and toxic heavy metals which distributed in nature and easily enter the food chain through a number of pathways, and tend to



# 4<sup>th</sup> Iran National Zeolite Conference

## Golpayegan University of Technology, Golpayegan, Iran

### August 23-24, 2017



accumulate in living organisms causing various diseases and disorders to the human health. Therefore, development of analysis methods for the accurate and precise determination of traces of these metals is meaningful for environmental monitoring. Solid phase extraction (SPE) using new adsorbent is currently one of the most widespread techniques for separation and preconcentration of metal ions. Among different sorbents, zeolites are most famous candidates because of their unique properties such as high cation exchange capacity and high adsorption capacity [1-5]. In this work, the SPE performance of modified clinoptilolite with 5(p-dimethylaminobenzylidene) rhodanine (PDR) as an adsorbent was investigated.

## 2. Experimental Part

First, the clinoptilolite/ZnO nanocomposite was synthesized by adding clinoptilolite nanoparticles to  $Zn(NO_3)_2$  solution. The obtained nanocomposite dried and calcined at 550 °C after washing. Then the prepared clinoptilolite/ZnO was treated with PDR solution using a simple method.

For performing vortex-assisted SPE, 80 mg of modified clinoptilolite with (PDR) was added to solution containing Cd(II) and Pb(II) and the solution was mixed on vortex mixture. Then, the adsorbent was separated and 1 mL of  $HNO_3$  solution was added to it. Finally, the concentration of eluted metal ions was determined by FAAS.

## 3. Results and discussion

In this work, clinoptilolite nanoparticles were modified with 5(p-dimethylaminobenzylidene) rhodanine (PDR) and used as a new adsorbent for simultaneous preconcentration of Pb(II) and Cd(II) using a rapid vortex-assisted SPE technique. The modified clinoptilolite nanoparticles was prepared according a simple method and characterized by Fourier transform infrared (FT-IR) spectra and scanning electron microscopy (SEM).

The adsorbed metal ions are eluted from the adsorbent with a solution of nitric acid and determined by flame atomic absorption spectrometry (FAAS). The adsorption conditions including pH of sample solution, adsorbent amount and sample volume as well as elution conditions were studied and optimized in order to achieve highest sensitivity and selectivity. The limit of detection based on  $3S_b$  was less than  $2 \text{ ng mL}^{-1}$  for Cd(II) and Pb(II). The relative standard deviation for eight replicate measurements of  $50 \text{ ng mL}^{-1}$  of both metal ions was less than 4 %. The effect of diverse ions on the recovery of Cd(II) and Pb(II) in SPE performance was investigated. The method was applied to the determination of Cd(II) and Pb(II) in different water samples.

## 4. Conclusions

In this study, a new sorbent consists of nano-sized clinoptilolite as a natural zeolite and PDR was used to developing a simple, low cost and time saving, vortex-assisted SPE technique coupled with FFAS for the simultaneous preconcentration and determination of Cd (II) and Pb (II) ions. The obtained results indicated that a careful choice of adsorption and elution conditions resulted in a reliable and selective method. Furthermore, the presented method was characterized by quantitative recovery, satisfactory accuracy and precision for the determination of trace Cd(II) and Pb(II) ions. The method showed minimum interferences with commonly found ions in real samples.

## Acknowledgments

The authors are grateful to Shahid Chamran University of Ahvaz Research Council for financial support of this work.

## References



4<sup>th</sup> Iran National Zeolite Conference  
Golpayegan University of Technology, Golpayegan, Iran  
August 23-24, 2017



- 1) Y. Han, Y. Li, W. Si, D. Wei, Z. Yao, X. Zheng, B. Du, Q. Wei, *Spectrochim. Acta A* 2011,79,1546.
- 2) L. Zhang, Z. Li, X. Du, R. Li, X. Chang, *Spectrochim. Acta A* 2012, 86, 443.
- 3) M. H. Mashhadizadeh, Z. Karami, *J. Hazard. Mater.* 2011, 190, 1023.
- 4) E.Yilmaz, M. Soylak, *Talanta* 2016, 158, 152.
- 5) M. Zendehtdel, A. Barati, H. Alikhani, *e-Polymers.* 2013, 11, 8.

**Mn(II)-substituted polyoxophosmolybdate supported on the amino-functionalized  
SBA-15 as catalyst for epoxidation reactions**

Maryam Zare<sup>\*a</sup>, Zeinab Moradi–Shoeili<sup>b</sup>, Hadighe Hoseini<sup>c</sup>, Mojtaba Bagherzadeh<sup>c</sup>

<sup>a</sup> *Materials Science & Engineering Department, Golpayegan University of Technology, P.O. Box 8771765651, Golpayegan, Iran*

<sup>b</sup> *Department of Chemistry, Faculty of Sciences, University of Guilan, P.O. Box 41335–1914, Rasht, Iran*

<sup>c</sup> *Department of Chemistry, Sharif University of Technology, Azadi Ave., P.O. Box 11155–3516, Tehran, Iran*

\*Email: m\_zare@gut.ac.ir (M. Zare)

## 1. Introduction

Ordered mesoporous SBA-15 materials present a series of some unique properties which recommend them as ideal host structures. These properties include an improved framework cross-linking and thick walls, high (hydro)thermal stability, large specific surface areas, well-defined dual pore structures composed of hexagonal arrays of large and tunable primary cylindrical mesopores, and also secondary (ultra) supermicropores or small mesopores [1–3]. Therefore, SBA-15 is suitable for successful anchoring platform materials for various kinds of catalysts [4, 5]. As the difficulty in separation and reuse of homogenous catalysts from the reaction medium, hamper their commercial applications, preparing the heterogeneous catalysts via immobilization of the catalytically active species onto/into the surface of traditional solid supports, has hence attracted a lot of attention [6].

Olefins epoxidation is an important reaction in the production of a wide variety of valuable materials used laboratorial and also industrial processes [7, 8]. As a result, enormous efforts have gone into designing and fabrication of suitable catalysts with high selectivity, stability and recyclability.

Herein, we report a simple method for grafting of the homogeneous Mn(II)-substituted phosphomolybdenum moiety on the amino-functionalized SBA-15 (Scheme 1). The synthesized nanomaterials, SBA–MnPOM have been identified by a series of characterization techniques. The catalytic properties of the nanocatalyst were investigated in the epoxidation of olefins using TBHP as oxygen source which exhibited excellent catalytic performance with high yields and selectivity.



# 4<sup>th</sup> Iran National Zeolite Conference

## Golpayegan University of Technology, Golpayegan, Iran

### August 23-24, 2017



## 2. Experimental Part

**Synthesis of SBA–MnPOM nanocomposite:** The ordered mesoporous silica containing amino groups (SBA-NH<sub>2</sub>) were synthesized on the basis of the procedure described previously [9]. The solution of MnPOM was synthesized by reported method by K. Patel [10] and then, 400 mg SBA-NH<sub>2</sub> was added to the solution. The resulting reaction mixture was refluxed for 24 h. The solid was separated and washed several times with water and ethanol. The final product dried in an oven at 70 °C for 8 h to afford SBA–MnPOM nanocomposite.

**Evaluation of catalytic properties in oxidation of olefins:** To a solution of alkene (1 mmol), SBA–MnPOM (0.0005 mmol Mo complex), chlorobenzene (1 mmol) as internal standard and C<sub>2</sub>H<sub>4</sub>Cl<sub>2</sub> (1 mL), 1mmol of TBHP was added as oxidant. The system was stirred for 1-4 h at 95 °C. The progress of the reaction was monitored by GC. All the reactions were performed at least two times and the products were compared with standard samples.

## 3. Results and discussion

**Nanocomposite synthesis and characterization:** The successful synthesis of the supported catalyst is confirmed by infrared spectroscopy. The FT-IR spectra of SBA-NH<sub>2</sub> and SBA–MnPOM in the range 400–4000 cm<sup>-1</sup> are depicted in Fig. 1. The typical vibration modes of SBA-NH<sub>2</sub> (OH, 3328 cm<sup>-1</sup>; Si–O–Si, 1076 and 803 cm<sup>-1</sup>; Si–OH, 956 cm<sup>-1</sup>; and Si–O, 462 cm<sup>-1</sup>) are observed in the IR spectra of SBA-15 and SBA–MnPOM [8]. Absorption bands at 893 and 767 cm<sup>-1</sup> appeared for SBA–MnPOM nanoparticles (Fig. 1b) corresponding to the symmetric stretching of W–O, and W–O–W bonds, respectively [11]. These peaks in FT–IR spectra reveal that MnPOM has been successfully supported on the surface of solid support.

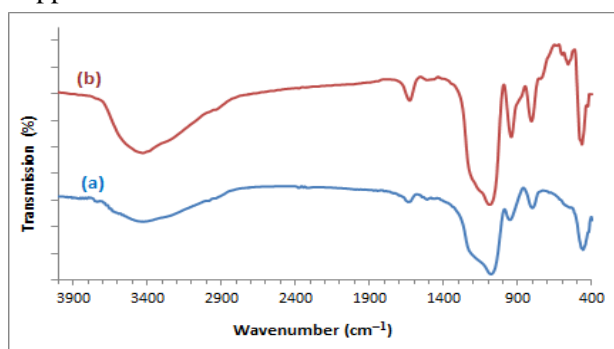


Fig. 1. FT–IR spectra of (a) SBA-NH<sub>2</sub>, (b) SBA–MnPOM

**The catalytic oxidation of olefins:** With the optimized conditions, the substrate scopes were next explored. As shown in Table 1, the epoxidation of cyclooctene, 1–octene in dichloroethane solution catalyzed by SBA–MnPOM give high yields of the corresponding epoxides. Styrene was converted into its epoxide in moderate yield and selectivity.

**Table 1.** Catalytic oxidation of various alkenes with TBHP in water by (SBA–MnPOM) catalyst.

Entry	Substrate	Conversion(%) <sup>b</sup>	Time(h)	Selectivity
1	Cyclooctene	98	2	95
2	1-octene	97	3	93
3	Styrene	70	4	50

The reactions were run under reflux in 1 mL dichloroethane.

<sup>a</sup> Reaction condition: 5 mg catalyst: 0.2 mmol alkene: 0.4 mmol TBHP in water.

<sup>b</sup> GC yield based on starting alkene.





# 4<sup>th</sup> Iran National Zeolite Conference

## Golpayegan University of Technology, Golpayegan, Iran

### August 23-24, 2017



#### 4. Conclusions

Heterogeneous nanoscale catalyst was successfully synthesized via anchoring of Mn(II)-substituted phosphomolybdenum complex on the amin-functionalized SBA-15. The mesoporous nanomaterials, SBA-MnPOM have been identified by a series of characterization techniques. The catalyst shows efficient reactivity in the olefins epoxidation reactions giving high yield and selectivity of the products, in most cases.

#### Acknowledgments

The authors are grateful to the University of Guilan and the Golpayegan University of Technology for financial support. Partial support by Sharif University of Technology is gratefully acknowledged.

#### References

- 1) H. Balcar, J. Čejka, *Coord. Chem. Rev.*, **2013**, 257, 3107–3124.
- 2) R. Maheswari, M.P. Pachamuthu, A. Ramanathan, B. Subramaniam, *Ind. Eng. Chem. Res.*, **2014**, 53, 18833–18839.
- 3) L. Duan, R. Fu, B. Zhang, W. Shi, Sh. Chen, Y. Wan, *ACS Catal.*, **2016**, 6, 1062–1074.
- 4) K. Ariga, A. Vinu, J.P. Hill, T. Mori, *Coord. Chem. Rev.*, **2007**, 251, 2562–2591.
- 5) A. Ungureanu, B. Dragoi, A. Chiriac, C. Ciotonea, S. Royer, D. Duprez, A.S. Mamede, E. Dumitriu, *ACS Appl. Mater. Interfaces*, **2013**, 5, 3010–3025.
- 6) Z. Moradi-Shoeili, M. Zare, M. Bagherzadeh *J. Nanopart. Res.*, **2016**, 18 (10), 298-306.
- 7) A.J. Burke, *Coord. Chem. Rev.*, **2008**, 252, 170–175.
- 8) M. Zare, Z. Moradi-Shoeili, F. Ashouri, M. Bagherzadeh, *Catal. Comm.* **2016**, 88, 9-12
- 9) R. Dobrowolski, M. Oszust-Cieniuch, J. Dobrzyńska, M. Barczak, *Colloids Surf. A. Physicochem. Eng. Asp.*, **2013**, 435, 63-70.
- 10) A. Patel, S. Pathan, *J. Coord. Chem.*, **2012**, 65, 3122–3132.
- 11) H. Salavati, N. Rasouli, *Mater Res Bulletin*, **2011**, 46, 1853–1859.



# 4<sup>th</sup> Iran National Zeolite Conference

## Golpayegan University of Technology, Golpayegan, Iran

### August 23-24, 2017



## Hydrothermal Synthesis of Aluminosilicate Zeolite Nanomaterials

Seyed Mahdi Rafiaei\*

*Dept. of Materials Science and Engineering, Golpayegan University of Technology, Golpayegan, Iran*

\*Email: [rafiaei@gut.ac.ir](mailto:rafiaei@gut.ac.ir)

### Abstracts

In this investigation, sodium included aluminosilicate zeolite was synthesized through a facile synthesizing method. To synthesize this material, tetraethylorthosilicate (TEOS) and aluminum-isopropoxide were used as the source of silicon and aluminum, respectively. Also, for characterizing crystal structures, microstructure and chemical bonds, x-ray diffraction (XRD), field emission scanning electron microscope (FESEM), Fourier transform infrared spectroscopy (FT-IR) were employed.

### 1. Introduction

Zeolite compounds are mainly composed from the aluminum, oxygen and silicon elements. Interestingly, these porous structure compounds can accommodate large numbers of cations, such as  $\text{Na}^+$ ,  $\text{K}^+$ ,  $\text{Ca}^{2+}$ ,  $\text{Mg}^{2+}$ . These positive cations which are rather loosely kept in the zeolite structure can be exchanged easily in a contact solution. Zeolites form with many different crystalline structures, which have large open pores (sometimes referred to as cavities) in a very regular arrangement and roughly the same size as small molecules. Zeolites are inorganic crystalline materials with a framework of tetrahedral  $\text{TO}_4$  building units (T=Si, Al, etc.). The three-dimensional crystalline porous skeletons of zeolite is formed by tetrahedral  $\text{TO}_4$  units linked by sharing of oxygen atoms. Chemical environmental synthesis conditions such as stirring rate, seeding, crystallization temperature, gel composition, alkalinity, Si/Al ratio and template concentration etc. are well known factors to control the crystal size. Among these factors, Si/Al ratio and crystallization temperatures are most important for crystal size control [1]. The inclusion of broad pores may help to suppress these problems. Thus, mesostructured zeolites have attracted significant attention. Current industrial post-synthesis treatments of zeolites, such as steaming, create mesoporous, but in a poorly controlled manner. Moreover, the intrinsic catalytic activity of zeolites is simultaneously affected as a result of aluminum extraction. [2-3]

### 2. Experimental

#### 2.1. Synthesis of nano-ZSM-5 zeolite

Raw materials consisting of tetraethylorthosilicate (TEOS), tetrapropyl-ammonium hydroxide (TPAOH), aluminum-isopropoxide and sodium hydroxide (NaOH) were purchased from sigma aldrich company. Specific amounts of NaOH, TPAOH, aluminum isopropoxide and de-ionized water were mixed and agitated for several hours to obtain a clear solution. Then TEOS was added drop wise and agitated at room temperature for several hours. Within the stirring of this solution on a hot plate, it was heated at 120 °C for 2 h. The precursor was centrifuged at 12000 rpm for 15 min. The deposited material was transferred to an autoclave and the hydrothermal process was done at 100 °C for time durations of 0, 12 and 24 hours. Finally, to remove the organic compounds, the calcination treatments were performed at 500 and 700 °C for 2 h.

#### 2.2. Characterization

The crystal structure of synthesized nanocrystalline ZSM-5 was characterized using x-ray diffraction (XRD, Rigaku, Japan) with  $\text{CuK}\alpha$  radiation ( $\lambda = 1.54 \text{ \AA}$ ). To study the microstructure of phosphors, field emission scanning electron microscope (FESEM, JSM 6330F, Japan) was used. In addition, high resolution transmission electron microscope



# 4<sup>th</sup> Iran National Zeolite Conference

## Golpayegan University of Technology, Golpayegan, Iran

### August 23-24, 2017



(HRTEM, JEOL 2100, Japan) was employed to study the structure of synthesized nano materials and their crystallinity. Also, FT-IR spectrum was employed to study the structure of prepared samples.

### 3. Results and discussion

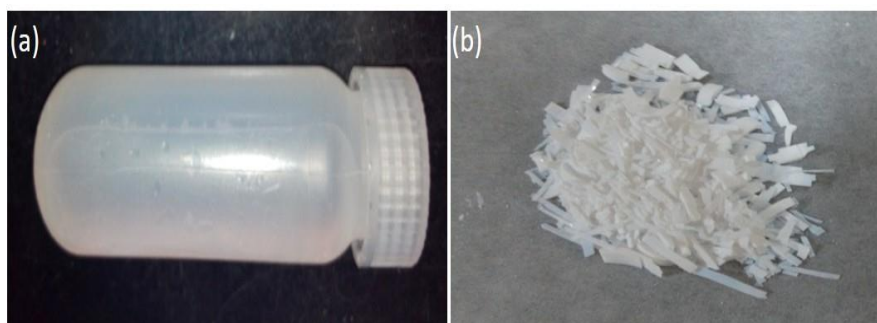


**Fig. 1.** Images of (a) precursor solutions after hydrothermal and centrifuge processes and (b) synthesized zeolite after drying.

Fig. 1 shows the images of productions at different steps. Fig. 1 (a) shows the obtained clear solution after hydrothermal and centrifuge processes. As it was explained in the experimental, after washing with centrifuge machine, the production should be dried at 100. Fig. 1 (b) presents the final zeolite material after being dried. Fig. 2 shows the XRD pattern of the synthesized nano sized ZSM 5 zeolite. Fig. 2 (a) indicates that the XRD spectrum of the precursor solutions after hydrothermal and centrifuge processes does not have any diffraction in crystallographic planes. In other words, it can be found that the precursor solutions after centrifuge process is not well crystallized. Fig. 2 (b) shows the XRD pattern of production after being calcined at 500°C. This spectrum reveals that the diffracted planes match with JCPDS No. 42-24 and the main diffraction can be seen at the angles of 7.9, 8.9, 23.2, 24.5 and 51 [20-22].

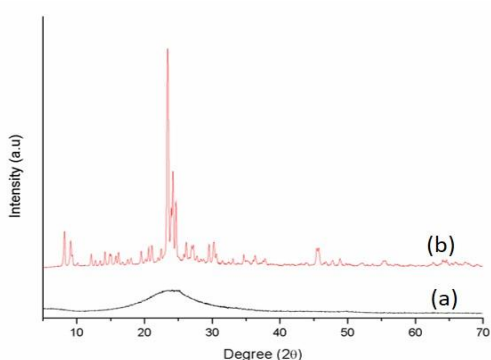


**Fig. 2.** XRD result of (a) precursor solutions after hydrothermal and centrifuge processes and (b) synthesized zeolite after drying.

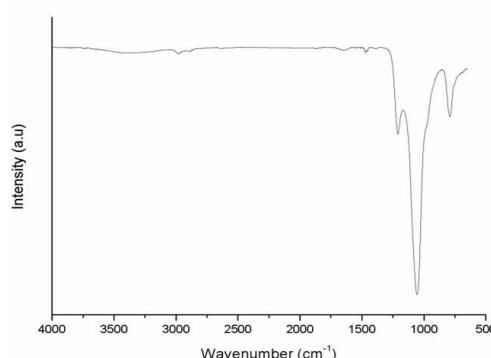


**Fig. 3.** FT-IR result of synthesized zeolite

The FT-IR spectrum of the synthesized nano crystalline ZSM-5 is illustrated in Fig. 3. Generally speaking, 950-1250cm<sup>-1</sup> bands are related to T-O stretching bands (T = Si or Al) respectively. The stretching modes are sensitive to the Si-Al composition of the framework and may shift to a lower frequency, while the bending mode may be related to the linkages between tetrahedral. The peaks between 700-850cm<sup>-1</sup> and 1000 to 1150cm<sup>-1</sup> are assigned to



# 4<sup>th</sup> Iran National Zeolite Conference

## Golpayegan University of Technology, Golpayegan, Iran

### August 23-24, 2017



symmetric and anti symmetric T-O-T stretching vibration. Accordingly, there is a very sharp absorption band at 1070 cm<sup>-1</sup> that is related to the anti symmetric T-O-T stretching vibration.

The very small size of synthesized material can accurately be determined by FESEM (see Fig. 4). Since, this observation method provide the ability to resolve individual particles. Accordingly, the nano particles can be easily observed in the range from less than 100 nm to about 150 nm. But noteworthy, most of the particles have a narrow size distribution and have a approximate size of 150 nm. Also, it is seen that there is not any aggregation, providing an efficient situation of surface of particles.

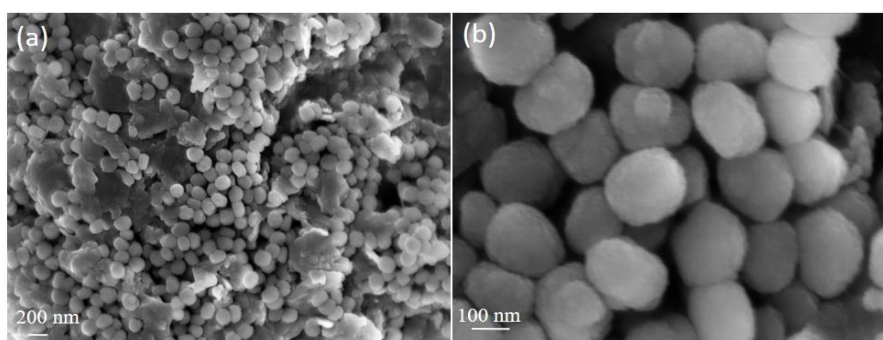


Fig. 4. FESEM images of synthesized zeolite after calcination at 700 °C.

#### References

1. B. Deepesh, T. Radha, K.S. Purnima, G. Yogesh, S. Pankaj, Hydrothermal Synthesis and Characterization of Zeolite: Effect of Crystallization Temperature, Research J Chemical Sciences, Vol. 3(9), 1-4(2013).
2. J. Wang, J.C. Groen, W. Yue, W. Zhou, M.O. Coppens, Facile synthesis of ZSM-5 composites with hierarchical porosity, J. Mater. Chem., 18, 468–474 (2008).
3. S. van Donk, A. H. Janssen, J. H. Bitter and K. P. de Jong, Catal. Rev. Sci. Eng., 2003, 45, 297.

## Synthesis, Characterization and antibacterial activity of a bis-acylhydrazone Cu(II) complex supported on MSN-APS

Leila Tahmasbi,<sup>a</sup> Tahereh Sedaghat<sup>\*a</sup>, Hossein Motamedi<sup>b</sup>

<sup>a</sup>Department of Chemistry, Faculty of Science, Shahid Chamran University of Ahvaz, Ahvaz, Iran

<sup>b</sup>Department of Biology, Faculty of Science, Shahid Chamran University of Ahvaz, Ahvaz, Iran

\*Email: [tsedaghat@scu.ac.ir](mailto:tsedaghat@scu.ac.ir)

#### 1. Introduction

According to pore diameter, Porous materials have been classified to microporous (< 2 nm such as zeolites), mesoporous (2-50 nm) and macroporous (50-100 nm) [1]. Zeolites may be had limitations in some applications because of their small dimension [2]. But mesoporous materials are suitable composites at different fields because had proper pore size, high surface area, good distribution, capability for functionalizing surface and stability [3]. M41S are



# 4<sup>th</sup> Iran National Zeolite Conference

## Golpayegan University of Technology, Golpayegan, Iran

### August 23-24, 2017



groups of mesoporous silica composites (2-10 nm pore size) including MCM-41, MCM-48 and MCM-50 [4]. Mesoporous silica nanoparticles (MSNs) are MCM-41 composites with particle size under 100 nm [5]. These composites were applied as catalysis, removal heavy metals, drug delivery, enzyme immobilization and etc. [6-8]. At this work we have supported bis-acyl-hydrazone metal complex on MSN-APS. These composites were characterized by several techniques successfully. Antibacterial activity of MSN-APS-complex was investigated against *S.aureus* and *E.coli*.

## 2. Experimental

MSNs were synthesized by sol-gel method. CTAB and NaOH were added to deionized water and then TEOS added to this solution slowly. The product was washed with deionized water and ethanol and dried in oven. Finally CTAB was extracted with chemical method.

For preparation of MSN-APS, 3-aminopropyl trimethoxy silane (APTMS) was added to MSNs at ethanol and refluxed at 80 °C.

Condensation of 2-hydroxy-benzaldehyde with succinic dihydrazide gives hydrazonic ligand and then Cu(II) complex was prepared by reaction of ligand with  $\text{Cu}(\text{OAc})_2 \cdot \text{H}_2\text{O}$  in EtOH. Then the solution of CuL was added to MSN-APS in ethanol and MSN-APS-CuL obtained.

## 3. Results and discussion

FE-SEM and TEM images of MSN, and MSN-CuL showed spherical morphology and particle size under 100 nm (Fig. 1). Low angle XRD indexed four peaks for MSN and two peaks for functionalized MSNs because of irregular arrangement of functional groups. BET and BJH analyzes showed high surface area (789  $\text{m}^2/\text{g}$ ) for MSN whereas it was decreased MSN-CuL. All composites showed same pore diameter about 2.42 nm. EDX analysis confirms the elements in the structure of composites. FT-IR spectroscopy of MSN showed the bonds assigned to O-H of silanol (1634 and 3463 $\text{cm}^{-1}$ ) and Si-O-Si (1084, 807 and 495  $\text{cm}^{-1}$ ). The spectra of MSN-AP show bands assigned to  $\text{CH}_2$  (1556-1471 $\text{cm}^{-1}$ ) as well as 1640  $\text{cm}^{-1}$  for  $\text{NH}_2$  group. Imine group at L, CuL and MSN-APS-CuL were appeared in 1620  $\text{cm}^{-1}$ , 1610 and 1617 $\text{cm}^{-1}$  respectively. Thermogravimetric analysis of nanocomposites was also investigated. Antibacterial activity evaluation for MSN-APS-CuL<sub>suc</sub> showed inhibitory effect against *S.aureus* and *E.coli*.

## 4. Conclusions

New functionalized nanoparticles were synthesized and characterized by FT-IR, TEM, FE-SEM, EDX, BET and TGA. The results showed spherical morphology and particle size under 100 nm. MSN-APS-CuL exhibited good antibacterial activity.

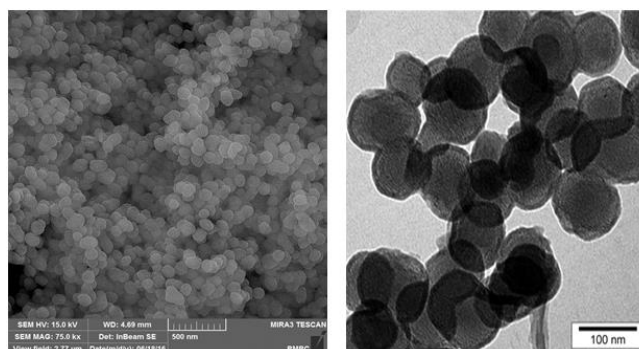


Figure 1. FE-SEM of MSN-APS-CuL (left) and TEM (right)



# 4<sup>th</sup> Iran National Zeolite Conference

## Golpayegan University of Technology, Golpayegan, Iran

### August 23-24, 2017



#### Acknowledgments

We acknowledge the financial support from Shahid Chamran University of Ahvaz, Iran.

#### References

- 1) N. Linares, A. Silvestre-Albero, E. Serrano, J. Silvestre-Albero, J. Garcia-Martinez, J. Chemical Society Reviews, 2014, 43, 7681-7717.
- 2) K. Thrane Leth, A. Krogh Rovik, M. Spangsborg Holm, M. Brorson, Applied Catalysis A: General 348 (2008) 257–265.
- 3) D. Margolese, J. Melero, S. Christiansen, B. Chmelka, G. Stucky, Chemistry of Materials 2000, 12, 2448.
- 4) F. Hoffmann, M. Cornelius, J. Morell, M. Fröba, Angewandte Chemie International Edition 2006, 45, 3216.
- 5) D. Zhang, X. Wang, Z. Qiao, D. Tang, Y. Liu, Q. Huo, J. Phys. Chem C 2010, 114, 12505.
- 6) D.B. Nale, S. Rana, K. Parida, B.M. Bhanage, *Applied Catalysis A: General*, **2014**, 469, 340-349.
- 7) R. Pogorilyi, Y.L. Zub, A. Beganskienė, A. Kareiva, *Chemija*, 2014, 25, 75-81.
- 8) R. Pogorilyi, Y.L. Zub, A. Beganskienė, A. Kareiva, *Chemija*, **2014**, 25, 75-81

## Introduce Ag on Natural Zeolites and Investigation of antibacterial activity

Scientific Society of Chemistry <sup>a</sup>, Zohreh Mortezaei<sup>a</sup>, Mojgan Zendehtdel\*<sup>a</sup>

<sup>a</sup> Department of Chemistry, Faculty of Science, Arak University, Arak 38156-8- 8349; Iran

\*Email: [m-zendehtdel@araku.ac.ir](mailto:m-zendehtdel@araku.ac.ir)

### 1. Introduction

The zeolites are a crystalline aluminosilicates with well defined channel and cavity that these cavities contain metal cations and removable water. Microorganisms are part of the organic matter in the wastewater. These organic materials can affect human health and are commonly found in wastewater because they are present in fecal material. Consequently, the treatment of wastewater is important and its success depends on its final use. The removal or inactivation of pathogenic microorganisms is the last step in the treatment of wastewater. Some chemical and physical agents, such as chlorine, ultraviolet light, reverse osmosis, and silver catalyst are well developed [1–3]. The bactericide activity of silver ions has been known for a long time. In nanoparticle form, silver becomes more reactive and shows catalytic properties, large surface area to volume ratio, unusual crystal morphologies, and thus toxic than silver ion [4]. To apply silver nanoparticles effectively in water disinfection, they should be impregnated in a substrate. Several studies have shown the use of silver nanoparticles coated on various substrates. For instance, silver nanoparticles were incorporated in materials such as montmorillonite, polysulfide, cellulose acetate, fiberglass, polyurethane foams, ceramic filters, and activated carbon [5]. In the last few years, several investigations were carried out using synthetic and natural zeolites that combined with silver ions to obtain disinfection agents for the treatment by microbiologically polluted water [6].



# 4<sup>th</sup> Iran National Zeolite Conference

## Golpayegan University of Technology, Golpayegan, Iran

### August 23-24, 2017



## 2. Experimental

### Synthesis of Ag<sup>0</sup>-Zeolite

In the first, AgNO<sub>3</sub> solution was added to natural zeolites (Clinoptilolite and Bentonite) and stirred for 48 h in room temperature and Ag<sup>+</sup> introduce on natural zeolites. Then by adding NaBH<sub>4</sub> solution, synthesis the solid compounds (Ag<sup>0</sup>-Clinoptilolite and Ag<sup>0</sup>-Bentonite). The products heated and dried at 120 °C for 3h in oven.

## 3. Results and discussion

silver–natural zeolite synthesized with two Natural zeolite (bentonite, clinoptilolite) successfully and characterized using FT-IR, XRD, TGA, SEM techniques.

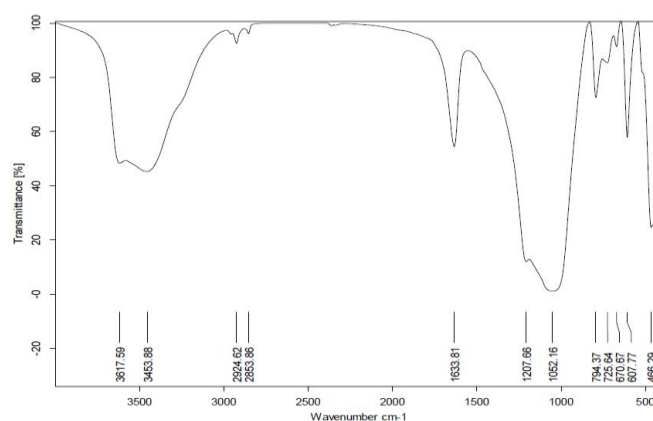


Figure 1. The FT-IR of Ag<sup>0</sup>-Clinoptilolite

The FT-IR spectra of Ag<sup>0</sup>-Clinoptilolite and Ag<sup>0</sup>-Bentonite indicate an intense band about ca.1052 , 1044 cm<sup>-1</sup> attributable to the asymmetric stretching of Al–O–Si chain of zeolite. The symmetric stretching and bending frequency bands of Al–O–Si framework of zeolite appear at ca.794, 791 and 466, 466 cm<sup>-1</sup>, respectively. Also broad peak at 3454 , 3447 cm<sup>-1</sup> respectively for Ag<sup>0</sup>-Clinoptilolite and Ag<sup>0</sup>-Bentonite is may be due to the presence of Van der Waals' interactions between the hydroxyl groups in the zeolite structure related to H<sub>2</sub>O and the partial positive charge on the surface of Ag.

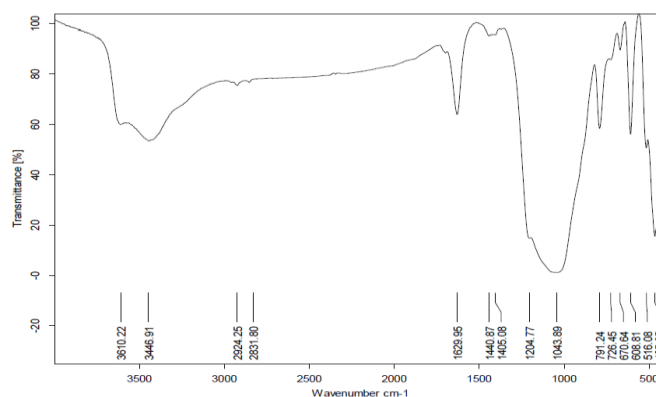


Figure 2. The FT-IR of Ag<sup>0</sup>-Bentonite



# 4<sup>th</sup> Iran National Zeolite Conference

## Golpayegan University of Technology, Golpayegan, Iran

### August 23-24, 2017



#### Antibacterial activity study

The in vitro antibacterial activity of the investigated compounds was tested against pathogenic Gram-negative bacteria's such as *P. aeruginosa* (ATCC 27853) and Gram-positive bacteria's such as *B. subtilis* (ATCC 6633) using the paper disc diffusion method according to the procedure described by Hwang and Ma [7]. This method is a way to measuring efficiency of an antibacterial agent against the mentioned bacterial growth. Mueller Hinton broth was used for preparing culture media for the bioassay of the organisms. A lawn culture from 0.5 Mac Farland suspension of each strain was prepared on Mueller Hinton agar. The agar medium was sterilized in autoclave, cooled to room temperature, and then poured into sterilized Petri dishes. The bacteria of interest are swabbed uniformly across a culture plate, while the Petri dishes are cooled over 24 h. Discs of samples were placed on the surface of the medium and finally, all Petri dishes containing bacteria and antibacterial reagents were incubated and maintained at 37 C for 24 h. After this period, the diameters of the inhibition zones formed around each disc were determined and presented in mm.

#### 4. Conclusions

The in vitro antibacterial activity of Ag<sup>0</sup>-natural zeolites was evaluated against *Bacillus subtilis* (as Gram-positive bacteria), *Pseudomonas aeruginosa* (as Gramnegative bacteria), and compared with standard drugs. The results show that Ag-Natural zeolite has more inhibition on bacterial growth.

#### Acknowledgments

Thanks are due to the Research Council of Arak University of Technology and Center of Excellence in the Chemistry Department of Arak University of Technology and Scientific Society of Chemistry for supporting of this work.

#### References

1. Finch G, Black E, Gyurek L (1994) Ozone and chlorine inactivation of *Cryptosporidium*. In: Water quality technology conference, AWWA, pp 1303–1309
2. Gujer W, von Gunten U (2003) A stochastic model of an ozonation reactor. *Water Res* 37:1667–1677
3. Hassinger E, Thomas AD, Paul BB (1994) Reverse osmosis units water facts
4. Marambio-Jones C, Hoek EMV (2010) A review of the antibacterial effects of silver nanomaterials and potential implications for human health and the environment. *J Nanopart Res* 12:1531–1551
5. Mthombeni NH, Mpenyana-Monyatsib L, Onyango MS, Momba MNB (2012) Breakthrough analysis for water disinfection using silver nanoparticles coated resin beads in fixed-bed column. *J Hazard Mater* 217–218:133–140.
6. Rivera-Garza M, Olguon MT, Garcoa-Sosa I, Alcantara D, Rodríguez-Fuentes G (2000) Silver supported on natural Mexican zeolite as an antibacterial material. *Microporous Mesoporous Mater* 39:431–444
7. Hwang JJ, Ma TW (2012) Preparation, morphology, and antibacterial properties of polyacrylonitrile/montmorillonite /silver nanocomposites. *Mater Chem Phys* 136:613–623





# 4<sup>th</sup> Iran National Zeolite Conference

## Golpayegan University of Technology, Golpayegan, Iran

### August 23-24, 2017



## Determination of Thymol by NaY nanozeolite modified carbon paste electrode

Seyed Karim Hassaninejad-Darzi\*, Behnaz Aghamohseni, Mohamad Asadollahi Baboli

Department of Chemistry, Faculty of Science, Babol Noshivani University of Technology, Babol, P.O.Box: 47148-71167, Iran.

\*Email: hassaninejad@nit.ac.ir

### 1. Introduction

Natural isopropyl cresols such as thymol (2-isopropyl-5-methylphenol) is credited with a series of pharmacological properties, including antimicrobial and antifungal effects. Thymol affect the surface electrostatics of the cell membrane and membrane integrity. Thymus pulegioides essential oil, consisting mainly of thymol, exhibits antifungal effects attributed to the formation of extensive membrane lesions and the reduction of ergosterol content [1]. Common methods was performed for quantification of thymol in different matrices including high performance liquid chromatography (HPLC) with different detection [2].

Zeolites are crystalline, porous solids whose intricate pore and channel systems in the molecular size range of 0.3 to about 1.5 nm are the basis for their immense importance in catalysis, separations, and ion exchange [3]. Zeolite Y can be viewed as the archetype zeolite owing to its enormous importance in catalysis (hydrocracking of petroleum) and its large stable pore structure, which makes it an ideal host for novel nanocomposites [3, 4].

In the present work, hydrothermally synthesis of NaY nanozeolite has been performed and characterized. Then, Mn(II)-exchanged Y nanozeolite were utilized for modification of carbon paste electrode (CPE) and applied for electrooxidation of thymol in phosphate buffer solution (pH = 10) using cyclic voltammetry technique.

### 2. Experimental Part

The synthesis of FAU-type (faujasite structure) from a clear aqueous solution with a molar composition of 0.15 Na<sub>2</sub>O: 5.5 (TMA)<sub>2</sub>O: 2.3 Al<sub>2</sub>O<sub>3</sub>: 10 SiO<sub>2</sub>: 570 H<sub>2</sub>O was performed at 100 °C. Tetramethylammonium hydroxide pentahydrate (TMAOH.5H<sub>2</sub>O; Aldrich) was added to an aqueous solution of aluminum isopropoxide (Aldrich) to give a clear solution. Then silica sol (30%, 5 nm, pH 10, Aldrich) was added while stirring, and the mixture was further stirred for about 30 min. Crystallization was carried out in Teflon-lined stainless steel autoclaves at 100 °C. Prior to analysis all samples were purified three times by high-speed centrifugation (10000 rpm), removal of the mother liquor, and re-dispersion in water and the filtrate was air dried [4].

For preparation of MnY, 0.3 g of the NaY powder was added to 25 mL of 0.5 M Mn(II) nitrate solution and shaken for 48 h. The suspension was centrifuged at 6000 rpm for 15 min, and the Mn(II)-exchanged Y nanozeolite re-suspended in very dilute (<0.01 M) hydrochloric acid and shaken 5 min to remove any Mn(II)-adsorbed ions or other materials. After centrifugation, the MnY exchanged sample air dried [5].

The electrochemical experiments were performed at room temperature using potentiostat galvanostat electrochemical analyzer (SAMA500, Iran) with a voltammetry cell in a three electrode configuration. The Ag|AgCl|KCl (3 M) and platinum wire were used as reference and auxiliary electrodes, respectively. The bare CPE and MnY modified carbon paste electrode (MnY/CPE) were used as working electrodes.

During preparation of the modified electrode (MnY) and graphite powder hand mixed with a mortar and then, paraffin oil was blended with the mixture in a mortar by hand mixing for 30 min until a uniformly wetted paste was obtained. This paste was packed into the end of a glass tube and the copper wire was utilized for electrical contact. The CPE was also prepared in the same way in the absence of MnY nanozeolite.



4<sup>th</sup> Iran National Zeolite Conference  
Golpayegan University of Technology, Golpayegan, Iran  
August 23-24, 2017



### 3. Results and discussion

XRD powder pattern and FESEM image of synthesized NaY nanozeolite is presented in Fig. 1. The crystallization products matched the characteristic peaks of NaY nanozeolite at  $2\theta$  values of 6.3, 15.7 and 23.7 degrees with the reference sample. Result indicated that pure phase of NaY nanozeolite was prepared [4]. The crystalline size ( $d$ ) of synthesized sample was also calculated using Scherrer equation [5, 6]:

$$d = \frac{0.89 \lambda}{\beta \cos \theta} \quad (1)$$

where  $\lambda$  is the wavelength of the X-ray source used in XRD (0.15418 nm),  $\beta$  is the breadth of the observed diffraction line at its half-intensity maximum in radian and  $\theta$  is the main Bragg peak angle. From the diffraction peaks at  $2\theta = 6.3^\circ$ , the average particles sizes of the sample was obtained to be about 52 nm. It is apparent that the diffraction lines are significantly broadened, which may indicate a smaller crystallite size [7].

The FESEM image of synthesized NaY nanozeolite is illustrated in inset of Fig. 1, which indicates the formation of semi-square shape of nanosized particle with average diameter of 80 nm.

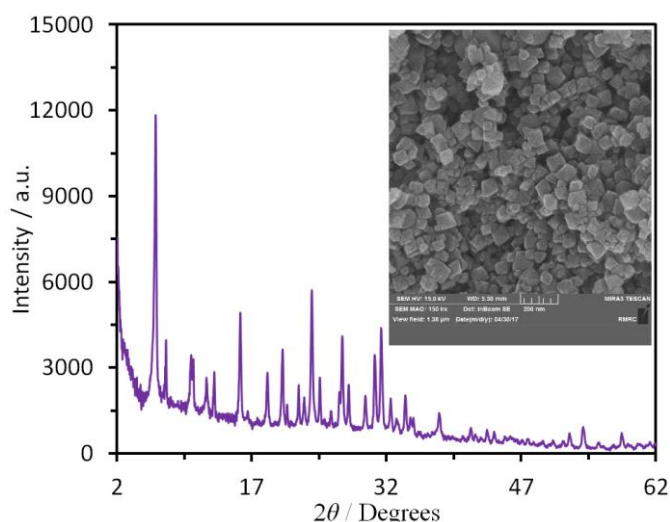
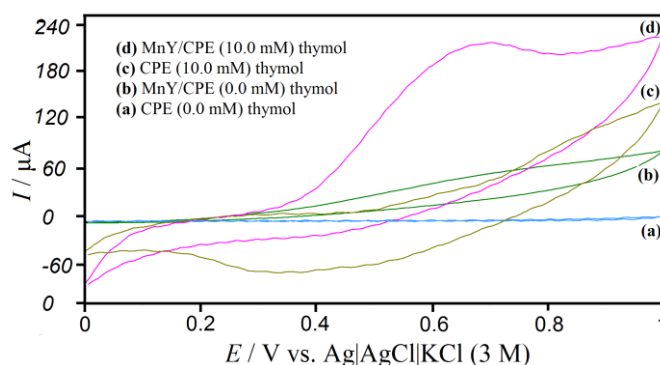


Figure 1. The representation XRD pattern of synthesized NaY nanozeolite. Inset shows FESEM image of this sample.

The electrochemical behavior of thymol was studied by cyclic voltammetric experiments using CPE and MnY/CPE in phosphate buffer solution at pH 10.0 at a scan rate of  $20 \text{ mV s}^{-1}$  (see Fig. 2). The oxidative electron transfer reactions characteristics of phenol derived molecules (thymol) are observed at the surface of MnY/CPE but no peak is appeared in the surface of CPE. It is possible to obtain reproducible current signals for the electro-oxidation of thymol by using the current signals obtained during the first voltammetric cycle. Thus, in the present study the electrochemical responses are showed those obtained during the first voltammetric cycle [2, 8].



4<sup>th</sup> Iran National Zeolite Conference  
Golpayegan University of Technology, Golpayegan, Iran  
August 23-24, 2017



**Figure 2.** Cyclic voltammograms of the CPE and MnY/CPE in the absence and presence of 10.0 mM thymol at pH 10 phosphate buffer solution at scan rate of 20 mV s<sup>-1</sup>.

#### 4. Conclusions

In this work, a Simple method was used to the synthesis of NaY nanozeolite and was modified by Mn(NO<sub>3</sub>) solution to obtain Mn(II)Y. Then, a novel modified CPE were fabricated by MnY nanozeolite. The modified CPE (MnY/CPE) has large electrochemical surface area, and exhibits the superior electrocatalytic performance for oxidation of thymol with decreasing over potential. Also, no oxidation signal was appeared in the surface of bare CPE for thymol.

#### References

- 1) A. Ahmad, A. Khan, F. Akhtar, S. Yousuf, I. Xess, L. A. Khan, N. Manzoor, *Eur. J. Clin. Microbiol. Infect. Dis.*, **2011**, 30, 41–50.
- 2) N. Tonello, M. B. Moressi, S. N. Robledo, F. Deramo, J. M. Marioli, *Talanta*, **2016**, 158, 306–314.
- 3) R. M. Barrer, *Hydrothermal Chemistry of Zeolites*, Academic Press, London, **1982**.
- 4) S. Mintova, N. H. Olson, T. Bein, *Angew. Chem. Int. Ed.* **1999**, 38, 3201–3204.
- 5) M S. Tohidi, A. Nezamzadeh-Ejehieh, *Int. J. Hydrogen Energy*, **2016**, 41, 8881–8892.
- 6) N. B. Castagnola, P. K. Dutta. *J. Phys. Chem. B*, **1998**, 102, 1696–1702.
- 7) W-C Oh, Jung A-R, Ko W-B. *Mater. Sci. Eng.-C*, **2009**, 29, 1338–1347.
- 8) E. S. Gil, R. O. Couto, *J. Braz. Pharm.*, **2013**, 23, 542–558.

## Hierarchical H-ZSM5 Zeolites synthesized from Iranian natural Kaolin clay for Methanol to Hydrocarbon conversion

Ahmad Asghari<sup>a\*</sup>, Mohammad Khanmohammadi khorrani<sup>a</sup>, Sayed habib kazemi<sup>b</sup>

<sup>a</sup> Department of Chemistry, Imam Khomeini International University, Qazvin, Iran

<sup>b</sup> Department of Chemistry, Institute for Advanced Studies in Basic Sciences (IASBS), Zanjan, 45137-66731, Iran

\*Email: a.asghari1367@gmail.com

### 1. Introduction

Hierarchical zeolites have some synthetic advantages of high stability and selectivity due to possessing both micro and meso pores. particularly, Various structure-directing agents has been explored for construction of hierarchical ZSM-5



# 4<sup>th</sup> Iran National Zeolite Conference

## Golpayegan University of Technology, Golpayegan, Iran

### August 23-24, 2017



structures. Herein, Hierarchical zeolites have been synthesized from Iranian natural kaolin clay as a low-cost silica and aluminum resource due to some synthetic advantages of high stability and selectivity. particularly, the steam assisted conversion with a low cost and green affordable monosaccharide structure-directing agents has been explored for direct construction of hierarchical HZSM-5 structures. The relation between precursor molar ratio and zeolites crystallinity, Acidity and porosity was studied for zeolites that was prepared with different Si/Al ratio.

## 2. Experimental

For direct synthesis of HZSM-5 from Iranian natural kaolin a hydrothermal process was performed in a 100-ml autoclave at 180 °C for 24h. Afterward FTIR, XRD, BET and NH<sub>3</sub>TPD analysis accompanied with Chemometric method was used to monitoring the pretreatment process and characterize obtained zeolites.

## 3. Results and discussion

Table 1 shows the textural properties of H-ZSM5 for Si/Al molar ratio 40 with different template concentration (A to C, from higher to lower template concentration, respectively). As we can see, at lower template concentration, the isotherm exhibited the formation of more micropores while at higher glucose concentration the porosity dramatically shifted into mesoporous.

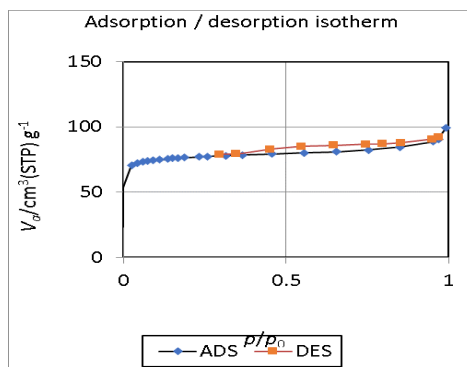


Figure 1. N<sub>2</sub> adsorption–desorption isotherms of the synthesized Zeolites.

Table 1. Textural properties of synthesized zeolites

HZSM5	SABET [m <sup>2</sup> g <sup>-1</sup> ]	Mean pore diameter [nm]
A	110.56	9.76
B	195.95	2.78
C	391.14	2.42

## 4. Conclusions

As a result, this work can be a great approach for large scale production of H-ZSM5 zeolites that was an overriding challenge facing to zeolites in methanol to hydrocarbon process.

## References

- [1]. Holmes, S.M., S.H. Khoo, and A.S. Kovo, *The direct conversion of impure natural kaolin into pure zeolite catalysts*. Green Chemistry, 2011. 13(5): p. 1152-1154.



# 4<sup>th</sup> Iran National Zeolite Conference

## Golpayegan University of Technology, Golpayegan, Iran

### August 23-24, 2017



## Introduce Zn on Natural Zeolites and Investigation of Antibacterial Activity

Mohammad Azarkish<sup>a</sup>, Mojgan Zendehtdel<sup>\*b</sup>

<sup>a</sup> Department of Chemistry, Faculty of Science, University of Ahvaz; Iran

<sup>b</sup> Department of Chemistry, Faculty of Science, Arak University, Arak 38156-8- 8349; Iran

\*Email: [m-zendehtdel@araku.ac.ir](mailto:m-zendehtdel@araku.ac.ir)

### 1. Introduction

Microorganisms are part of the organic matter in the wastewater. These organic materials can affect human health and are commonly found in wastewater because they are present in fecal material. The removal or inactivation of pathogenic microorganisms is the last step in the treatment of wastewater. Some chemical and physical agents, such as chlorine, ultraviolet light, reverse osmosis, and silver catalyst are well developed [1–3]. The bactericide activity of Zinc ions has been known for a long time. Zinc is an essential mineral perceived by the public today as being of "exceptional biologic and public health importance", especially regarding prenatal and postnatal development [4]. Zinc deficiency affects about two billion people in the developing world and is associated with many diseases. In the last few years, several investigations were carried out using synthetic and natural zeolites that combined with silver ions to obtain disinfection agents for the treatment by microbiologically polluted water.

### 2. Experimental

#### Synthesis of Zn<sup>0</sup>-Zeolite

In the first, Zn(Cl)<sub>2</sub>.4H<sub>2</sub>O solution was added to natural zeolites (Clinoptilolite and Bentonite) and stirred for 48 h in room temperature and Zn<sup>2+</sup> introduce on natural zeolites. Then by adding NaBH<sub>4</sub> solution, synthesis the solid compounds (Zn<sup>0</sup>-Clinoptilolite and Zn<sup>0</sup>-Bentonite). The products heated and dried at 120 °C for 3h in oven.

### 3. Results and discussion

Zinc–Natural zeolite synthesized with two Natural zeolite (bentonite, clinoptilolite) successfully and characterized using FT-IR, XRD, SEM techniques.

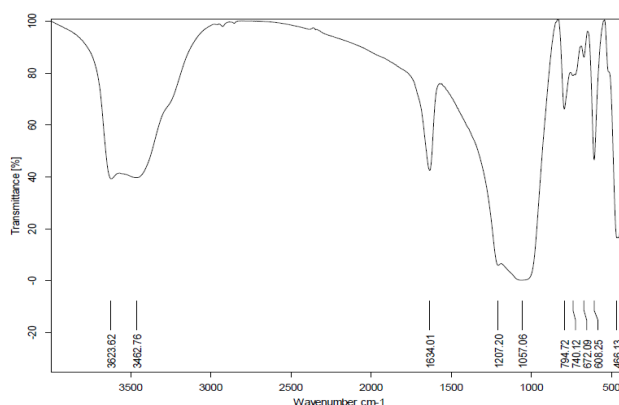


Figure 1. The FT-IR of Zn<sup>0</sup>-Clinoptilolite



4<sup>th</sup> Iran National Zeolite Conference  
Golpayegan University of Technology, Golpayegan, Iran  
August 23-24, 2017

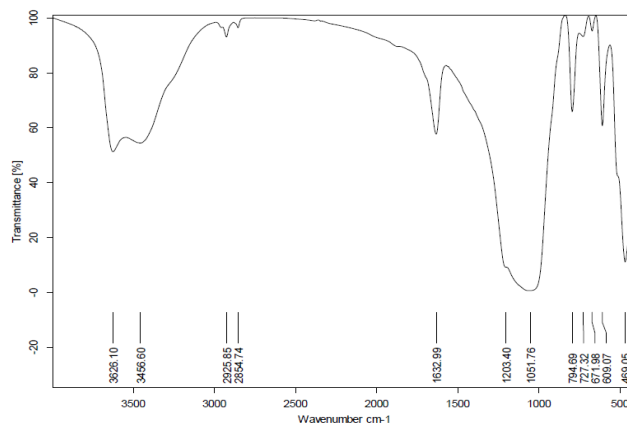


Figure 2. The FT-IR of Zn<sup>0</sup>-Bentonite

The FT-IR spectra of Zn<sup>0</sup>-Clinoptilolite and Zn<sup>0</sup>-Bentonite indicate an intense band about ca.1057 , 1052 cm<sup>-1</sup> attributable to the asymmetric stretching of Al–O–Si chain of zeolite. The symmetric stretching and bending frequency bands of Al–O–Si framework of zeolite appear at ca.795, 795 and 466, 469 cm<sup>-1</sup>, respectively.

#### Antibacterial activity study

The in vitro antibacterial activity of the investigated compounds was tested against pathogenic Gram-negative bacteria's such as *P. aeruginosa* (ATCC 27853) and Gram-positive bacteria's such as *B. subtilis* (ATCC 6633) using the paper disc diffusion method according to the procedure described by Hwang and Ma [5]. This method is a way to measuring efficiency of an antibacterial agent against the mentioned bacterial growth. Mueller Hinton broth was used for preparing culture media for the bioassay of the organisms. A lawn culture from 0.5 Mac Farland suspension of each strain was prepared on Mueller Hinton agar. The agar medium was sterilized in autoclave, cooled to room temperature, and then poured into sterilized Petri dishes. The bacteria of interest are swabbed uniformly across a culture plate, while the Petri dishes are cooled over 24 h. Discs of samples were placed on the surface of the medium and finally, all Petri dishes containing bacteria and antibacterial reagents were incubated and maintained at 37 C for 24 h. After this period, the diameters of the inhibition zones formed around each disc were determined and presented in mm.

#### 4. Conclusions

The in vitro antibacterial activity of Zn<sup>0</sup>-Natural zeolites was evaluated against *Bacillus subtilis* (as Gram-positive bacteria), *Pseudomonas aeruginosa* (as Gramnegative bacteria), and compared with standard drugs. The results show that Zn<sup>0</sup>-Natural zeolite has more inhibition on bacterial growth.

#### References

1. Finch G, Black E, Gyurek L (1994) Ozone and chlorine inactivation of *Cryptosporidium*. In: Water quality technology conference, AWWA, pp 1303–1309
2. Gujer W, von Gunten U (2003) A stochastic model of an ozonation reactor. *Water Res* 37:1667–1677
3. Hassinger E, Thomas AD, Paul BB (1994) Reverse osmosis units water facts
4. Hambidge, K. M. & Krebs, N. F. (2007). "Zinc deficiency: a special challenge". *J. Nutr.* 137 (4): 1101–5.
5. Hwang JJ, Ma TW (2012) Preparation, morphology, and antibacterial properties of polyacrylonitrile/montmorillonite /silver nanocomposites. *Mater Chem Phys* 136:613–623



# 4<sup>th</sup> Iran National Zeolite Conference

## Golpayegan University of Technology, Golpayegan, Iran

### August 23-24, 2017



## Optimization of bisphenol A removal from water using NaP: HAp nanocomposite and modeling of experimental results by artificial neural networks

B. Shoshtari-Yeganeh,<sup>a</sup> M. Zendehtdel,<sup>a\*</sup> , G. Cruciani<sup>b</sup>

<sup>a</sup> Department of Chemistry, Faculty of Science, Arak University, Arak38156-8- 8349; Iran

<sup>b</sup> Department of Physics and Earth Sciences, University of Ferrara , Via G. Saragat 1, I-44122 Ferrara, Italy

\*Email: m-zendehtdel@araku.ac.ir

### 1. Introduction

The increasing population and urbanization of society caused to increase production and distribution of toxic chemicals, containing the endocrine-disrupting chemicals (EDCs) into the environment [1]. Many EDCs excluding natural estrogens (e.g. estrone (E1), 17 $\beta$ -strodial (E2), and estriol (E3)), synthesized estrogen (e.g. ethinylestradiol (EE2)), and industrial compounds (e.g. bisphenol A (BPA) and nonylphenol) are organic compounds that they have various adverse health effect as be reported in recent years [2]. One of the known endocrine disruptors is Bisphenol A (BPA; 2, 2-bis(4-hydroxyphenyl) propane that has an important toxicity to aquatic organisms in the range of 1–10 mg/ml for freshwater and marine species [3,4]. BPA is widely used as a raw material in the production of polycarbonate plastics, polyesters, phenol resins, polyacrylates, epoxy resins and lacquer coatings on food cans [5]. Due to the widespread utilization of BPA, there is increasing interest in effective remediation technologies for its removal from contaminated water. Some methods such as, adsorption [6], membrane separation [7], solvent extraction [8] and photo degradation [9] are used. Among these methods, Adsorption is widely used to remove refractory trace compounds with a high potential of adsorption because of simplicity and high efficiency. In this study NaP:HAp nanocomposite was used as an effective adsorbent for removal of BPA and Also in this study, an artificial neural networks (ANNs) model type (i) was developed to predict the performance adsorption process over synthesized adsorbent based on data from bath experiments. A comparison between the predicted results of the designed ANN model and experimental data was also conducted.

### 2. Experimental Part or Theoretical Details

The starting materials used in this study included Silica gel, sodium hydroxide, aluminum hydroxide, calcium nitrate (CNT), potassium dihydrogen phosphate (KPP), ammonia and deionized water. All chemical materials supplied by Merck and aqueous solutions were made dissolving them in deionized water. XRD, FT-IR, TGA and SEM were used to characterization of obtained product. At first NaP zeolite and hydroxyapatite was prepared separately and then nanocomposite of NaP:HAp synthesized with hydrothermal method at 100°C for 26h. Batch experiments were carried out using synthetic NaP:HAp. The effect of contact time, NaP:HAp dosage, initial pH , initial metal concentration and temperature on removal efficiency were also investigated. Measuring final concentration of BPA was recorded by high-performance liquid chromatography( HPLC) system.

### 3. Results and discussion

X-ray diffraction pattern of NaP:HAp is shown in Fig.1.a A, Some diffraction peaks such as  $2\theta = 26.033^\circ, 32.036^\circ, 33.65^\circ$  and  $38.36^\circ$  can be indexed as the NaP and  $2\theta = 12.62^\circ, 18.44^\circ, 21.79^\circ, 28.42^\circ, 29.56^\circ, 44.26^\circ, 46.11^\circ, 48.61^\circ, 50.11^\circ, 51.63^\circ, 53.41^\circ, 55.21^\circ$  can be indexed as the hydroxyapatite. Similar to other observation found in the literature, both cactus-like and diamond like morphology with the 1-2  $\mu\text{m}$  size of each diamond-shape particle were appeared in the SEM image of NaP:HAp nanocomposite [26]. The result in Fig.1.b showed that the synthesized Hydroxyapatite powder were particle Shape with the diameter of 40-70 nm and were made.



4<sup>th</sup> Iran National Zeolite Conference  
Golpayegan University of Technology, Golpayegan, Iran  
August 23-24, 2017

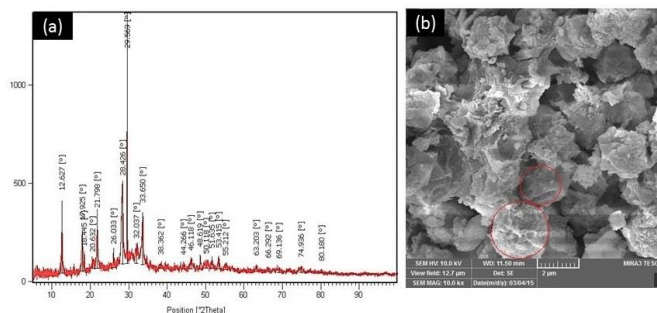


Figure 1. a. XRD pattern of NaP:HAp nanocomposite, b. SEM micrograph of NaP:HAp nanocomposite

In the present work, the prediction of total adsorption by NaP:HAp nanocomposite was done by using three-layered feed forward back propagation, multi-layer perceptron (MLP) type of ANN. BP algorithm with three-layer architecture (5:12:1) with a tangent sigmoid transfer function (tansig) at input and hidden layer and a linear transfer function (purelin) at output layer used for the modeling of BPA sorption by NaP:HAp nanocomposite. In this study, pH (over range 5-12), initial concentration (over range of 5-50 ppm), contact time (over range 30-120 min), adsorbent dosage (over range 1-4 g/L) and temperature (over range 298-318K) was chosen as an input variable, and percent removal of BPA from aqueous solution was selected as an output variable. The network is tested with different number of neurons in range of 2 to 25 to find the optimal number of neurons at the hidden layer by observing the mean squared error. Each topology was repeated three times. As shown in Fig.2, it was tried to showing correlation between predicted data and experimental data. We can see a high degree of correlation between ANN outputs (predicted data) and the corresponding targets (experimental data). Test outputs showed a very small deviation in efficiency values from the experimental data.

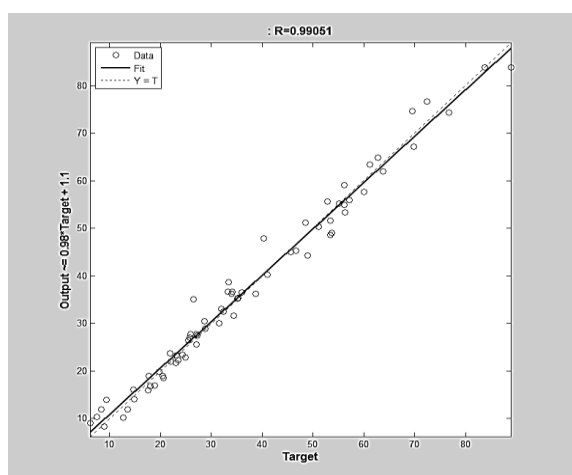


Figure 2. Regression analysis for adsorption of BPA

#### 4. Conclusions

The results obtained in this work demonstrated that BPA can be effectively removed by adsorption in NaP:HAp. ANN model was employed for modeling of removal of BPA from aqueous solutions by NaP:HAp nanocomposite. The model and the test data are in perfect match with  $R^2$  value of 0.9905.

#### Acknowledgments

Thanks are due to the Iranian Nanotechnology Initiative and the Research Council of Arak University of Technology and Center of Excellence in the Chemistry Department of Arak University of Technology for supporting of this work.





# 4<sup>th</sup> Iran National Zeolite Conference

## Golpayegan University of Technology, Golpayegan, Iran

### August 23-24, 2017



#### References

- 1) D. P. Mohapatra, S. K. Brar, R. D. Tyagi, R. Y. Surampalli, *Chemosphere* **2010**, 78, 923-941.
- 2) H. S. Chang, K. H. Choo, B. Lee, S. J. Choi, *Journal of Hazardous Materials* **2009**, 172, 1–12.
- 3) A. V. Krishnan, P. Stathis, S. F. Permeth, L. Tokes, D. Feldman, *Endocrinology* **1993**, 132, 2279–2286.
- 4) H. C. Alexander, D. C. Dill, L. W. Smith, P. D. Guiney, P. B. Dorn, *Environ Toxicol. Chem* **1988**, 7, 19–26.
- 5) C. A. Staples, P. B. Dorn, G. M. Klecka, S. T. O'Block, L. R. Hariis, *Chemosphere* **1998**, 36, 2149–2173.
- 6) B. Pan, D.H. Lin, H. Mashayekhi, B.S. Xing, *Environ. Sci. Technol* **2008**, 42, 5480-5485.
- 7) J.H. Chen, X. Huang, D.J. Lee, *Process Biochem* **2008**, 43, 451-456.
- 8) Y. Wang, Sh. Jin, Q. Wang, G. Lu, J. Jiang, D. Zhu, *Journal of Chromatography A* **2013**, 1291, 27– 32.
- 9) V.M. Mboula, V. Héquet, Y. Andrès, L.M. Pastrana-Martínez, J.M. DoñaRodríguez, A.M.T. Silva, P. Falaras, *Water Res* **2013**, 47, 3997-4005.

## Synthesis and characterization of nano-road RuO<sub>2</sub> by sol-gel method

Mahdieh Sheikhshoae<sup>a</sup>, Hassan Karimi-Maleh<sup>a</sup>, Iran Sheikhshoae<sup>a\*</sup>, Mohammad Ranjbar<sup>a</sup>

<sup>a</sup>Department of Chemistry faculty of science, Shahid Bahonar University, Kerman, Iran

\*Email: i\_shoae@yahoo.com

#### Abstract

In this study a nano sized V<sub>2</sub>O<sub>5</sub> as nao-roads was synthesized with sol-gel method and were characterized by SEM, MAP, EDS and XRD methods.

#### 1. Introduction

Nanomaterials were considered for modification of electrochemical sensors due to high surface area and low charge transfer resistance [1-3]. Some published papers reported coupling of ionic liquids and nano materials for fabrication of high sensitive voltammetric sensors in the recent years [4-6]. Sol-gel method is used for the fabrication of metal oxides. The sol-gel process is a wet-chemical technique that uses either a chemical solution (sol short for solution) or colloidal particles (sol for nanoscale particle) to produce an integrated network (gel). Metal alkoxides and metal chlorides are typical precursors. They undergo hydrolysis and polycondensation reactions to form a colloid, a system composed of nanoparticles dispersed in a solvent. The sol evolves then towards the formation of an inorganic continuous network containing a liquid phase (gel). Formation of a metal oxide involves connecting the metal centers with oxo (M-O-M) or hydroxo (M-OH-M) bridges, therefore generating metal-oxo or metal-hydroxo polymers in solution. After a drying process, the liquid phase is removed from the gel. Then, a thermal treatment (calcination) may be performed in order to favor further polycondensation and enhance mechanical properties.



4<sup>th</sup> Iran National Zeolite Conference  
Golpayegan University of Technology, Golpayegan, Iran  
August 23-24, 2017



## 2. Experimental Part or Theoretical Details

In this work, we synthesized nano-road  $\text{RuO}_2$  by sol-gel method and characterized by SEM, XRD, TEM, EDAX analysis and Map. Firstly, 0.8 g of starch and 80 ml of water mixed together and placed in a 60 °C water bath to achieve a clear solution, and then 0.012 mol ruthenium chloride salt was added to the clear solution, and then set pH to 10.0 with 1.0 M ammonia. The color of solution changed to black. The solution were stirred for 2 h and then filtered. After washing with water and ensuring complete withdrawal of chlorine, precipitated was dried and calcined at 450 °C for 2h.

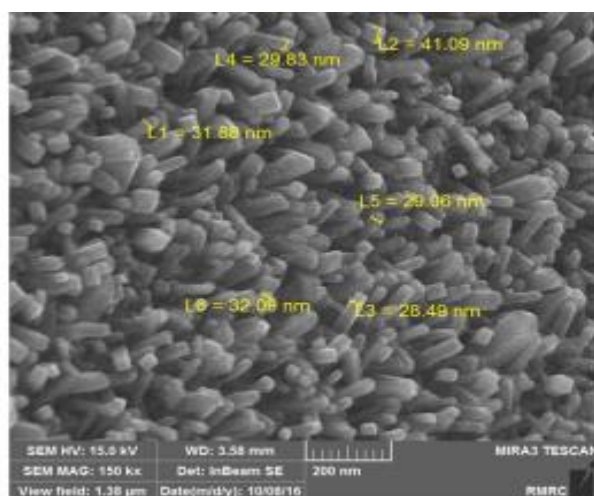


Figure 1. The SEM spectra for nano sized  $\text{RuO}_2$ .

## 3. Results and discussion

The SEM image (Fig. 1) of  $\text{RuO}_2$  shows nano-road morphology, the obtained result of X-ray diffraction pattern shows these miller indexes: (110); (101); (200); (211); (220); (002); (310); (112); (301) and (202) in  $2\theta$  range of 28.2137; 35.1206; 39.7071; 54.3658; 58.1207; 59.3685; 65.3274; 66.7619; 69.1320 and 73.7794. The EDAX (Fig. 2) and MAP (Fig. 3) analysis of  $\text{RuO}_2$  nano-road are presence in Fig. 4 and can be seen, Ru and O elements are presence in synthesized nano-powder that confirms high purity of  $\text{RuO}_2$  nano-road.

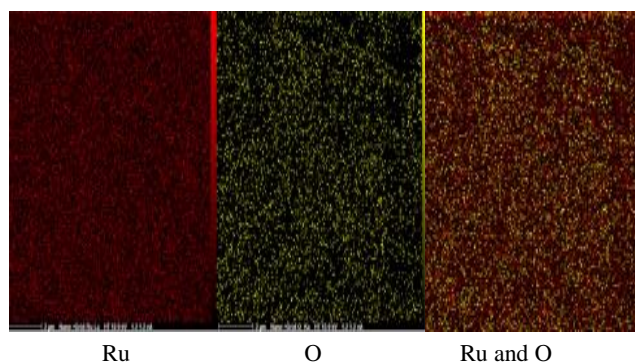


Figure 2. The MAP analysis of nano sized  $\text{RuO}_2$



4<sup>th</sup> Iran National Zeolite Conference  
Golpayegan University of Technology, Golpayegan, Iran  
August 23-24, 2017

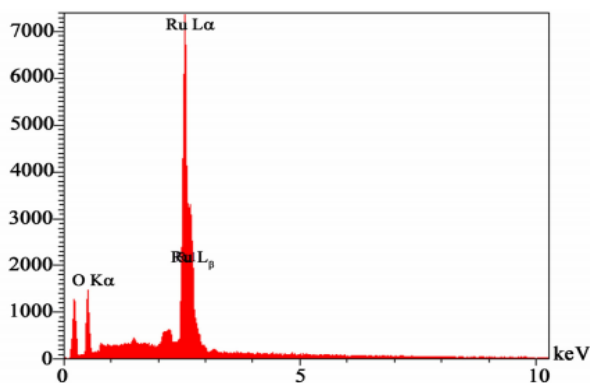


Figure 3. The EDAX analysis of nano sized RuO<sub>2</sub>

#### 4. Conclusions

In this study we prepared nano sized RuO<sub>2</sub> with sol-gel rapid method and characterized and confirmed the structure of this nano oxide with some spectroscopic methods such as SEM, MAP, EDAX and XRD.

#### References

- 1) F.-H. Wu, G.-C. Zhao, X.-W. Wei, Z.-S. Yang, , *Microchim. Acta*, 2004, 144, 243.
- 2) Y. Xu, Y. Jiang, H. Cai, P.-G. He, Y.-Z. Fang, *Anal. Chim. Acta*, 2004, 516, 19.
- 3) Y. Xu, X. Ye, L. Yang, P. He, Y. Fang, *Electroanalysis*, 2006, 18, 1471.
- 4) T. Tavana, M.A. Khalilzadeh, H. Karimi-Maleh, A.A. Ensafi, H. Beitollahi, D. Zareyee, *J. Mol. Liq.* 2012, 168, 69.
- 5) E. Afsharmanesh, H. Karimi-Maleh, A. Pahlavan, J. Vahedi, *Mol. Liq.* 2013, 181, 8,
- 6) H. Beitollah, M. Goodarzian, M.A. Khalilzadeh, H. Karimi-Maleh, M. Hassanzadeh, M. Tajbakhsh, *J. Mol. Liq.* 2012, 173, 137.

## Electrocatalytic activities of Cu(II)Schiff base complexes encapsulated in nanocavities of zeolite-Y towards a new method for olefins oxidation

Saeed Rayati<sup>\*a</sup>, Elham Khodaei<sup>a</sup>

<sup>a</sup> Department of Chemistry, K.N. Toosi University of Technology, P.O. Box 16315-1618, Tehran 15418, Iran

\*Email: rayati@kntu.ac.ir

#### 1. Introduction

Metal transition complexes of Schiff base were considered among the other metal complexes due to their potential application in catalytic systems [1-4]. In addition, electrocatalytic performance of transition metal complexes have been becomes a popular research topic in the oxidation process. The work reported herein presents a modified



4<sup>th</sup> Iran National Zeolite Conference  
Golpayegan University of Technology, Golpayegan, Iran  
August 23-24, 2017



procedure in electrocatalytic oxidation of olefins by  $\text{CuL}_1\text{-Y}$  and  $\text{CuL}_2\text{-Y}$  as heterogeneous catalysts. However, no such studies are reported for the oxidation of chemical substrates. The results showed that the Schiff base complexes encapsulated in zeolite convert olefins into the corresponding epoxide products. Results showed the excellent conversion and selectivity for substrates in green system after 90 second at room temperature [6-12].

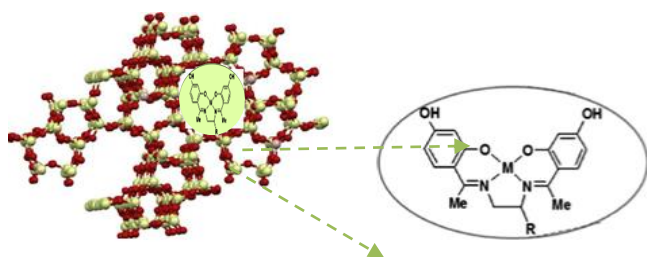
## 2. Experimental

### 2.1. Preparation of the Cu-Y

To stabilize copper into the zeolite structure Na-Y, copper(II) nitrate (3.1 g, 12 mmol) was dissolved in 100 mL distilled water then to this solution 1.25 g Na-Y was added and the resulted mixture was *stirred under reflux* for 24 h then filtered to obtain a gray precipitate, which was washed with distilled water, and finally dried in 150 °C.

### 2.2. Preparation of the $\text{CuL}_1\text{-Y}$ and $\text{CuL}_2\text{-Y}$

Encapsulation of metal complexes was performed with the flexible ligand method. Cu-Y (0.7 g) and 1.25 g of ligands were mixed in 50 mL of methanol, and the reaction mixture was refluxed for 17 h in an oil bath with stirring. The resulting material was separated by filtration and then extracted with methanol using Soxhlet extractor for 72 h to remove unreacted ligands from the cavities of the zeolite as well as those located on the surface of the zeolite along with neat complexes. The unreacted metal ions present in the zeolite were removed by stirring with aqueous 0.01 M NaCl solution. The resulting solid was filtered and washed with distilled water until free from chloride ions. Finally, it was dried at 120 °C. Scheme 1 shows the structure of  $\text{CuL}\text{-Y}$ .



**Scheme 1.** Proposed framework structure of zeolite encapsulated metal Schiff base complexes ( $\text{CuL}_1$  and  $\text{CuL}_2$ ).

## 3. Results and discussion

### 3.1. Characterization of the heterogeneous catalyst $\text{CuL}_1\text{-Y}$ and $\text{CuL}_2\text{-Y}$

FTIR studies of  $\text{CuL}_1\text{-Y}$  and  $\text{CuL}_2\text{-Y}$  are shown in Fig 1. The azomethine C=N groups stretching frequency are observed around 1620 and 1611  $\text{cm}^{-1}$  for  $\text{CuL}_1\text{-Y}$  and  $\text{CuL}_2\text{-Y}$ , respectively. The C=C and C-H stretching frequency are observed as abroad bands around 1536, 2981  $\text{cm}^{-1}$  for  $\text{CuL}_1\text{-Y}$  and 1524, 2926 for  $\text{CuL}_2\text{-Y}$ , respectively. The new fairly less intense bands appearing at the lower frequency region around 540 and 450  $\text{cm}^{-1}$  for  $\text{CuL}_1\text{-Y}$  and 528 and 445 for  $\text{CuL}_2\text{-Y}$  in the encapsulated complexes originate from Cu-O and Cu-N vibrations [18]. These observations suggest that there is a very weak involvement of metal ion in coordination with the zeolite. FTIR spectral analysis provided evidence for the encapsulation.

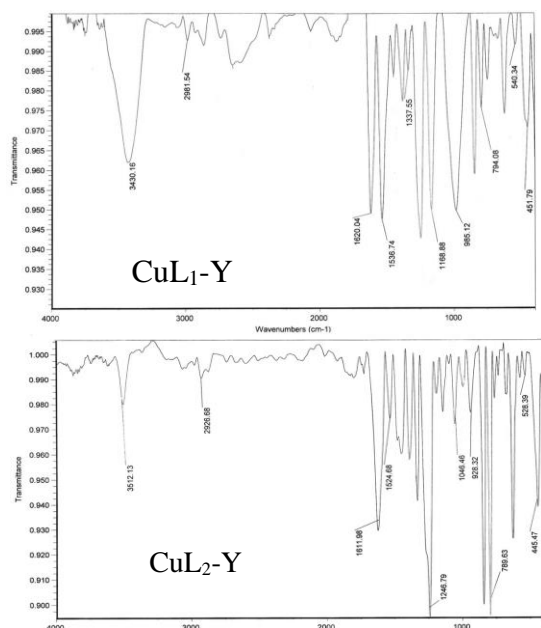


Fig 1. IR spectra of CuL<sub>1</sub>-Y and CuL<sub>2</sub>-Y

The UV-Vis spectra of Fig 2 confirm the inclusion of the Cu(II) Schiff base complexes within the zeolite cages. The spectra suggest the existence of Cu(II) Schiff base complexes in the cage of zeolite even though the peaks exhibit some shift and broadening compared to Cu-Y. This might be due to some distortions of the Cu(II) Schiff base complexes happening inside the zeolite cage. A relatively intense absorption band is seen around 300-400 nm can be attributed to ligand-to-metal charge transfer and gives a strong evidence for the formation of Cu(II) Schiff base complex molecules inside the cavity of zeolite Y.

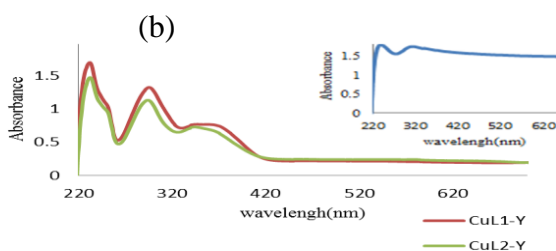


Fig 2. UV-visible spectrum of (a) CuL<sub>1</sub>-Y, CuL<sub>2</sub>-Y and (b) Cu-Y

The thermal properties of the copper(II) Schiff-base complexes encapsulated in zeolite-Y were investigated by TGA measurements with a view to compare their thermal stabilities. The encapsulated copper complexes were heated from 100 °C to 700 °C at a rate of 10° min<sup>-1</sup> in nitrogen atmosphere. The thermograms are given in Fig 3. The TGA curves of encapsulated complexes, CuL<sub>1</sub>-Y and CuL<sub>2</sub>-Y, are found to be almost similar. The endothermic peak observed at below 200 °C in the TGA curve is due to desorption of physically adsorbed and occluded water. The exothermic peaks above 200 °C are attributed to the combustion of copper complexes encaged in the host. However, the mass loss in TG



curves of the encapsulated complexes was extremely small, due to the very low concentration of metal complexes within the supercages of the zeolite.

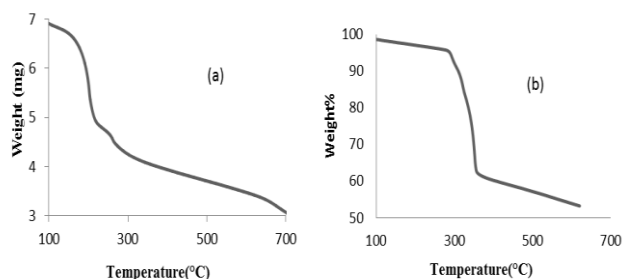


Fig 3. (a) TGA curves of the CuL<sub>1</sub>-Y and (b) CuL<sub>2</sub>-Y

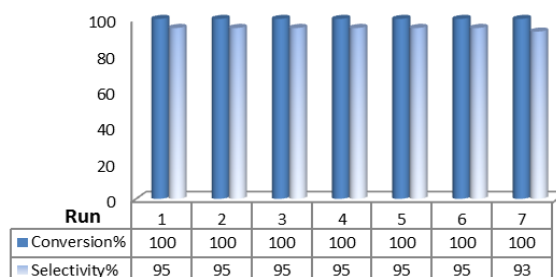


Fig 4. Reuse of the catalytic system in the oxidation of cyclooctene

### 3.2. Electrochemical Oxidation of olefins by nanocatalysts (CuL<sub>1</sub>-Y)

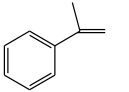
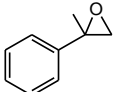
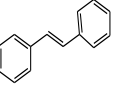
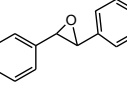
Catalytic efficiency of the heterogeneous catalysts has been examined on epoxidation of cyclooctene by applying a potential to the reaction solution. Oxidation of cyclooctene with different amount of H<sub>2</sub>O<sub>2</sub> as an efficient and green oxidant in the presence of catalytic amounts of CuL<sub>1</sub>-Y was investigated. In this study the highest conversion was obtained at 5:1 (H<sub>2</sub>O<sub>2</sub> to cyclooctene) molar ratio. The effect of potential value and time on the electrochemical oxidation of cyclooctene catalyzed by CuL<sub>1</sub>-Y in ethanol has been examined. In addition the oxidation of cyclooctene in the presence of different solvents was investigated. The highest conversion (100%) was obtained for polar solvents. In this study EtOH was selected as green solvent for further investigation. To examine the effect of the potential value and time different amount of potential in different time was applied. The heterogeneous nanocatalysts (CuL<sub>1</sub>-Y and CuL<sub>2</sub>-Y) could be separated and reused multiple times and recover efficiently in the epoxidation of cyclooctene (Fig 4). In order to examine the efficiency of the heterogeneous nanocatalysts, further investigations were carried out on a broad range of olefins.

Substrate	products	Time (min)	Conversion %	Epoxide products %
		60	100	100
		60	100	100
		60	100	97(3) <sup>b</sup>
		60	100	99(1) <sup>c</sup>
		60	91	100



4<sup>th</sup> Iran National Zeolite Conference  
Golpayegan University of Technology, Golpayegan, Iran  
August 23-24, 2017



		60	100	89(11) <sup>d</sup>
		60	100	100

Reaction conditions: catalyst (mmol): imidazole: alkene: H<sub>2</sub>O<sub>2</sub>: is 1:100:150:750 at room temperature for 90 second reaction time in EtOH in the presence of 60 V potential.

#### 4. Conclusion

In this search, copper(II) Schiff base complexes were prepared and encapsulated in zeolite. The heterogeneous catalysts characterized and utilized for the oxidation of various olefins in the presence potential as a new method using H<sub>2</sub>O<sub>2</sub> as a green oxidant in ethanol by approaching to the green chemistry. The results indicated the superior catalytic activity of catalysts compared to the blank one. In addition heterogeneous nanocatalysts were reused multiple consecutive times without loss in activity or selectivity of catalysts.

#### References

- [1] H. H. Gong, K. Baathulaa, J. S. Lv, G. X. Cai, C. H. Zhou, *Med. Chem. Commun.* **2016**, 7, 924-931.
- [2] M. Aghayee, M. A. Zolfigol, H. Keypour, M. Yarie, L. Mohammadi, *Appl. Organomet. Chem.* **2016**, 30, 612-618.
- [3] W. G. Jia, H. Zhang, T. Zhang, D. Xie, S. Ling, E. H. Sheng, *J. Organomet. Chem.* **2016**, 35, 503-512.
- [4] S. Kato, M. Kanai, S. Matsunaga, *Chem-Asian J.* **2013**, 8, 1768-1771.
- [5] X. Qiu, S. Han, Y. Hu, M. Gao, H. Wang, *J. Mater. Chem. A.* **2014**, 2, 1493-1501.
- [6] H. L. Singh, J. Singh, A. Mukherjee, *Bioinorg. Chem. Appl.* **2013**; 2013: 425832.
- [7] L.Chen, B. Li, D. Liu. *Catal. Lett.* **2014**, 144, 1053-1061.
- [8] M. Navidi, B. Movassagh, S. Rayati, *Appl. Organomet. Chem.* **2013**, 452, 24-28.
- [9] V. Ganesan, M. Pal, M. Tiwari. *Bull. Mater. Sci.* **2014**, 37, 623-628.
- [10] R. Malakooti, G. R. Bardajee, S. Hadizadeh, H. Atashin, H. Khanjari, *Transit Metal Chem.* **2014**, 39, 47.
- [11] Z. Tohidyan, I. Sheikhshoaie; M. Khaleghi. *Int. J. Nano Dimens.* **2016**, 7, 127-136.
- [12] G. R. Reddy, S. Balasubramanian, K. Chennakesavulu. *J. Mater. Chem. A.* **2014**, 2, 15598-15610.



4<sup>th</sup> Iran National Zeolite Conference  
Golpayegan University of Technology, Golpayegan, Iran  
August 23-24, 2017



study of CO<sub>2</sub>, N<sub>2</sub> and CH<sub>4</sub> adsorption in zeolites by Grand Canonical Monte Carlo simulation

Daniel Lotfi moghadam <sup>\*a</sup>, Behruz Bayati <sup>b</sup>, Mona Khodai Pour <sup>c</sup>

<sup>a</sup> Daniel Lotfi moqdm, Department of Chemical Engineering, University of Ilam, Ilam, Iran

<sup>b</sup> Department of Chemical Engineering, University of Ilam, Ilam, Iran

<sup>c</sup> Chemical Engineering faculty, sahand University of technology, Tabriz, Iran

\*Email: [lotfi.dani70@yahoo.com](mailto:lotfi.dani70@yahoo.com)

### abstract

We present a molecular model for the adsorption of CO<sub>2</sub>, N<sub>2</sub>, CH<sub>4</sub>, in zeolite Na-4A. Grand Canonical Monte Carlo simulation is used to study adsorption of nitrogen and methane and Carbon dioxide on new type of zeolites LTA (4A) at temperature range 273–393 K and pressures up to 10000 kpa. Lennard-Jones potential and evaluation of the simulation results are examined. The cvff force field was considered for methane and Carbon dioxide adsorption isotherm and Compass force field is used for simulation of nitrogen adsorption. Besides, the effects of temperature, pressure in unit cell on the adsorption isotherms are investigated, at constant temperature, pressure increases in absorbed and Increasing pressure effect of pressure in absorption decreases. zeolite LTA simulated 96-silicate, aluminum 96 and 384 oxygen atom and includes 8 cells, which is considered to be three-dimensional.

Keywords: Adsorption – zeolites - force field - simulation

### 1. Introduction

Adsorption is an important method in the gas separation processing. Synthesis, characterization and implications of porous sorbent, such as zeolites is receiving increasing attention. Zeolites are crystalline, microporous materials with molecular size pore structure and large surface areas. Zeolites crystals have a uniform three-dimensional pore structure, with pores that vary in shape and of well-defined diameters of molecular dimensions. Zeolites are widely used in various processes for minimizing emissions to the environment, of mainly volatile organic compounds [1-3]. LTA zeolite (3A, 4A, and 5A, where the n in nA refers to the pore size in Å) are widely used as drying industrials and gas separation. Due to small temperature and pressure range limitations of the experimental apparatus, molecular simulation methods are an effective and complementary tool for studying the sorption thermodynamics of nanoporous systems [2-5].

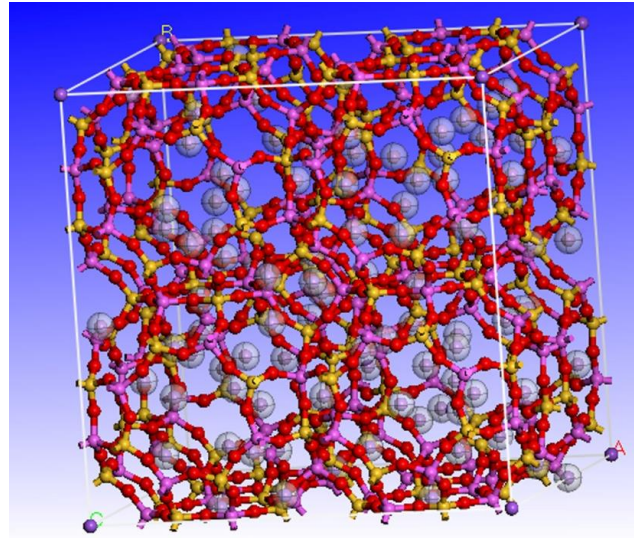
Grand Canonical Monte Carlo (GCMC) techniques are, particularly, well suited method for simulation of adsorption phenomena. Molecular simulation of adsorption by GCMC methods are growing, because these methods provide fair agreement with the results of adsorption experiments [6-10]. The GCMC simulation technique simulates the equilibrium of a collection of adsorbates in a sorbent pore at constant chemical potential, volume, and temperature or pressure [11,12].

In this work the set of Monte Carlo simulations on the grand canonical (m,V,T) ensemble have been used for calculation of the adsorption isotherm of nitrogen and methane and Carbon dioxide on zeolites(4A). A comparison to available experimental data is also shown.





4<sup>th</sup> Iran National Zeolite Conference  
Golpayegan University of Technology, Golpayegan, Iran  
August 23-24, 2017



Schem .1. Diagram of zeolite 4A with silicon atoms shown in yellow, aluminum in purple, oxygen in red, and sodium in blue.

## 2. Simulation details

The LTA zeolite structure was assumed to be rigid structure during the sorption process. The simulated box contains of eight unit cells of zeolite, and periodic boundary conditions are applied in three-dimensions in order to simulate an infinite system.

The dimension of cell is  $a = b = c = 24.610 \text{ \AA}$  (see Schem. 1). In this simulation, Lennard- Jones (L-J) potential is used to calculate the thermodynamics properties of gases. The Lennard- Jones potential is in the following form:

$$U_{ij} = 4\varepsilon_{ij} \left( \left( \frac{\sigma_{ij}}{r_{ij}} \right)^{12} - \left( \frac{\sigma_{ij}}{r_{ij}} \right)^6 \right)$$

$$\varepsilon_{ij} = \sqrt{\varepsilon_i \varepsilon_j}$$

$$\sigma_{ij} = \sqrt{\sigma_i \sigma_j}$$

Where  $r$  and  $e$  are the L-J potential parameters and  $r_{ij}$  is the interatomic distance between  $j$ th and  $i$ th atoms [13-14].

Its interactions parameters of L-J potential are summarized in Table 1, where all the pair interactions were truncated at a cutoff distance  $9.5 \text{ \AA}$ . The partial charges and Lennard-Jones parameters used in our simulations ( Ozeo: -1.025, C: +0.6512 , Oco2: -0.3256 , N: -40484 , Dummy(N<sub>2</sub>): 0.80968)[16] .



4<sup>th</sup> Iran National Zeolite Conference  
 Golpayegan University of Technology, Golpayegan, Iran  
 August 23-24, 2017



**Table 1** Partial charges and Lennard-Jones force field parameters for adsorbent-adsorbate and adsorbate-adsorbate interactions. Top-left corner  $\epsilon/kB$  (K). Bottom-right corner  $\sigma$  (Å)[16]

	O <sub>zeo</sub>	CH <sub>4</sub>	C	O <sub>co2</sub>	N
CH <sub>4</sub>	115	158.5	66.77	112.96	75.96
	3.47	3.72	3.24	3.52	3.52
C	50.2	66.77	28.129	32.0	32.0
	2.78	3.24	2.76	3.04	3.04
O <sub>co2</sub>	84.93	112.96	47.59	54.13	54.13
	2.9192	3.38	2.89	3.18	3.18
N	58.25	75.96	32.0	36.04	36.04
	3.062	3.52	3.04	3.32	3.32

### 3. Results and discussion

Adsorption of N<sub>2</sub> -CO<sub>2</sub> -CH<sub>4</sub> on LTA zeolite at different temperatures was calculated and the results of simulations with experimental data have been compared. In Figures 1, 2 and 3 respectively the calculated adsorption isotherms for nitrogen, methane and carbon dioxide have been compared with experimental data from literatures. The results, from former studies, show that the simulation results are in good agreement with the experimental data and confirm the simulation calculation. Therefore, the used force fields in the simulation studies are suitable. because, selection of appropriate force field can be considered of special importance in this type of molecular simulation studies.

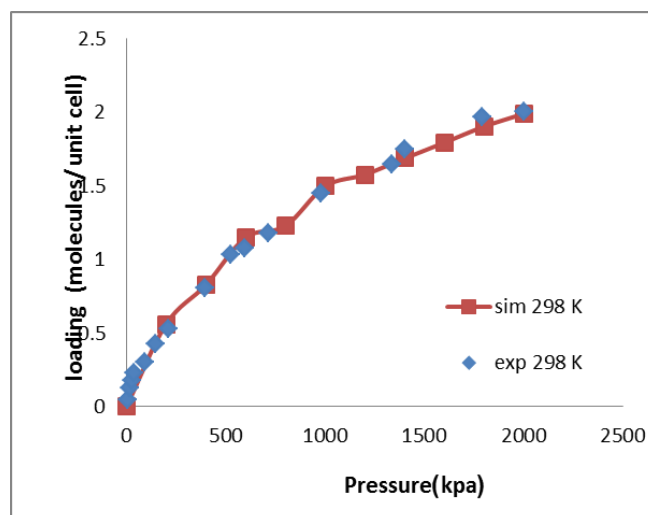


Fig. 1. Experimental [22] and simulated nitrogen adsorption isotherm for zeolite LTA (4 A) temperatures 298 k



4<sup>th</sup> Iran National Zeolite Conference  
Golpayegan University of Technology, Golpayegan, Iran  
August 23-24, 2017

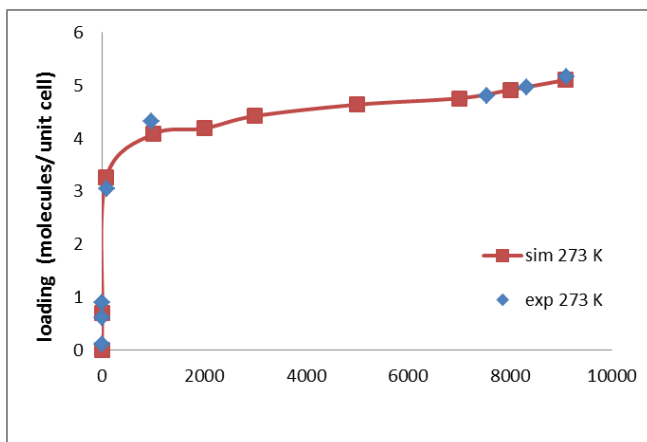


Fig. 2. Experimental [23] and simulated methane adsorption isotherm for zeolite (4 A) LTA temperatures 273 K

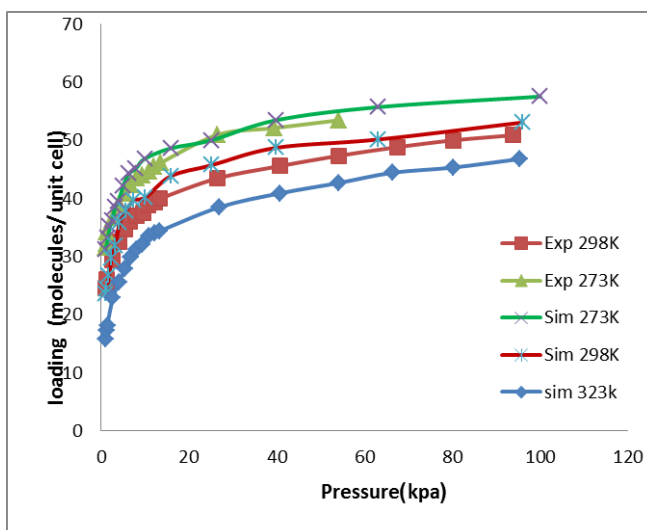


Fig.3. Experimental [24] and simulated carbon dioxide in the zeolite LTA (4 A) temperatures 298-332-273K

Figure 4. nitrogen adsorption isotherm for zeolite 4A in 3 temperatures of 273 to 343 K and pressure of 0.001 to 10000 kpa simulated, is evident from the graph that the temperature increases have reduced absorption.

The adsorption process is completely spontaneous. So, free energy is negative ( $\Delta G < 0$ ), because the molecules adsorb degrees of freedom when the surface area they lose as a result of changes in entropy during adsorption process normally is negative so due to the negative free energy, enthalpy variations must be sufficiently negative to negative  $\Delta G = \Delta H - T\Delta S < 0$  once the absorption process is exothermic and when the high temperature and absorb advanced in the opposite direction will be reduced. Fig. 5. shows the pressure in the range of 0.001 to 10000 kpa. As it is clear that the most effective pressure is a pressure of 1000 kPa and then absorb the impact of increased pressure due to approaching saturation decreases and is almost a straight line.

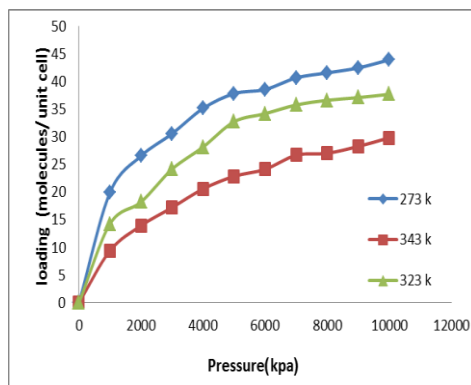


Fig 4. The adsorption isotherm of nitrogen on zeolite LTA (4A) at 273- 323-343 K.

Fig.5. shows that the relative variations of adsorption isotherms (methane molecules for 8 unit cells) versus temperature in the pressures of 0.0001-10000 kpa for a temperature range 273-393 K. As it is well known, the adsorbed methane is decrease when the adsorption temperature is increased. Other zeolites show similar dependencies on adsorption temperature.

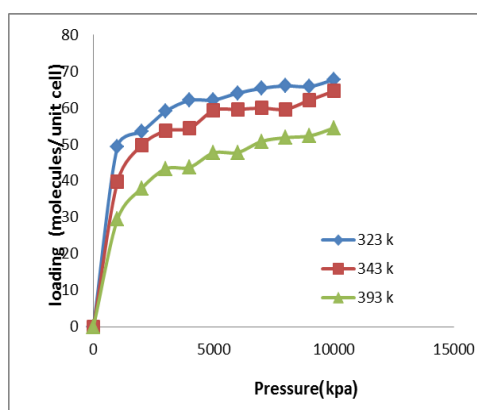


Fig. 5. The adsorption isotherm of methane on zeolite LTA (4A) at 273- 323-343 K.

The potential parameters for CO<sub>2</sub> adsorption were fit to the experimental isotherm at 298 K and then used to calculate the isotherms at 277 and 323 K. Figure 5 shows the adsorption isotherms for CO<sub>2</sub> on zeolite 4A at different temperatures and their comparison with the experimental isotherms from the manufacturer. The agreement between the experimental and simulated isotherms is excellent for pressures greater than 10 kPa. At lower pressures, there is a deviation of the simulated isotherms toward lower loadings. These results are also in agreement with the experimental isotherms obtained at different temperatures.

Simulation in Fig. 6 in the range of 0.0001 to 100 kPa pressure is taken as the figure increases to absorb the increased pressure. At high pressures due to absorption approaching saturation, the effect of pressure is adjusted. The process of temperatures in all of this is true. the pressure 40 Kpa, slope dropped sharply due to full capacity in high-pressure chambers. Fig. 6. shows that with increasing temperature we uptake. This pattern is visible. The adsorption process is completely spontaneous.



4<sup>th</sup> Iran National Zeolite Conference  
Golpayegan University of Technology, Golpayegan, Iran  
August 23-24, 2017

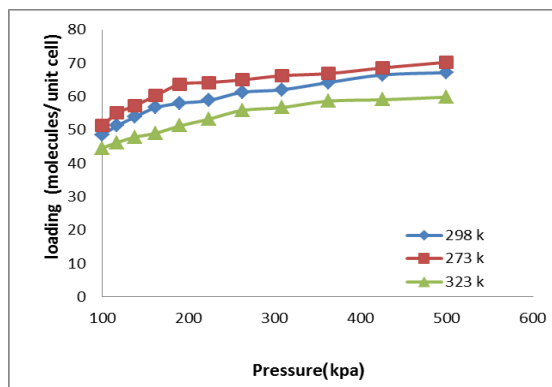


Fig 6. The adsorption isotherm of carbon dioxide on zeolite LTA (4A) at 273- 323-343 K.

#### 4. Conclusions

utilizing molecular simulation systems attractive behavior was studied on the molecular scale, and the influence of process parameters for adsorption in zeolite LTA  $N_2$ ,  $CH_4$  and  $CO_2$  was investigated by GCMC. The use of appropriate force field makes good agreement between the simulation and experimental results exist. The results of the simulation shows that the absorption capacity increases with increasing pressure and absorption is reduced with increasing temperature.

#### References

- 1) Zhang, J.F., Burke, N., Yang, Y.X., 2012. J.Phys.Chem.C116,9666–9674.
- 2) E. Jaramillo and M. Chandross., J. Phys. Chem., B 2004, 108, 20155-20159
- 3) T. Ohkubo, J. Miyawaki, K. Kaneko, R. Ryoo, N.A. Seaton, J. Phys. Chem. B 106 (2002) 6523.
- 4) E.A. Ustinov, D.D. Do, M. Jaroniec, Appl. Surf. Sci. 252 (2005) 548.
- 5) J. Jiang, S.I. Sandler, Langmuir 20 (2004) 10910.
- 6) B. Smit, J. Ilja Siepmann, J. Phys. Chem. 98 (1994) 8442.
- 7) T. Ohkubo, J. Miyawaki, K. Kaneko, R. Ryoo, N.A. Seaton, J. Phys. Chem. B 106 (2002) 6523.
- 8) A.J.P. Carvalho, T. Ferreira, A.J. Estevao Candeias, J.P.P. Ramalho, J. Mol. Struct. (THEOCHEM) 729 (2005) 65.
- 9) E.A. Ustinov, D.D. Do, M. Jaroniec, Appl. Surf. Sci. 252 (2005) 548.
- 10) S. Furmaniak, A.P. Terzyk, P.A. Gauden, K. Lota,
- 11) D. Zhang, W. Li, Z. Liu, R. Xu, J. Mol. Struct. (THEOCHEM) 804 (2007) 89.
- 12) C. Baerlocher, L.B. McCusker, D.H. Olson, Atlas of Zeolite Structure Types, Elsevier, Amsterdam, 2007.
- 13) J.D. Sherman, Proc. Nat. Acad. Sci. USA 96 (1999) 3471.
- 14) M. Rahmati, H. Modarress / Journal of Molecular Structure: THEOCHEM 901 (2009) 110–116
- 15) J. Liu, M. Dong, Z. Qin, J. Wang, J. Mol. Struct. (THEOCHEM) 679 (2004) 95.
- 16) J. Pikunic, P. Llewellyn, R. Pellenq, K.E. Gubbins, Langmuir 21 (2005) 4431.
- 17) J. Sebastian, S.A. Peter, R.V. Jasra, Langmuir 21 (2005) 11220.
- 18) S. Gavalda, K.E. Gubbins, Y. Hanzawa, K. Kaneko, K.T. Thomson, Langmuir 18 (2002) 2141.
- 19) X. Zhang, W. Wang, J. Chen, Z. Shen, Langmuir 19 (2003) 6088.
- 20) R. Denoyel, J.M. Meneses, G.S. Armatas, J. Rouquerol, K.K. Unger, P.J. Pomonis, Langmuir 22 (2006) 5350.
- 21) Y. Li, R.T. Yang, J. Phys. Chem. B 110 (2006) 17175.
- 22) E. Demet Akten, Ranjani Siriwardane, David S. Sholl, Energy & Fuels 2003, 17, 977-983
- 23) A. Garcí'a-Sa'nchez, D. Dubbeldam, S. Calero J. Phys. Chem. C 2010, 114, 15068–15074
- 24) E. Jaramillo, M. Chandross, J. Phys. Chem. B 2004, 108, 20155-20159



## Isomorphous substituted of Fe and Ce in the framework of dealuminated Y zeolite by post-synthesis treatment: Evaluation by 4-Nitrophenol photodegradation

Sara Akbari <sup>a</sup>, Maryam Moosavifar <sup>\*a</sup>

<sup>a</sup>Department of Chemistry, Faculty of Science, University of Maragheh, P.O. Box 55181-83111, Maragheh, Iran

\*Email: m.moosavifar90@gmail.com)

### 1. Introduction

Color is one of the permanent features of surface water. Industrial effluents from textile and dyeing and other operations associated with the streams and rivers of the treatment process has become essential. Many of the chemicals used in the textile industry is causing environmental and health problems. Environmental problems associated with pollution caused by the discharge of untreated water is investigating [1]. Nitrophenols, toxic, inhibitory and biorefractory organic compounds, are extensively use in chemical industries for the manufacture of pesticides, dyes and pharmaceuticals [2]. One of the methods to remove contaminants affordable optical degradation process is carried out using heterogeneous catalysts. During recent years the use of recyclable heterogeneous catalyst considerable importance due to the environmental aspects of economic and industry. Clay, silica alumina and other platforms that are common examples of heterogeneous catalysts are widely used [3]. Zeolite, with unique micropore structure, high thermal stability and high acidity, is widely applied as adsorbent, catalyst or catalyst supports in lots of fields, such as basic petrochemistry, oil refining and fine chemicals synthesis [4]. In this post-synthesis using metallic iron and cerium encapsulated within the zeolite and its photocatalytic activity will be examined. 4-nitro phenol photocatalytic system for optical degradation will be tested

and it will be removed by the technique of spectroscopy [5].

### 2. Experimental Part

All materials were of the commercial reagent grade and were used without any purification. In a typical procedure, NaY zeolite was dealuminated by chemical operation with EDTA treatment.

In a typical procedure, metal of Fe and Ce Pasted in the nanocage of the dealuminated Y zeolite by Post-synthesis method. The prepared photocatalysts were used in the photodecoloration of 4-Nitrophenol.

### 3. Results and discussion

The synthesis of dealuminated Y zeolite-encapsulated cerium (IV) sulfate and iron nitrate was carried out by Post-synthesis method. FESEM analysis, EDS analysis indicated the cubo-octahedral units that proved zeolite structure was preserved after the insertion of metals in the nanocage of zeolite ( Fig. 1) and (Fig. 2).

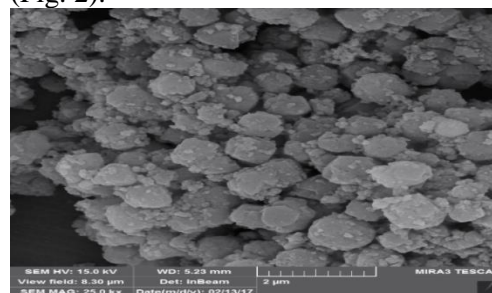


Fig. 1. FESEM analysis of a Ce,Fe zeolite



# 4<sup>th</sup> Iran National Zeolite Conference

## Golpayegan University of Technology, Golpayegan, Iran

### August 23-24, 2017

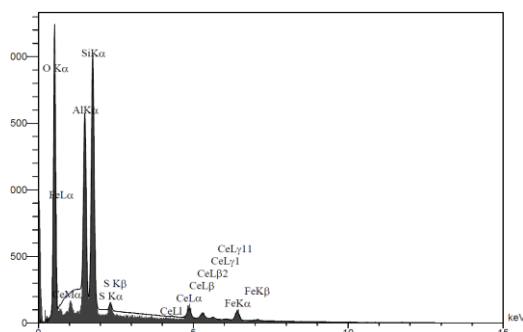


Fig. 2. EDS analysis of a Ce,Fe zeolite

The photocatalytic activity of these systems investigated in the photodecoloration of 4-nitrophenol. The results showed The optimum amount of catalyst and H<sub>2</sub>O<sub>2</sub> and concentration of 4-nitrophenol is Is probably (Fig. 3).

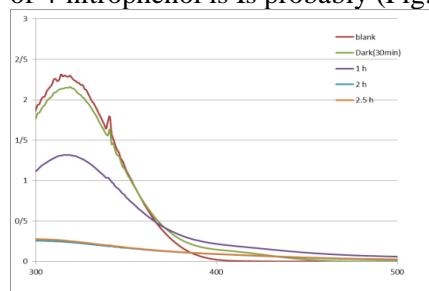


Fig. 3. The optimum amount of catalyst

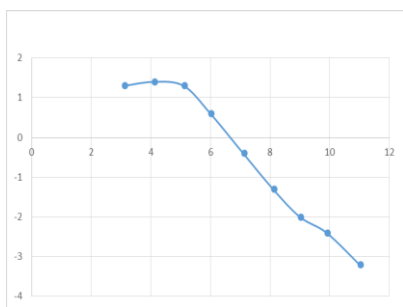


Fig. 4. The effect of pH

#### 4. Conclusions

In this study, the preparation of Ce-Fe zeolites photocatalyst was performed using Post-synthesis methods. The prepared photocatalyst was characterized by SEM, EDSs techniques. The catalyst displays an efficient photocatalytic activity for the degradation 4-Nitrophenol in the presence of H<sub>2</sub>O<sub>2</sub> under UV illumination. The best results were obtained within 2.5 h for a concentration of  $5 \times 10^{-5}$  of 4-NP, 0.03 g of catalyst, and 20 microLiter H<sub>2</sub>O<sub>2</sub> under UV irradiation.

In order to investigation of pH effect, reaction was performed in the range of (pH=3-11). The best condition is related to neutral pH with high efficiency .Isobestic point is another reason to prove this claim. Isobestic point is 6.4. Because pollutant molecule is fairly large and density of charge on extra surface isn't enough, therefore, there isn't noticeable electrostatic repulsive or attractive on contaminants with photocatalyst surface (Fig. 4).

#### References

- 1) Khan, S., & Malik, A. 2014. In Environmental Deterioration and Human Health2014. (pp. 55-71). Springer Netherlands.
- 2) Ma, Y. S., Huang, S. T., & Lin, J. G. Water science and technology, 2000. 42(3-4), 155-160
- 3) Mohammadpoor-Baltork, I., Khosropour, A. R., & Hojati, S. F. Catalysis Communications, 2007.8(12), 1865-1870.
- 4) Xing, C., Yang, G., Wu, M., Yang, R., Tan, L., Zhu, P., ... & Tsubaki, N. Fuel, 2015.148, 48-57.
- 5) Moosavifar, M., Nikkhoo, M., & Mansouri, F. Research on Chemical Intermediates, 2016.42(10), 7417-7427.



4<sup>th</sup> Iran National Zeolite Conference  
Golpayegan University of Technology, Golpayegan, Iran  
August 23-24, 2017



<u>Name</u>	<u>Page</u>	<u>Name</u>	<u>Page</u>
Abedini F	53	Farhangi M	85,172,175
Akhbari K	24	Fazli Shokouhi S	166,167, 215
Asghari A	251	Gheitani S	233
Ameri Dehabadi V	35	Ghetmiri S.H	68
Amiri Zare S	127	Hatamzadeh S	116
Aghamohseni B	249	Hosseini H.S	88
Azarkish M	253	Hashemi M	190
Akbari S	270	Jabbari Manjili T	90
Behyar H	98	Jalalvandi Fard S	221
Bodaghi Fard M	37	Jafari Sh	197
Bahadori E	30	Kalateh Z	178
Behroozibakhsh A.H	170	Khodaei E	122,259
bibakian sangsar H	214	Karami Z	212
Banibairami S	69	Karami M	191
Barghi B	73	Khaghaninejad S	193
Cruciani G	9	Khajeh Ebrahimi A	228
Divband B	33, 160	Kalhor M	43,145
Dehghani M	142	Kazemi Zangeneh F	60
Esmaeili S	52	Koohsaryan E	195
Eslami M	102	Khatamian M	32
Eskandarzade M	114, 182	Lotfi moghadam D	132, 264
		Mir N	80





4<sup>th</sup> Iran National Zeolite Conference  
Golpayegan University of Technology, Golpayegan, Iran  
August 23-24, 2017



<u>Name</u>	<u>Page</u>	<u>Name</u>	<u>Page</u>
Malakzadeh Rusta Sh	207	Sohrabi Noor A	93,230
Mortezaei Z	129, 246	Shahrokh B	63
Mohammadi Manesh H	49,119	Sepehrian M	218
Mahdi Babaei N	236	Taheri Mirghaed S	210
Moosavifar M	46,77	Tarighi S	201
Mahdavi hezaveh S	111	Tahmasbi L	244
Moghadam Z	75	Tavakoli F	163
Mangoli M	100	Usefi S	83
Maleki P	91	Vinu A	22
Nasiri Sh	204	Zare M	105,239
Niakan M	108,180		
Nademi A	153		
Pourmoghadam M	14		
Parchegani F	96		
Pour Amini M.M	12		
Rajabpour Nikfam M	141		
Rafiaei S.M	56,242		
Rastegarzadeh S	237		
Rostamnia S	26, 39, 185		
Shoshtari-Yeganeh B	255		
Sheikh shoaie M	257		
Sedighi P	148,223		



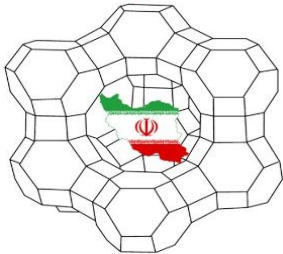
4<sup>th</sup> Iran National Zeolite Conference  
Golpayegan University of Technology, Golpayegan, Iran  
August 23-24, 2017



Sponsors



چهارمین کنفرانس ملی زئولیت ایران  
اول مرداد شهریور ۱۳۹۶



4<sup>th</sup> Iran International Zeolite Conference  
August 23-24, 2017



انجمن آهن و فولاد ایران



International Zeolite Association





4<sup>th</sup> Iran National Zeolite Conference  
Golpayegan University of Technology, Golpayegan, Iran  
August 23-24, 2017



**Phone:**

+98 31 57243160

+98 901 4520600

+98 901 4520601

**Fax:**

+98 31 57240067

**Email:**

[iizc4@gut.ac.ir](mailto:iizc4@gut.ac.ir)

[m\\_zendehdel.iizc4@yahoo.com](mailto:m_zendehdel.iizc4@yahoo.com)



**4<sup>th</sup> Iran National Zeolite Conference**  
**Golpayegan University of Technology, Golpayegan, Iran**  
**August 23-24, 2017**

---

